

Distribution Agreement

In presenting this thesis or dissertation as a partial fulfillment of the requirements for an advanced degree from Emory University, I hereby grant to Emory University and its agents the non-exclusive license to archive, make accessible, and display my thesis or dissertation in whole or in part in all forms of media, now or hereafter known, including display on the world wide web. I understand that I may select some access restrictions as part of the online submission of this thesis or dissertation. I retain all ownership rights to the copyright of the thesis or dissertation. I also retain the right to use in future works (such as articles or books) all or part of this thesis or dissertation.

Signature:

Aaron R. Thornton

Date

**Metallonitrene/Alkyne Cascade Reactions:
Development of a Versatile Process for Organic Synthesis**

By

Aaron R. Thornton
Doctor of Philosophy

Department of Chemistry

Dr. Simon B. Blakey
Advisor

Dr. Huw M. L. Davies
Committee Member

Dr. Frank E. McDonald
Committee Member

Accepted:

Lisa A. Tedesco, Ph.D.
Dean of the James T. Laney School of Graduate Studies

Date

**Metallonitrene/Alkyne Cascade Reactions:
Development of a Versatile Process for Organic Synthesis**

By

Aaron R. Thornton

Bachelor of Arts with Honors in Chemistry (2006),
Knox College, Galesburg, IL, USA

Advisor: Dr. Simon B. Blakey

An abstract of
A dissertation submitted to the Faculty of the
James T. Laney School of Graduate Studies of Emory University
in partial fulfillment of the requirements for the degree of
Doctor of Philosophy
in Chemistry
2010

Abstract

Metallonitrene/Alkyne Cascade Reactions: Development of a Versatile Process for Organic Synthesis

By Aaron R. Thornton

This dissertation outlines our efforts towards the discovery, development, and application of a novel Rh(II)-catalyzed metallonitrene/alkyne cascade reaction. Chapter 1 provides an introduction and background to the field of metallonitrene chemistry, focusing on the development and application of aziridination and C-H amination reactions. Following this, Chapter 2 outlines our efforts towards the discovery and development of a novel metallonitrene/alkyne cascade reaction. In this chapter we first discuss the initial concept for catalyst selection and substrate design, followed by the examination of various substrates in an attempt to better understand this new cascade process. Additionally, experiments designed to elucidate a potential mechanism for this transformation are presented. These studies have led to the successful development of four different cascade termination processes, with each providing access to a range of densely functionalized *N*-containing molecules from remarkably simple starting materials.

Chapter 3 outlines our efforts towards the synthesis of the Securinega alkaloids. A brief background discussing the history, biological importance, and prior syntheses of these natural products is presented. This is followed by our efforts towards the construction of (\pm)-allonorsecurine and (\pm)-allosecurinine through the use of our newly developed cascade reaction. Lastly, the studies that have evolved from this endeavor,

including the development of conditions for the intermolecular termination of this cascade process, are highlighted.

**Metallonitrene/Alkyne Cascade Reactions:
Development of a Versatile Process for Organic Synthesis**

By

Aaron R. Thornton

Bachelor of Arts with Honors in Chemistry (2006),
Knox College, Galesburg, IL, USA

Advisor: Dr. Simon B. Blakey

A dissertation submitted to the Faculty of the
James T. Laney School of Graduate Studies of Emory University
in partial fulfillment of the requirements for the degree of
Doctor of Philosophy
in Chemistry
2010

Acknowledgements

First and foremost thank you Dr. Simon Blakey. The last four years have been a learning experience for everyone in our lab and I cannot thank you enough for the time and energy that you have devoted to making me a better scientist. We may not always see eye-to-eye, but I know that no matter what you are always behind me. Also, thank you to my committee members, Drs. Davies, Liebeskind, and McDonald for all of your help along the way. Emory has a dynamic chemistry department and it has been great knowing that I can step into any of your offices without a second thought.

Thank you to everyone within the Blakey group. You guys are amazing to work with everyday and I could not imagine working with a better group. Clay, I take pride in the fact that I “lured” you into Emory and the Blakey group. It was always great to have someone else around who liked American things...like football, baseball, and everything else awesome. Danny, it's been great sharing a lab with you for the last two years, you are a great chemist and an even better guy. Véronique, I cannot thank you enough for your help. I don't know too many other people that would put up with me while writing this thing and I cannot thank you enough for letting me live with you. Last but not least, Ricardo. You and I did not exactly hit-it-off when I joined the group. We are incredibly different people, but for some reason you have managed to become my closest friend at Emory. Your over-the-top pessimism and paranoia, combined with your wit and personality managed to put a smile on my face everyday. Seriously, you are an insanely smart guy and you can do anything that you want, thank you for keeping my eyes and mind open.

My family is the reason I am the person that I am, thank you. No matter what I do, or don't do, I know that you guys are 100 % behind me. That doesn't mean I won't hear your opinion, but thank you for supporting me. I love you all so much more than I can write here.

And Liz, thank you, thank you, thank you! You have put up with an awful lot and I cannot begin to tell you how important you were to me the last four years. Whenever things were rough in lab I always knew that you were there to keep me sane. You, Chester, Lindsey and Lucille are the ligands to my metal center, attenuating my reactivity and keeping me stable. Thank you.

Contents

Chapter 1: Introduction and Background: The Development and Application of Transition Metal Catalyzed Nitrene Transfer Reactions

1.1.	Prevalence of Nitrogen-Containing Molecules.....	2
1.2.	Aziridination Reactions	3
1.3.	C-H Amination Reactions.....	8
1.4.	Future Directions	15
1.5.	Metallonitrene/Alkyne Metathesis Reaction	16
	References.....	20

Chapter 2: The Discovery and Development of a Metallonitrene/Alkyne Cascade Reaction

2.1.	Design of a Metallonitrene/Alkyne Metathesis Reaction	24
2.1.1.	Potential Catalysts.....	24
2.1.2.	Substrate Design	26
2.2.	Reaction Discovery and Initial Studies.....	28
2.2.1.	Reaction Discovery.....	28
2.2.2.	Control Experiments and Mechanistic Hypothesis.....	31
2.2.3.	Metallonitrene/Alkyne Cascade Reaction Optimization	34

2.2.4.	Substrate Scope for Metallonitrene/Alkyne Cascade Reaction Termination Through Ylide Formation/Group Migration	36
2.3.	Alternate Cascade Terminations and Mechanistic Insight	42
2.3.1.	Reactivity Studies and the Discovery of Metallonitrene/Alkyne Cascade Reaction Termination Through Friedel-Crafts Reaction	42
2.3.2.	Substrate Scope for Cascade Termination Through Friedel-Crafts Reaction.....	45
2.3.3.	Discovery of and Substrate Scope for Cascade Termination Through Cyclopropanation.....	53
2.3.4.	Revised Mechanistic Hypothesis Based on Reactivity Patterns.....	54
2.4.	Conclusions and Future Directions.....	56
	Experimental Procedures and Compound Characterization	57
	X-Ray Crystallographic Data.....	95
	References.....	132

Chapter 3: Application of Metallonitrene/Alkyne Cascade Reactions: Towards the Synthesis of the Securinega Alkaloids and the Development of Intermolecular Cascade Termination

3.1.	The Securinega Alkaloids.....	136
------	-------------------------------	-----

3.1.1.	Introduction.....	136
3.1.2.	History and Biological Importance.....	137
3.1.3.	Recent Syntheses of The Securinega Alkaloids	138
3.1.4.	Metallonitrene/Alkyne Cascade Reactions to Streamline Synthesis	143
3.2.	Synthetic Utility of Cyclic Sulfamidates	144
3.2.1.	Previous Methods for the Use of 1,2- and 1,3-Cyclic Sulfamidates.....	144
3.2.2.	Seven-Membered Oxathiazepane Ring-Opening	145
3.3.	First Generation Approach Towards (\pm)-Allonorsecurinine	146
3.3.1.	Retrosynthetic Analysis of (\pm)-Allonorsecurinine.....	146
3.3.2.	Towards the Synthesis of (\pm)-Allonorsecurinine Through Allyl Acetal Tethered Alkynyl Sulfamate Ester 37	149
3.4.	Intermolecular Metallonitrene/Alkyne Cascade Reaction Termination.....	153
3.4.1.	Concept and Preliminary Results.....	153
3.4.2.	Retrosynthetic Analysis for (\pm)-Allosecurinine Through Intermolecular Cascade Termination	156
3.4.3.	Towards the Synthesis of Allosecurinine Through Intermolecular Cascade Termination	160
3.5.	Re-evaluation of Cascade Termination Through Intermolecular Ylide Fomation/Allyl Migration.....	168
3.5.1.	Examination of Etheral Traps	168

3.5.2.	Examination of Alkyne Substitution.....	169
3.5.3.	Utility of Intermolecular Cascade Termination Cyclization Adducts	171
3.6.	Conclusions and Future Directions.....	178
	Experimental Procedures and Compound Characterization	180
	References.....	215

Appendix: Copper-Catalyzed Olefin Aminoacetoxylation

A.1.	Background and Previous Studies on Olefin Aminoacetoxylation ...	219
A.1.1.	Introduction and Background	219
A.1.2.	Previous Studies Within the Blakey Group	222
A.2.	Results and Discussion	225
A.2.1.	Intramolecular Olefin Aminoacetoxylation	225
A.3.	Conclusions.....	231
	Experimental Procedures and Compound Characterization	232
	X-Ray Crystallographic Data.....	247
	References.....	282

List of Schemes

Chapter 1:

Scheme 1.1.	Metallonitrene chemistry	3
Scheme 1.2.	Early advances in the field of metallonitrene chemistry.....	4
Scheme 1.3.	Evans' and Jacobsen's asymmetric aziridination protocols	5
Scheme 1.4.	Introduction of $\text{PhI}=\text{NSes}$ and one-pot aziridinations	6
Scheme 1.5.	$\text{Rh}_2(\text{tfacam})_4$ as an effective aziridination catalyst	6
Scheme 1.6.	Du Bois' synthesis of (-)-agelastatin A.....	7
Scheme 1.7.	Che's $\text{Ru}(\text{II})$ -porphyrin catalyzed C-H amination	9
Scheme 1.8.	Selective methods for intramolecular C-H amination	10
Scheme 1.9.	Du Bois' synthesis of (-)-tetrodotoxin	11
Scheme 1.10.	$\text{Rh}_2(\text{esp})_2$ as an effective and general catalyst for C-H amination.....	12
Scheme 1.11.	Che's original precedent for enantioselective C-H amination.....	13
Scheme 1.12.	Blakey's $\text{Ru}(\text{II})$ -pybox complex for enantioselective C-H amination.....	14
Scheme 1.13.	Du Bois' $\text{Rh}_2(\text{S-nap})_4$ for enantioselective C-H amination	15
Scheme 1.14.	Ene/yne metathesis mechanism	18
Scheme 1.15.	Odom's stable imido/alkyne metathesis	19

Chapter 2:

Scheme 2.1.	Rh(II)-catalyzed metallocarbene/alkyne cascade reaction.....	26
Scheme 2.2.	Substrate design for a tandem metallonitrene/alkyne metathesis/C-H insertion reaction.....	28
Scheme 2.3.	Rh(II)-catalyzed metallonitrene/alkyne cascade reaction discovery .	29
Scheme 2.4.	Cascade reaction followed by <i>in situ</i> reduction provides stable oxathiazepane 13	31
Scheme 2.5.	Metallonitrene/alkyne cascade reaction mechanism.....	32
Scheme 2.6.	π -Activation as an alternate mechanism for the formation of <i>N</i> -sulfonyl imine 11	33
Scheme 2.7.	Control experiments suggest cascade reaction is initiated by metallonitrene formation.....	34
Scheme 2.8.	Synthesis of allyl ether tethered sulfamate ester 24	35
Scheme 2.9.	Synthesis of alkyl and aryl substituted alkynyl sulfamate esters for substrate scope examination	38
Scheme 2.10.	Substrate scope for intramolecular ylide formation/group migration termination	39
Scheme 2.11.	Synthesis of sulfamate esters with alternate tether lengths.....	40
Scheme 2.12.	Examination of sulfamate esters with alternate tether lengths	41
Scheme 2.13.	Synthesis of aromatic tethered alkynyl sulfamate ester 49	43
Scheme 2.14.	Reactivity studies suggest vinyl cation intermediate	44

Scheme 2.15. Synthesis of simple aromatic tethered alkynyl sulfamate esters 56 and 58	45
Scheme 2.16. Effect of tether length on Friedel-Crafts cascade termination	46
Scheme 2.17. Synthesis of electronically biased aromatic tethered alkynyl sulfamate esters 61 and 62	47
Scheme 2.18. Metallonitrene/alkyne cascade reaction termination through Friedel-Crafts reaction	48
Scheme 2.19. Synthesis on <i>N</i> -benzyl indole tethered sulfamate ester 70 and unsuccessful cyclization attempts.....	50
Scheme 2.20. Synthesis of <i>N</i> -Boc indole tethered sulfamate ester 75	51
Scheme 2.21. Cascade termination through selective C-2 and C-3 additions of <i>N</i> -Boc indole 75	53
Scheme 2.22. Representative substrate scope for cascade termination through cyclopropanation.....	54
Scheme 2.23. Revised metallonitrene/alkyne cascade reaction mechanism	55

Chapter 3:

Scheme 3.1. Horii's synthesis of (\pm)-securinine	139
Scheme 3.2. Kerr's method for the synthesis of densely functionalized pyrrolidines	140
Scheme 3.3. Kerr's synthesis of (-)-allosecurinine	142
Scheme 3.4. 1,2- and 1,3-cyclic sulfamidates as versatile electrophilic reagents ..	144

Scheme 3.5.	Ring-opening reactions of <i>N</i> -acyl oxathiazepanes and the development of NaI mediated pyrrolidine synthesis	146
Scheme 3.6.	Securinega alkaloids inspire the development of novel metallonitrene/alkyne cascade reaction termination.....	147
Scheme 3.7.	Retrosynthetic analysis for the construction of allonorsecurinine through a metallonitrene/alkyne cascade reaction strategy	148
Scheme 3.8.	Initial route to cyclization precursor 37 and unsuccessful attempts at oxirane opening.....	149
Scheme 3.9.	Attempted synthesis of cyclization precursor 37 and unsuccessful oxidation protocols	150
Scheme 3.10.	Synthesis of allyl acetal tethered alkynyl sulfamate ester 37	151
Scheme 3.11.	Cyclization of sulfamate ester 37 yields an unexpected product.....	152
Scheme 3.12.	Mechanism for the intermolecular termination of metallonitrene/alkyne cascade reactions and potential non-productive pathways	155
Scheme 3.13.	Preliminary examination of intermolecular cascade termination with <i>bis</i> -allyl ether leads to intermolecular C-H amination products	156
Scheme 3.14.	Du Bois' Rh ₂ (tfacam) ₄ for intra- and intermolecular aziridination reactions	157
Scheme 3.15.	Catalyst tuning provides proof-of-principle for intermolecular cascade termination.....	158
Scheme 3.16.	Retrosynthetic analysis for the construction of allosecurinine through intermolecular cascade termination.....	159
Scheme 3.17.	Synthesis of alkynyl sulfamate ester 70	160

Scheme 3.18. Optimization of intermolecular cascade termination with <i>bis</i> -allyl ether towards the synthesis of allosecurinine	162
Scheme 3.19. Unsuccessful attempts at <i>N</i> -alkyl oxathiazepane ring-opening and initial positive results	163
Scheme 3.20. Limited success at <i>N</i> -alkyl oxathiazepane ring-opening with H ₂ O ...	164
Scheme 3.21. Attempts at <i>N</i> -acylation and unsuccessful ring-opening with H ₂ O ...	165
Scheme 3.22. Unsuccessful attempts to produce bicyclic <i>N</i> -acylated oxathiazepane 84	167
Scheme 3.23. Examination of various ethereal traps for intermolecular cascade termination	169
Scheme 3.24. Examination of alkyne substitution patterns and interesting reactivity differences.....	171
Scheme 3.25. Temperature dependent facial selectivity for the addition of allylmagnesium chloride to <i>N</i> -sulfonyl imine 90	172
Scheme 3.26. Examination of Grignard reagents	175
Scheme 3.27. Synthesis of aliphatic amines via intermolecular cascade termination	176
Scheme 3.28. Synthesis of <i>N</i> -heterocycles via intermolecular cascade termination	177
Scheme 3.29. Synthesis of functionalized carbocycles via intermolecular cascade termination	178

Appendix:

Scheme A.1. Previously developed Pd-catalyzed olefin aminoxygenation methodologies.....	220
Scheme A.2. Chemler's Cu-catalyzed olefin aminoxygenation methodology	221
Scheme A.3. Metal-free aminoxygenation reactions for the synthesis of functionalized piperidines.....	222
Scheme A.4. Cu(I)-catalyzed olefin aminoacetoxylation reaction discovery	223
Scheme A.5. Intramolecular aminoacetoxylation of metallonitrene/alkyne cyclization adducts 3 and 5	226
Scheme A.6. Synthesis of 1,2-disubstituted γ -aminoolefins 7 and 8	227
Scheme A.7. Cyclization of 1,2-disubstituted γ -aminoolefins 7 and 8	227
Scheme A.8. Cylization of <i>cis</i> - and <i>trans</i> -phenyl γ -aminoolefins 12 and 13	229
Scheme A.9. Synthesis of TBS-protected γ -aminoolefin 18	230
Scheme A.10. Cylization of TBS-protected γ -aminoolefin 18	231

List of Figures

Chapter 1:

- Figure 1.1. Metallonitrene and metallocarbene chemistries16
- Figure 1.2. Metallonitrene/alkyne metathesis reaction concept17
- Figure 1.3. Common Ru(II) based catalyst for ene/yne metathesis17

Chapter 2:

- Figure 2.1. Potential catalysts for metallonitrene/alkyne metathesis reaction25
- Figure 2.2. Metallonitrene/alkyne cascade reaction optimization and versatility36

Chapter 3:

- Figure 3.1. Representative members of the Securinega alkaloids.....136
- Figure 3.2. Metallonitrene/alkyne cascade reaction constructs the 1,2-amino oxygenated core of the Securinega alkaloids in a single reaction143
- Figure 3.3. Key nOe correlations for oxathiazepane **73** and ring-closed product **100**174

Appendix:

Figure A.1. Proposed mechanism for Cu(I)-catalyzed intramolecular
aminoacetoxylation.....225

List of Tables

Chapter 2:

Table 2.1.	Optimization for the coupling of 73 with THP-protected 3-butyn-1-ol	51
------------	---	----

Appendix:

Table A.1.	Optimization studies for Cu(I)-catalyzed olefin aminoacetoxylation	224
------------	---	-----

List of Abbreviations

Ac	Acetyl
Aq	Aqueous
Bn	Benzyl
Bz	Benzoyl
d	doublet
DIBAL-H	diisobutylaluminum hydride
DMAP	<i>N,N</i> -dimethylaminopyridine
DMPU	1,3-dimethyl-3,4,5,6-tetrahydro-2(1H)-pyrimidinone
dppe	1,3-bis(diphenylphosphino)ethane
DMF	<i>N,N</i> -dimethylformamide
EtOAc	ethyl acetate
imid	imidazole
m	multiplet
MeCN	acetonitrile
mL	milliliter
mmol	millimole
ⁿ BuLi	<i>n</i> -butyllithium
Ph	phenyl
s	singlet
SO ₃ :pyr	sulfur trioxide-pyridine
t	triplet

TBAF	tetrabutylammonium fluoride
TBAI	tetrabutylammonium iodide
TBS	<i>tert</i> -butyldimethylsilyl
THF	tetrahydrofuran

Chapter 1:

Introduction and Background:

The Development and Application of Transition Metal

Catalyzed Nitrene Transfer Reactions

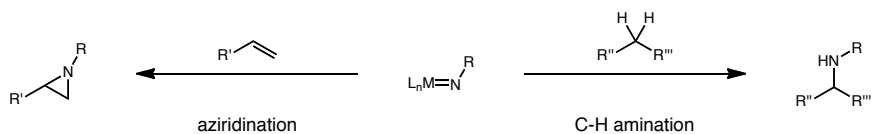
1.1. Prevalence of Nitrogen-Containing Molecules

Nitrogen containing compounds are prevalent in many biological systems and are commonly utilized as pharmaceutical agents as well as functional materials. The ubiquitous nature of C-N bonds has ensured that the development of efficient methods for *N*-incorporation has remained at the forefront of synthetic research. However, while progress has been made, still today the most commonly utilized methods to construct C-N bonds are deeply rooted in the 20th, or even 19th, centuries. Indicating the need for new methods for C-N bond construction, in 2007 the ACS Green Chemistry Pharmaceutical Roundtable identified that the development of “*N*-centered chemistries avoiding azides, hydrazine, etc.” was a “key research area”.¹ This sentiment should not be surprising considering the fact that 47 of the top 50 selling drugs worldwide actually contain this important connection.²

In light of this intense need for *N*-containing molecules, methods that have the ability to selectively introduce *N*-containing functionality into simple organic substrates with little or no prefunctionalization represent an overtly attractive strategy for synthesis. In turn, the development of such methods has grown into a burgeoning field of study. One area within this field that has garnered considerable attention from the synthetic community is the use of transition metal catalyzed nitrene transfer reactions. These reactions take advantage of the unique reactivity that is offered by these short-lived intermediates, and methods for C-N bond construction using these species has quickly developed into a significant area of research. Traditionally, metallonitrene facilitated C-N bond-forming reactions have focused on efficient protocols for both aziridination

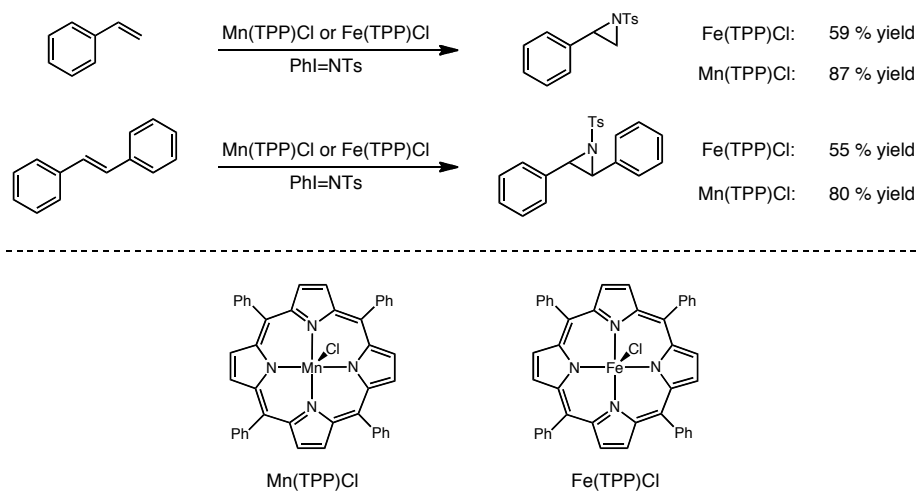
and C-H amination (Scheme 1.1).³

Scheme 1.1. Metallonitrene Chemistry.

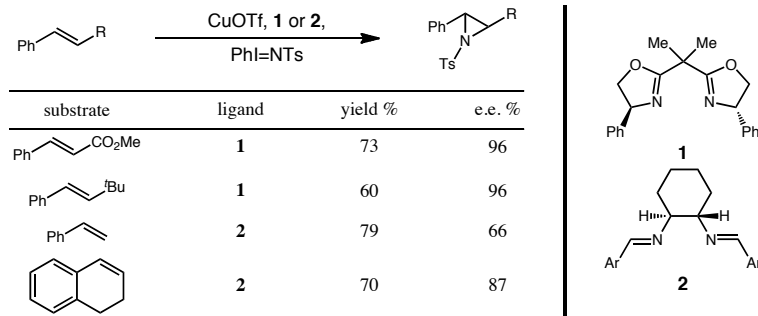


1.2. Aziridination Reactions

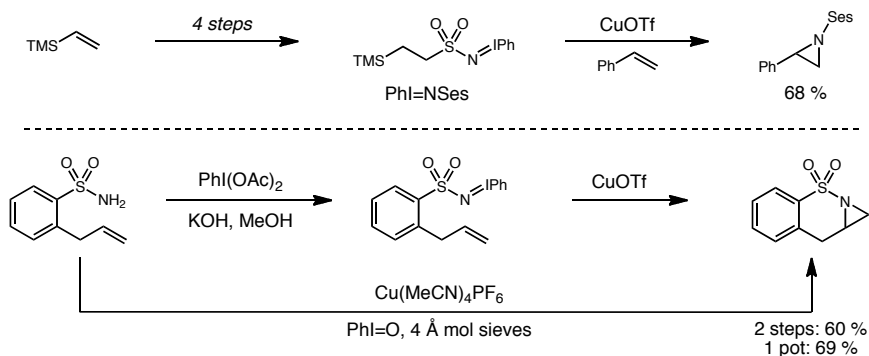
The aziridine moiety is an important structural motif found in molecules possessing antitumor activity.⁴ In addition to this, these three-membered ring *N*-heterocycles have long been revered as useful electrophilic intermediates in organic synthesis, and are often referred to as the *N*-equivalent of epoxides.⁵ Even with their obvious utility, the development of broadly applicable methods for aziridine construction still remains a challenge to the synthetic community. Early work in this field was inspired by the cytochrome P-450 catalyzed epoxidation of olefins with iodosylbenzene,⁶ and showed that similar Mn(III) and Fe(III)-tetraphenylporphyrin (TPP) based catalysts were capable of analogous *N*-atom transfer from tosylimino phenyliodine (PhI=NTs) (Scheme 1.2).⁷ Although these transformations were of only limited applicability, this early work laid the foundation for the future development of synthetically useful nitrene transfer reactions.

Scheme 1.2. Early advances in the field of metallonitrene chemistry.

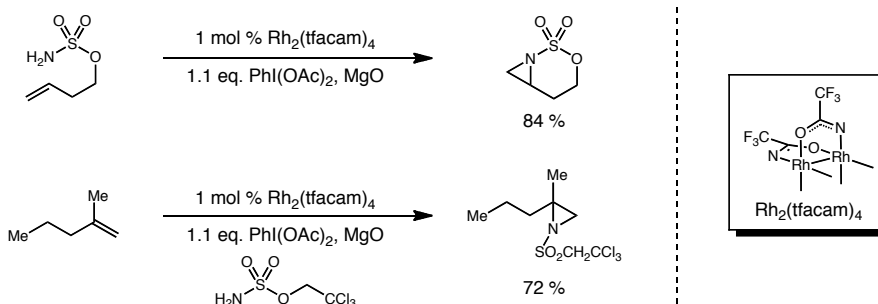
Since this initial work, efforts within the field have shown that an array of transition metal catalysts are capable of effecting this transformation,^{3a} but it was the Evans group who first developed this transformation into a practical process. In addition to powerful racemic aziridination protocols,⁸ their work also provided evidence that CuOTf, supported by various chiral bis(oxazoline) ligands, could effectively catalyze this reaction in an enantioselective manner (Scheme 1.3).⁹ Simultaneous efforts from the Jacobsen laboratory illustrated that similar chiral diimine/CuOTf based systems could catalyze asymmetric olefin aziridination with PhI=NTs as well.¹⁰ Although these systems afforded similar yields and enantioselectivities, the significant advantage of Jacobsen's method may be attributed to the use of olefinic substrates as the limiting reagent. Even with this advance, the constraint of styrenal substrates and the use of PhI=NTs as the only applicable *N*-source limited the use of metallonitrene facilitated aziridination reactions in organic synthesis.

Scheme 1.3. Evans' and Jacobsen's asymmetric aziridination protocols.

To address these limitations Dauban and Dodd introduced $\text{PhI}=\text{NSes}$ ($\text{Ses}=\text{trimethylsilylethanesulfonyl}$) as a readily accessible nitrene precursor for olefin aziridination (Scheme 1.4).¹¹ With the successful isolation of imino phenyliodinanes derived from aliphatic sulfonamides, the work of Dauban and Dodd opened the door for the development intramolecular aziridination reactions.¹² On top of this significant finding, the development of reaction conditions that allowed for the one-pot conversion of sulfonamides and sulfamate esters to aziridines drastically expanded the applicability of transition metal catalyzed olefin aziridination reactions. Still, despite this important progress, these transformations' limited substrate scope has hindered their widespread use within the synthetic community.

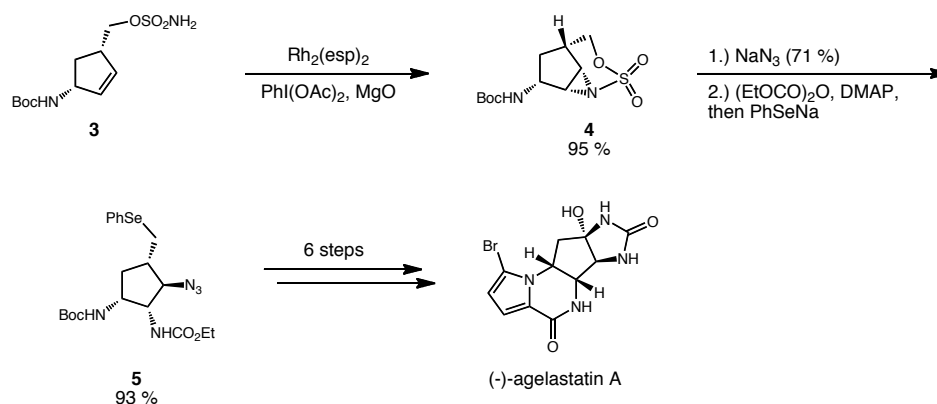
Scheme 1.4. Introduction of PhI=NSes and one-pot aziridinations.

Traditionally copper catalysis has proven to be most effective for olefin aziridination reactions. More recently however, Rh(II) based systems have been shown to be highly useful for nitrene transfer reactions.¹³ The Du Bois group's studies on the complex interplay between catalyst structure, the nature of the *N*-source, and the hypervalent iodine oxidant have all led to significant advances in both olefin aziridination and C-H amination chemistries. In fact it was not until this group demonstrated that Rh₂(tfacam)₄ was an exceptionally efficient catalyst for both intra- and intermolecular olefin aziridinations that aliphatic olefins possessing multiple reactive sites could be aziridinated selectively (Scheme 1.5).¹⁴ This development helped to establish Rh(II)-catalyzed aziridination as a useful tool for the synthesis of biologically relevant natural products, and numerous syntheses have utilized this method since.¹⁵

Scheme 1.5. Rh₂(tfacam)₄ as an effective aziridination catalyst.

Highlighting the utility of transition metal catalyzed aziridination methods, the Du Bois group's recent synthesis of (-)-agelastatin A commenced with intramolecular aziridination of alkenyl sulfamate ester **3** (Scheme 1.6).¹⁶ The corresponding heterocycle was then easily derivatized using sequential regioselective nucleophilic ring-opening reactions, in turn underscoring the value of efficient intramolecular aziridination methods as well as the utility of the sulfamate ester nitrene precursor. With densely functionalized cyclopentane **5** hand, the total synthesis of (-)-agelastatin A was then completed in just six additional steps.

Scheme 1.6. Du Bois' synthesis of (-)-agelastatin A.

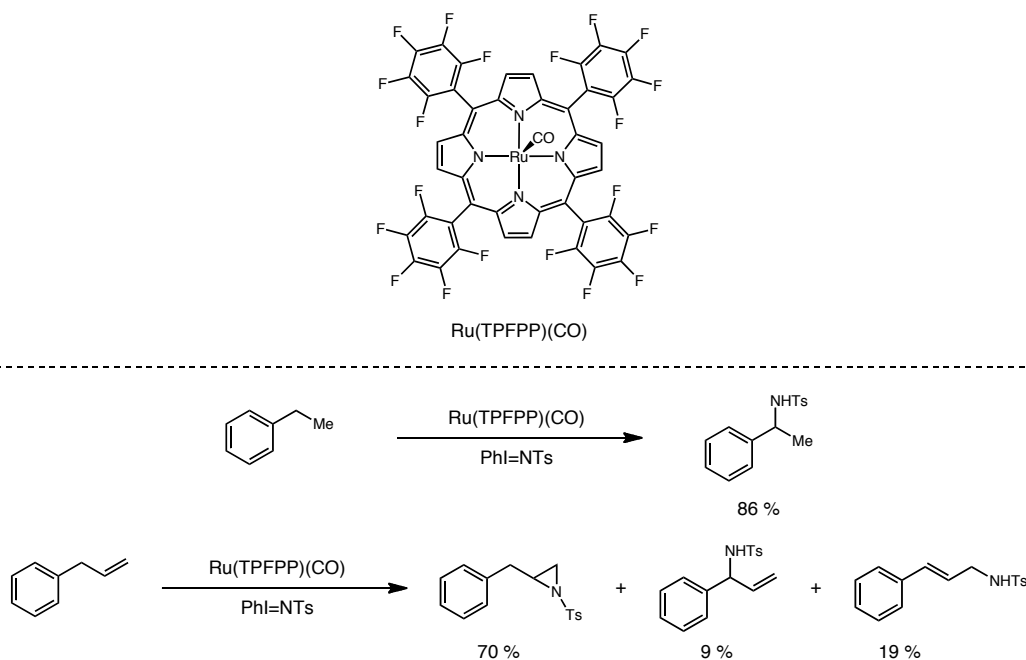


The successful development of selective and predictable protocols for metallonitrene facilitated aziridination have helped to establish this method as a powerful tool for organic synthesis. While progress is continuously made within the field, much of the recent work focusing on the use of reactive metallonitrenes has been devoted to the development of efficient methods for C-H amination.

1.3. C-H Amination Reactions

Along with metallonitrene facilitated aziridination reactions the field of C-H amination has developed into a growing area of interest.^{3b,c} While both reactions offer extremely attractive alternatives to classical methods for C-N bond formation, the similarities displayed by aziridination and C-H amination reactions has led to significant issues of chemoselectivity, and in turn has detracted from their use in synthesis. Because of this lack of selectivity, considerable effort has been put into the development of predictable methods for C-H amination, while suppressing competitive aziridination.

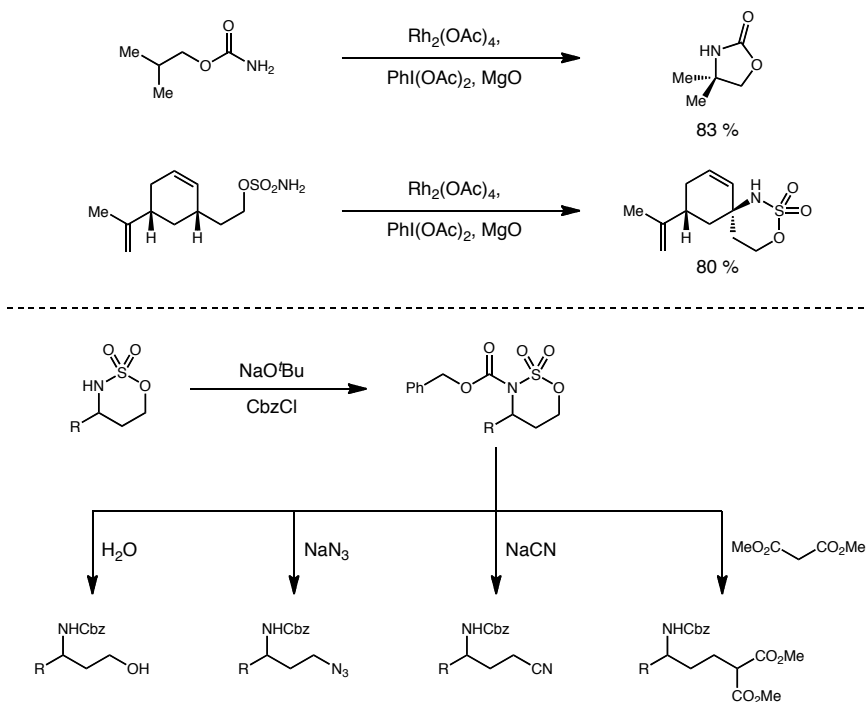
In 2000 Che and Du Bois disclosed independent reports for the *in situ* formation of imino phenyliodinanes for C-H amination, similar to the method of Dauban and Dodd for aziridination.^{17,18} The work of Che's group revolved around the use of a Ru(II)-porphyrin based catalyst system, Ru(TPFPP)(CO) (Scheme 1.7). Although this catalyst was able to carry out C-H amination reactions with exceptionally high turnover numbers, up to 2,600 in certain cases, many substrates lead to unselective nitrene transfer, resulting in the formation of both C-H amination as well as aziridination products. These issues of chemoselectivity limited the application of this method, and further highlighted the need for chemoselective protocols.

Scheme 1.7. Che's Ru(II)-porphyrin catalyzed C-H amination.

In contrast to Che's work, the work of the Du Bois group primarily focused on intramolecular C-H amination reactions. Their work showed that primary carbamates and sulfamate esters could be smoothly transformed into their corresponding cyclic amine products (Scheme 1.8).^{18a,b} These reactions have been shown to exhibit an impressive level of stereo- and regioselectivity, with carbamates leading to the formation of five-membered rings while sulfamate esters cyclize to give six-membered ring products. While carbamates are known to undergo a range of organic transformations, methods for the utilization of cyclic sulfamidates are often less obvious. In addition to these powerful methods for C-H amination, the Du Bois group has also shown that these cyclic sulfamidates may be used as versatile electrophilic reagents. Following *N*-acylation the cyclic sulfamidate is activated for nucleophilic extrusion of SO₃, thereby allowing for the introduction of a wide range on nucleophilic reagents.¹⁹ These

complimentary *N*-sources in turn allow access to both 1,2- and 1,3-amino functionalized products selectively and predictably.

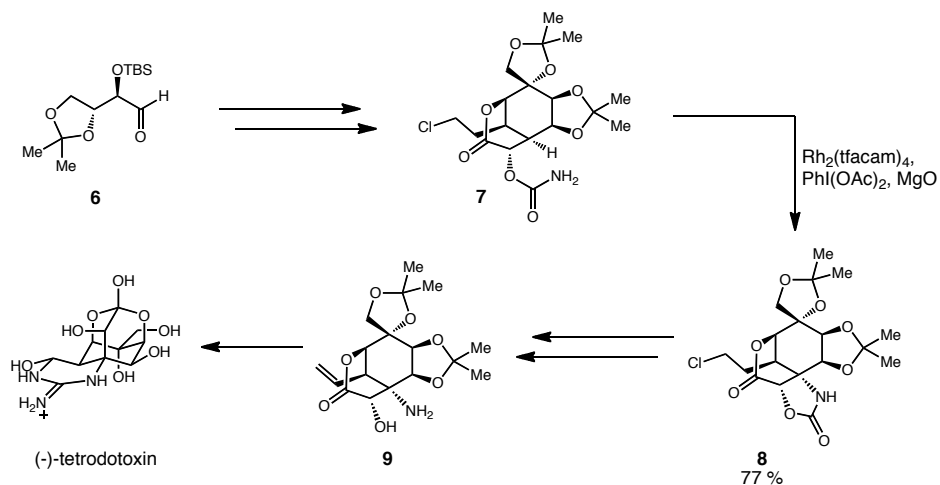
Scheme 1.8. Selective methods for intramolecular C-H amination.



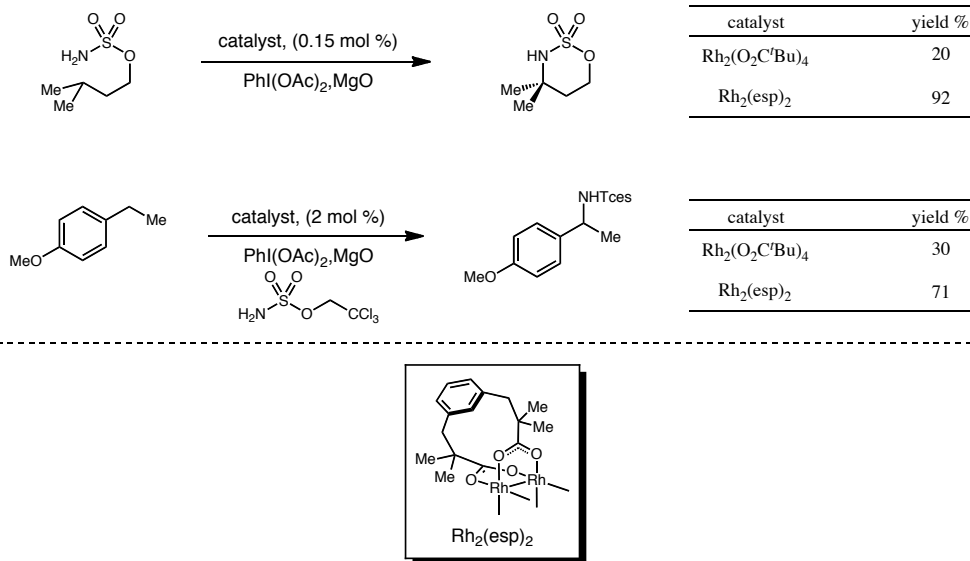
With these powerful methods established, the utility of intramolecular C-H amination was elegantly illustrated in the Du Bois group's synthesis of (-)-tetrodotoxin (Scheme 1.9).²⁰ Because chemo- and regioselective C-H amination strategies had been developed, C-H amination could be utilized late in their synthetic route on a highly functionalized intermediate. The conversion of carbamate **7** to oxazolidinone **8** in 77 % yield with 10 mol % $\text{Rh}_2(\text{tfacam})_4$ constitutes a major advance in the field of metallonitrene chemistry. Following this key C-H amination, a straightforward seven-step sequence was undertaken to then furnish the natural product. This work established C-H amination as a useful tool for organic synthesis and helped pave the way

for future developments within the field.

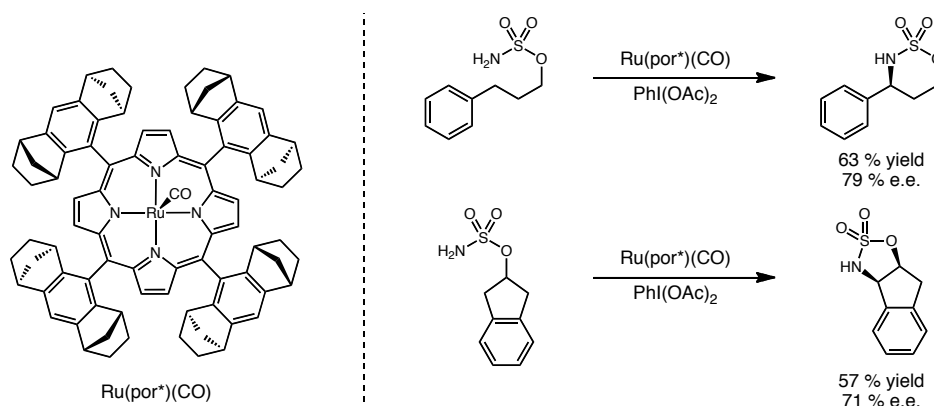
Scheme 1.9. Du Bois' synthesis of (-)-tetrodotoxin.



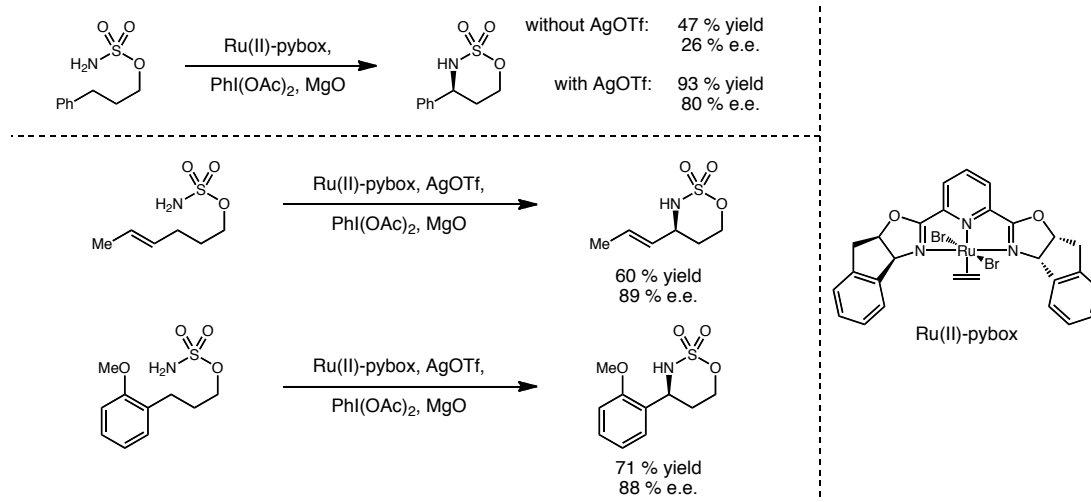
While the synthesis of (-)-tetrodotoxin demonstrated Rh(II) catalysts' exquisite selectivity for C-H amination, the use of 10 mol % plainly illustrates their limited activity. Cognizant of this, the Du Bois group created $\text{Rh}_2(\text{esp})_2$ (Scheme 1.10), a catalyst reminiscent of those developed by the groups of Taber and Davies for analogous metallocarbene chemistries.^{21,22} Owing to its two bridging carboxylate ligands, $\text{Rh}_2(\text{esp})_2$ has proven to be an exceptionally effective and general catalyst for C-H amination. With catalyst loadings as low as 0.15 mol %, this complex has been shown to be superior to other Rh(II)-tetracarboxylates, including its isosteric counterpart $\text{Rh}_2(\text{O}_2\text{C}^t\text{Bu})_4$ for intra- and intermolecular C-H aminations. Importantly, the enhanced reactivity and stability of $\text{Rh}_2(\text{esp})_2$ also allows for intermolecular C-H aminations to be carried out with the C-H bond containing substrate as the limiting reagent.

Scheme 1.10. Rh₂(esp)₂ as an effective and general catalyst for C-H amination.

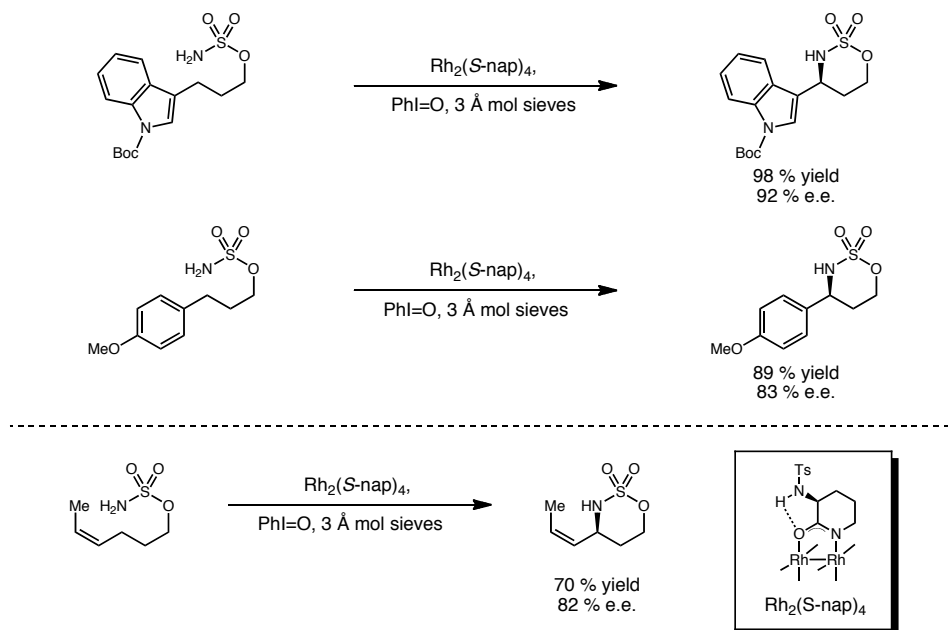
New catalysts and *N*-sources have both vastly broadened the scope of C-H amination. However, until very recently practical methods for enantioselective variants of this powerful transformation had yet to be developed. Che and coworkers' original precedent using a chiral Ru(II)-porphyrin complex, Ru(por*)(CO), was a landmark discovery (Scheme 1.11).²³ Unfortunately the use of this system was quite limited, once again due to a lack of chemoselectivity.

Scheme 1.11. Che's original precedent for enantioselective C-H amination.

To address this issue, a range of catalysts based around a Rh(II) framework have also been examined. Although a number of chiral Rh(II)-tetracarboxylate and -carboxamidate catalysts have been developed for asymmetric metallocarbene transformations, these systems have not proven to be particularly effective for asymmetric C-H amination.^{24,25} Keeping this in mind, the Blakey group re-examined the use of ruthenium and has recently developed a highly modular catalyst system based on a chiral Ru(II)-pybox framework (Scheme 1.12).²⁶ Halide abstraction from this catalyst with AgOTf furnishes a cationic metal center and an active catalyst that has been found to effectively aminate a variety of benzylic and allylic C-H bonds. Allylic C-H bonds of *trans*-olefins appear to be particularly amenable, and notably, aziridination byproducts are not observed under the reaction conditions.

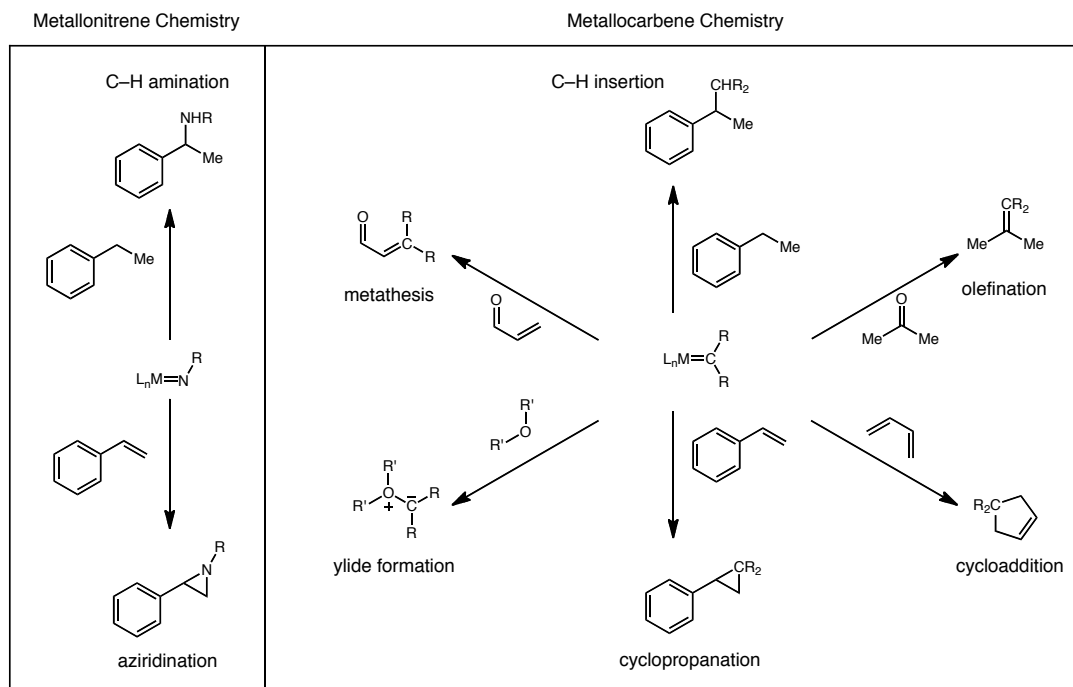
Scheme 1.12. Blakey's Ru(II)-pybox complex for enantioselective C-H amination.

Even with the limited success of chiral Rh(II) catalysis for asymmetric C-H amination, the Du Bois group has remained focused in this area. Recently this group developed a chiral Rh(II)-carboxamidate complex capable of impressive reactivity and selectivity (Scheme 1.13).²⁷ Although there are challenges associated with the use of carboxamidate ligands, many of which render them incompatible with oxidative conditions, the Du Bois group has developed Rh₂(*S*-nap)₄, taking advantage of intramolecular hydrogen-bonding to raise the complex's redox potential. In addition, the electron donating carboxamidate ligands are thought to increase the ability of the rhodium center to back-bond to the π -acidic nitrene ligand, in turn attenuating its reactivity and potentially imparting selectivity on the reaction pathway. The Du Bois group has shown that benzylic C-H bonds are aminated with excellent efficiency, and complementary to Blakey's Ru(II)-pybox system, Rh₂(*S*-nap)₄ is effective for the amination of allylic C-H bonds of *cis*-olefins, again with high selectivity for C-H amination over competitive aziridination.

Scheme 1.13. Du Bois's $\text{Rh}_2(\text{S-nap})_4$ for enantioselective C-H amination.

1.4. Future Directions

The ability to introduce *N*-containing functionality into starting materials with little or no prefunctionalization offers an attractive alternative to classical methods for C-N bond formation, and thus has provided the motivation for the development of metallonitrene mediated transformations such as aziridination and C-H amination. In spite of the obvious potential of these methods, the field of metallonitrene chemistry still remains underdeveloped. This fact becomes glaringly obvious when the reactivity of metallonitrenes is compared to their analogous carbon-based counterparts, metallocarbenes (Figure 1.1).^{24,28}

Figure 1.1. Metallonitrene and metallocarbene chemistries.

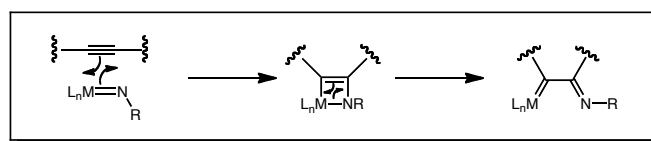
While the reactivity scope of metallonitrenes has remained limited to primarily two reaction types, aziridination and C-H amination, metallocarbenes are known to undergo a multitude of bond forming processes. With this in mind, the development of novel C-N bond forming processes based on the use of reactive metallonitrenes would represent a significant advance within the field, and in turn has provided us the impetus to explore the development of such processes.

1.5. Metallonitrene/Alkyne Metathesis Reaction

At the outset of our studies we were intrigued by the possibility of developing a conceptually novel metallonitrene/alkyne metathesis reaction. In developing this new

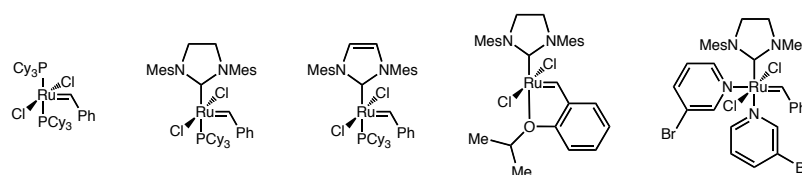
transformation we envisioned a process in which a metal-bound reactive nitrene would undergo a metathesis reaction with an alkyne (Figure 1.2). Such a reaction would mechanistically mirror the key steps of well-established ene/yne metathesis (*vide infra*), but in the present case would yield a new carbon–nitrogen double bond, as well as a reactive metallocarbene species capable of cascading into a variety of secondary transformations.

Figure 1.2. Metallonitrene/alkyne metathesis reaction concept.



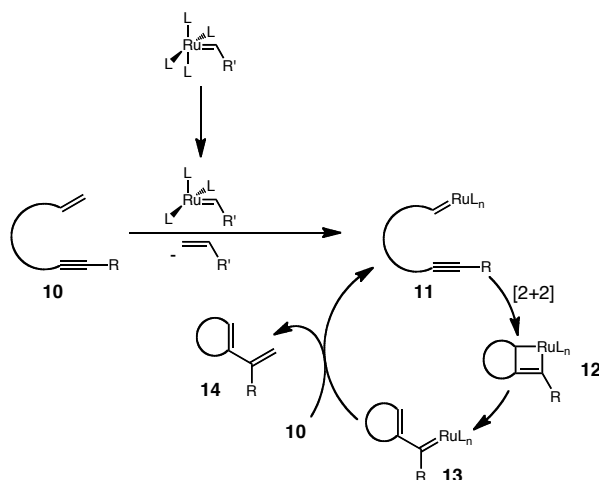
Over the past 30 years ene/yne metathesis has emerged as a powerful method for the construction of 1,3-dienes via the reorganization of an alkene and alkyne.²⁹ It has been shown that a variety of transition metal complexes are capable of catalyzing this type of transformation, with the most widely used being the same Ru(II) based systems used for alkene metathesis (Figure 1.3).

Figure 1.3. Common Ru(II) based catalysts for ene/yne metathesis.



Ene/yne metathesis is considered to proceed through a mechanistic pathway quite similar to its alkene metathesis counterpart.^{29b} Thus, after initial reaction of the metal catalyst with an alkene to generate a metallocarbene intermediate **11**, subsequent [2+2] addition across a tethered alkyne leads to strained metallocyclobutene intermediate **12** (Scheme 1.14). This intermediate can then reorganize to give a new C-C double bond as well as an adjacent metallocarbene, **13**. This intermediate can then continue on the catalytic cycle by engaging a second molecule of starting material **10** to produce 1,3-diene **14**, and regenerate intermediate **11**.

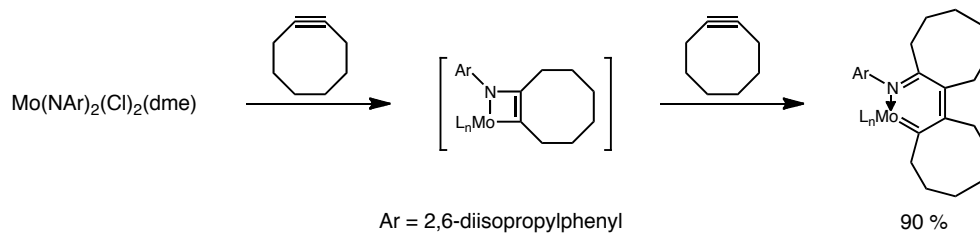
Scheme 1.14. Ene/yne metathesis mechanism.



In addition to this well-established precedent for such a carbon-based metathesis reaction, it is also important to note that Odom and co-workers recently observed such a metathesis using a *stable* molybdenum imido complex and a strained alkyne to in turn generate a *stable* molybdenum alkylidene complex (Scheme 1.15).³⁰ While this literature precedent was encouraging, we felt that in order to identify useful catalysts for our novel transformation it would be important to focus on transition metals that are known to

support *reactive* nitrene and *reactive* carbene ligands.

Scheme 1.15. Odom's stable imido/alkyne metathesis.



Building upon these literature precedents, the following chapters of this thesis will outline the development and application of a novel metallonitrene/alkyne cascade reaction that is based on this metathesis concept. More specifically, the initial discovery and development of this reaction along with reactivity studies designed to elucidate a potential mechanism will be presented. In addition, the application of this methodology towards the synthesis of biologically relevant natural products, and the subsequent studies that have evolved from this endeavor, will be discussed.

References

- (1) Constable, D., J., C.; Dunn, P.J.; Hayler, J. D.; Humphrey, G. R.; Leazer, J. L.; Linderman, R. J.; Lorenz, K.; Manley, J.; Pearlman, B. A.; Wells, A.; Zaks, A.; Zhang, T. *Y. Green Chem.* **2007**, *9*, (5), 411.
- (2) Humphreys, A. *MedAdNews*, **2007**, *13*, (7).
- (3) For reviews see: (a) Muller, P.; Fruit, C. *Chem. Rev.* **2003**, *103*, 2905. (b) Dick, A. R.; Sanford, M. S. *Tetrahedron* **2006**, *62*, 2439. (c) Davies, H. M. L.; Long, M. S. *Angew. Chem. Int. Ed.* **2005**, *44*, 3518.
- (4) Louw, A.; Swart, P.; Allie, F. *Biochem. Pharmacol.* **2000**, *60*, 749.
- (5) Padwa, A.; Murphree, S. S. In *Progress in Heterocyclic Chemistry*; Gribble, G. W., Gilchrist, T. L. Eds.; Elsevier Science; Oxford, 2000; Vol 12 Chapter 4.1, pg 57.
- (6) (a) Ullrich, V. *Top. Curr. Chem.* **1979**, *83*, 68. (b) Hill, C. L.; Schardt, B. C. *J. Am. Chem. Soc.* **1980**, *102*, 6375.
- (7) (a) Breslow, R.; Gellman, S. H. *J. Chem. Soc., Chem. Commun.* **1982**, 1400. (b) Mansuy, D. Mahy, J. -P; Dureault, A.; Bedi, G.; Battioni, P. *J. Chem. Soc., Chem. Commun.* **1984**, 1161.
- (8) Evans, D. A.; Bilodeau, M. T. *J. Org. Chem.* **1991**, *56*, 6744.
- (9) Evans, D. A.; Faul, M. M.; Bilodeau, M. T.; Anderson, B. A.; Barnes, D. M. *J. Am. Chem. Soc.* **1993**, *115*, 5328.
- (10) Li, Z.; Conser, K. R.; Jacobsen, E. N. *J. Am. Chem. Soc.* **1993**, *115*, 5326.
- (11) Dauban, P.; Dodd, R. H. *J. Org. Chem.* **1999**, *64*, 5304.
- (12) (a) Dauban, P.; Dodd, R. H. *Org. Lett.* **2000**, *2*, 2327. (b) Dauban, P.; Sanière, L.; Tarrade, A.; Dodd, R. H. *J. Am. Chem. Soc.* **2001**, *123*, 7707. (c) Duran,

-
- F.; Leman, L.; Ghini, A.; Burton, G.; Dauban, P.; Dodd, R. H. *Org. Lett.* **2002**, *4*, 2481.
- (13) Espino, C. G.; Du Bois, J. *Modern Rhodium-Catalyzed Organic Reactions*; Wiley-VCH: Weinheim, Germany, 2005, p 379.
- (14) Guthikonda, K.; Du Bois, J. *J. Am. Chem. Soc.* **2002**, *124*, 13672.
- (15) (a) Baron, E.; O'Brien, P.; Towers, T. D. *Tetrahedron Lett.* **2002**, *43*, 723. (b) Brase, S.; Gil, C.; Knepper, K.; Zimmerman, V. *Angew. Chem. Int. Ed.* **2005**, *44*, 5188.
- (16) Wehn, P. M.; Du Bois, J. *Angew. Chem. Int. Ed.* **2009**, *48*, 3802.
- (17) Yu, X. -Q.; Huang, J. -S.; Zhou, X. -G.; Che, C. -M. *Org. Lett.* **2000**, *15*, 2233.
- (18) (a) Espino, C. G.; Du Bois, J. *Angew. Chem. Int. Ed.* **2001**, *40*, 598. (b) Espino, C. G.; Wehn, P. M.; Chow, J.; Du Bois, J. *J. Am. Chem. Soc.* **2001**, *123*, 6935.
- (19) For review see: Melendez, R. E.; Lubell, W. D. *Tetrahedron* **2003**, 2581.
- (20) Hinman, A.; Du Bois, J. *J. Am. Chem. Soc.* **2003**, *125*, 11510.
- (21) (a) Espino, C. G.; Fiori, K. W.; Kim, M.; Du Bois, J. *J. Am. Chem. Soc.* **2004**, *126*, 15378. (b) Fiori, K. W.; Du Bois, J. *J. Am. Chem. Soc.* **2007**, *129*, 562.
- (22) (a) Taber, D. F.; Meagley, R. P.; Louey, J. P.; Rheingold, A. L. *Inorg. Chim. Acta* **1995**, *239*, 25. (b) Davies, H. M. L. *Eur. J. Org. Chem.* **1999**, 2459.
- (23) Liang, J. L.; Yuan, S. -X.; Huang, J. -S.; Yu, W. -Y.; Che, C. -M. *Angew. Chem. Int. Ed.* **2002**, *41*, 3465.
- (24) Davies, H. M. L.; Beckwith, R. E. *Chem. Rev.* **2003**, *103*, 2861.
- (25) (a) Yamawaki, M.; Tsutsui, H.; Kitagaki, S.; Anada, M.; Hashimoto, S. *Tetrahedron Lett.* **2002**, *43*, 6561. (b) Fruit, C.; Muller, P. *Helv. Chim. Acta* **2004**, *87*, 1607.
- (26) Milczek, E.; Boudet, N.; Blakey, S. *Angew. Chem. Int. Ed.* **2008**, *47*, 6825.

-
- (27) Zalatan, D. N.; Du Bois, J. J. *Am. Chem. Soc.* **2008**, *130*, 9220.
- (28) Doyle, M. P.; Forbes, D. C. *Chem. Rev.* **1998**, *98*, 911.
- (29) (a) Diver, S. T.; Giessert, A. J. *Chem. Rev.* **2004**, *104*, 1317. (b) Mori, M. *Top. Organomet. Chem.* **1998**, *1*, 133. (c) Hansen, E. C.; Lee, D. *Acc. Chem. Res.* **2006**, *39*, (8), 509.
- (30) Lokare, K. S.; Ciszewski, J. T.; Odom, A. L. *Organometallics* **2004**, *23*, (23), 5386.

Chapter 2:

The Discovery and Development of a Metallonitrene/Alkyne Cascade Reaction

2.1. Design of a Metallonitrene/Alkyne Metathesis Reaction

2.1.1. Potential Catalysts

In designing this novel metallonitrene/alkyne metathesis reaction, we felt that the examination of catalysts that are known to support reactive nitrene and carbene ligands would be essential. In addition to this, based on our proposed mechanistic hypothesis, it would also be important to examine metal complexes containing a vacant coordination site adjacent to the initially formed metallonitrene. This is based on the well-documented necessity for such a site within effective ene/yne metathesis catalysts.¹ Previous work in this field has established that this site is needed for both initial π -coordination and subsequent [2+2] cycloaddition across the alkyne.^{1b} Therefore, if our new transformation is going to work through a similar mechanism, this vacant coordination site will also be necessary.

With these guiding principles for catalyst selection established, we were immediately drawn to a small group of metal complexes (Figure 2.1). First, based on our mechanistic hypothesis and our goal of developing a new metathesis reaction, we felt that examination of well-established Ru(II)-based metathesis catalysts would be useful. While such complexes are known to catalyze the analogous carbon-based ene/yne metathesis reaction, to date there is no precedent for their use within the field of metallonitrene chemistry, potentially due to the oxidative sensitivity of these complexes and their phosphine ligands.² Second, we were attracted to the Ru(II)-pybox catalyst which the Blakey group has utilized for enantioselective C-H amination reactions.³ In

addition to this precedent, a review of the literature reveals that there are also examples for the use of similar Ru(II)-pybox complexes for metallocarbene facilitated cyclopropanation reactions.⁴ In addition to this, it was thought at the time of these studies that following dissociation of ethylene in solution, halide abstraction from the Ru(II)-pybox furnishes a cationic catalyst that now possesses two vacant coordination sites. With both of our initial requirements met, we were particularly attracted to this catalyst system.

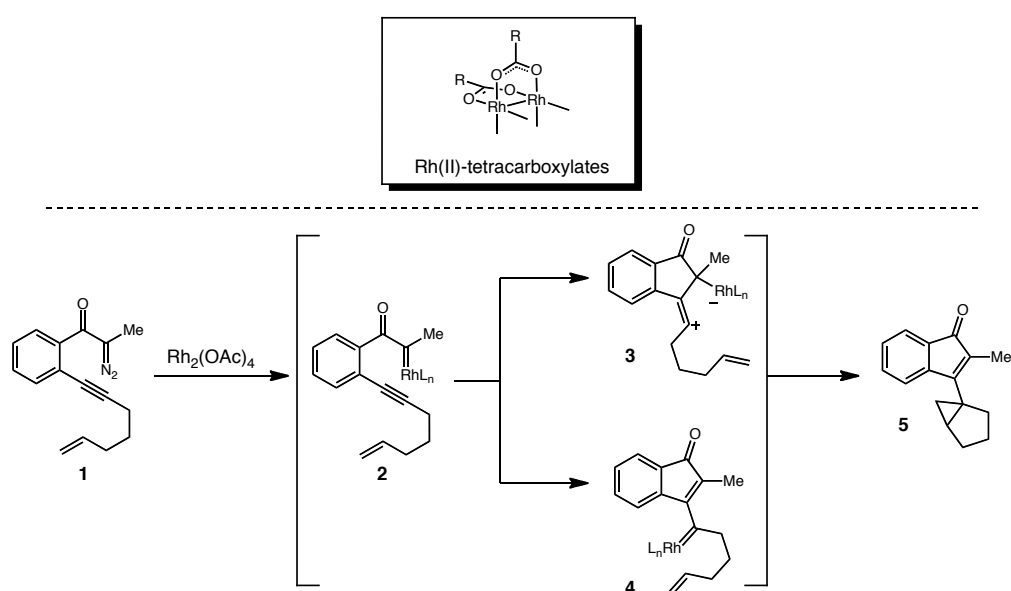
Figure 2.1. Potential catalysts for a new metallonitrene/alkyne metathesis reaction.



In addition to catalysts based around a ruthenium metal center, the last family of catalysts to attract our attention were the dirhodium(II)-tetracarboxylates. As outlined in Chapter 1, there is significant precedent for the use of these catalysts in the fields of both reactive nitrene and carbene chemistry.⁵ Also, it is important to note that while there is computational evidence suggesting that these systems contain only one open coordination site at each rhodium center,^{6a} work by the groups of Padwa and Hoyer have shown that these complexes are able to catalyze the analogous metallocarbene/alkyne cascade reactions (Scheme 2.1).⁷ For example, when alkynyl α -diazo ketone **1** is exposed to catalytic amounts of Rh₂(OAc)₄, the resulting metallocarbene **2** undergoes a metathesis-type transformation across the tethered alkyne.^{7b} While there is some uncertainty as to

the formation of vinyl cation **3** or metallocarbene **4**, it has been shown that the new reactive center at the distal position of the alkyne may be trapped by a variety of tethered functionalities.^{7a} In this case, the new reactive intermediate is trapped by a tethered olefin, terminating the cascade process through a cyclopropanation event and leading to the formation of **5**.

Scheme 2.1. Rh(II)-catalyzed metallocarbene/alkyne cascade reaction.

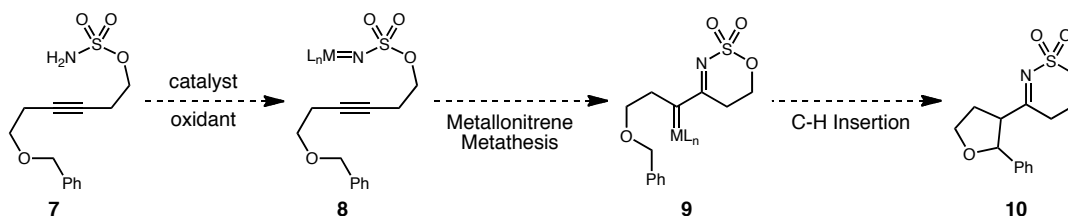
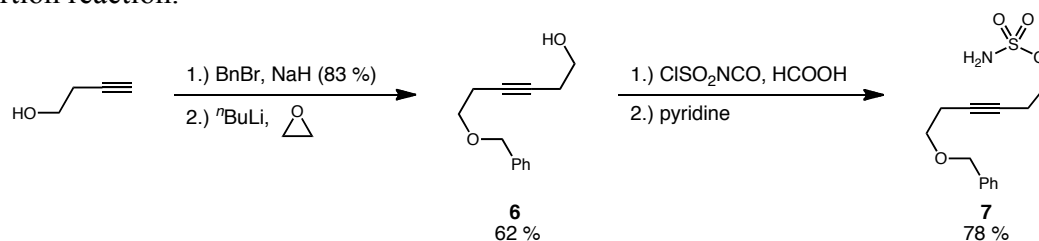


2.1.2. Substrate Design

In order to examine the feasibility of this novel metallonitrene metathesis reaction, we first needed to develop a substrate with a number of geometric and electronic prerequisites. Specifically, we needed to develop a substrate that places a known reactive nitrene precursor on one side of an alkyne, and on the opposite side, a trap for the potentially newly formed reactive metallocarbene. This led us to the

development of sulfamate ester **7** (Scheme 2.2). This substrate is easily prepared in three steps from commercially available 3-butyn-1-ol. Thus, deprotonation and benzylation with NaH and BnBr, followed by deprotonation of the resulting terminal alkyne with ⁿBuLi at -78 °C and addition to oxirane furnished homopropargylic alcohol **6** in 62 % yield.⁸ This alcohol was then smoothly converted to sulfamate ester **7** under standard conditions developed by Du Bois and co-workers in 78 % yield.⁹ In this process sulfamoyl chloride is first generated by reaction of chlorosulfonyl isocyanate and formic acid while evolving CO₂ and CO, addition of alcohol **6** in pyridine then leads to desired sulfamate ester **7**. With this substrate the nitrogen atom of a sulfamate ester, a known metallonitrene precursor, is placed six atoms away from an alkyne. On the opposite side of this alkyne is a trap for the new metallocarbene. In designing this substrate we postulated that the cascade process would be terminated through C-H insertion of α -imino metallocarbene species **9** into the doubly activated ethereal and benzylic C-H bonds of the tethered benzyl ether, in turn leading to the formation of *N*-sulfonyl imine **10**.

Scheme 2.2. Substrate design for a tandem metallonitrene/alkyne metathesis/C-H insertion reaction.



2.2. Reaction Discovery and Initial Studies

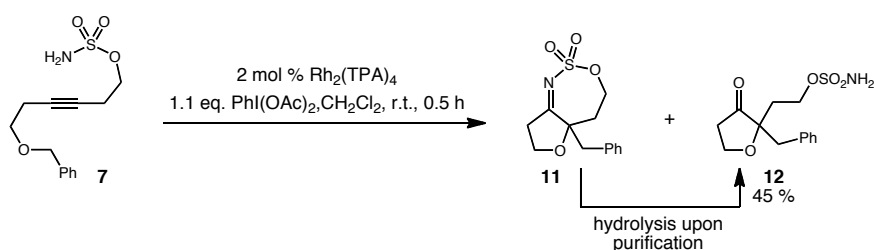
2.2.1. Reaction Discovery

With both catalysts and test substrate **7** in hand, we next set out to examine the potential for the development of a new metallonitrene/alkyne metathesis reaction. To commence our studies we first examined the use of Ru(II)-based metathesis catalysts developed by Grubbs and coworkers.¹⁰ However, when sulfamate ester **7** was exposed to 5 mol % Grubbs II catalyst and varying amounts of PhI(OAc)₂ in CH₂Cl₂, benzene, or toluene at ambient and elevated temperatures, no reaction was observed and starting sulfamate ester **7** was returned in nearly quantitative yield. While somewhat uncertain, this inactivity could be attributed to the oxidative sensitivity of this complex and its ligands.² Next we pursued the use of the same Ru(II)-pybox complex that the Blakey group showed to be effective for enantioselective C-H amination.³ Again, while varying

amounts of $\text{PhI}(\text{OAc})_2$ and multiple reaction solvents were examined at a range of temperatures, no reaction was observed. While this result is somewhat surprising (*vide infra*), later computational studies of this complex suggest that the previously mentioned metallonitrene facilitated C-H amination reactions are in fact proceeding through a radical based mechanism, inconsistent with our mechanistic hypothesis.¹¹

With these results established we then turned our attention to the Rh(II)-tetracarboxylate family of catalysts. To our delight, when sulfamate ester **7** was exposed to catalytic $\text{Rh}_2(\text{TPA})_4$ and stoichiometric $\text{PhI}(\text{OAc})_2$ in CH_2Cl_2 at ambient temperature, we observed complete consumption of starting material within just 30 minutes (Scheme 2.3). While TLC and crude ^1H NMR indicated that a single compound, *N*-sulfonyl imine **11**, was being produced as the major product, upon purification by flash column chromatography with silica gel, a different product, ketone **12**, was isolated as the major product.

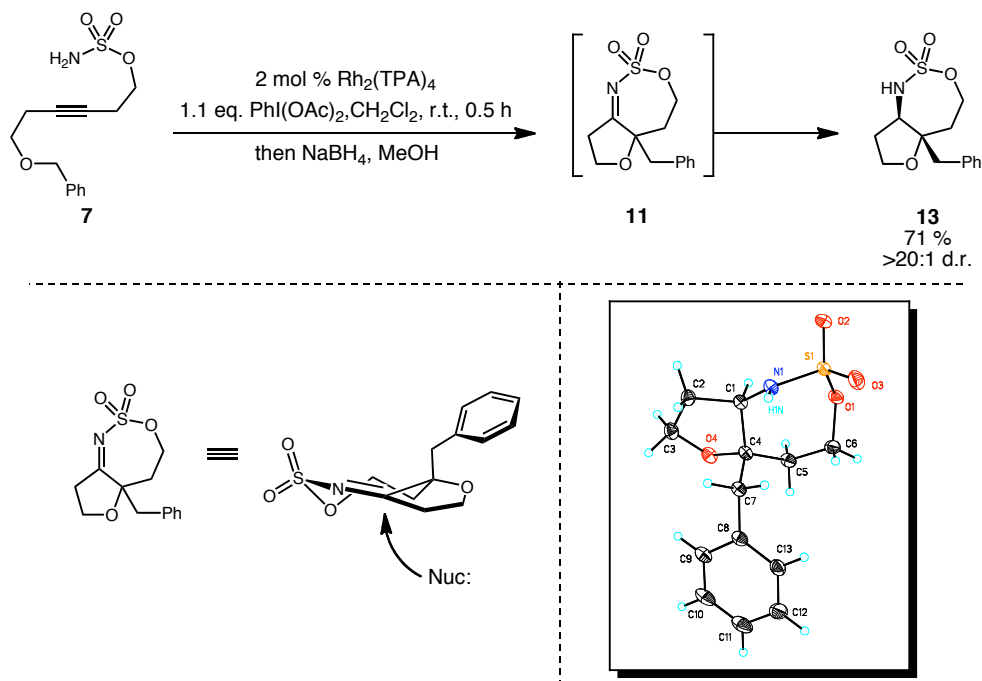
Scheme 2.3. Rh(II)-catalyzed metallonitrene/alkyne cascade reaction discovery.



Realizing that ketone **12** was in fact coming from the hydrolysis of *N*-sulfonyl imine **11** motivated us to adopt a reductive work-up. Thus, submitting sulfamate ester **7** to 2 mol % $\text{Rh}_2(\text{TPA})_4$ and 1.1 equivalents of $\text{PhI}(\text{OAc})_2$ in CH_2Cl_2 at ambient temperature, followed by *in situ* reduction with NaBH_4 and MeOH led to an isolated

yield of oxathiazepane **13** in 71 % with a diastereomeric ratio of >20:1 as determined by ^1H NMR analysis (Scheme 2.4). The facial selectivity for the addition of NaBH_4 to *N*-sulfonyl imine **11** may be attributed to the steric congestion that is provided by the adjacent oxygenated center. Due to the rigidity of this imine's 7,5-bicyclic ring system, the migrating benzyl group is forced into a pseudo-axial position. This benzyl group effectively blocks one face of the imine and in turn allows for the selective addition of nucleophiles to the opposite face. While all of the obtained spectroscopic data were consistent with the formation of oxathiazepane **13**, X-ray crystallography provided unambiguous confirmation of both connectivity as well as relative stereochemistry for this cyclization adduct. While the production of oxathiazepane **13** was initially unexpected, it is important to note that in this single transformation new C-N, C-C, and C-O bonds, as well as adjacent stereocenters have all been generated, and overall, a readily accessible substrate has been transformed into a densely functionalized *N*-containing molecule.

Scheme 2.4. Cascade reaction followed by *in situ* reduction provides stable oxathiazepane **13**.

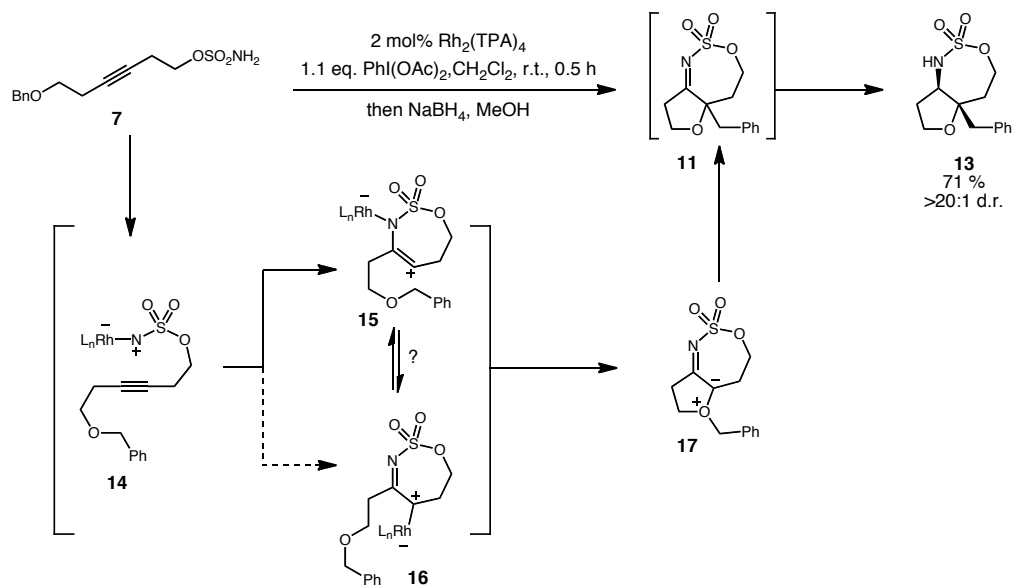


2.2.2. Control Experiments and Mechanistic Hypothesis

While there is no question that significant molecular complexity has been generated in this transformation, initially it was unclear as to how this product was being produced. Sulfamate ester **7** was designed with the thought that initial cyclization would lead to the corresponding six-membered α -imino metallocarbene **9** (Scheme 2.2). This new reactive metallocarbene was then expected to undergo a C-H insertion reaction to generate *N*-sulfonyl imine **10**. However, the formation of seven-membered oxathiazepane **13** clearly indicates that an alternate cascade process is taking place. Cyclization of the sulfamate ester onto the distal carbon of the alkyne precludes a [2+2]

metathesis mechanism. Taking this into account, we propose that the tethered alkyne attacks the initially formed electrophilic rhodium nitrene **14** to in turn generate a transient vinyl cation **15** (*vide infra*) (Scheme 2.5). This species was initially speculated to be in equilibrium with isomeric α -imino metallocarbene **16**. However, based on reactivity studies (*vide infra*) it is thought that this intermediate collapses directly to oxonium ylide **17**, without migration of the metal center. Subsequent rearrangement of this species produces *N*-sulfonyl imine **11** and diastereoselective reduction furnishes the stable oxathiazepane product **13**.

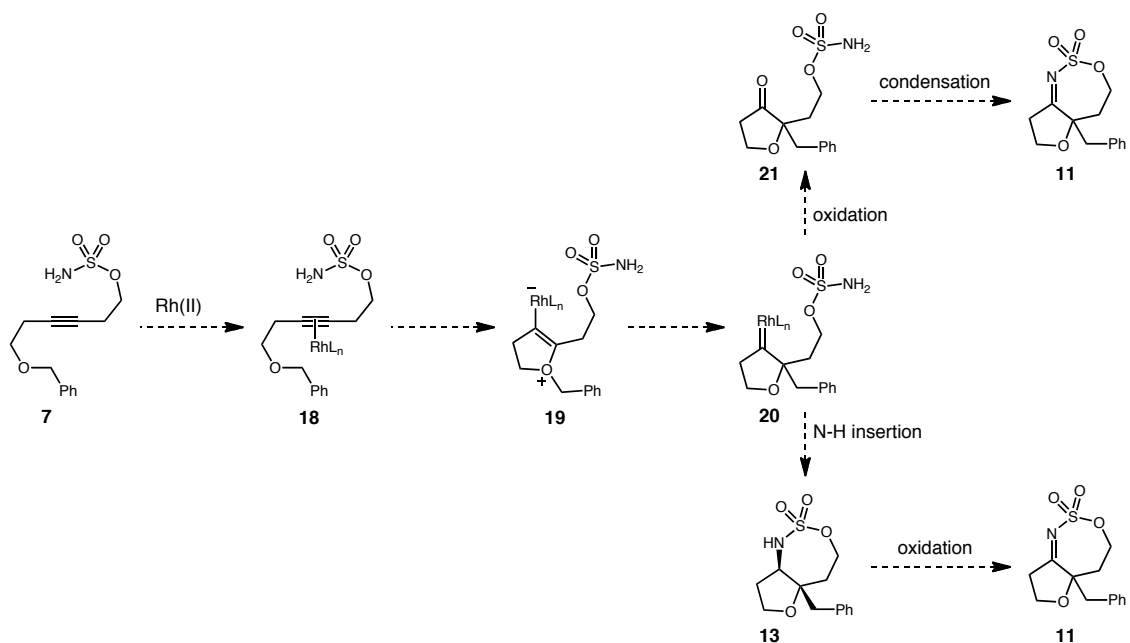
Scheme 2.5. Metallonitrene/alkyne cascade reaction mechanism.



It is also possible to envision a mechanism that does not involve the formation of a reactive metallonitrene species (Scheme 2.6). In this mechanism the rhodium catalyst acts as a Lewis acid,¹² coordinating to alkyne **7** and activating it for addition from a tethered nucleophile, mechanistically similar to Au(I)-catalyzed alkynyl isomerizations.¹³

Rearrangement of the intermediate resulting from attack of the tethered benzyl ether (**19**) would then lead to the formation of carbene species **20**. This intermediate may undergo N-H insertion to give oxathiazepane **13** which is then oxidized to the same *N*-sulfonyl imine **11**. Alternately, this same carbene intermediate **20** could undergo oxidation to generate ketone **21**. This ketone may then undergo condensation with the tethered sulfamate ester moiety to give *N*-sulfonyl imine **11** once again.

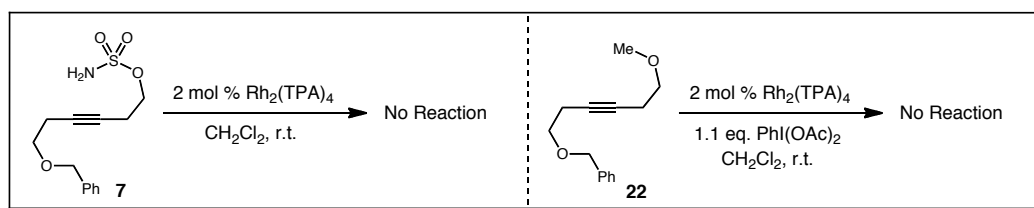
Scheme 2.6. π -Activation as an alternate mechanism for the formation of *N*-sulfonyl imine **11**.



In an attempt to distinguish between these potential mechanisms we have conducted a number of control experiments (Scheme 2.7). We have found that when sulfamate ester **7** is exposed to a Rh(II) catalyst in the absence of an oxidant no reaction is observed, and starting material is recovered cleanly after 24 hours. Knowing that Rh(II)-tetracarboxylates may undergo oxidation to their corresponding electron deficient

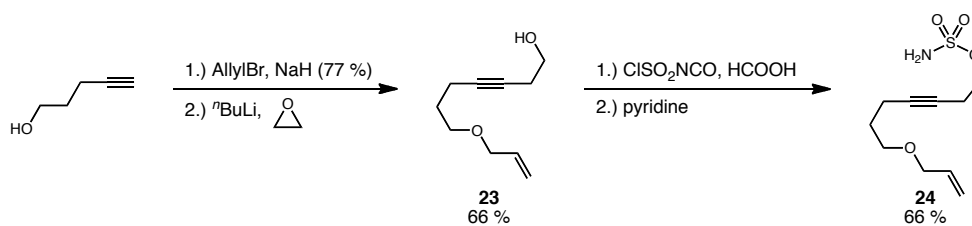
Rh(II/III) dimer,¹⁴ we also examined the combination of Rh(II) catalyst and hypervalent iodine oxidant with a similar alkyne. Thus, when methyl ether **22** was exposed to both Rh₂(TPA)₄ and PhI(OAc)₂, we still observe no reaction. Observing that reaction only takes place when known conditions for the generation of a reactive metallonitrene intermediate are employed strongly suggests that the cascade process is in fact initiated by metallonitrene formation, and in turn not by π -activation of the alkyne followed by nucleophilic attack.

Scheme 2.7. Control experiments suggest cascade reaction is initiated by metallonitrene formation.



2.2.3. Metallonitrene/Alkyne Cascade Reaction Optimization

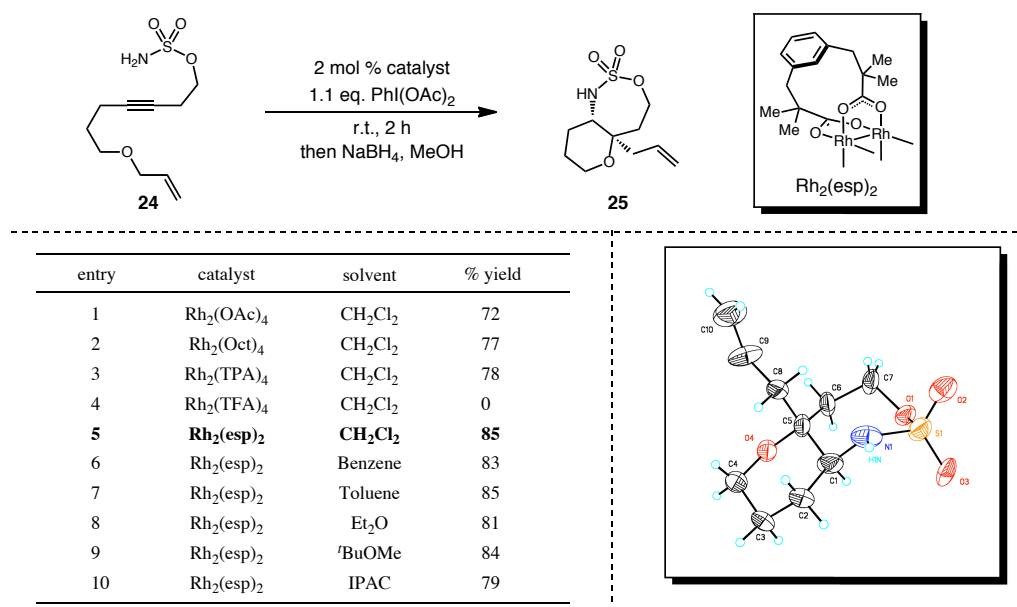
After the initial discovery of this novel cascade process an optimization was undertaken to examine what role both the structure of the catalyst and solvent play on reaction efficiency. We chose to perform this optimization study using substrate **24**, synthesized in an analogous manner to sulfamate ester **7** (Figure 2.8). Thus, deprotonation of 4-pentyn-1-ol with NaH and subsequent allylation was followed by deprotonation of the resulting terminal alkyne with ⁿBuLi at -78 °C and addition of oxirane, furnishing the desired homopropargylic alcohol **23** in 66 % yield.⁸ Alcohol **23** was then converted to sulfamate ester **24** in 66 % yield.

Scheme 2.8. Synthesis of allyl ether tethered sulfamate ester **24**.

We have found that allyl ether tethered sulfamate ester **24** may undergo cyclization to give oxathiazepane **25** in good yield and diastereoselectivity (10:1 determined by ^1H NMR) under a variety of conditions, with the connectivity and relative stereochemistry of oxathiazepane **25** confirmed by X-ray crystallography (Figure 2.2). The use of substrate **24** confirms that allyl groups may be transferred in this cascade process, and also illustrates that tether lengths which result in the formation of six-membered rings are useful for efficient cascade termination. While the initial goal of this study was to determine the optimal conditions for this new reaction, in reality we discovered that this process is quite versatile, and that a range of catalysts and common organic solvents may be utilized. For example, sterically unencumbered $\text{Rh}_2(\text{OAc})_4$, as well as its more soluble counterpart $\text{Rh}_2(\text{oct})_4$, produced the desired bicyclic amine **25** in good yields (Entries 1, 2). Likewise, sterically demanding $\text{Rh}_2(\text{TPA})_4$ led to oxathiazepane **25** in 78 % yield (Entry 3). The only catalyst that did not produce any of the desired oxathiazepane product was the highly electron deficient $\text{Rh}_2(\text{TFA})_4$ (Entry 4). The highest yields were realized when Du Bois' bridged carboxylate catalyst, $\text{Rh}_2(\text{esp})_2$,¹⁵ was utilized (Entry 5). In addition to this catalyst diversity, a range of common organic solvents may be utilized. For example, comparable yields were

obtained with aromatic solvents benzene and toluene (Entries 6 and 7) as well as ethereal solvents Et₂O and ^tBuOMe (Entries 8 and 9). Highest yields were produced when CH₂Cl₂ was employed as a reaction medium. Additionally, while it has been shown in many instances that metallonitrene facilitated transformations benefit from certain additives such as MgO, K₂CO₃, or mol. sieves, we have not found this to be the case for our metallonitrene/alkyne cascade reaction.¹⁶ Based on these studies we have adopted Rh₂(esp)₂ as our catalyst of choice and CH₂Cl₂ as solvent for our future studies (Entry 5).

Figure 2.2. Metallonitrene/alkyne cascade reaction optimization and versatility.

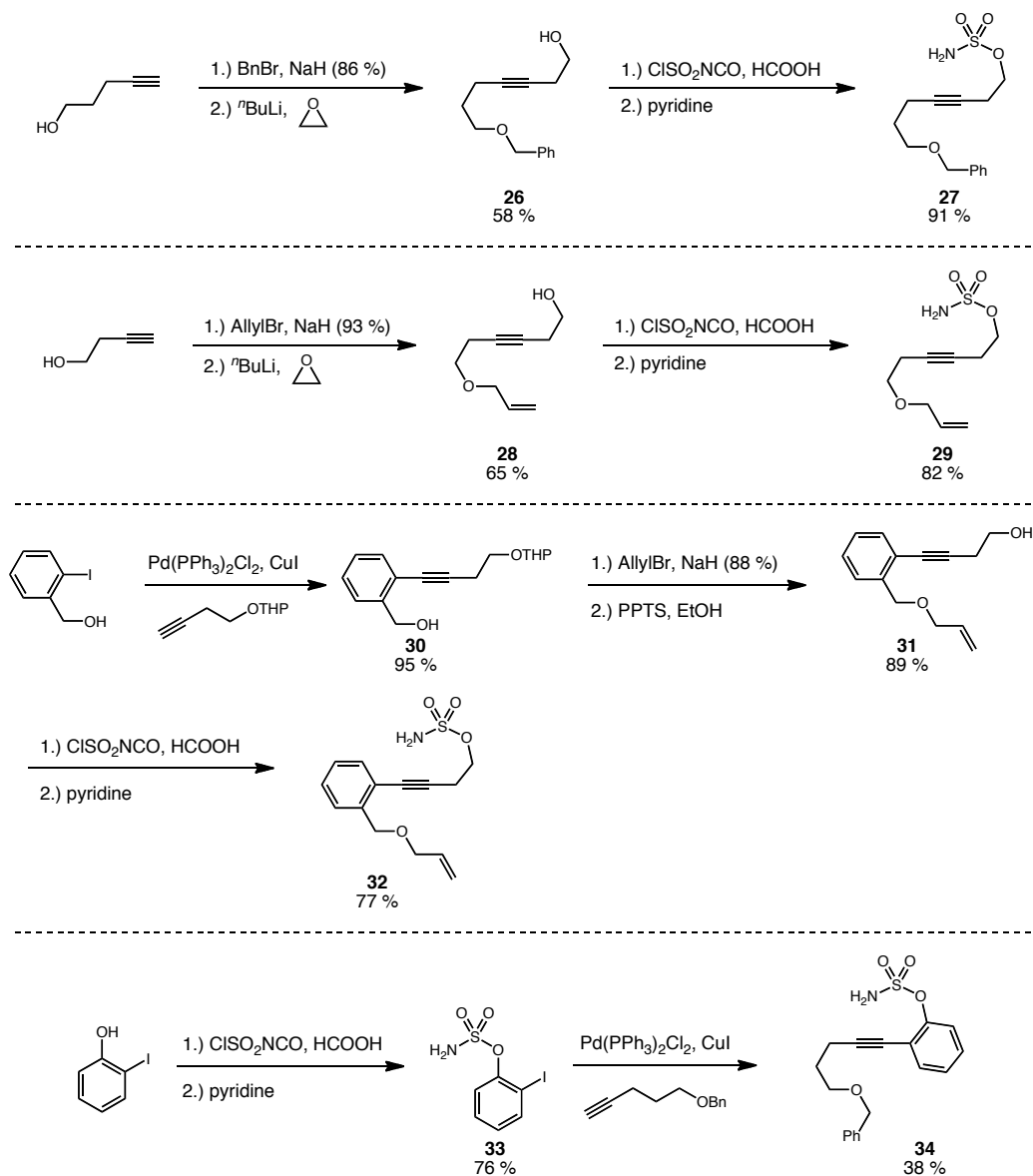


2.2.4. Substrate Scope for Metallonitrene/Alkyne Cascade Reaction Termination Through Ylide Formation/Group Migration

In order to examine the scope of this new reaction we needed to produce a range of potential cyclization precursors. Thus, similar to sulfamate esters **7** and **24**,

compounds **27** and **29** were produced in three-step protocols as outlined in Scheme 2.9. Aromatic sulfamate esters **32** and **34** required slightly different synthetic routes, but both could be readily assembled through a Sonagashira coupling strategy. The alcohol precursor of **32** was produced following Sonagashira coupling of 2-iodo-benzyl alcohol and THP-protected 3-butyn-1-ol using Pd(PPh₃)₂Cl₂ and CuI followed by allylation of the resulting benzyl alcohol with NaH and AllylBr in 89 % yield. THP removal with PPTS in EtOH provided alcohol **31** which was then cleanly converted to sulfamate ester **32** in 77 % yield. Sulfamate ester **34** was produced through a similar strategy but alternate reaction order. Thus, conversion of 2-iodo phenol to aryl sulfamate ester **33** was carried out under slightly altered reaction conditions as described by Fruit and Müller for use with phenolic substrates in 76 % yield.¹⁷ While a review of the literature showed no precedent for the use of Sonagashira coupling in the presence of a sulfamate ester, we were still motivated to attempt such a transformation based on the incredible selectivity and functional group tolerance displayed by these reactions.¹⁸ Aromatic sulfamate ester **33** underwent Sonagashira coupling with benzyl-protected 4-pentyn-1-ol with Pd(PPh₃)₂Cl₂ and CuI in 38 % yield. While low yielding, the production sulfamate ester **34** in 38 % yield was sufficient for our purposes and no optimization was undertaken. With this group of substrates produced, we next turned our attention to examining the scope to this new transformation.

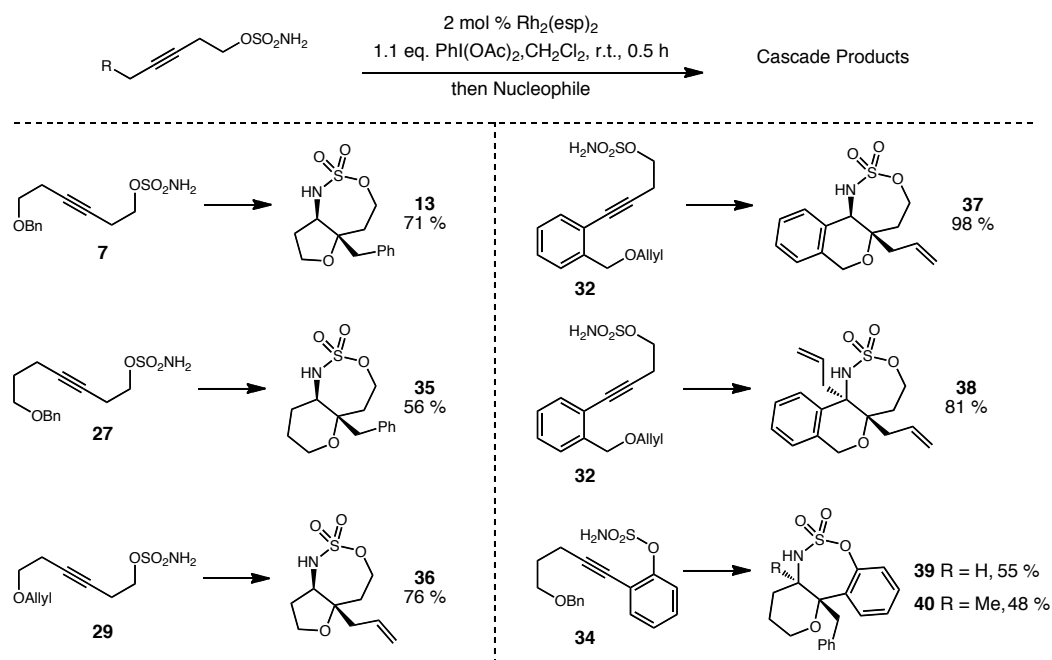
Scheme 2.9. Synthesis of alkyl and aryl substituted alkynyl sulfamate esters for substrate scope examination.



We have found that this intramolecular metallonitrene/alkyne cascade reaction is effective for the cyclization of a variety of sulfamate esters derived from homopropargylic alcohols (Scheme 2.10).¹⁹ Both benzyl and allyl units may be cleanly transferred in this cascade process via oxonium ylide formation and [1,2] or [2,3] group migrations (**13**, **36**). In addition, we have found that tether lengths which result in both

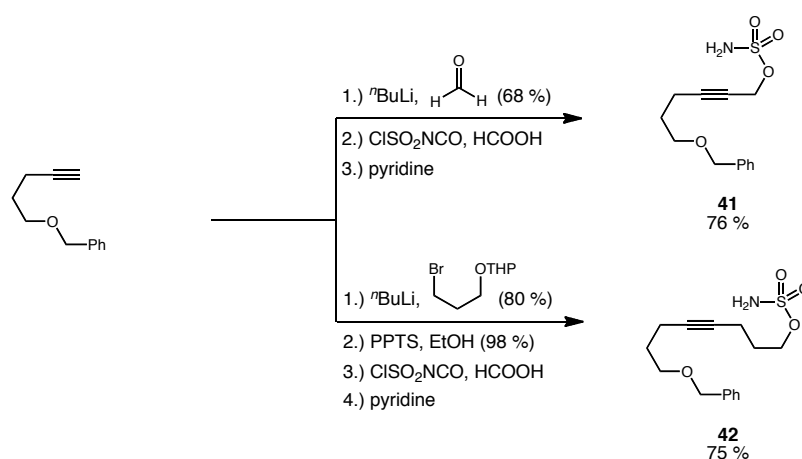
7,6 and 7,5 bicyclic ring systems are amenable (**35**, **13**). We have shown that alkyl as well as aryl substituents are tolerated at either terminus of the alkyne (**37**, **13**), and to further increase molecular complexity, the *N*-sulfonyl imine generated upon cyclization may also undergo highly diastereoselective additions by Grignard reagents *in situ* (**38**, **40**), with the relative stereochemistry of **40** confirmed by X-ray crystallography (see experimental section for details). The facial selectivity for the addition of nucleophiles to these *N*-sulfonyl imines may be attributed to the steric congestion that is provided by the migrating benzyl or allyl groups, similar to the reduction of **11** (Figure 2.2). This in turn allows for the construction of highly congested bicyclic systems containing adjacent quaternary amino-oxygenated stereocenters in a single transformation from simple starting materials.

Scheme 2.10. Substrate scope for intramolecular ylide formation/group migration termination.



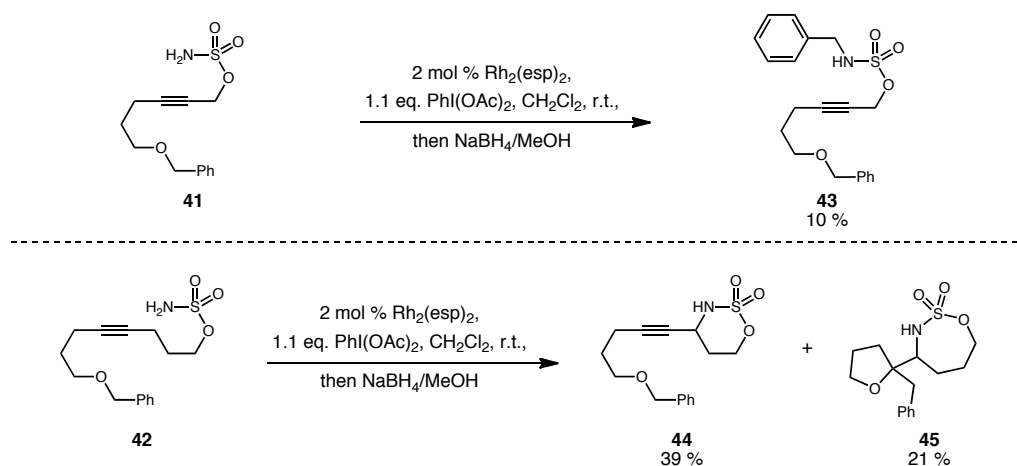
In addition to these substrates we were also interested in examining what effect the tether length between the alkyne and sulfamate ester moiety had on this transformation. Thus, sulfamate esters **41** and **42**, containing one and three carbon units between the sulfamate ester and alkyne were produced (Scheme 2.11). The alcohol precursor to sulfamate ester **41** was constructed from benzylated 4-pentyn-1-ol following deprotonation with *n*BuLi at -78 °C and addition to paraformaldehyde in 68 % yield. The resulting propargylic alcohol was then converted to sulfamate ester **41** under standard conditions in 76 % yield. Additionally, sulfamate ester **42**, containing a three carbon tether between the sulfamate ester and alkyne, was constructed from the same benzylated 4-pentyn-1-ol following deprotonation with *n*BuLi at -78 °C and addition to THP-protected 1-bromo-propane-3-ol in 80 % yield. Subsequent removal of the THP protecting group was then followed by conversion of the resulting alcohol to sulfamate ester **42** in 75 % yield.

Scheme 2.11. Synthesis of sulfamate esters with alternate tether lengths.



Interestingly, when sulfamate ester **41** was exposed to our general reaction conditions we did not observe formation of the expected six-membered cyclization adduct (Scheme 2.12). Instead, due to the geometric constraints associated with this substrate's shortened tether length, we only observe products arising from intermolecular C-H amination. For example, compound **43**, which results from the insertion **41** into the benzylic and ethereal position of a second molecule of **41** followed by *in situ* reduction, is isolated in 10 % yield. Also, when sulfamate ester **42**, now with a three-carbon tether, is exposed to the same reaction conditions we isolate a mixture of intramolecular C-H amination product **44** in 39 % as well as the cyclization adduct resulting from addition of the reactive metallonitrene onto the proximal carbon of the alkyne, **45**, in 21 % yield. While interesting, these results suggest that a two-carbon linker between the sulfamate ester and alkyne is essential for efficient cyclization.

Scheme 2.12. Examination of sulfamate esters with alternate tether lengths.



At the outset of these studies we were intrigued by the development of a novel metallonitrene/alkyne metathesis reaction as a way to produce *N*-containing molecules in

a highly concise manner. While our initial mechanistic hypothesis may not have been accurate, based on this metallonitrene/alkyne metathesis concept we have in fact been successful in developing a novel metallonitrene facilitated cascade reaction. These studies have successfully established that this new metallonitrene/alkyne cascade reaction is able to construct multiple bonds and stereocenters in a single transformation, and thus allows for the construction of a diverse series of congested bicyclic systems. Importantly, all of this is done from remarkably simple starting materials and commercially available reagents.

While cascade termination through ylide formation/group migration is significant, we felt that to further develop this novel transformation into a synthetically useful process it would be crucial to implement new methods for terminating this cascade process, and in turn motivated our subsequent research efforts.

2.3. Alternate Cascade Terminations and Mechanistic Insight

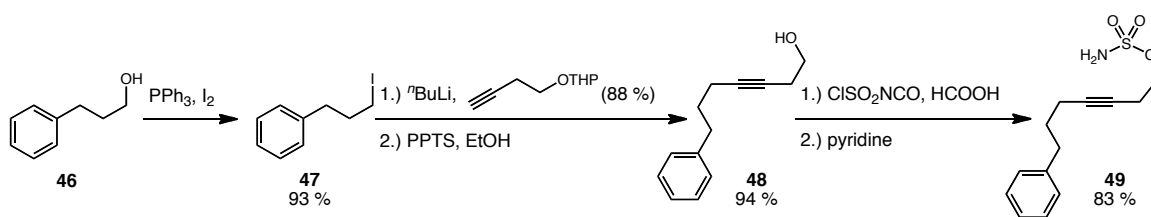
2.3.1. Reactivity Studies and the Discovery of Metallonitrene/Alkyne Cascade Reaction Termination Through Friedel-Crafts Reaction

In further developing this reaction we felt the true power of this cascade process would lie beyond the simple amination of an alkyne, but instead in the ability of the vinyl cation/metallocarbene intermediate (**15/16**, Scheme 2.5) to cascade into a diverse range of C–C, C–O and C–N bond forming reactions. To harness this power, we would need to gain a better understanding of the reactive intermediates at play throughout this process

so that we may determine how best to take advantage of their reactivity and this transformation's potential.

To probe the nature of the reactive intermediate we first needed to develop a substrate that would allow us to potentially differentiate between the two initially proposed reactive intermediates, vinyl cation **15** and α -imino metallocarbene **16** (Scheme 2.5). With this in mind we produced sulfamate ester **49** in a four-step sequence outlined in Scheme 2.13. Commercially available alcohol **46** was first converted to its corresponding primary iodide in 93 % yield with PPh_3 and I_2 . This alkyl iodide then underwent $\text{S}_{\text{N}}2$ displacement with the lithiate formed via deprotonation of THP-protected 3-butyne-1-ol with $n\text{BuLi}$ at $-78\text{ }^\circ\text{C}$ in 88 % yield. Removal of the THP protecting group with PPTS in EtOH was followed by conversion of the resulting alcohol to sulfamate ester **49** under standard reaction conditions in 83 % yield.

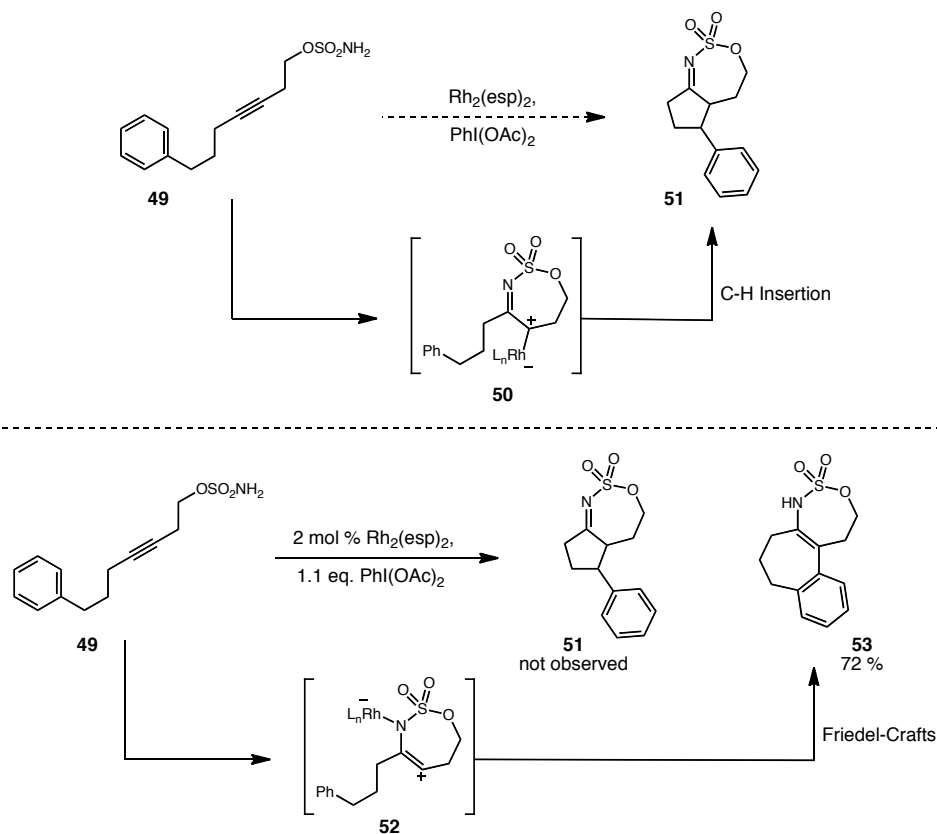
Scheme 2.13. Synthesis of aromatic tethered alkynyl sulfamate ester **49**.



Substrate **49**, containing a simple aryl group tethered onto an alkyne, was designed with the thought that if the α -imino metallocarbene intermediate **50** is produced, we expect the cascade process to be terminated through a facile C-H insertion into the tether's benzylic position, in turn leading to the formation of *N*-sulfonyl imine **51** (Scheme 2.14). However, when sulfamate ester **49** was exposed to our general reaction

conditions we do not observe the expected C-H insertion product **51**, but instead, β -amino styrene compound **53** is isolated in 72 % yield.²⁰

Scheme 2.14. Reactivity studies suggest vinyl cation intermediate.

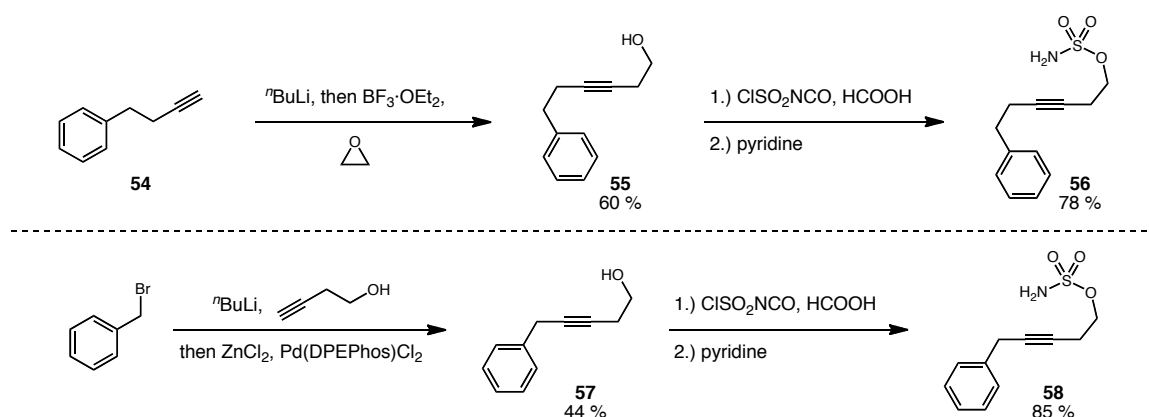


Observing that no products typical of reactive metallocarbene intermediates, such as C-H insertion, aryl cyclopropanation, or β -hydride elimination, are formed in this cascade process strongly suggests that the reactive intermediate is more accurately represented as a vinyl cation intermediate (**52**), with **53** being formed via an electrophilic aromatic substitution pathway.

2.3.2. Substrate Scope for Cascade Termination Through Friedel-Crafts Reaction

Inspired by this potentially powerful reactive intermediate, we next underwent a study of other possible aromatic traps. Cyclization precursor **56** was constructed from commercially available alkyne **54** following deprotonation with $n\text{BuLi}$, and $\text{BF}_3 \cdot \text{OEt}_2$ facilitated opening of oxirane (Scheme 2.15). Subsequent conversion of the resulting alcohol **55** to sulfamate ester **56** under standard conditions then went smoothly in 78 % yield. The homopropargylic alcohol **57** needed to access sulfamate ester **58**, with a shortened tether length, was produced through a modified Negishi coupling of 3-butyne-1-ol and BnBr with $\text{Pd}(\text{DPEPhos})\text{Cl}_2$ as described by Negishi himself.²¹ Subsequent conversion of alcohol **57** to sulfamate ester **58** went smoothly in 85 % yield.

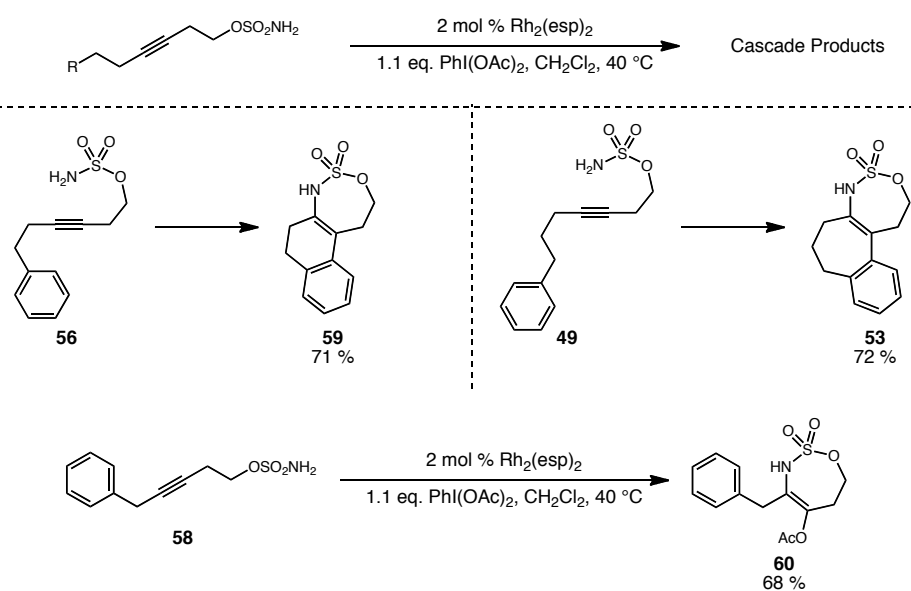
Scheme 2.15. Synthesis of simple aromatic tethered alkynyl sulfamate esters **56** and **58**.



With these alkynyl sulfamate esters we have shown that tether lengths which result in the formation of both six- and seven-membered β -amino styrene systems are useful for efficient termination of this cascade process (Scheme 2.16, **59** and **53**).

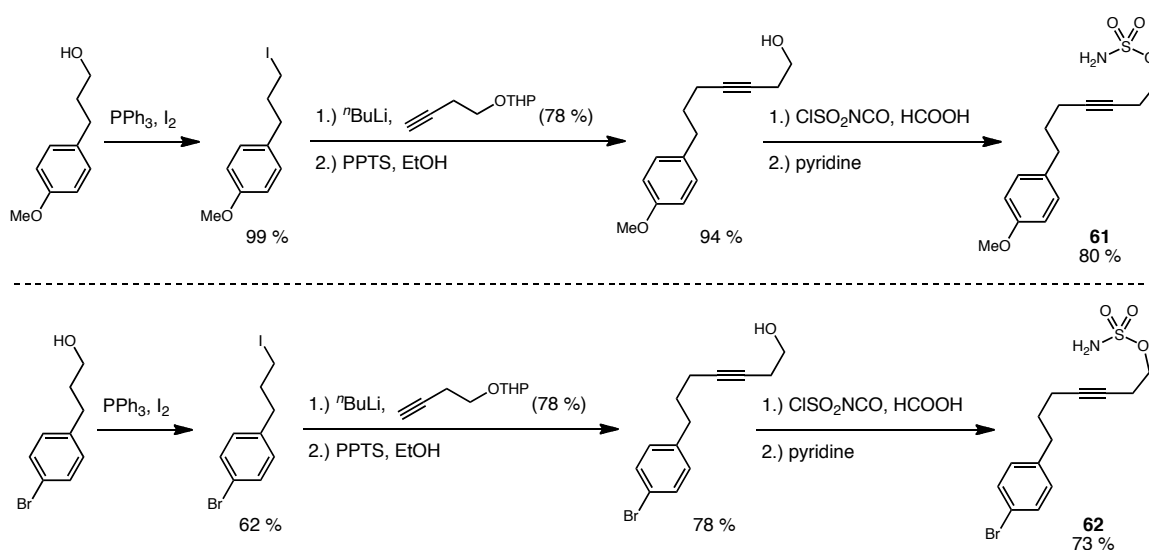
However, when this tether length is shortened by a single carbon unit (**58**), due to geometric constraints we do not observe the expected five-membered ring product. Instead, the product resulting from intermolecular trapping of the reactive intermediate with acetic acid, the byproduct of $\text{PhI}(\text{OAc})_2$, is isolated. Amino acetoxylation product **60** showed a propensity to hydrolyze upon purification, but it was found that column chromatography under acidic conditions (1 % HOAc in 2:1 hexanes/EtOAc) allowed for the successful isolation of **60** in 68 % yield. This intermolecular trapping of the reactive intermediate results in an efficient amino acetoxylation reaction, and provides the first example for the intermolecular termination of this new cascade process. In addition, this finding is consistent with the proposed vinyl cation intermediate, and suggests that a variety of other nucleophiles may be used to terminate this cascade process. However, these studies have yet to be undertaken, and fall outside the scope of this dissertation.

Scheme 2.16. Effect of tether length on Friedel-Crafts cascade termination.



In addition to electron-neutral substrates, we have also examined the effect of electronically biased systems. Thus, electron-rich and electron-poor aromatic substrates (**61** and **62**) were accessed in a similar manner to substrate **49**, as outlined in Scheme 2.17.

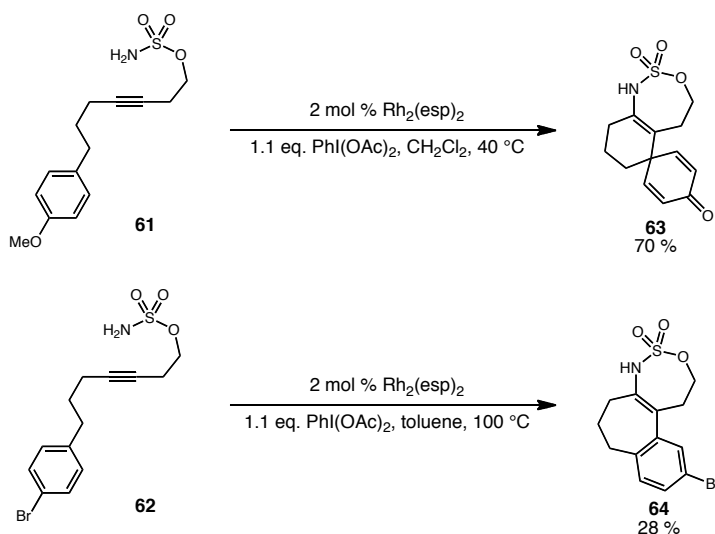
Scheme 2.17. Synthesis of electronically biased aromatic tethered alkynyl sulfamate esters **61** and **62**.



These studies reveal that electron-rich aromatic traps may also be used to terminate the cascade process (Scheme 2.18). However, electron-poor aromatic moieties have proven to be less effective, with bromobenzene substrate **62** leading to the desired β -amino styrene **64** in only 28 % yield, even when temperatures are raised to 100 °C in toluene. In addition to these findings, it is also important to note that in all cases the products observed are consistent with an electrophilic aromatic substitution (Friedel-Crafts) mechanism. This provides further evidence for the involvement of a vinyl cation reactive intermediate, and in turn has provided us with a working model for

the further development of novel cascade terminations.

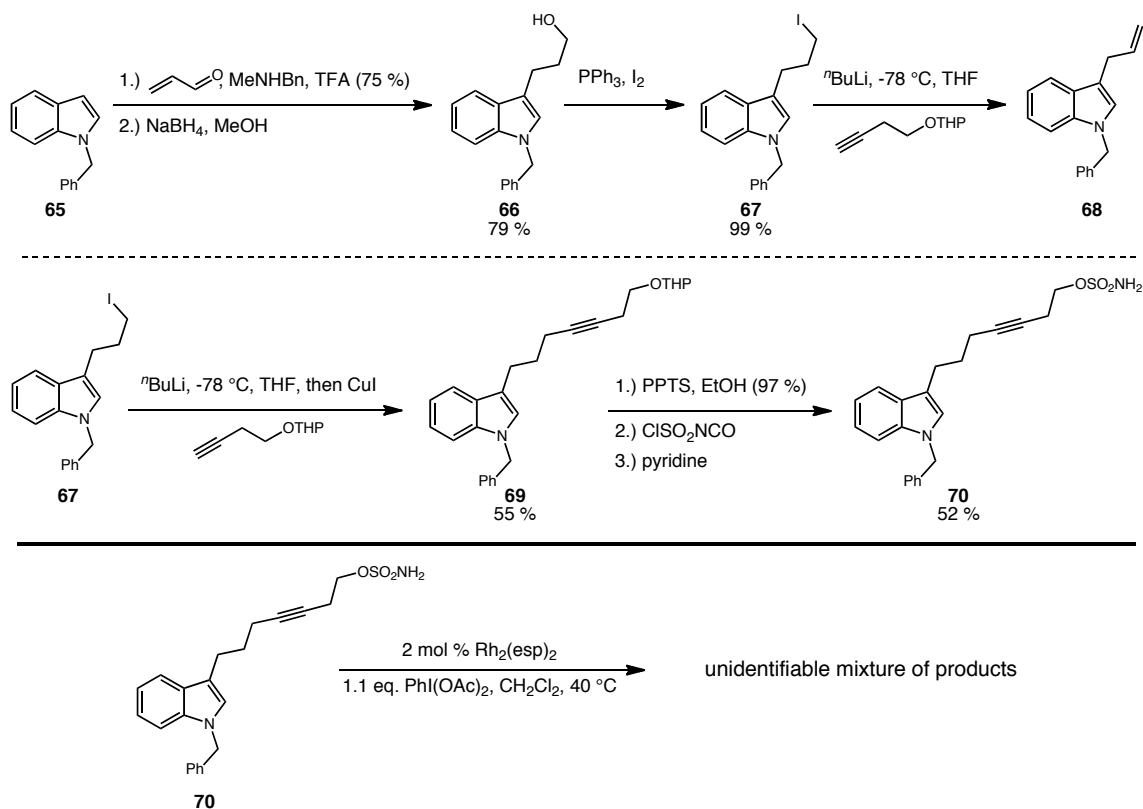
Scheme 2.18. Metallonitrene/alkyne cascade reaction termination through Friedel-Crafts reaction.



In addition to these simple aromatic tethers, we were also interested in examining the potential use of heteroaromatic traps for this metallonitrene/alkyne cascade reaction. In particular, because of its overwhelming presence in biologically interesting natural products, we were interested in terminating this cascade process through the addition of an indole nucleus. With this in mind, we needed to develop an efficient method to access indole tethered alkynyl sulfamate esters. Borrowing from our past work, we began the construction of such a substrate from *N*-benzyl indole **65** (Scheme 2.19). The benzyl group was selected due to its electron-donating capabilities, with the thought that this characteristic would facilitate the subsequent cascade termination. Indole **65** underwent conjugate addition to the iminium ion formed from the reaction of acrolein and *N*-methyl benzyl amine with catalytic TFA in 75 % yield.²² The resulting aldehyde was

immediately reduced with NaBH₄ in MeOH to give indole **66** in 79 % yield. Alcohol **66** was then smoothly converted to its corresponding alkyl iodide in 99 % yield using PPh₃ and I₂. Iodide **67** was then exposed to our general reaction conditions for S_N2 displacement with the anion of THP-protected 3-butyne-1-ol. Interestingly, under these conditions we obtained minimal amounts of the desired displacement product **69**, but instead, the elimination product **68** was produced. In an attempt to attenuate the basicity of the alkynyllithium formed via deprotonation of THP-protected 3-butyne-1-ol, we turned to a transmetalation strategy using CuI. Thus, after deprotonation with ⁿBuLi at -78 °C, a slurry of CuI in THF was added and allowed to stir for one hour. A solution of alkyl iodide **67** was then added to this solution and the mixture was warmed to ambient temperature. This procedure yielded the desired displacement product **69** in 55 % yield. While not ideal, this yield was sufficient for our purposes and no further optimization was undertaken. Subsequent removal of the THP protecting group and conversion of this alcohol to sulfamate ester **70** was then carried out without any issues. This substrate was then exposed to our general reaction conditions for cascade termination through Friedel-Crafts reaction. Accordingly, when indole tethered sulfamate ester **70** was reacted with 1.1 equivalents PhI(OAc)₂ and 2 mol % Rh₂(esp)₂ in CH₂Cl₂ at 40 °C we observed the formation of a complex mixture of products. Multiple attempts at purification led to the isolation of one constituent of this mixture combined with minor amounts of unidentifiable products. Typical methods for the characterization of this compound (¹H, ¹³C, IR, MS, COSY) proved to be unsuccessful and with simultaneous efforts underway to construct alternative indole tethered alkynyl sulfamate esters, the examination of substrate **70** was abandoned.

Scheme 2.19. Synthesis on *N*-benzyl indole tethered sulfamate ester **70** and unsuccessful cyclization attempts.



Hoping to protect the indole nucleus from oxidative degradation under the cascade reaction conditions, we chose to install a Boc group on the indole nitrogen. Thus, the synthesis of Boc-protected indole **75** commenced from readily available Boc-protected indole **71** (Scheme 2.20).²³ **71** was reduced with LiBH_4 to give alcohol **72** in 99 % yield and subsequent conversion of this alcohol to alkyl iodide **73** took place in 92 % yield. Again, as seen with *N*-benzyl indole **67**, *N*-Boc indole **73** was not amenable to our general conditions for the addition of THP-protected 3-butyne-1-ol, and only elimination products were observed. Inspired by our success with using a transmetallation strategy, we then underwent an optimization study employing CuI as a

metal source (Table 2.1). As outlined in Table 2.1, observing that product **74** was formed only when the temperature during the transmetallation step was raised, suggested that transmetallation does not occur at $-78\text{ }^{\circ}\text{C}$ and thus motivated our future efforts. In addition, the discovery that polar aprotic co-solvent DMPU also increased the yield of desired product **74** was crucial. Combining these findings, in addition to altering the order of addition, led to our optimized conditions and an isolated yield of **74** in 75 % yield. THP removal and conversion of this alcohol to sulfamate ester **75** was then carried out without issue.

Scheme 2.20. Synthesis of *N*-Boc indole tethered sulfamate ester **75**.

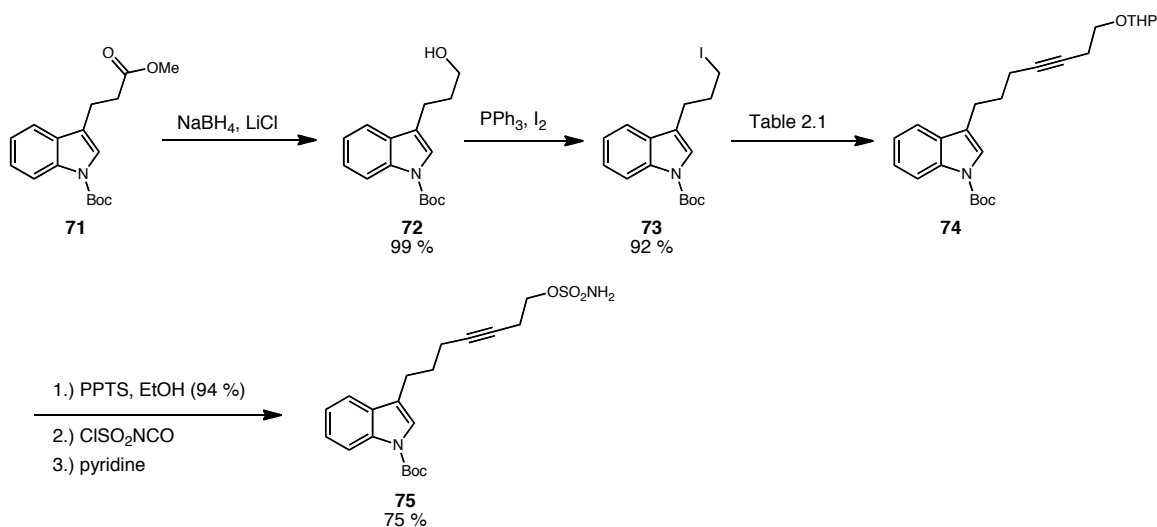
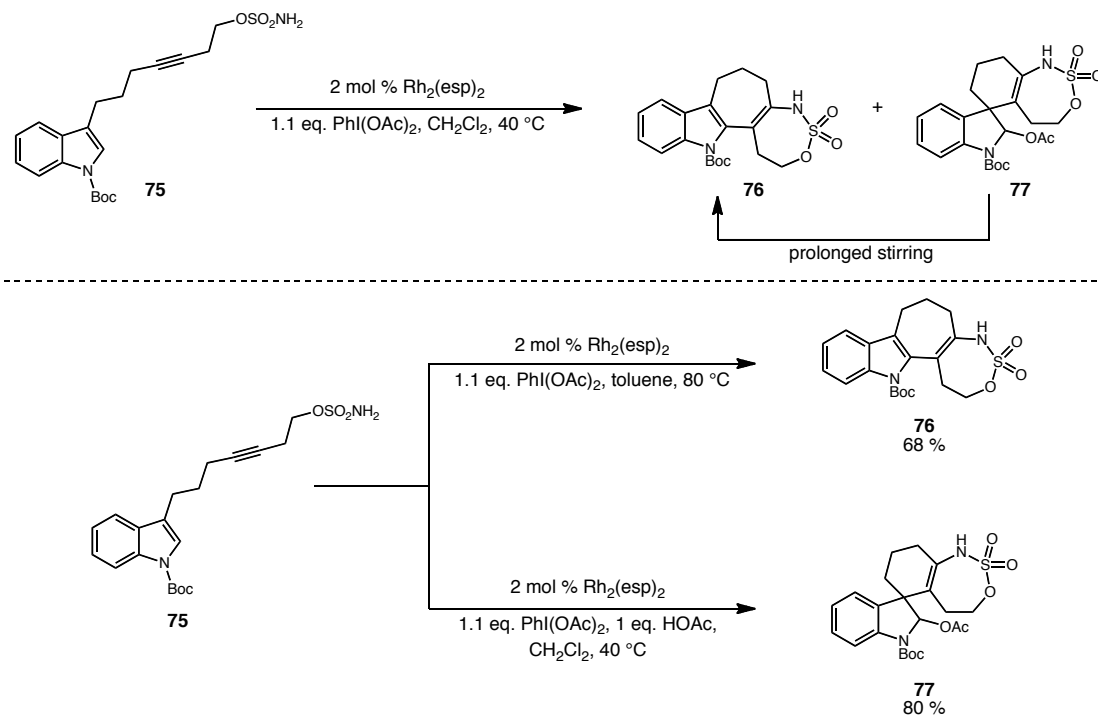


Table 2.1. Optimization for the coupling of **73** with THP-protected 3-butyn-1-ol.

base	transmetallation T ($^{\circ}\text{C}$)	co-solvent	order of addition	yield
$n\text{BuLi}$ ($-78\text{ }^{\circ}\text{C}$)	CuI , $-78\text{ }^{\circ}\text{C}$	--	73 to alkyne	0 %
$n\text{BuLi}$ ($-78\text{ }^{\circ}\text{C}$)	CuI , $-40\text{ }^{\circ}\text{C}$	--	73 to alkyne	16 %
$n\text{BuLi}$ ($-78\text{ }^{\circ}\text{C}$)	CuI , $-78\text{ }^{\circ}\text{C}$	DMPU	73 to alkyne	25 %
$n\text{BuLi}$ ($-78\text{ }^{\circ}\text{C}$)	CuI , $-40\text{ }^{\circ}\text{C}$	DMPU	73 to alkyne	53 %
$n\text{BuLi}$ ($-78\text{ }^{\circ}\text{C}$)	CuI , $-40\text{ }^{\circ}\text{C}$	DMPU	alkyne to 73	75 %

Subjecting *N*-Boc indole tethered sulfamate ester **75** to our general reaction conditions for Friedel-Crafts termination of this metallonitrene/alkyne cascade reaction resulted in a mixture of products **76** and **77**, the C-2 and C-3 addition products respectively (Scheme 2.21). Control experiments suggested the C-2 addition product **76** was in fact arising from rearrangement of C-3 addition adduct **77**, and in turn motivated us to develop conditions for the selective formation of each product. With this in mind, we have found that this C-3 to C-2 shift may be facilitated simply by prolonged heating of the reaction mixture. Thus, conducting the reaction in toluene at 80 °C for eight hours led to the desired C-2 addition product **76** in 68 % yield, while conducting the reaction in acidic media (1 eq. HOAc) resulted in an isolated yield of the desired C-3 addition product **77** in 80 %. Importantly, by making these simple alterations we are now able to take a single substrate and selectively form tetracyclic compound **76** as well as spirocyclic compound **77** in good yields.

Scheme 2.21. Cascade termination through selective C-2 and C-3 additions of *N*-Boc indole **75**.

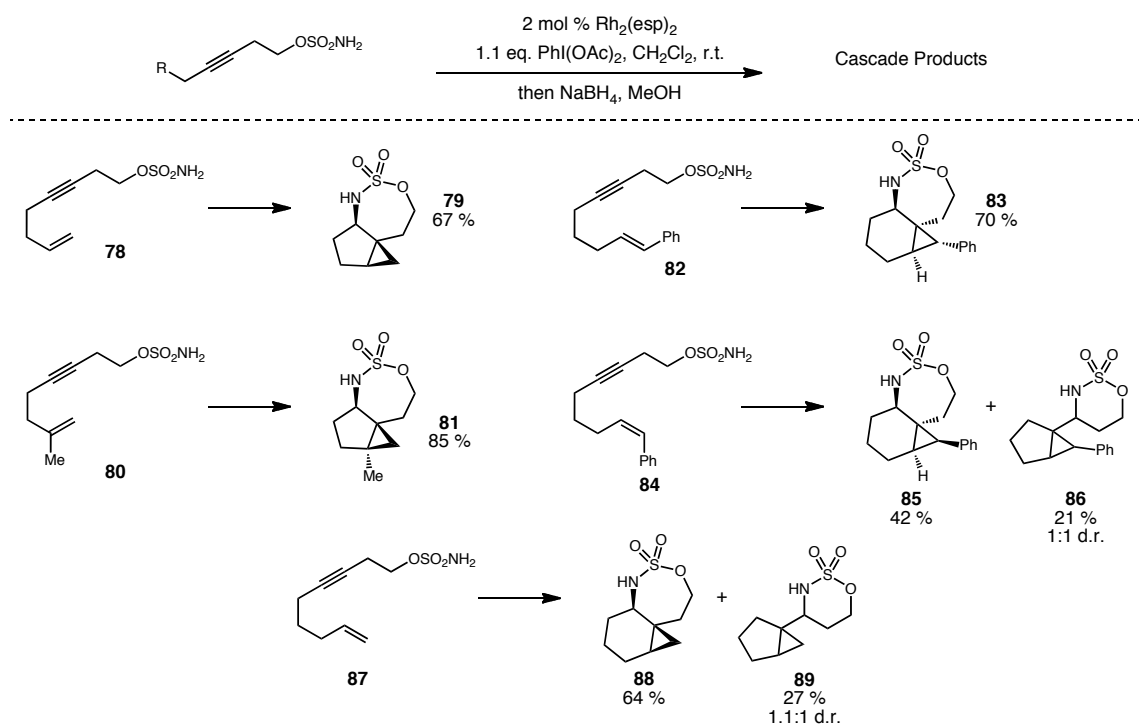


2.3.3. Discovery and Substrate Scope for Cascade Termination Through Cyclopropanation

In addition to aromatic traps, we have also shown that olefins may be used to terminate this cascade process. In our initial studies, I showed that simple alkenyl sulfamate ester **78** could undergo this reaction in 67 % yield. Subsequently, Véronique Martin further expanded the scope of this reaction (Scheme 2.22). Our work showed that tether lengths which result in both five- and six-membered ring systems may be used to terminate this cascade process (**79**, **88**). Also, her work illustrated that various substitution patterns on the alkene may be tolerated. For example, both 1,1-disubstituted (**80**) as well as 1,2-disubstituted (**82**, **84**) olefins may be used to terminate the cascade

process. Interestingly, she observed that the stereochemistry of the starting olefin is conserved in the corresponding cyclopropane products. Thus, *trans*-olefin **82** leads to *trans*-cyclopropane **83** and *cis*-olefin **84** leads to *cis*-cyclopropane **85**. While these results are not conclusive, they do suggest that the cyclopropanation event takes place in a concerted fashion, potentially inconsistent with an ionic intermediate.

Scheme 2.22. Representative substrate scope for cascade termination through cyclopropanation.

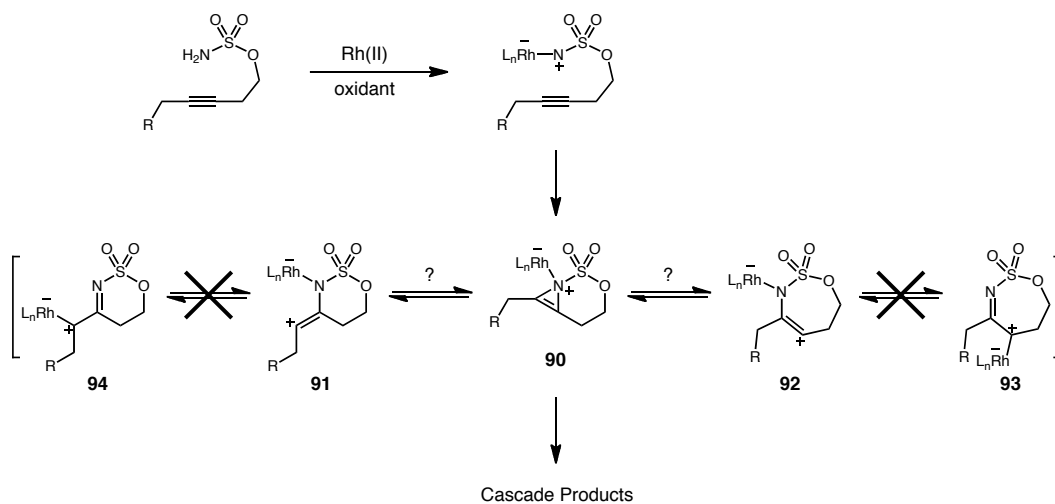


2.3.4. Revised Mechanistic Hypothesis Based on Reactivity Patterns

In addition to these findings, her work also showed that product regioselectivity is dependent on tether length. For example, both alkenyl sulfamate esters **84** and **87** led to the production of both regioisomeric α -amino cyclopropane products, **85/86** and **88/89**

respectively. Taking our combined results into consideration, we now propose that the initial reaction between a sulfamate ester derived metallonitrene and a tethered alkyne leads to a strained metal-bound azirine species, **90** (Scheme 2.23). Consistent with literature precedent for the nucleophilic ring-opening of aziridines due to the increased ring-strain associated with six-membered cyclic sulfamates, addition by the tethered nucleophile takes place at the internal position of this strained three-membered ring.²⁴ When tether lengths will not allow for efficient orbital overlap between the tethered nucleophile and the internal position of this reactive intermediate, we see formation of the regioisomeric products, as in the case of alkenyl sulfamate esters **84** and **87**. Based on these reactivity studies, we are confident in the conclusion that the formation of α -imino metalcarbene species **93** and **94** are highly unlikely. At this point, it is still unclear whether this reaction leads to the formation of discrete vinyl cation intermediates **91** or **92**, and detailed computational studies will be required to further understand the subtle details of this reaction pathway.

Scheme 2.23. Revised metallonitrene/alkyne cascade reaction mechanism.



2.4. Conclusions and Future Directions

In conclusion we have developed a new, versatile process for the formation of C-N bonds. This novel transformation leads to the generation of significant molecular complexity from simple and readily accessible starting materials and reagents in a selective and predictable fashion. We have shown that four different classes of nucleophiles may be used to terminate the cascade process; tethered ethers, aromatic groups, and olefins, as well as intermolecular trapping with carboxylates.

With this effective method developed, the value of our methodology will lie in its ability to facilitate the synthesis of complex chemical architectures. Inspired by this reaction's ability generate multiple bonds and stereocenters in a single transformation, we were intrigued by the possibility of utilizing our newly developed metallonitrene/alkyne cascade reaction to streamline the synthesis of biologically interesting and medicinally relevant natural products. These efforts, and the studies that have evolved from this work, will be discussed in the subsequent chapter.

Experimental Procedures and Compound Characterization

General Information.

^1H and ^{13}C NMR spectra were recorded on a Varian Inova 600 spectrometer (600 MHz ^1H , 150 MHz ^{13}C) or a Varian Inova 400 spectrometer (400 MHz ^1H , 100 MHz ^{13}C) at room temperature in CDCl_3 with internal CHCl_3 as the reference (7.27 ppm for ^1H and 77.23 ppm for ^{13}C) unless stated otherwise. Chemical shifts (δ values) were reported in parts per million (ppm) and coupling constants (J values) in Hz. Multiplicity is indicated using the following abbreviations: s = singlet, d = doublet, t = triplet, q = quartet, qn = quintet, m = multiplet, b = broad signal. Infrared (IR) spectra were recorded using Thermo Electron Corporation Nicolet 380 FT-IR spectrometer. High resolution mass spectra were obtained using a Thermo Electron Corporation Finigan LTQFTMS (at the Mass Spectrometry Facility, Emory University) and we acknowledge the use of shared instrumentation provided by grants from the NIH and the NSF. Melting points (mp) were taken using a Fisher-Johns melting point apparatus and are not corrected. Analytical thin layer chromatography (TLC) was performed on precoated glass backed EMD 0.25 mm silica gel 60 plates. Visualization was accomplished with UV light or ethanolic anisaldehyde followed by heating. Flash column chromatography was carried out using EMD Geduran® silica gel 60 (40-63 μm).

All reactions were conducted with anhydrous solvents in oven dried or flame-dried and argon charged glassware unless stated otherwise. Anhydrous solvents were purified by passage through activated alumina using a *Glass Contours* solvent purification system unless otherwise noted. Benzene, DMA, and DMF were dried over

activated 4 Å molecular sieves. Acetone was purified by distillation from CaCl₂. Solvents for workup, extraction and column chromatography were used as received from commercial suppliers. All reagents were purchased from Sigma-Aldrich and used as received unless otherwise noted. *Bis*-acetoxy-iodobenzene was dried under vacuum (0.02 mmHg) for 12 hours prior to use. Pyridine, pyrrolidine, 2,6 lutidine, and DMPU were purified by distillation from calcium hydride. Rhodium catalysts were purchased from Sigma-Aldrich and used as received.

Procedures and Characterization for the Preparation of Sulfamate Esters

General procedure (A) for the benzylation or allylation of alkynyl alcohols.²⁵

Alkynyl alcohol (1 eq.) was added to a solution of NaH (60 % dispersion, 1.2 eq.) in THF (0.20 M) at 0 °C. The resulting solution was warmed to ambient temperature and stirred until thin layer chromatography indicated complete consumption of the starting alkyne. At this point the reaction was quenched by the addition of 1 N HCl at 0 °C. The organic phase was collected and the aqueous phase was extracted with Et₂O (2x), washed with brine, and dried over MgSO₄. Following filtration and concentration *in vacuo*, the resulting oil was purified by flash column chromatography (100 % pentane).

General procedure (B) for the addition of terminal alkynes to oxirane.⁸

ⁿBuLi (1.6 M, 1.2 eq.) was added slowly to a solution of the terminal alkyne (1 eq.) in THF/DMPU (10:1, 0.25 M) at -78 °C and stirred at this temperature for 0.5 h. After this time, distilled oxirane (2 eq.) was added in a single portion via syringe. The resulting

solution was warmed to ambient temperature and stirred for 14 h. After this time the reaction was quenched by the addition of sat. aqueous NH_4Cl . The organic layer was separated, and the aqueous layer was extracted with Et_2O (2x). The combined organic extracts were dried over MgSO_4 , filtered, and concentrated *in vacuo* to give the resulting crude oil that was purified via flash column chromatography.

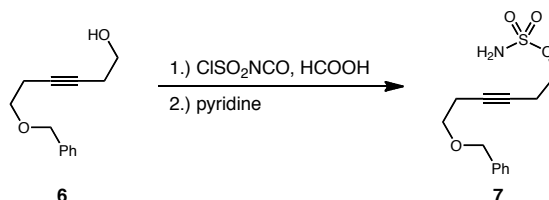
General procedure (C) for the preparation of homopropargylic alcohols via THP removal.

PPTS (0.4 eq.) was dissolved in EtOH (0.1 M). The starting THP protected alcohol (1.0 eq.) was added and the resulting solution was heated to 55 °C until thin layer chromatography indicated complete consumption of starting material. The reaction mixture was cooled to room temperature and concentrated *in vacuo*. Purification by flash chromatography as indicated afforded the desired homopropargylic alcohol.

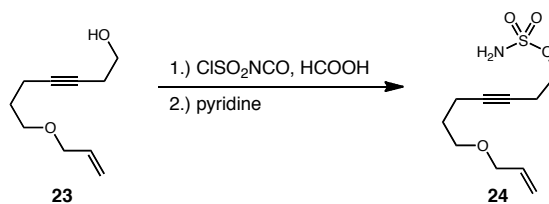
General Procedure (D) for the preparation of sulfamate esters.

Formic acid was added to neat chlorosulfonyl isocyanate (1.5 eq.) at 0 °C with stirring. The resulting white solid was dissolved in CH_2Cl_2 (1 M). The solution was warmed to 25 °C and allowed to stir overnight. The reaction mixture was cooled to 0 °C and a solution of the starting alcohol (1.0 eq.) and pyridine (1.5 eq.) in CH_2Cl_2 (1.4 M) was added dropwise. The solution was warmed to ambient temperature and stirred until thin layer chromatography indicated complete consumption of starting material (15 min – 1 h). The reaction was quenched by the addition of EtOAc and H_2O . The organic phase was collected and the aqueous layer was extracted with EtOAc (2 x 25 mL). The

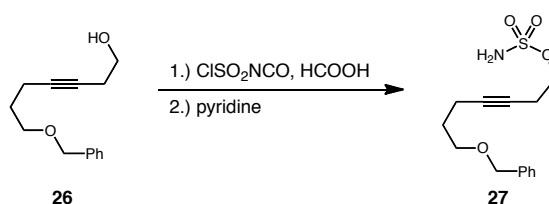
combined organic extracts were washed with brine (50 mL), dried over MgSO₄, and concentrated *in vacuo*. Purification by column chromatography on silica gel as indicated afforded the desired sulfamate ester.



6-(benzyloxy)hex-3-yn-1-yl sulfamate (7). Prepared according to general procedure **D** using 6-benzyloxy-hex-3-yn-1-ol²⁶ (**6**) (2.8 g, 14 mmol), chlorosulfonyl isocyanate (1.8 mL, 20 mmol) and formic acid (0.78 mL, 20 mmol). After 0.25 h the reaction was quenched by the addition of EtOAc (30 mL) and H₂O (15 mL). Purification by flash column chromatography (3:1 → 1:1 hexanes/EtOAc) afforded 6-(benzyloxy)hex-3-yn-1-yl sulfamate (**7**) as a pale yellow oil (3.0 g, 78 %); **R_f** 0.13 (3:1 hexanes/EtOAc); **IR** (thin film, cm⁻¹) 3310, 3280, 2868, 1364, 1179, 1094, 916, 738; **¹H NMR** (CDCl₃, 600 MHz) δ 7.37-7.32 (m, 5H), 5.11 (s, 2H), 4.56 (s, 2H), 4.26 (t, 2H, *J* = 6.7 Hz), 3.57 (t, 2H, *J* = 6.4 Hz), 2.61 (tt, 2H, *J* = 6.7, 2.5 Hz), 2.47 (tt, 2H, *J* = 6.7, 2.5 Hz); **¹³C NMR** (CDCl₃, 150 MHz) δ 138.0, 128.7, 128.2, 128.1, 80.0, 76.1, 73.1, 69.1, 68.5, 20.2, 20.0; **HRMS** (+ESI) calculated for C₁₃H₁₈NO₄S 284.0957, found 284.0950 [M+H]⁺.

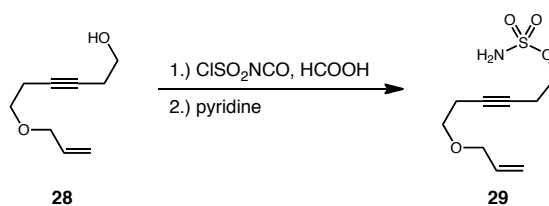


7-(allyloxy)hept-3-yn-1-yl sulfamate (24). Prepared according to general procedure **D** using 7-allyloxy-hept-3-yn-1-ol⁸ (**23**) (2.5 g, 15 mmol), chlorosulfonyl isocyanate (1.9 mL, 22 mmol) and formic acid (0.86 mL, 22 mmol). After 0.5 h the reaction was quenched by the addition of EtOAc (25 mL) and H₂O (12 mL). Flash chromatography (3:1 hexanes/EtOAc) afforded 7-(allyloxy)hept-3-yn-1-yl sulfamate (**24**) (3.7 g, 88 %) as a pale yellow viscous oil; **R_f** 0.13 (3:1 hexanes/EtOAc); **IR** (thin film, cm⁻¹) 3380, 3285, 3082, 2866, 1363, 1177, 987, 920; **¹H NMR** (CDCl₃, 600 MHz) δ 5.92 (ddt, 1H, *J* = 17.1, 10.5, 5.6 Hz), 5.28 (dq, 1H, *J* = 17.2, 1.6 Hz), 5.19 (dq, 1H, *J* = 10.2, 1.6 Hz), 5.13 (s, 2H), 4.25 (t, 2H, *J* = 6.7 Hz), 3.98 (dt, 2H, *J* = 5.7, 1.3 Hz), 3.54 (t, 2H, *J* = 6.4 Hz), 2.62 (tt, 2H, *J* = 6.7, 2.2 Hz), 2.26 (tt, 2H, *J* = 7.0, 2.2 Hz), 1.76 (qn, 2H, *J* = 6.4 Hz); **¹³C NMR** (CDCl₃, 150 MHz) δ 134.9, 117.3, 82.3, 75.2, 71.9, 69.3, 68.7, 28.7, 19.9, 15.6; **HRMS** (+ ESI) calculated for C₁₀H₁₈NO₄S 248.0957, found 248.0949 [M+H]⁺.



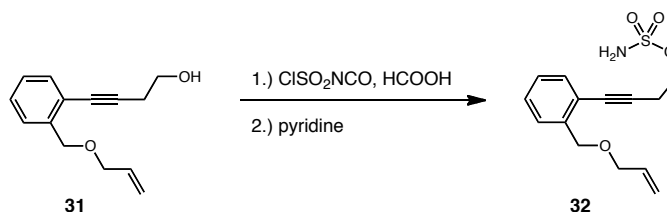
7-(benzyloxy)hept-3-yn-1-yl sulfamate (27). Prepared according to general procedure **D** using 7-benzyloxy-hept-3-yn-1-ol⁸ (**26**) (3.7 g, 17 mmol), chlorosulfonyl isocyanate (2.2

mL, 25 mmol) and formic acid (0.98 mL, 25 mmol). After 30 mins the reaction was quenched by addition of EtOAc (15 mL) and H₂O (8 mL). Flash chromatography (3:1 hexanes/EtOAc) afforded 7-(benzyloxy)hept-3-yn-1-yl sulfamate (**27**) as a pale yellow oil (3.3 g, 91 %); **R_f** 0.14 (3:1 hexanes/EtOAc); **IR** (thin film, cm⁻¹) 3369, 3284, 2926, 1363, 1178, 918; **¹H NMR** (CDCl₃, 600 MHz) δ 7.39-7.28 (m, 5H), 4.83 (s, 2H), 4.53 (s, 2H), 4.23 (t, 2H, *J* = 7.0 Hz), 3.60 (t, 2H, *J* = 6.4 Hz), 2.61 (tt, 2H, *J* = 6.7, 2.2 Hz), 2.29 (tt, 2H, *J* = 7.0, 2.5 Hz), 1.79 (qn, 2H, *J* = 6.4 Hz); **¹³C NMR** (CDCl₃, 150 MHz) δ 138.5, 128.6, 127.9, 127.8, 82.4, 75.2, 73.0, 69.3, 68.8, 28.8, 19.9, 15.7; **HRMS** (+ESI) calculated for C₁₄H₂₀NO₄S 298.1113, found 298.1106 [M+H]⁺.

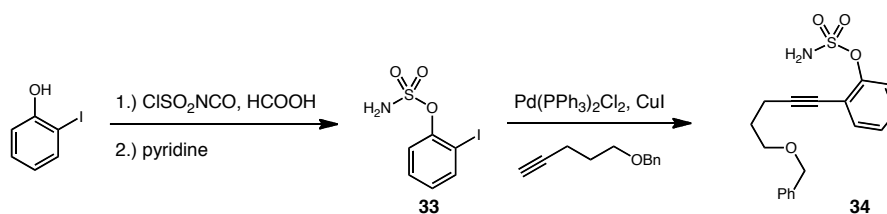


6-(allyloxy)hex-3-yn-1-yl sulfamate (29). Prepared according to general procedure **D** using 6-allyloxy-hex-3-yn-1-ol⁸ (**28**) (0.25 g, 1.6 mmol), chlorosulfonyl isocyanate (2.7 mL, 30 mmol) and formic acid (1.2 mL, 30 mmol). After 45 mins the reaction was quenched by addition of EtOAc (10 mL) and H₂O (5 mL). Flash chromatography (3:1 hexanes/EtOAc) afforded 6-(allyloxy)hex-3-yn-1-yl sulfamate (**29**) as a pale yellow oil (0.19 g, 50 %); **R_f** 0.13 (3:1 hexanes/EtOAc); **IR** (thin film, cm⁻¹) 3350, 3279, 3085, 2917, 1361, 1177, 1086, 921; **¹H NMR** (CDCl₃, 600 MHz) δ 5.92 (ddt, 1H *J* = 17.2, 10.5, 5.7 Hz), 5.30 (dq, 1H, *J* = 17.6, 1.9 Hz), 5.25 (dd, 1H, *J* = 10.5, 1.4 Hz), 5.20 (s, 2H), 4.27 (t, 2H, *J* = 6.2 Hz), 4.15 (dt, 2H, *J* = 6.2, 1.4 Hz), 3.54 (t, 2H, *J* = 6.2 Hz), 2.61

(tt, 2H, $J = 6.2, 2.4$ Hz), 2.45 (tt, 2H, $J = 6.7, 2.4$ Hz); $^{13}\text{C NMR}$ (CDCl_3 , 150 MHz) δ 134.4, 118.0, 80.0, 76.3, 72.1, 69.1, 68.5, 20.2, 20.0; **HRMS** (+ESI) calculated for $\text{C}_9\text{H}_{16}\text{NO}_4\text{S}$ 234.0800, found 234.0794 $[\text{M}+\text{H}]^+$.



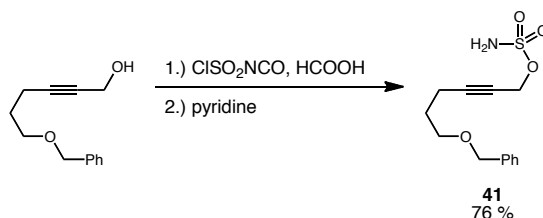
4-(2-((allyloxy)methyl)phenyl)but-3-yn-1-yl sulfamate (32). Prepared according to general procedure **D** using 4-(2-((allyloxy)methyl)phenyl)but-3-yn-1-ol (**31**) (0.33 g, 1.5 mmol), chlorosulfonyl isocyanate (0.20 mL, 2.3 mmol) and formic acid (0.09 mL, 2.3 mmol). After 1 h the reaction was quenched by addition of EtOAc (20 mL) and H_2O (10 mL). Flash chromatography (3:1 to 1:1 hexanes/EtOAc) afforded 4-(2-((allyloxy)methyl)phenyl)but-3-yn-1-yl sulfamate (**32**) as a colorless oil (0.34 g, 77 %); R_f 0.20 (3:1 hexanes/EtOAc); **IR** (thin film, cm^{-1}) 3320, 3279, 2917, 1362, 1178, 1065, 920, 758; $^1\text{H NMR}$ (CDCl_3 , 600 MHz) δ 7.44 (d, 1H, $J = 7.2$ Hz), 7.40 (d, 1H, $J = 7.6$ Hz), 7.32 (t, 1H, $J = 7.6$ Hz), 7.27 (t, 1H, $J = 7.6$ Hz), 5.96 (ddt, 1H, $J = 17.2, 10.5, 5.7$ Hz), 5.34 (d, 1H, $J = 17.2$), 5.24 (d, 1H, $J = 10.5$ Hz), 5.14 (bs, 2H), 4.67 (s, 2H), 4.38 (t, 2H, $J = 6.2$ Hz), 4.06 (d, 2H, $J = 5.7$ Hz), 2.92 (t, 2H, $J = 6.2$ Hz); $^{13}\text{C NMR}$ (CDCl_3 , 150 MHz) δ 139.6, 134.6, 132.6, 129.0, 128.5, 128.0, 122.5, 118.0, 89.2, 80.7, 71.3, 70.6, 68.7, 21.0; **HRMS** (-ESI) calculated for $\text{C}_{14}\text{H}_{16}\text{NO}_4\text{S}$ 294.0800, found 294.0813 $[\text{M}-\text{H}]^-$.



2-Iodophenyl sulfamate (33).¹⁷ Formic acid (0.69 mL, 18 mmol) was added to a flask containing chlorosulfonyl isocyanate (1.6 mL, 18 mmol). The resulting mixture was stirred under argon at 0 °C for 8 h. A solution of 2-iodophenol (1.4 g, 6.4 mmol) in NMP (4.2 mL) was added, the reaction was warmed to ambient temperature, stirred for 10 h and then quenched with brine (50 mL). After dilution with EtOAc (50 mL), the organic layer was collected. The aqueous layer was extracted with EtOAc (2 x 30 mL) and the combined organic extracts were washed with brine (100 mL), dried over MgSO₄ and concentrated *in vacuo*. Purification by flash chromatography (2:1 hexanes/EtOAc) afforded 2-iodophenyl sulfamate (**33**) as a white solid (1.2 g, 65 %); **R_f** 0.22 (3:1 hexanes/EtOAc); **IR** (thin film, cm⁻¹) 3395, 3287, 1462, 1380, 1175; **¹H NMR** (CDCl₃, 600 MHz) δ 7.90 (dd, 1H, *J* = 7.6, 1.0 Hz), 7.55 (dd, 1H, *J* = 8.3, 1.3 Hz), 7.42 (t, 1H, *J* = 7.3), 7.06 (dt, 1H, *J* = 7.3, 1.0 Hz), 5.10 (bs, 2H); **¹³C NMR** (CDCl₃, 150 MHz) δ 150.5, 144.1, 140.2, 130.2, 129.0, 123.3; **m.p.** 72-73 °C **HRMS** (-ESI) calculated for C₆H₅INO₃S 297.9033, found 297.9041 [M-H]⁻.

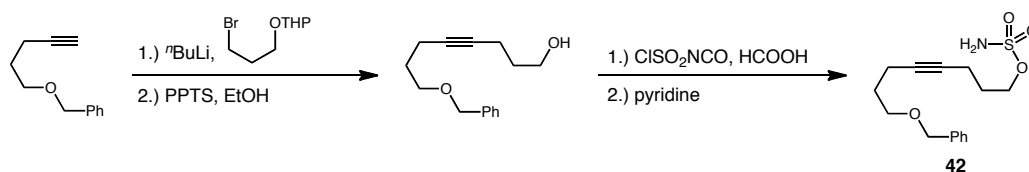
2-(5-(benzyloxy)pent-1-yn-1-yl)phenyl sulfamate (34). CuI (5mg, 0.026 mmol), 5-benzyloxypentyne²⁷ (0.23 g, 1.3 mmol) and Et₃N (0.50 mL) were combined in a flask under an atmosphere of nitrogen. To this mixture, a solution of PdCl₂(PPh₃)₂ (18 mg, 0.026 mmol) and 2-iodophenyl sulfamate (**33**) (0.39 g, 1.3 mmol) in Et₃N (0.75 mL) and

THF (0.5 mL) was added dropwise. The resulting solution was stirred at ambient temperature for 9 h, diluted with CH₂Cl₂ (9 mL) and concentrated onto silica (*ca.* 0.5 g). Purification by flash chromatography (3:2 hexanes/EtOAc) gave 2-(5-(benzyloxy)pent-1-yn-1-yl)phenyl sulfamate (**34**) as a pale yellow oil (0.13 g, 28 %); **R_f** 0.23 (3:1 hexanes/EtOAc); **IR** (thin film, cm⁻¹) 3395, 3289, 1487, 1386, 1177; **¹H NMR** (CDCl₃, 600 MHz) δ 7.48 (dd, 1H, *J* = 7.6, 1.4 Hz), 7.40 (d, 1H, *J* = 8.6 Hz), 7.31-7.38 (m, 4H), 7.24-7.31 (m, 2H), 5.26 (s, 2H), 4.57 (s, 2H), 3.78 (t, 2H, *J* = 5.7 Hz), 2.61 (t, 2H, *J* = 6.2 Hz), 1.29 (qn, 2H, *J* = 6.2 Hz); **¹³C NMR** (CDCl₃, 150 MHz) δ 150.6, 138.0, 133.5, 129.5, 128.7, 128.2, 128.1, 127.3, 123.8, 118.5, 108.7, 95.3, 72.9, 68.8, 27.8, 16.9; **HRMS** (+ESI) calculated for C₁₈H₂₀NO₄S 346.1113, found 346.1108 [M+H]⁺.



6-(benzyloxy)hex-2-yn-1-yl sulfamate (41). Prepared according to general procedure **D** using 6-benzyloxy-hex-2-yn-1-ol²⁸ (1.3 g, 6.1 mmol), chlorosulfonyl isocyanate (0.80 mL, 9.2 mmol) and formic acid (0.36 mL, 9.2 mmol). After 20 mins the reaction was quenched by addition of EtOAc (35 mL) and H₂O (17 mL). Flash chromatography (3:1 hexane/EtOAc) afforded 6-(benzyloxy)hex-2-yn-1-yl sulfamate (**41**) as a pale yellow oil (1.3 g, 77 %); **R_f** 0.15 (3:1 hexanes/EtOAc); **IR** (thin film, cm⁻¹) 3380, 3288 1368, 1183; **¹H NMR** (CDCl₃, 600 MHz) δ 7.29-7.40 (m, 5H), 4.94 (s, 2H), 4.79 (t, 2H, *J* = 2.2 Hz), 4.52 (s, 2H), 3.57 (t, 2H, *J* = 6.0 Hz), 2.40 (tt, 2H, *J* = 7.0, 2.2 Hz), 1.83 (2H, qn, *J* = 6.4

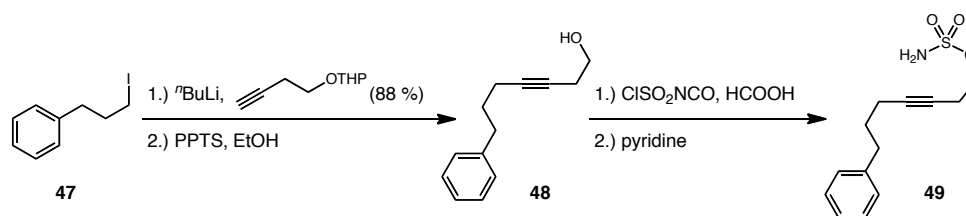
Hz); ^{13}C NMR (CDCl_3 , 150 MHz) δ 138.3, 128.7, 128.0, 90.6, 73.1, 72.9, 68.7, 59.4, 28.3, 16.1; HRMS (+ESI) calculated for $\text{C}_{13}\text{H}_{18}\text{NO}_4\text{S}$ 284.0957, found 284.0950 $[\text{M}+\text{H}]^+$.



8-(benzyloxy)oct-4-yn-1-ol. $n\text{-BuLi}$ (1.6 M, 2.0 mL, 3.2 mmol) was added dropwise to a solution of 5-benzyloxypentyne²⁹ (0.55 g, 3.2 mmol) in THF/DMPU (1:1, 20 mL total) at $-78\text{ }^\circ\text{C}$ and stirred for 1 h. After this time 2-(3-bromopropoxy)tetrahydro-2H-pyran³⁰ (0.77 g, 3.5 mmol) was added slowly. The resulting solution was warmed to ambient temperature and stirred for 3 h. After this time the reaction was cooled to $0\text{ }^\circ\text{C}$ and quenched by the addition of 1 N HCl. The organic layer was separated and the aqueous layer was extracted with Et_2O (2 x 25 mL). The combined organic extracts were washed with brine, dried over MgSO_4 , and concentrated *in vacuo*. The resulting crude oil was immediately dissolved in EtOH (17 mL) and PPTS (0.14 g, 0.50 mmol) was added as a solid in a single portion. The resulting solution was warmed to $40\text{ }^\circ\text{C}$ and stirred for 12 h. After this time the reaction mixture was concentrated *in vacuo* on to SiO_2 and purified by flash column chromatography (7:1 hexanes/EtOAc) to afford 8-(benzyloxy)oct-4-yn-1-ol (0.57 g, 78 %) as a clear oil; R_f 0.20 (8:1 hexanes/EtOAc); IR (thin film, cm^{-1}) 3379, 2944, 2862, 1453, 1104, 1075, 698; ^1H NMR (CDCl_3 , 600 MHz) δ 7.36-7.28 (m, 5H), 4.52 (s, 2H), 3.74 (t, 2H, $J = 6.0$ Hz), 3.56 (t, 2H, $J = 6.0$ Hz), 2.31-2.25 (m, 4H), 1.82-1.69 (m, 4H), 1.52 (bs, 1H); ^{13}C NMR (CDCl_3 , 150 MHz) δ 138.7, 128.6, 127.8, 127.7,

81.7, 80.5, 73.1, 69.1, 62.2, 31.7, 29.4, 15.8, 15.6; **HRMS** (+ESI) calculated for $C_{15}H_{20}O_2$ 232.1463, found 233.1535 $[M+H]^+$.

8-(benzyloxy)oct-4-yn-1-yl sulfamate (42). Prepared according to general procedure **D** using 8-(benzyloxy)oct-4-yn-1-ol (0.58 g, 2.5 mmol), chlorosulfonyl isocyanate (0.33 mL, 3.7 mmol) and formic acid (0.14 mL, 3.7 mmol). After 0.5 h the reaction was quenched by addition of EtOAc (15 mL) and H_2O (8 mL). Flash chromatography (3:1 hexanes/EtOAc) afforded 8-(benzyloxy)oct-4-yn-1-yl sulfamate (**42**) as a colorless oil (0.57 g, 75 %); R_f 0.19 (3:1:1 hexanes/EtOAc/ CH_2Cl_2); **IR** (thin film, cm^{-1}) 3373, 3286, 2929, 2856, 2358, 1367, 1182; 1H NMR ($CDCl_3$, 600 MHz) δ 7.36-7.29 (m, 5H), 4.80 (s, 2H), 4.53 (s, 2H), 4.32 (t, 2H, $J = 6.2$ Hz), 3.58 (t, 2H, $J = 5.2$ Hz), 2.32 (tt, 2H, $J = 6.7$, 1.4 Hz), 2.28 (tt, 2H, $J = 7.2$, 1.9 Hz), 1.79 (qn, 2H, $J = 6.2$ Hz), 1.79 (qn, 2H, $J = 6.2$ Hz); ^{13}C NMR ($CDCl_3$, 150 MHz) δ 138.5, 128.6, 127.9, 127.8, 81.3, 78.4, 73.0, 70.0, 69.0, 29.1, 28.1, 15.7, 15.2; **HRMS** (+ESI) calculated for $C_{15}H_{22}NO_4S$ 312.1270, found 312.1257 $[M+H]^+$.

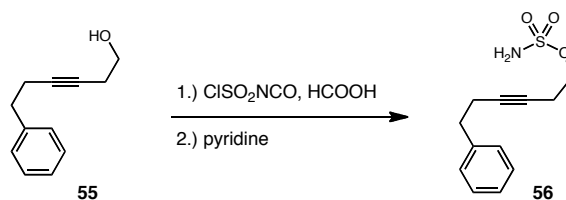


2-(7-phenylhept-3-ynyloxy)tetrahydro-2H-pyran. 2-(but-3-ynyloxy)tetrahydro-2H-pyran³¹ (0.30 g, 1.9 mmol) was stirred in THF (12 mL) with triphenylmethane (2 mg) and DMPU (2.0 mL) at -78 °C. $t-BuLi$ (1.4 mL, 1.6 M in hexanes, 1.9 mmol) was added dropwise until the solution's color remained consistent. After stirring for 1 h

(3-iodopropyl)benzene³² (**47**) (0.53 g, 2.1 mmol) in THF (1.5 mL) was added dropwise. The reaction was warmed to 65 °C. After 20 h the reaction was cooled to ambient temperature and quenched by the addition of H₂O. Purification by flash chromatography afforded 2-(7-phenylhept-3-ynoxy)tetrahydro-2H-pyran (**48**) as a colorless oil (0.42 g, 81 %); **R_f** 0.75 (8:1 hexanes/EtOAc); **IR** (thin film, cm⁻¹) 2939, 2869, 1456, 1136, 1121, 1034; **¹H NMR** (CDCl₃, 600 MHz) 7.30-7.18 (m, 5H), 4.66 (t, 1H, *J* = 3.8 Hz), 3.90 (ddd, 1H, *J* = 11.9, 8.6, 3.3 Hz), 3.82 (dt, 1H, *J* = 9.5, 7.2 Hz), 3.59-3.50 (m, 2H), 2.72 (t, 1H, *J* = 7.2 Hz), 2.49 (tt, 2H, *J* = 7.2, 2.4 Hz), 2.17 (tt, 2H, *J* = 6.7, 1.9 Hz), 1.86-1.78 (m, 3H), 1.75-1.70 (m, 1H), 1.63-1.50 (m, 4H); **¹³C NMR** (CDCl₃, 150 MHz) 142.0, 128.7, 128.5, 126.0, 98.9, 81.0, 77.4, 66.5, 62.4, 34.9, 30.8, 30.7, 25.6, 20.5, 19.6, 18.4; **HRMS** (+ESI) calculated for C₁₈H₂₅O₂ 273.1849, found 273.1745 [M+H]⁺.

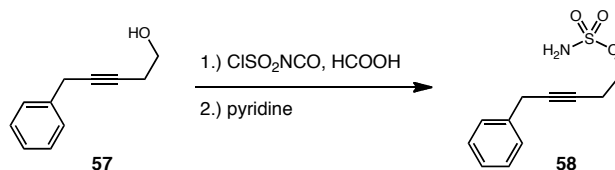
7-phenylhept-3-yn-1-ol (48). Prepared according to general procedure C using 2-(7-phenylhept-3-ynoxy)tetrahydro-2H-pyran (0.42 g, 1.5 mmol). Purification by flash chromatography afforded 7-phenylhept-3-yn-1-ol (**48**) as a colorless oil (0.23 g, 81 %); **R_f** 0.27 (3:1 hexanes/EtOAc); **IR** (thin film, cm⁻¹) 3346, 3026, 2938, 2859, 1498 1454, 1045; **¹H NMR** (CDCl₃, 600 MHz) 7.31-7.20 (m, 5H), 3.71 (t, 2H, *J* = 6.9 Hz), 2.72 (t, 2H, *J* = 7.6 Hz), 2.47 (tt, 2H, *J* = 6.2, 2.4 Hz), 2.20 (tt, 2H, *J* = 7.1, 2.4 Hz), 1.83 (qn, 2H, *J* = 7.1 Hz); **¹³C NMR** (CDCl₃, 150 MHz) 141.8, 128.7, 128.5, 126.1, 82.4, 77.1, 61.6, 35.0, 30.7, 23.4, 18.4; **HRMS** (+ESI) calculated for C₁₃H₁₇O 189.1274, found 189.1309 [M+H]⁺.

7-phenylhept-3-yn-1-yl sulfamate (49). Prepared according to general procedure **D** using 7-phenylhept-3-yn-1-ol (**48**) (0.29 g, 1.5 mmol), chlorosulfonyl isocyanate (0.20 mL, 2.3 mmol) and formic acid (0.09 mL, 2.3 mmol). After 30 mins the reaction was quenched by the addition of EtOAc (30 mL) and H₂O (15 mL). Purification by flash chromatography (3:1 → 2:1 hexanes/EtOAc) afforded 7-phenylhept-3-yn-1-yl sulfamate (**49**) as a colorless oil (0.27 g, 83 %); **R_f** 0.26 (3:1 hexanes/EtOAc); **IR** (thin film, cm⁻¹) 3383, 3287, 3026, 2936, 1365, 1183; **¹H NMR** (CDCl₃, 600 MHz) 7.31-7.19 (m, 5H), 4.77 (bs, 2H), 4.28 (t, 2H, *J* = 7.1 Hz), 2.72 (t, 2H, *J* = 7.6 Hz), 2.67 (t, 2H, *J* = 7.2 Hz), 2.18 (tt, 2H, *J* = 7.2, 2.4 Hz), 1.82 (qn, 2H, *J* = 7.2 Hz). **¹³C NMR** (CDCl₃, 150 MHz) 141.8, 128.7, 128.6, 126.1, 82.8, 75.0, 69.4, 34.9, 30.5, 19.9, 18.3; **HRMS** (+ESI) calculated for C₁₃H₁₈NO₃S 268.1002, found 268.0996 [M+H]⁺.

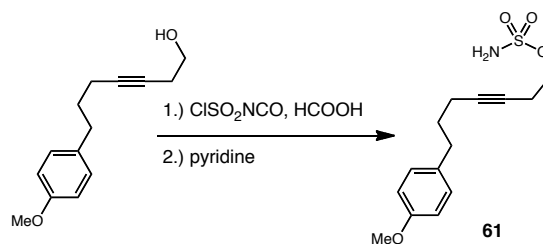


6-phenylhex-3-yn-1-yl sulfamate (56). Prepared according to general procedure **D** using 6-phenylhex-3-yn-1-ol³³ (**55**) (0.69 g, 4.0 mmol), chlorosulfonyl isocyanate (0.60 mL, 6.9 mmol) and formic acid (0.27 mL, 6.9 mmol). After 15 mins the reaction was quenched by the addition of EtOAc (30 mL) and H₂O (15 mL). Purification by flash chromatography (3:1→2:1 hexanes/EtOAc) afforded 6-phenylhex-3-yn-1-yl sulfamate (**56**) as a white amorphous solid (0.80 g, 78 %); **R_f** 0.21 (3:1 hexanes/EtOAc); **IR** (thin film, cm⁻¹) 3382, 3284, 3027, 2926, 1360, 1177; **¹H NMR** (CDCl₃, 600 MHz) 7.34-7.22

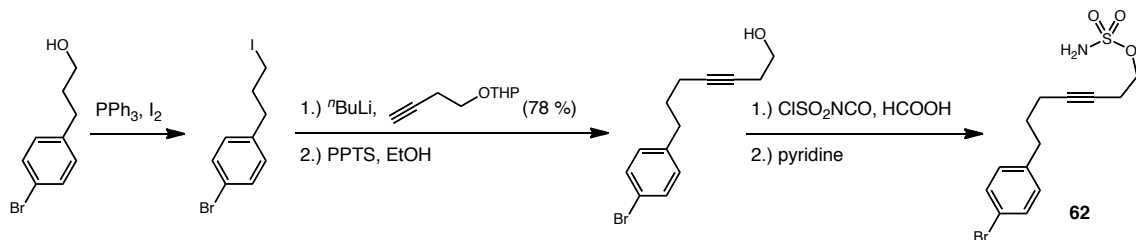
(m, 5H), 4.70 (bs, 2H), 4.22 (t, 2H, $J = 6.7$ Hz), 2.81 (t, 2H, $J = 7.3$ Hz), 2.62 (tt, 2H, $J = 7.0, 2.2$ Hz), 2.47 (tt, 2H, $J = 7.3, 2.2$ Hz). ^{13}C NMR (CDCl₃, 150 MHz) 140.8, 128.7, 128.6, 126.5, 82.3, 75.5, 69.3, 35.2, 20.9, 19.9; **HRMS** (+ESI) calculated for C₁₂H₁₆NO₃S 254.0845, found 254.0857 [M+H]⁺.



5-phenylpent-3-yn-1-yl sulfamate (58). Prepared according to general procedure **D** using 5-phenylpent-3-yn-1-ol²¹ (**57**) (0.25 g, 1.5 mmol), chlorosulfonyl isocyanate (0.45 mL, 5.1 mmol) and formic acid (0.19 mL, 5.1 mmol). After 15 mins the reaction was quenched by the addition of EtOAc (30 mL) and H₂O (15 mL). Purification by flash chromatography (3:1→2:1 hexanes/EtOAc) afforded 5-phenylpent-3-yn-1-yl sulfamate (**58**) as a white amorphous solid (0.31 g, 85 %); R_f 0.28 (3:1 hexanes/EtOAc); **IR** (thin film, cm⁻¹) 3383, 3285, 3029, 1364, 1180; ^1H NMR (CDCl₃, 600 MHz) 7.34-7.24 (m, 5H), 4.79 (bs, 2H), 4.29 (t, 2H, $J = 7.2$ Hz), 3.58 (t, 2H, $J = 2.4$ Hz), 2.70 (tt, 2H, $J = 7.2, 2.3$ Hz). ^{13}C NMR (CDCl₃, 150 MHz) 137.0, 128.8, 128.1, 126.9, 80.8, 76.9, 69.3, 25.2, 19.9; **HRMS** (+ESI) calculated for C₁₁H₁₄NO₃S 240.0689, found 240.0685 [M+H]⁺.



7-(4-methoxyphenyl)hept-3-yn-1-yl sulfamate (61). Prepared according to general procedure **D** using 7-(4-methoxyphenyl)hept-3-yn-1-ol (0.80 g, 3.0 mmol), chlorosulfonyl isocyanate (0.39 mL, 4.5 mmol) and formic acid (0.17 mL, 4.5 mmol). After 1.5 h the reaction was quenched by the addition of EtOAc (30 mL) and H₂O (15 mL). Purification by flash chromatography (2:1 hexanes/EtOAc) afforded 7-(4-methoxyphenyl)hept-3-yn-1-yl sulfamate (**61**) as a white amorphous solid (0.61 g, 73 %); **R_f** 0.27 (3:1 hexanes/EtOAc); **IR** (thin film, cm⁻¹) 3384, 3285, 2940, 1488, 1365, 1183; **¹H NMR** (CDCl₃, 600 MHz) 7.41 (d, 2H, *J* = 8.3 Hz), 7.07 (d, 2H, *J* = 8.3 Hz), 4.86 (bs, 2H), 4.27 (t, 2H, *J* = 7.0 Hz), 2.67-2.64 (m, 4H), 2.17-2.14 (m, 2H), 1.78 (qn, 2H, *J* = 7.0 Hz). **¹³C NMR** (CDCl₃, 150 MHz) 140.7, 131.6, 130.5, 119.8, 82.5, 75.2, 69.4, 34.3, 30.3, 19.9, 18.2; **HRMS** (-ESI) calculated for C₁₄H₁₈NO₄S 296.0962, found 296.0963 [M-H]⁻.



1-bromo-4-(3-iodopropyl)benzene. I₂ (3.5 g, 14 mmol) in Et₂O (8 mL) was added to a solution of PPh₃ (3.7 g, 14 mmol), imidazole (0.95 g, 14 mmol), and 3-(4-bromophenyl)propan-1-ol³⁴ (2.0 g, 9.3 mmol) in Et₂O/MeCN (3:1, 34 mL total) at 0 °C. This solution was warmed to ambient temperature. After 45 mins the reaction was diluted with Et₂O, passed through a pad of SiO₂ and eluted with Et₂O. Purification by flash chromatography (100 % pentane) afforded 1-bromo-4-(3-iodopropyl)benzene as a colorless oil (1.9 g, 62 %); **R_f** 0.33 (100 % hexanes); **IR** (thin film, cm⁻¹) 2935, 2855, 1487, 1210, 1071, 1010; **¹H NMR** (CDCl₃, 600 MHz) 7.42 (dt, 2H, *J* = 8.3, 1.9 Hz), 7.09 (dt, 2H, *J* = 8.3, 1.9 Hz), 3.16 (t, 2H, *J* = 6.7 Hz), 2.70 (t, 2H, *J* = 7.3 Hz), 2.10 (qn, 2H, *J* = 7.0 Hz). **¹³C NMR** (CDCl₃, 150 MHz) 139.5, 131.8, 130.5, 120.2, 35.8, 34.8, 6.2; **HRMS** (+APCI) calculated for C₉H₁₀Br⁸¹I 325.8990, found 325.8081 [M]⁺.

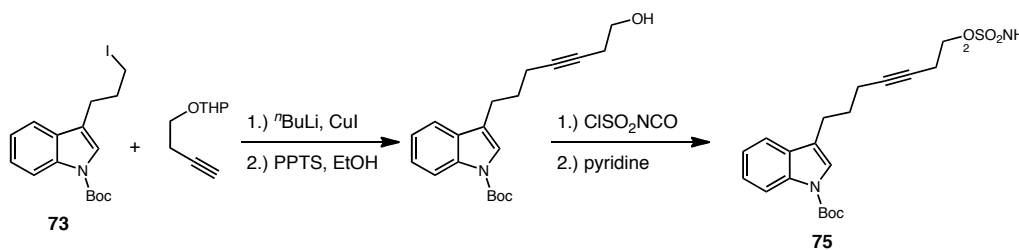
2-(7-(4-bromophenyl)hept-3-ynoxy)tetrahydro-2H-pyran. 2-(but-3-ynoxy)tetrahydro-2H-pyran³¹ (0.60 g, 3.9 mmol) was stirred in THF (26 mL) with triphenylmethane (2 mg) and DMPU (5.2 mL) at -78 °C. ⁿBuLi (2.5 mL, 1.6 M in hexanes, 3.9 mmol) was added dropwise until the solution's color remained consistent. After stirring the mixture for 1 h at -78 °C, 1-bromo-4-(3-iodopropyl)benzene (1.4 g, 4.3 mmol) was added dropwise. The reaction was warmed to ambient temperature. After 4 h the reaction was quenched by the addition of H₂O and extracted with Et₂O (3 x 25 mL).

Purification by flash chromatography (10:1 hexanes/EtOAc) afforded 2-(7-(4-bromophenyl)hept-3-ynyloxy)tetrahydro-2H-pyran as a colorless oil (1.1 g, 78 %); R_f 0.32 (10:1 hexanes/EtOAc); **IR** (thin film, cm^{-1}) 2940, 2867, 1488, 1033; **^1H NMR** (CDCl_3 , 400 MHz) 7.40 (d, 2H, $J = 8.6$ Hz), 7.07 (d, 2H, $J = 8.1$ Hz), 4.66 (t, 1H, $J = 3.3$ Hz), 3.90 (ddd, 1H, $J = 11.4, 8.6, 2.6$ Hz), 3.82 (dt, 1H, $J = 9.5, 7.2$ Hz), 3.57-3.50 (m, 2H), 2.67 (t, 2H, $J = 7.6$ Hz), 2.49 (tt, 2H, $J = 7.1, 2.4$ Hz), 2.16 (tt, 2H, $J = 6.7, 2.4$ Hz), 1.87-1.82 (m, 1H), 1.79-1.50 (m, 4H); **^{13}C NMR** (CDCl_3 , 100 MHz) 140.9, 131.5, 130.5, 119.7, 98.9, 80.7, 77.9, 66.4, 62.4, 34.2, 30.8, 30.5, 25.6, 20.4, 19.6, 18.2; **HRMS** (+ESI) calculated for $\text{C}_{18}\text{H}_{24}\text{Br}^{81}\text{O}_2$ 353.0939, found 353.0946 $[\text{M}+\text{H}]^+$.

7-(4-bromophenyl)hept-3-yn-1-ol. Prepared according to general procedure **C** using 2-(7-(4-bromophenyl)hept-3-ynyloxy)tetrahydro-2H-pyran (1.0 g, 3.1 mmol). The reaction mixture was concentrated and purification by flash chromatography (8:1 \rightarrow 4:1 hexanes/ Et_2O) afforded 7-(4-bromophenyl)hept-3-yn-1-ol as a colorless oil (0.66 g, 78 %); R_f 0.20 (8:1 hexanes/EtOAc); **IR** (thin film, cm^{-1}) 3352, 2942, 1488, 1044; **^1H NMR** (CDCl_3 , 600 MHz) 7.40 (d, 2H, $J = 8.3$ Hz), 7.07 (d, 2H, $J = 8.3$ Hz), 3.70 (q, 2H, $J = 6.0$ Hz), 2.67 (t, 2H, $J = 7.3$ Hz), 2.46 (tt, 2H, $J = 6.4, 2.2$ Hz), 2.19 (tt, 2H, $J = 7.0, 2.5$ Hz), 1.79 (qn, 2H $J = 7.3$ Hz); **^{13}C NMR** (CDCl_3 , 150 MHz) 140.8, 131.6, 130.5, 119.8, 82.1, 77.4, 61.6, 34.4, 30.5, 23.4, 18.3; **HRMS** (+ESI) calculated for $\text{C}_{13}\text{H}_{16}\text{Br}^{81}\text{O}$ 269.0364, found 269.0359 $[\text{M}+\text{H}]^+$.

7-(4-bromophenyl)hept-3-yn-1-yl sulfamate (62). Prepared according to general procedure **D** using 7-(4-bromophenyl)hept-3-yn-1-ol (0.80 g, 3.0 mmol), chlorosulfonyl

isocyanate (0.39 mL, 4.5 mmol) and formic acid (0.17 mL, 4.5 mmol). After 1.5 h the reaction was quenched by the addition of EtOAc (30 mL) and H₂O (15 mL). Purification by flash chromatography (2:1 hexanes/EtOAc) afforded 7-(4-bromophenyl)hept-3-yn-1-yl sulfamate (**62**) as a white amorphous solid (0.61 g, 73 %); *R_f* 0.23 (3:1 hexanes/EtOAc); **IR** (thin film cm⁻¹) 3384, 3285, 2940, 1488, 1365, 1183; **¹H NMR** (CDCl₃, 600 MHz) 7.41 (d, 2H, *J* = 8.3 Hz), 7.07 (d, 2H, *J* = 8.3 Hz), 4.86 (bs, 2H), 4.27 (t, 2H, *J* = 7.0 Hz), 2.67-2.64 (m, 4H), 2.17-2.14 (m, 2H), 1.78 (qn, 2H, *J* = 7.0 Hz). **¹³C NMR** (CDCl₃, 150 MHz) 140.7, 131.6, 130.5, 119.8, 82.5, 75.2, 69.4, 34.3, 30.3, 19.9, 18.2; **HRMS** (-ESI) calculated for C₁₃H₁₅Br⁷⁹NO₃S 343.9962, found 343.9964 [M-H]⁻.



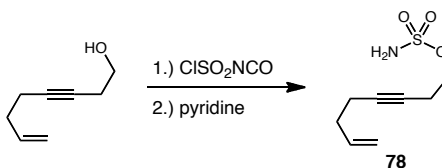
^tButyl 3-(6-(tetrahydro-2H-pyran-2-yloxy)hex-3-ynyl)-1H-indole-1-carboxylate.

ⁿBuLi (2.3 mL, 1.6 M in hexanes, 3.7 mmol) was added dropwise to 2-(but-3-ynyloxy)tetrahydro-2H-pyran³¹ (0.52 g, 3.4 mmol) stirring in THF (5.3 mL) at -78 °C. After 1 h CuI (0.71 g, 3.7 mmol) in THF (5.3 mL) was added slowly, this solution was warmed to -40 °C and stirring was continued 1 h. This solution was then added via cannula to a stirring solution of ^tbutyl 3-(3-iodopropyl)-1H-indole-1-carboxylate³⁵ (**73**) (1.30 g, 3.4 mmol) in THF (5.3 mL) and DMPU (4.0 mL) at -40 °C. After 8 h the reaction was quenched by the addition of satd. aq. NH₄Cl at 0 °C. Purification by flash chromatography (15:1 hexanes/EtOAc) afforded ^tbutyl 3-(6-

(tetrahydro-2H-pyran-2-yloxy)hex-3-ynyl)-1H-indole-1-carboxylate as a colorless oil (1.0 g, 75 %); R_f 0.59 (8:1 hexanes/EtOAc); **IR** (thin film, cm^{-1}) 2938, 2869, 1731, 1454, 1370, 1157; **$^1\text{H NMR}$** (CDCl_3 , 400 MHz) 8.12 (bs, 1H), 7.54 (d, 1H, $J = 7.6$ Hz), 7.37 (bs, 1H), 7.31 (t, 1H, $J = 7.6$ Hz), 7.24 (t, 1H, $J = 7.2$ Hz), 4.66 (t, 1H, $J = 3.3$ Hz), 3.92-3.81 (m, 2H), 3.58-3.50 (m, 2H), 2.80 (t, 2H, $J = 7.6$ Hz), 2.50 (t, 2H, $J = 7.2$ Hz), 2.25 (t, 2H, $J = 7.2$ Hz), 1.19-1.81 (m, 3H), 1.74-1.68 (m, 10H), 1.63-1.57 (m, 2H), 1.54-1.51 (m, 2H); **$^{13}\text{C NMR}$** (CDCl_3 , 100 MHz) 150.0, 135.7, 130.9, 124.4, 122.7, 122.5, 120.6, 119.2, 115.4, 99.0, 83.5, 80.9, 77.7, 66.4, 62.4, 30.8, 29.8, 28.7, 25.6, 24.1, 20.5, 19.7, 18.7; **HRMS** (+APCI) calculated for $\text{C}_{25}\text{H}_{34}\text{NO}_4$ 412.2482, found 412.2489 $[\text{M}+\text{H}]^+$.

t Butyl 3-(6-hydroxyhex-3-ynyl)-1H-indole-1-carboxylate. Prepared according to general procedure **C** using t butyl 3-(6-(tetrahydro-2H-pyran-2-yloxy)hex-3-ynyl)-1H-indole-1-carboxylate (1.0 g, 2.5 mmol). The solution was concentrated *in vacuo*, and the residue was purified by flash chromatography (12:1 hexanes/EtOAc) to afford t butyl 3-(6-hydroxyhex-3-ynyl)-1H-indole-1-carboxylate as a colorless oil (0.77 g, 94 %); R_f 0.19 (8:1 hexanes/EtOAc); **IR** (thin film, cm^{-1}) 3395, 2977, 2935, 1729, 1453, 1370, 1156; **$^1\text{H NMR}$** (CDCl_3 , 600 MHz) 8.13 (bs, 1H), 7.54 (d, 1H, $J = 7.6$ Hz), 7.39 (bs, 1H), 7.32 (t, 1H, $J = 8.1$ Hz), 7.25 (t, 1H, $J = 7.6$ Hz), 3.71 (q, 2H, $J = 6.2$ Hz), 2.80 (t, 2H, $J = 7.6$ Hz), 2.47 (tt, 2H, $J = 6.2, 1.9$ Hz), 2.27 (tt, 2H, $J = 7.2, 1.9$ Hz), 1.91 (qn, 2H, $J = 7.2$ Hz), 1.79 (bs, 1H), 1.68 (s, 9H); **$^{13}\text{C NMR}$** (CDCl_3 , 150 MHz) 150.1, 135.7, 130.9, 124.5, 122.8, 122.5, 120.5, 119.2, 115.5, 83.6, 82.3, 77.5, 61.6, 28.6, 28.4, 24.1, 23.4, 18.7; **HRMS** (+ESI) calculated for $\text{C}_{20}\text{H}_{26}\text{NO}_3$ 328.1907, found 328.1906 $[\text{M}+\text{H}]^+$.

^tButyl 3-(7-(sulfamoyloxy)hept-4-yn-1-yl)-1H-indole-1-carboxylate (75). Prepared according to general procedure **D** using ^tbutyl 3-(6-hydroxyhex-3-ynyl)-1H-indole-1-carboxylate (0.76 g, 2.3 mmol), chlorosulfonyl isocyanate (0.31 mL, 3.5 mmol) and formic acid (0.14 mL, 3.5 mmol). After 1 h the reaction was quenched by the addition of EtOAc (20 mL) and H₂O (10 mL). Purification by flash chromatography (3:1→1:1 hexanes/EtOAc) afforded ^tbutyl 3-(7-(sulfamoyloxy)hept-4-yn-1-yl)-1H-indole-1-carboxylate (**75**) as a white amorphous solid (0.70 g, 74 %); **R_f** 0.14 (3:1 hexanes/EtOAc); **IR** (thin film, cm⁻¹) 3278, 2978, 2935, 1728, 1370, 1183, 1156; **¹H NMR** (CDCl₃, 600 MHz) 8.09 (bs, 1H), 7.54 (d, 2H, *J* = 7.6 Hz), 7.41 (bs, 1H), 7.32 (t, 1H, *J* = 7.6 Hz), 7.25 (t, 1H, *J* = 7.6 Hz), 4.90 (bs, 2H), 4.28 (t, 2H, *J* = 7.2 Hz), 2.82 (t, 2H, *J* = 7.2 Hz), 2.66 (tt, *J* = 6.7, 2.4 Hz), 2.23 (t, 2H, *J* = 7.1 Hz), 1.89 (qn, 2H, *J* = 7.1 Hz), 1.68 (s, 9H); **¹³C NMR** (CDCl₃, 150 MHz) 150.2, 135.7, 130.9, 124.5, 122.9, 122.6, 120.3, 119.2, 115.5, 83.9, 82.5, 75.4, 69.3, 28.5, 23.8, 20.0, 18.3; **HRMS** (-ESI) calculated for C₂₀H₂₅N₂O₅S 405.1490, found 405.1489 [M-H]⁻.



Oct-7-en-3-yn-1-yl sulfamate (78). Prepared according to general procedure **D** using oct-7-en-3-yn-1-ol³⁶ (68 mg, 0.55 mmol), chlorosulfonyl isocyanate (0.032 mL, 0.83 mmol) and formic acid (0.072 mL, 0.83 mmol). After 1 h the reaction was quenched by the addition of EtOAc (8 mL) and H₂O (4 mL). Purification by flash chromatography

(3:1 hexanes/EtOAc) afforded oct-7-en-3-yn-1-yl sulfamate (**78**) as a white amorphous solid (47 mg, 43 %); R_f 0.13 (3:1 hexanes/EtOAc); **IR** (thin film, cm^{-1}) 3272, 2923, 2869, 1437, 1351, 1173; **$^1\text{H NMR}$** (CDCl_3 , 400 MHz) 5.91-5.79 (m, 1H), 5.14 (bs, 2H), 5.13-5.03 (m, 2H), 4.24 (t, 2H, $J = 7.2$ Hz), 2.63 (t, 2H, $J = 6.8$ Hz), 2.22 (s, 4H); **$^{13}\text{C NMR}$** (CDCl_3 , 100 MHz) 137.1, 115.9, 82.4, 75.0, 69.3, 33.0, 19.8, 18.6; **HRMS** (+ESI) calculated for $\text{C}_8\text{H}_{14}\text{NO}_3\text{S}$ 204.0689, found 204.0650 $[\text{M}+\text{H}]^+$.

Procedures and Characterization for Metallonitrene/Alkyne Cascade Reactions

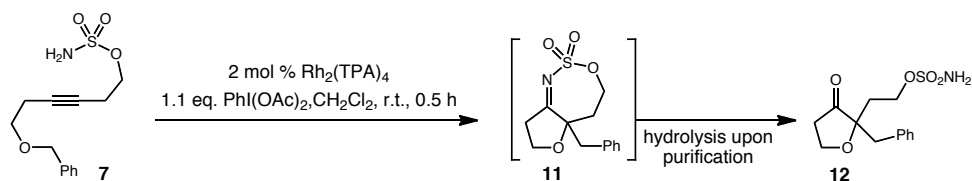
General procedure (E) for oxathiazepane synthesis.

Sulfamate ester (1.0 eq.), $\text{PhI}(\text{OAc})_2$ (1.1 eq.) and $\text{Rh}_2(\text{esp})_2$ (2 mol %) were combined in a 2 dram reaction vial and capped with a teflon lined septum. CH_2Cl_2 was added and the reaction was stirred under argon at ambient temperature until thin layer chromatography indicated complete consumption of starting material (15 - 30 min). MeOH (1.5 mL) and NaBH_4 (3 eq.) were added and the reaction was stirred for 1 h. SiO_2 (*ca.* 250 mg) was added and the resulting mixture was concentrated. The silica was then eluted with $\text{CH}_2\text{Cl}_2/\text{Et}_2\text{O}$ (1:1, 10 mL). The eluent was concentrated *in vacuo* and the residue was purified by flash chromatography on silica gel as indicated.

General procedure (F) for oxathiazepane synthesis.

Sulfamate ester (1.0 eq.), $\text{PhI}(\text{OAc})_2$ (1.1 eq.) and $\text{Rh}_2(\text{esp})_2$ (2 mol %) were combined in a 2 dram reaction vial and capped with a teflon lined septum. CH_2Cl_2 (0.175 M) was added and the reaction was stirred under argon at 40 °C until thin layer chromatography

indicated complete consumption of starting material (15 min - 2 h). The resulting solution was concentrated *in vacuo* and the residue was purified by flash chromatography on silica gel as indicated.



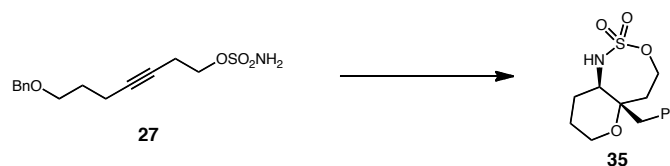
2-(2-benzyl-3-oxotetrahydrofuran-2-yl)ethyl sulfamate (12). 6-(benzyloxy)hex-3-yn-1-yl sulfamate (**7**) (50 mg, 0.18 mmol), PhI(OAc)₂ (63 mg, 0.19 mmol) and Rh₂(TPA)₄ (5.4 mg mg, 0.004 mmol) were combined in a 2 dram reaction vial and capped with a teflon lined septum. CH₂Cl₂ was added and the reaction was stirred under argon at ambient temperature until thin layer chromatography indicated complete consumption of starting material (15 min). The reaction mixture was concentrated *in vacuo* and the residue purified by flash chromatography (3:1 hexanes/EtOAc) to afford 2-(2-benzyl-3-oxotetrahydrofuran-2-yl)ethyl sulfamate (**12**) (22 mg, 45 %); **R_f** 0.37 (3:1 hexanes/EtOAc); **IR** (thin film, cm⁻¹) 3365, 3277, 2921, 2851, 1749, 1369, 1180, 935; **¹H NMR** (CDCl₃, 600 MHz) δ 7.31-7.17 (m, 5H), 4.82 (bs, 2H), 4.36 (dt, 1H, *J* = 12.0, 6.0 Hz), 4.31-4.26 (m, 1H), 4.21-4.16 (m, 1H), 3.87 (q, 1H, *J* = 6.0 Hz), 2.95 (d, 1H, *J* = 18.0 Hz), 2.74 (d, 1H, *J* = 18.0 Hz), 2.58-2.52 (m, 1H), 2.39-2.30 (m, 1H), 2.40-1.91 (m, 2H); **HRMS** (-ESI) calculated for C₁₃H₁₇NO₅S 299.0827, found 298.0807 [M-H]⁻.



5a-benzylhexahydro-1H-furo[3,2-d][1,2,3]oxathiazepine 2,2-dioxide (13). Prepared by general procedure **E** using 6-(benzyloxy)hex-3-yn-1-yl sulfamate (**7**) (50 mg, 0.18 mmol), $\text{PhI}(\text{OAc})_2$ (63 mg, 0.19 mmol) and $\text{Rh}_2(\text{esp})_2$ (1.6 mg, 0.004 mmol) in CH_2Cl_2 (1.0 mL). Flash chromatography (3:1 hexanes/EtOAc) afforded 5a-benzylhexahydro-1H-furo[3,2-d][1,2,3]oxathiazepine 2,2-dioxide (**13**) as a white crystalline solid (33 mg, 65 %); R_f 0.17 (3:1 hexanes/EtOAc); **IR** (thin film, cm^{-1}) 3289, 2893, 1360, 1179, 1720; **^1H NMR** (CDCl_3 , 600 MHz) δ 7.33 (t, 2H, $J = 7.6$ Hz), 7.28 (t, 1H, $J = 7.2$ Hz), 7.22 (d, 2H, $J = 7.5$ Hz), 4.82 (d, 1H, $J = 10.5$), 4.47-4.52 (m, 1H), 4.44 (ddd, 1H, $J = 12.9, 5.2, 3.3$ Hz), 4.18 (td, 1H, $J = 9.5, 3.3$ Hz), 4.09 (dd, 1H, $J = 17.6, 8.6$ Hz), 3.91 (td, 1H, $J = 11.4, 8.1$ Hz), 2.86 (s, 2H), 2.44 (dtd, 1H, $J = 11.4, 8.6, 3.3$ Hz), 1.94-2.02 (m, 2H), 1.82 (ddd, 1H, $J = 15.3, 11.4, 5.2$ Hz); **^{13}C NMR** (CDCl_3 , 150 MHz) δ 135.9, 130.6, 128.7, 127.2, 82.0, 68.3, 64.3, 60.0, 36.0, 33.6, 28.6; **m.p.** 159-160 °C; **HRMS** (-ESI) calculated for $\text{C}_{13}\text{H}_{16}\text{NO}_4\text{S}$ 282.0800, found 282.0807 $[\text{M}-\text{H}]^-$.

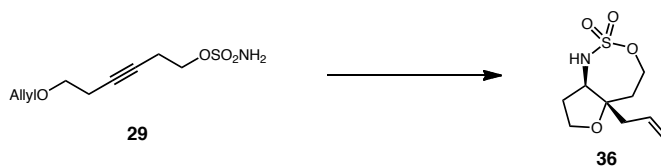


5a-allyloctahydropyrano[3,2-d][1,2,3]oxathiazepine 2,2-dioxide (25). Prepared by general procedure **E** using 7-(allyloxy)hept-3-yn-1-yl sulfamate (**24**) (50 mg, 0.20 mmol), $\text{PhI}(\text{OAc})_2$ (72 mg, 0.22 mmol) and $\text{Rh}_2(\text{esp})_2$ (1.8 mg, 0.004 mmol) in CH_2Cl_2 (1.2 mL). Flash chromatography (3:1 hexanes/EtOAc) afforded 5a-allyloctahydropyrano[3,2-d][1,2,3]oxathiazepine 2,2-dioxide (**25**) as a white crystalline solid (34 mg, 67 %, 3:1 anti:syn); R_f 0.17 (3:1 hexanes/EtOAc); **IR** (thin film, cm^{-1}) 3293, 2956, 1437, 1339, 1179, 1090, 1026; **$^1\text{H NMR}$** (CDCl_3 , 600 MHz) δ 5.76 (dddd, 1H, $J = 17.2, 10.0, 9.1, 5.2$ Hz), 5.24 (d, 1H, $J = 10.5$ Hz), 5.18 (d, 1H, $J = 17.2$ Hz), 5.04 (1H, d, $J = 10.0$ Hz), 4.32 (t, 1H, $J = 12.9$ Hz), 4.22-4.28 (m, 2H), 3.64 (m, 1H), 3.51 (td, 1H, $J = 11.9, 4.3$ Hz), 3.33-3.41 (m, 2H), 2.81 (ddd, 1H, $J = 15.3, 4.8, 1.9$ Hz), 2.30 (dd, 1H, $J = 15.2, 8.6$ Hz), 2.04-2.11 (m, 1H), 1.88-1.98 (m, 3H), 1.68-1.76 (m, 3H), 1.58-1.66 (m, 1H); **$^{13}\text{C NMR}$** (CDCl_3 , 150 MHz) δ 131.8, 119.8, 76.3, 60.2, 56.1, 38.9, 28.5, 25.9, 25.7; **m.p.** 137-139 °C; **HRMS** (-ESI) calculated for $\text{C}_{10}\text{H}_{16}\text{NO}_4\text{S}$ 246.0800, found 246.0807 $[\text{M}-\text{H}]^-$.



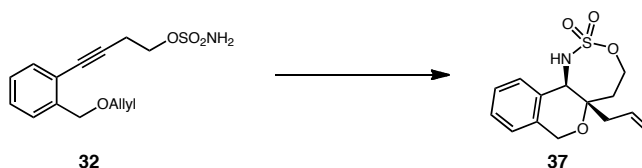
5a-benzyloctahydropyrano[3,2-d][1,2,3]oxathiazepine 2,2-dioxide (35). Prepared by general procedure **E** using 7-(benzyloxy)hept-3-yn-1-yl sulfamate (**27**) (50 mg, 0.17

mmol), $\text{PhI}(\text{OAc})_2$ (60 mg, 0.19 mmol), $\text{Rh}_2(\text{esp})_2$ (2.5 mg, 0.003 mmol) in CH_2Cl_2 (1.0 mL). Flash chromatography (3:1 hexanes/EtOAc) afforded 5a-benzyl octahydro-pyrano[3,2-d][1,2,3]oxathiazepine 2,2-dioxide (**35**) as a white crystalline solid (28 mg, 56 %); R_f 0.18 (3:1 hexanes/EtOAc); **IR** (thin film, cm^{-1}) 3294, 2946, 1437, 1339, 1180, 1086, 1036, 930; **^1H NMR** (CDCl_3 , 600 MHz) δ 7.32 (t, 2H, $J = 7.6$ Hz), 7.26 (t, 2H, $J = 7.2$ Hz), 7.20 (d, 1H, $J = 7.2$ Hz), 4.80 (d, 1H, $J = 9.5$ Hz), 4.40 (td, 1H, $J = 12.9, 1.4$ Hz), 4.17 (dt, 1H, $J = 12.9, 3.8$ Hz), 3.91 (td, 1H, $J = 11.9, 3.8$ Hz), 3.82 (m, 1H), 3.53 (ddd, 1H, $J = 13.3, 10.0, 4.8$ Hz), 3.46 (d, 1H, $J = 15.3$ Hz), 2.77 (d, 1H, $J = 15.3$ Hz), 2.02 (m, 1H), 1.82-1.91 (m, 3H), 1.78 (ddd, 1H, $J = 13.8, 3.3, 1.4$ Hz), 1.71 (qd, 1H, $J = 12.9, 5.2$ Hz); **^{13}C NMR** (CDCl_3 , 150 MHz) δ 136.0, 130.4, 129.0, 127.2, 77.5, 67.5, 28.6, 26.2, 25.9; **m.p.** 168-170 °C; **HRMS** (-ESI) calculated for $\text{C}_{13}\text{H}_{16}\text{NO}_4\text{S}$ 296.0957, found 296.0966 $[\text{M}-\text{H}]^-$.



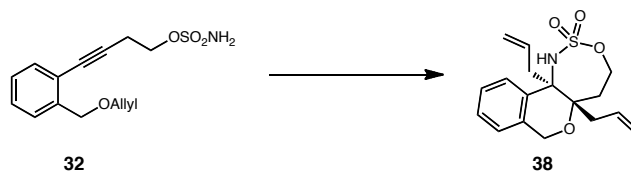
5a-allylhexahydro-1H-furo[3,2-d][1,2,3]oxathiazepine 2,2-dioxide (36). Prepared by general procedure **E** using 6-(allyloxy)hex-3-yn-1-yl sulfamate (**29**) (50 mg, 0.21 mmol), $\text{PhI}(\text{OAc})_2$ (76 mg, 0.24 mmol) and $\text{Rh}_2(\text{esp})_2$ (3.2 mg, 0.004 mmol) in CH_2Cl_2 (1.2 mL). Flash chromatography (3:1 hexanes/EtOAc) afforded 5a-allylhexahydro-1H-furo[3,2-d][1,2,3]oxathiazepine 2,2-dioxide (**36**) as a white crystalline solid (38 mg, 76 %); R_f 0.17 (3:1 hexanes/EtOAc); **IR** (thin film, cm^{-1}) 3281, 2894, 1457, 1360, 1180, 1035; **^1H NMR** (CDCl_3 , 600 MHz) δ 5.86 (dddd, 1H, $J = 17.2, 10.0, 8.6, 5.2$ Hz), 5.24 (d, 1H, $J =$

10.0 Hz), 5.19 (d, 1H, $J = 17.2$), 4.54 (d, 1H, $J = 11.4$ Hz), 4.47 (ddd, 1H, $J = 13.0, 5.2, 3.8$ Hz), 4.38 (ddd, 1H, $J = 13.3, 11.4, 3.3$ Hz), 3.96-4.03 (m, 2H), 3.83 (td, 1H, $J = 11.0, 8.1$ Hz), 2.29-2.43 (m, 3H), 2.27 (dt, 1H, $J = 14.8, 3.3$ Hz) 1.87-1.98 (m, 2H); ^{13}C NMR (CDCl₃, 150 MHz) δ 131.8, 119.8, 81.4, 68.1, 64.3, 59.6, 36.1, 33.2, 28.5; **m.p.** 106-109 °C; **HRMS** (-ESI) calculated for C₉H₁₄NO₄S 232.0644, found 232.0651 [M-H]⁻.



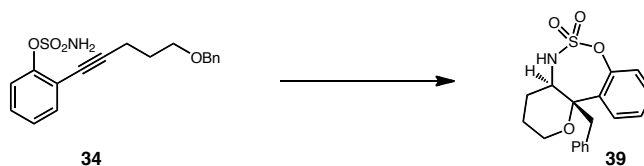
5a-allyl-1,4,5,5a,7,11b-hexahydroisochromeno[4,3-d][1,2,3]oxathiazepine 2,2-dioxide (37). Prepared by general procedure **E** using ((4-(2-((allyloxy)methyl)phenyl)but-3-yn-1-yl)oxy)(aminoperoxy)sulfane (**32**) (50 mg, 0.17 mmol), PhI(OAc)₂ (60 mg, 0.19 mmol) and Rh₂(esp)₂ (2.6 mg, 0.003 mmol) in CH₂Cl₂ (1 mL). Flash chromatography (3:1 hexanes/EtOAc) afforded 5a-allyl-1,4,5,5a,7,11b-hexahydroisochromeno[4,3-d][1,2,3]oxathiazepine 2,2-dioxide (**37**) as a white amorphous solid (48 mg, 98 %); **R_f** 0.28 (3:1 hexanes/EtOAc); **IR** (thin film, cm⁻¹) 3289, 2924, 1455, 1351, 1181, 1081, 945; ^1H NMR (CDCl₃, 600 MHz) δ 7.64 (d, 1H, $J = 7.2$ Hz), 7.34-7.28 (m, 2H), 7.04 (d, 1H, $J = 6.7$ Hz), 5.84 (dddd, 1H, $J = 17.2, 10.0, 8.6, 5.2$ Hz), 5.27 (d, 1H, $J = 10.5$ Hz), 5.19 (d, 1H, 17.1), 4.82 (dd, 2H, $J = 15.7, 7.8$ Hz), 4.76 (d, 1H, $J = 11.0$ Hz), 4.60 (d, 1H, $J = 11.4$ Hz), 4.43 (td, 1H, $J = 12.9, 1.4$ Hz), 4.38 (dt, 1H, $J = 12.9, 3.8$ Hz), 2.44 (m, 1H), 2.38 (dd, 1H, $J = 15.7, 8.6$ Hz), 2.29 (ddd, 1H, $J = 15.2, 3.3, 1.4$ Hz), 2.16 (m, 1H); ^{13}C NMR (CDCl₃, 150 MHz) δ 134.2, 131.5, 130.4, 128.1, 127.7, 126.4, 124.0, 120.4, 75.1, 67.0,

62.7, 56.4, 38.1, 30.4; **HRMS** (-ESI) calculated for C₁₄H₁₆NO₄S 294.0800, found 294.0810 [M-H]⁻.



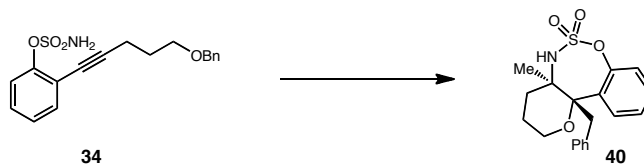
5a,11b-diallyl-1,4,5,5a,7,11b-hexahydroisochromeno[4,3-d][1,2,3]oxathiazepine 2,2-dioxide (38). ((4-(2-((allyloxy)methyl)phenyl)but-3-yn-1-yl)oxy)(aminoperoxy)sulfane (**32**) (50 mg, 0.17 mmol), PhI(OAc)₂ (60 mg, 0.19 mmol) and Rh₂(esp)₂ (2.6 mg, 0.003 mmol) were combined in CH₂Cl₂ (1 mL) and stirred at ambient temperature for 30 mins. The solution was cooled to -78 °C and allylmagnesium bromide (1.0 M in Et₂O, 0.54 mL, 0.54 mmol) was added dropwise. The reaction was stirred at -78 °C for 30 mins, quenched by addition of silica (*ca.* 250 mg) and concentrated *in vacuo*. Flash chromatography (4:1 hexanes/ EtOAc) afforded 5a,11b-diallyl-1,4,5,5a,7,11b-hexahydroisochromeno[4,3-d][1,2,3]oxathiazepine 2,2-dioxide (**38**) as a white crystalline solid (46 mg, 81 %); **R_f** 0.33 (3:1 hexanes/EtOAc); **IR** (thin film, cm⁻¹) 3284, 3075, 2976, 1429, 1347, 1177, 920; **¹H NMR** (CDCl₃, 600 MHz) δ 7.49-7.52 (m, 1H), 7.24-7.28 (m, 2H), 7.00-7.03 (m, 1H), 5.78-5.86 (m, 1H), 5.71-5.78 (m, 1H), 5.22 (d, 1H, *J* = 10.5 Hz), 5.13 (d, 1H *J* = 16.7 Hz), 4.66 (d, 1H, *J* = 17.2 Hz), 4.55 (s, 2H), 4.45 (t, 1H, *J* = 12.4 Hz), 4.38 (dt, 1H, *J* = 13.3, 3.3 Hz), 3.19 (dd, 1H, *J* = 14.8, 5.7 Hz), 2.89 (dd, 1H, *J* = 14.8, 8.6 Hz), 2.52 (dd, 1H, *J* = 15.2, 9.1 Hz), 2.38-2.44 (m, 2H), 2.12 (dd, 1H, *J* = 14.3, 2.4 Hz); **¹³C NMR** (CDCl₃, 150 MHz) δ 135.2, 133.5, 133.2, 132.5, 128.0, 126.8, 126.5,

123.8, 119.9, 118.4, 78.5, 66.5, 63.5, 63.4, 38.6, 33.3, 33.2; **m.p.** 166-168 °C; **HRMS** (-ESI) calculated for C₁₇H₂₀NO₄S 334.1113, found 334.1123 [M-H]⁻.



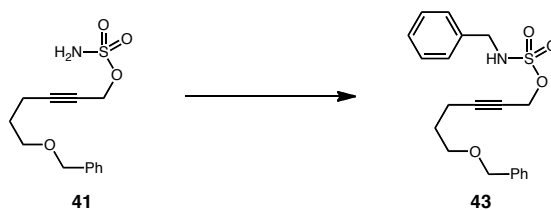
11b-benzyl-2,3,4,4a,5,11b-hexahydrobenzo[f]pyrano[3,2-d][1,2,3]oxathiazepine 6,6-dioxide (39). 2-(5-(benzyloxy)pent-1-yn-1-yl)phenyl sulfamate (**34**) (0.03 g, 0.86 mmol), $\text{PhI}(\text{OAc})_2$ (0.31 g, 0.095 mmol) and $\text{Rh}_2(\text{esp})_2$ (0.0013 g, 0.0017 mmol) were combined in a 2 dram reaction vial and capped with a teflon lined septum. CH_2Cl_2 (0.49 mL) was added and the reaction was stirred under argon at 40 °C for 1 h. The reaction was cooled to -78 °C and LAH (0.19 mL, 2 M in THF, 0.39 mmol) was added. The reaction was stirred at -78 °C for 9 h. It was quenched by the addition of SiO_2 (ca. 250 mg), warmed to ambient temperature and the resulting mixture was concentrated *in vacuo*. The silica was then eluted with $\text{CH}_2\text{Cl}_2/\text{Et}_2\text{O}$ (1:1, 10 mL). The eluent was concentrated *in vacuo* and the residue was purified by flash chromatography (6:1 hexanes/EtOAc) to give 11b-benzyl-2,3,4,4a,5,11b-hexahydrobenzo[f]pyrano[3,2-d][1,2,3]oxathiazepine 6,6-dioxide (**39**) as a white crystalline solid (0.017 g, 57 %); **R_f** 0.33 (3:1 hexanes/EtOAc); **IR** (thin film, cm^{-1}) 3284, 2951, 1479, 1438, 1373, 1192, 1164, 1090; **¹H NMR** (CDCl_3 , 600 MHz) δ 7.38 (dd, 1H, $J = 7.9, 1.6$ Hz), 7.24 (m, 1H), 7.18 (dd, 1H, $J = 7.9, 1.3$ Hz), 7.00-7.08 (m, 4H), 5.03 (d, 1H, $J = 10.8$ Hz), 4.01 (m, 2H), 3.79 (td, 1H, $J = 11.1, 4.8$ Hz), 3.45 (dd, 2H, $J = 14.0, 7.0$ Hz), 2.12-2.20 (m, 1H), 1.71-1.91 (m, 3H); **¹³C NMR** (CDCl_3 , 150 MHz) δ 146.6, 136.2, 135.2, 130.1, 129.6, 128.7, 127.8, 127.0, 126.5, 122.6, 79.8,

60.8, 57.1, 30.3, 27.7. 25.6; **m.p.** 191-193 °C; **HRMS (-ESI)** calcd for C₁₈H₁₈NO₄S 344.0957, found 344.0961 [M-H]⁻.

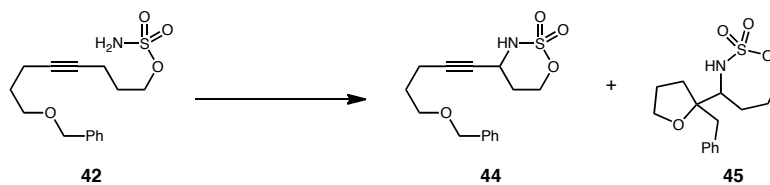


11b-benzyl-4a-methyl-2,3,4,4a,5,11b-hexahydrobenzo[f]pyrano[3,2-

d][1,2,3]oxathiazepine 6,6-dioxide (40). 2-(5-(benzyloxy)pent-1-yn-1-yl)phenyl sulfamate (**34**) (30 mg, 0.087 mmol), PhI(OAc)₂ (31 mg, 0.096 mmol) and Rh₂(esp)₂ (1.3 mg, 0.0017 mmol) were combined in CH₂Cl₂ (1 mL) and stirred at ambient temperature for 30 mins. The solution was cooled to -78 °C and methylmagnesium bromide (3 M in THF, 0.90 mL, 0.27 mmol) was added dropwise. The reaction was stirred at -78 °C for 2 h, quenched by addition of silica (*ca.* 250 mg) and concentrated *in vacuo*. Flash chromatography (5:1 hexanes/ EtOAc) afforded 11b-benzyl-4a-methyl-2,3,4,4a,5,11b-hexahydrobenzo[f]pyrano[3,2-d][1,2,3]oxathiazepine 6,6-dioxide (**40**) as a white crystalline solid (18 mg, 58 %); **R_f** 0.32 (3:1 hexanes/EtOAc); **IR** (thin film, cm⁻¹) 3278, 2950, 1480, 1445, 1370. 1199, 1164, 1085; **¹H NMR** (CDCl₃, 600 MHz) δ 7.37 (dd, 1H, *J* = 8.3, 1.6 Hz), 7.14-7.24 (m, 2H), 7.00-7.09 (m, 3H), 6.84-6.89 (m, 2H), 5.22 (bs, 1H), 4.17 (td, 1H, *J* = 12.4, 2.9 Hz), 4.03 (dd, 1H, *J* = 11.8, 5.4 Hz), 3.73 (s, 2H), 2.02-2.19 (m, 1H), 1.98 (td, 1H, *J* = 13.0, 3.5 Hz), 1.88 (bd, 1H, *J* = 12.7 Hz), 1.76 (bd, 1H, *J* = 13.3 Hz), 1.31 (s, 3H); **¹³C NMR** (CDCl₃, 150 MHz) δ 145.4, 136.2, 135.6, 130.0, 129.4, 128.9, 127.8, 127.1, 126.4, 123.1, 82.3, 60.3, 59.9, 34.3, 30.5, 22.2, 19.9; **m.p.** 202-207 °C; **HRMS (-ESI)** calcd for C₁₉H₂₀NO₄S 358.1113, found 358.1117 [M-H]⁻.

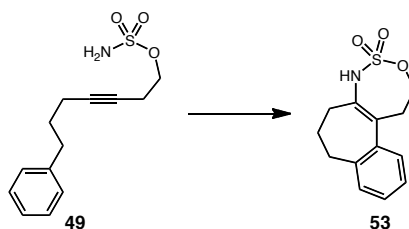


6-(benzyloxy)hex-2-yn-1-yl benzylsulfamate (43). Prepared by general procedure **E** using 6-(benzyloxy)hex-2-yn-1-yl sulfamate (**41**) (50 mg, 0.18 mmol), $\text{PhI}(\text{OAc})_2$ (63 mg, 0.19 mmol) and $\text{Rh}_2(\text{esp})_2$ (2.7 mg, 0.0035 mmol) in CH_2Cl_2 (1.0 mL). Flash chromatography (4:1 hexanes/EtOAc) afforded 6-(benzyloxy)hex-2-yn-1-yl benzylsulfamate (**43**) as a colorless oil (6.5 mg, 10 %); R_f 0.32 (3:1 hexanes/EtOAc); ^{13}C NMR (CDCl_3 , 150 MHz) δ 138.4, 136.1, 129.1, 128.6, 128.4, 128.3, 127.9, 127.8, 90.0, 73.0, 72.9, 68.6, 61.9, 59.1, 52.0, 48.2, 28.4, 16.0; HRMS (-ESI) calculated for $\text{C}_{20}\text{H}_{23}\text{NO}_4\text{S}$ 373.1348, found 372.1273 $[\text{M}-\text{H}]^-$,



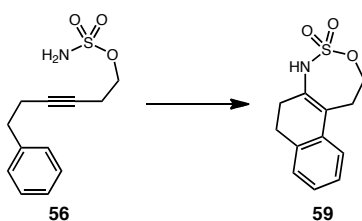
4-(5-(benzyloxy)pent-1-yn-1-yl)-1,2,3-oxathiazinane 2,2-dioxide (44) and 4-(2-benzyltetrahydrofuran-2-yl)-1,2,3-oxathiazepane 2,2-dioxide (45). Prepared by general procedure **E** using 8-(benzyloxy)oct-4-yn-1-yl sulfamate (**42**) (27 mg, 0.087 mmol), $\text{PhI}(\text{OAc})_2$ (31 mg, 0.096 mmol) and $\text{Rh}_2(\text{esp})_2$ (1.3 mg, 0.0018 mmol) in CH_2Cl_2 (0.5 mL). Flash chromatography (3:1:1 hexanes/EtOAc/ CH_2Cl_2) afforded 4-(5-

(benzyloxy)pent-1-yn-1-yl)-1,2,3-oxathiazinane 2,2-dioxide (**44**) as a colorless oil (11 mg, 39 %); R_f 0.32 (3:1:1 hexanes/EtOAc/CH₂Cl₂); **IR** (thin film, cm⁻¹) 3265, 2922, 2852, 2242, 1367, 1181, 1010; **¹H NMR** (CDCl₃, 600 MHz) δ 7.4-7.3 (m, 5H), 4.7 (ddd, 1H, $J = 11.8, 3.2, 2.9$ Hz), 4.53- 4.46 (m, 4H), 4.09 (d, 1H, $J = 10.2$ Hz), 3.54 (t, 2H, $J = 6.0$ Hz), 2.34 (dt, 1H, $J = 7.0, 2.2$ Hz), 2.05-1.88 (m, 2H), 1.80 (tt, 2H, $J = 6.7, 6.0$ Hz); **¹³C NMR** (CDCl₃, 150 MHz) δ 138.6, 128.6, 128.0, 127.9, 86.6, 76.1, 73.1, 71.4, 68.4, 47.9, 31.4, 28.6, 15.6; **HRMS** (-ESI) calculated for C₁₅H₁₉NO₄S 308.0957, found 308.0962 [M-H]⁻, and 4-(2-benzyltetrahydrofuran-2-yl)-1,2,3-oxathiazepane 2,2-dioxide (**45**) as a white amorphous solid (5.7 mg, 21%); R_f 0.26 (3:1:1 hexanes/EtOAc/CH₂Cl₂); **IR** (thin film, cm⁻¹) 3276, 2923, 2852, 2242, 1351, 1180, 935; **¹H NMR** (CDCl₃, 600 MHz) δ 7.31-7.28 (m, 4H), 7.26-7.26 (m, 1H), 4.79 (d, 1H, $J = 9.5$ Hz), 4.35-4.33 (m, 2H), 3.75 (dd, 1H, $J = 8.1, 6.7$ Hz), 3.57 (dd, 1H, $J = 8.1, 6.7$ Hz), 3.30 (dt, 1H, $J = 9.5, 1.9$ Hz), 2.99 (d, 1H, $J = 13.8$ Hz), 2.70 (d, 1H, $J = 13.3$ Hz), 2.26 (bd, 1H, $J = 12.9$ Hz), 2.08-2.02 (m, 2H, Hz), 1.96-1.86 (m, 2H), 1.76- 1.68 (m, 2H), 1.44-1.36 (m, 1H); **¹³C NMR** (CDCl₃, 150 MHz) δ 137.0, 131.0, 128.3, 126.8, 86.5, 70.7, 69.3, 60.5, 41.4, 32.1, 29.4, 28.6, 26.5; **HRMS** (-ESI) calculated for C₁₅H₂₁NO₄S 310.1113, found 310.1119 [M-H]⁻.



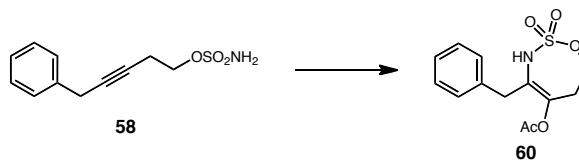
1,2,5,6,7,8-hexahydrobenzo[3,4]cyclohepta[1,2-d][1,2,3]oxathiazepine 4,4-dioxide

(53). Prepared according to general procedure **F** using 7-phenylhept-3-yn-1-yl sulfamate (**49**) (30 mg, 0.088 mmol), $\text{PhI}(\text{OAc})_2$ (39 mg, 0.12 mmol) and $\text{Rh}_2(\text{esp})_2$ (1.7 mg, 0.0022 mmol) in CH_2Cl_2 (0.50 mL). Purification by flash chromatography (6:1 hexanes/EtOAc) afforded 1,2,5,6,7,8-hexahydrobenzo[3,4]cyclohepta[1,2-d][1,2,3]oxathiazepine 4,4-dioxide (**53**) as a white amorphous solid (21 mg, 72 %); R_f 0.45 (2:1 hexanes/EtOAc); **IR** (thin film, cm^{-1}) 3280, 2927, 2857, 1364, 1173, 756; **^1H NMR** (CDCl_3 , 600 MHz) 7.30-7.25 (m, 1H), 7.23-7.16 (m, 3H), 6.07 (bs, 1H), 4.52 (t, 2H, $J = 3.5$ Hz), 3.05 (t, 2H, $J = 5.1$ Hz), 2.77 (t, 2H, $J = 7.0$ Hz), 2.33 (qn, 2H, $J = 7.3$ Hz), 1.97 (t, 2H, 7.0 Hz); **^{13}C NMR** (CDCl_3 , 150 MHz) 141.0, 140.9, 133.8, 129.5, 128.2, 127.6, 126.8, 126.7, 71.4, 34.6, 34.4, 31.9, 31.8; **HRMS** (-ESI) calculated for $\text{C}_{13}\text{H}_{14}\text{NO}_3\text{S}$ 264.0700, found 264.0695 $[\text{M}-\text{H}]^-$.



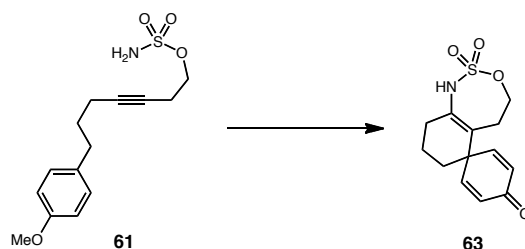
2,5,6,7-tetrahydro-1H-naphtho[2,1-d][1,2,3]oxathiazepine 4,4-dioxide (59). Prepared according to general procedure **F** using 6-phenylhex-3-yn-1-yl sulfamate (**56**) (22 mg,

0.088 mmol), $\text{PhI}(\text{OAc})_2$ (31 mg, 0.096 mmol) and $\text{Rh}_2(\text{esp})_2$ (1.3 mg, 0.0018 mmol) in CH_2Cl_2 (0.5 mL). Purification by flash chromatography (4:1 hexanes/EtOAc) afforded 2,5,6,7-tetrahydro-1H-naphtho[2,1-d][1,2,3]oxathiazepine 4,4-dioxide (**59**) as a white amorphous solid (15 mg, 71 %); R_f 0.34 (2:1 hexanes/EtOAc); **IR** (thin film, cm^{-1}) 3280, 2924, 2853, 1423, 1349, 1172, 1013; **^1H NMR** (CDCl_3 , 600 MHz) 7.26-7.16 (m, 4H), 5.99 (bs, 1H), 4.60 (t, 2H, $J = 2.4$ Hz), 3.10 (t, 2H, $J = 4.8$ Hz), 2.87 (t, 2H, $J = 7.8$ Hz), 2.43 (t, 2H, $J = 7.8$ Hz); **^{13}C NMR** (CDCl_3 , 150 MHz) 135.0, 134.4, 132.2, 127.9, 127.3, 127.0, 124.3, 122.7, 119.2, 71.8, 30.2, 28.7; **HRMS** (-ESI) calculated for $\text{C}_{12}\text{H}_{12}\text{NO}_3\text{S}$ 250.0543, found 250.0544 $[\text{M}-\text{H}]^-$.

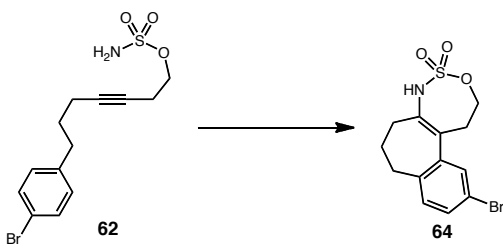


4-benzyl-2,2-dioxido-6,7-dihydro-3H-1,2,3-oxathiazepin-5-yl acetate (60). Prepared according to general procedure **E** using 5-phenylpent-3-yn-1-yl sulfamate (**58**) (21 mg, 0.088 mmol), $\text{PhI}(\text{OAc})_2$ (31 mg, 0.096 mmol) and $\text{Rh}_2(\text{esp})_2$ (1.3 mg, 0.0018 mmol) in CH_2Cl_2 (0.50 mL). Purification by flash chromatography (2:1 hexanes/EtOAc, 1 % HOAc) afforded 4-benzyl-2,2-dioxido-6,7-dihydro-3H-1,2,3-oxathiazepin-5-yl acetate (**60**) as a white amorphous solid (8.3 mg, 68 %); R_f 0.71 (1:1 hexanes/EtOAc); **IR** (thin film, cm^{-1}) 3280, 2924, 2853, 1423, 1349, 1172, 1013; **^1H NMR** (CDCl_3 , 600 MHz) 4.46 (d, 1H, $J = 10.5$ Hz), 4.43 (d, 1H, $J = 2.4$ Hz), 4.41 (t, 1H, $J = 2.4$ Hz), 3.94 (dt, 1H, $J = 10.5, 8.1$ Hz), 2.60 (ddd, 1H, $J = 15.2, 7.1, 1.4$ Hz), 1.98 (dt, 1H, $J = 15.7, 8.1$ Hz), 1.89-1.83 (m, 1H), 1.76 (dd, 1H, $J = 12.9, 8.1$ Hz); **^{13}C NMR** (CDCl_3 , 150 MHz) 70.6, 58.9,

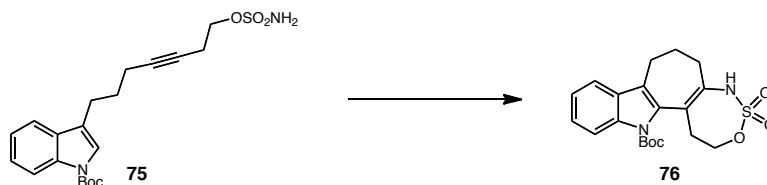
35.2, 32.3, 26.8, 25.5, 24.2; **HRMS** (-ESI) calculated for $C_{13}H_{14}NO_5S$ 296.0598, found 296.0597 $[M-H]^-$.



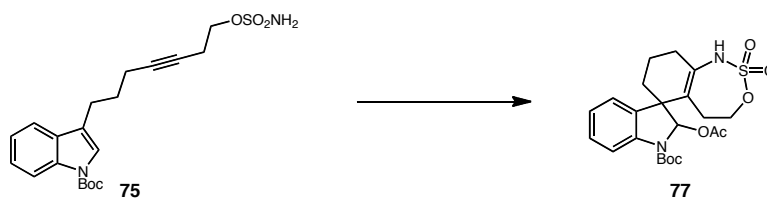
1,4,5,7,8,9-hexahydrospiro[benzo[d][1,2,3]oxathiazepine-6,1'-cyclohexa[2,5]dien]-4'-one 2,2-dioxide (63). Prepared according to general procedure **F** using 7-(4-methoxyphenyl)hept-3-yn-1-yl sulfamate (**61**) (39 mg, 0.13 mmol), $PhI(OAc)_2$ (46 mg, 0.14 mmol) and $Rh_2(esp)_2$ (2.0 mg, 0.0026 mmol) in CH_2Cl_2 (0.75 mL). Purification by flash chromatography (2:1 hexanes/EtOAc) afforded 1,4,5,7,8,9-hexahydrospiro[benzo[d][1,2,3]oxathiazepine-6,1'-cyclohexa[2,5]dien]-4'-one 2,2-dioxide (**63**) as a white amorphous solid (25 mg, 70 %); R_f 0.20 (1:1 hexanes/EtOAc); **IR** (thin film, cm^{-1}) 3261, 2926, 2854, 1654, 1615, 1351, 1167; **1H NMR** ($CDCl_3$, 600 MHz) 6.81 (d, 2H, $J = 15.0$ Hz), 6.38 (d, 2H, $J = 15.0$ Hz), 5.85 (bs, 1H), 4.24 (t, 2H, $J = 7.8$ Hz), 2.29 (t, 2H, $J = 9.0$ Hz), 2.25 (t, 2H, $J = 7.8$ Hz), 1.91-1.85 (m, 2H), 1.80-1.77 (m, 2H); **^{13}C NMR** ($CDCl_3$, 150 MHz) 185.6, 152.5, 134.8, 130.5, 124.0, 67.9, 46.4, 32.8, 30.6, 29.9, 18.9; **HRMS** (-ESI) calculated for $C_{13}H_{14}NO_4S$ 280.0649, found 280.0651 $[M-H]^-$.



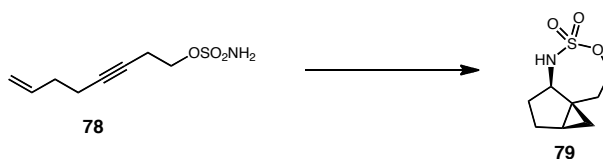
11-bromo-1,2,5,6,7,8-hexahydrobenzo[3,4]cyclohepta[1,2-d][1,2,3]oxathiazepine 4,4-dioxide (64). 7-(4-bromophenyl)hept-3-yn-1-yl sulfamate (**62**) (30 mg, 0.088 mmol), $\text{PhI}(\text{OAc})_2$ (31 mg, 0.096 mmol) and $\text{Rh}_2(\text{esp})_2$ (1.3 mg, 0.0018 mmol) were combined in a 2 dram reaction vial and capped with a teflon lined septum. Toluene (0.50 mL) was added and the solution was stirred at 100 °C for 8 h. Purification by flash chromatography (4:1 \rightarrow 2:1 hexanes/EtOAc) afforded 11-bromo-1,2,5,6,7,8-hexahydrobenzo[3,4]cyclohepta[1,2-d][1,2,3]oxathiazepine 4,4-dioxide (**64**) as a colorless oil (8.2 mg, 28 %); R_f 0.56 (2:1 hexanes/EtOAc); **IR** (thin film, cm^{-1}) 3276, 2926, 2857, 1419, 1174; **$^1\text{H NMR}$** (CDCl_3 , 600 MHz) 7.33-7.30 (m, 2H), 7.08 (d, 1H, $J = 11.4$ Hz), 6.03 (bs, 1H), 4.51 (t, 2H, $J = 7.2$ Hz), 3.01 (t, 2H, $J = 7.2$ Hz), 2.72 (t, 2H, $J = 10.8$ Hz), 2.31 (qn, 2H, $J = 10.2$ Hz), 1.96 (t, 2H, $J = 10.2$ Hz); **$^{13}\text{C NMR}$** (CDCl_3 , 150 MHz) 143.1, 139.8, 134.9, 131.1, 130.5, 129.9, 126.7, 120.4, 71.3, 34.4, 34.2, 31.9, 31.5; **HRMS** (+ESI) calculated for $\text{C}_{13}\text{H}_{15}\text{Br}^{79}\text{NO}_3\text{S}$ 343.9951, found 343.9950 $[\text{M}+\text{H}]^+$.



^tButyl 5,6,7,8-tetrahydro-1H-[1,2,3]oxathiazepino[4',5':6,7]cyclohepta[1,2-b]indole-13(2H)-carboxylate 4,4-dioxide (76). ^tbutyl 3-(7-(sulfamoyloxy)hept-4-yn-1-yl)-1H-indole-1-carboxylate (**75**) (60 mg, 0.15 mmol), PhI(OAc)₂ (53 mg, 0.16 mmol), and Rh₂(esp)₂ (2.2 mg, 0.003 mmol) were combined in a 2 dram reaction vial and capped with a teflon lined septum. Toluene (0.85 mL) was added and the solution was stirred at 80 °C for 7 h. Purification by flash chromatography (11:1:1 hexanes/EtOAc/CH₂Cl₂) afforded ^tbutyl 5,6,7,8-tetrahydro-1H-[1,2,3]oxathiazepino[4',5':6,7]cyclohepta[1,2-b]indole-13(2H)-carboxylate 4,4-dioxide (**76**) as a white amorphous solid (40 mg, 68 %); **R_f** 0.60 (3:1 hexanes/EtOAc); **IR** (thin film, cm⁻¹) 3264, 2933, 1728, 1708, 1361, 1171, 1146; **¹H NMR** (*d*₆-DMSO, 600 MHz, 70 °C) 9.66 (s, 1H), 7.97 (d, 1H, *J* = 8.6 Hz), 7.58 (d, 1H, *J* = 7.6 Hz), 7.30 (t, 1H, *J* = 8.1 Hz), 7.24 (t, 1H, *J* = 7.6 Hz), 4.37 (t, 2H, *J* = 4.3 Hz), 2.75-2.71 (m, 4H), 2.31 (qn, 2H, *J* = 6.7 Hz), 2.15 (t, 2H, *J* = 7.2 Hz), 1.62 (s, 9H); **¹³C NMR** (*d*₆-DMSO, 150 MHz, 70 °C) 150.1, 136.6, 136.4, 135.8, 129.7, 126.1, 125.0, 124.1, 123.2, 118.6, 115.9, 84.6, 71.7, 36.2, 33.5, 33.3, 28.4, 20.3; **HRMS** (-ESI) calculated for C₂₀H₂₃N₂O₅S 403.1333, found 403.1333 [M-H]⁻.



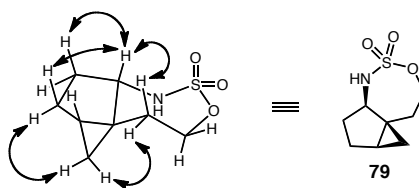
^tButyl 2'-acetoxy-1,4,5,7,8,9-hexahydrospiro[benzo[d][1,2,3]oxathiazepine-6,3'-indoline]-1'-carboxylate 2,2-dioxide (77). ^tbutyl 3-(7-(sulfamoyloxy)hept-4-yn-1-yl)-1H-indole-1-carboxylate (**75**) (36 mg, 0.088 mmol), $\text{PhI}(\text{OAc})_2$ (31 mg, 0.096 mmol), acetic acid (0.005 mL, 0.096 mmol) and $\text{Rh}_2(\text{esp})_2$ (1.3 mg, 0.0018 mmol) were combined in a 2 dram reaction vial and capped with a teflon lined septum. CH_2Cl_2 (0.50 mL) was added and the solution was stirred at ambient temperature for 2 h. Purification by flash chromatography (7:1:1 hexanes/EtOAc/ CH_2Cl_2) afforded ^tbutyl 2'-acetoxy-1,4,5,7,8,9-hexahydrospiro[benzo[d][1,2,3]oxathiazepine-6,3'-indoline]-1'-carboxylate 2,2-dioxide (**77**) as a colorless oil (33 mg, 80 %); R_f 0.43 (3:1 hexanes/EtOAc); **IR** (thin film, cm^{-1}) 3272, 2977, 2936, 1717, 1483, 1389, 1169; **¹H NMR** (d_6 -DMSO, 600 MHz, 70 °C) 9.47 (s, 1H), 7.71 (bs 1H), 7.27 (t, 1H, $J = 7.6$ Hz), 7.09 (t, 1H, $J = 7.6$ Hz), 7.01 (d, 1H, $J = 7.2$ Hz), 6.57 (s, 1H), 4.16 (dd, 1H, $J = 11.4, 6.2$ Hz), 4.08 (t, 1H, $J = 10.5$ Hz), 2.38 (dd, 1H, $J = 16.2, 10.0$ Hz), 2.25-2.19 (m, 1H), 2.10-1.99 (m, 5H), 1.94-1.86 (m, 1H), 1.81-1.74 (m, 2H), 1.58-1.48 (m, 10H); **¹³C NMR** (d_6 -DMSO, 150 MHz, 70 °C) 168.3, 150.5, 135.9, 134.8, 128.2, 124.1, 123.3, 114.1, 113.6, 88.7, 86.8, 81.7, 70.1, 53.6, 35.7, 32.4, 29.6, 27.7, 20.6, 18.1; **HRMS** (-ESI) calculated for $\text{C}_{22}\text{H}_{27}\text{N}_2\text{O}_7\text{S}$ 463.1544, found 463.1545 [M-H]⁻.



Octahydrocyclopropa[2,3]cyclopenta[1,2-d][1,2,3]oxathiazepine 4,4-dioxide (79).

Prepared according to general procedure **F** using oct-7-en-3-yn-1-yl sulfamate (**78**) (20 mg, 0.098 mmol), $\text{PhI}(\text{OAc})_2$ (35 mg, 0.26 mmol) and $\text{Rh}_2(\text{esp})_2$ (1.5 mg, 0.0046 mmol) in CH_2Cl_2 (0.55 mL). Purification by preparative TLC (3:2 hexanes/EtOAc) afforded oxathiazepane **79** as a white amorphous solid (13 mg, 67 %); R_f 0.47 (1:1 hexanes/EtOAc); **IR** (thin film, cm^{-1}) 3272, 2923, 2869, 1437, 1351, 1173; **^1H NMR** (CDCl_3 , 600 MHz) 4.46 (d, 1H, $J = 10.5$ Hz), 4.43 (d, 1H, $J = 2.4$ Hz), 4.41 (t, 1H, $J = 2.4$ Hz), 3.94 (dt, 1H, $J = 10.5, 8.1$ Hz), 2.60 (ddd, 1H, $J = 15.2, 7.1, 1.4$ Hz), 1.98 (dt, 1H, $J = 15.7, 8.1$ Hz), 1.89-1.83 (m, 1H), 1.76 (dd, 1H, $J = 12.9, 8.1$ Hz); **^{13}C NMR** (CDCl_3 , 150 MHz) 70.6, 58.9, 35.2, 32.3, 26.8, 25.5, 24.2, 10.6 ; **HRMS** (-ESI) calculated for $\text{C}_8\text{H}_{12}\text{NO}_3\text{S}$ 202.0543, found 202.0539 $[\text{M}-\text{H}]^-$.

Key NOE correlations for compound oxathiazepane 79:



X-Ray Crystallographic Data

5a-benzylhexahydro-1H-furo[3,2-d][1,2,3]oxathiazepine 2,2-dioxide (13).

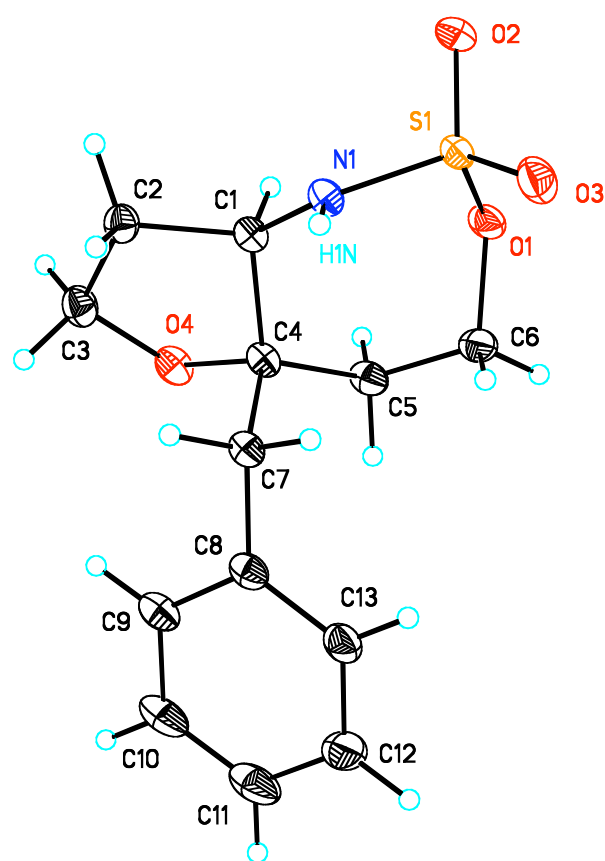


Table 1. Crystal data and structure refinement for oxathiazepane **13**

Identification code	art_2_157s	
Empirical formula	C ₁₃ H ₁₇ N O ₄ S	
Formula weight	283.34	
Temperature	173(2) K	
Wavelength	1.54178 Å	
Crystal system	Orthorhombic	
Space group	P2(1)2(1)2(1)	
Unit cell dimensions	a = 6.6794(3) Å	α = 90°.
	b = 9.7679(5) Å	β = 90°.
	c = 20.0851(9) Å	γ = 90°.
Volume	1310.43(11) Å ³	
Z	4	
Density (calculated)	1.436 Mg/m ³	
Absorption coefficient	2.301 mm ⁻¹	
F(000)	600	
Crystal size	0.36 x 0.25 x 0.20 mm ³	
Theta range for data collection	5.03 to 64.91°.	
Index ranges	-7<=h<=6, -9<=k<=11, -21<=l<=23	
Reflections collected	5250	
Independent reflections	2033 [R(int) = 0.0128]	
Completeness to theta = 64.91°	96.2 %	
Absorption correction	Semi-empirical from equivalents	
Max. and min. transmission	0.6561 and 0.4913	
Refinement method	Full-matrix least-squares on F ²	
Data / restraints / parameters	2033 / 0 / 177	
Goodness-of-fit on F ²	1.079	
Final R indices [I>2sigma(I)]	R1 = 0.0217, wR2 = 0.0573	
R indices (all data)	R1 = 0.0217, wR2 = 0.0573	

Absolute structure parameter	0.507(15)
Largest diff. peak and hole	0.125 and -0.290 e.Å ⁻³

Table 2. Atomic coordinates (x 10⁴) and equivalent isotropic displacement parameters (Å²x 10³)

for art_2_157s. U(eq) is defined as one third of the trace of the orthogonalized U^{ij} tensor.

	x	y	z	U(eq)
C(1)	3119(2)	8733(2)	6757(1)	23(1)
C(2)	4580(2)	9855(2)	6960(1)	27(1)
C(3)	5843(3)	9999(2)	6330(1)	32(1)
C(4)	2854(3)	8996(2)	6002(1)	23(1)
C(5)	2076(3)	7741(2)	5632(1)	28(1)
C(6)	147(3)	7138(2)	5901(1)	31(1)
C(7)	1607(2)	10298(2)	5857(1)	24(1)
C(8)	1459(3)	10655(2)	5126(1)	27(1)
C(9)	3105(3)	11195(2)	4786(1)	33(1)
C(10)	2975(4)	11494(2)	4112(1)	43(1)
C(11)	1208(4)	11261(2)	3773(1)	49(1)
C(12)	-437(4)	10753(2)	4103(1)	48(1)
C(13)	-314(3)	10456(2)	4782(1)	35(1)
N(1)	1258(2)	8688(1)	7139(1)	23(1)
O(1)	509(2)	6474(1)	6549(1)	30(1)
O(2)	927(2)	6399(1)	7703(1)	32(1)
O(3)	-2019(2)	7601(1)	7270(1)	37(1)
O(4)	4899(2)	9206(1)	5810(1)	29(1)
S(1)	48(1)	7272(1)	7210(1)	24(1)

Table 3. Bond lengths [\AA] and angles [$^\circ$] for art_2_157s.

C(1)-N(1)	1.461(2)
C(1)-C(2)	1.523(2)
C(1)-C(4)	1.549(2)
C(1)-H(1)	1.0000
C(2)-C(3)	1.528(2)
C(2)-H(2A)	0.9900
C(2)-H(2B)	0.9900
C(3)-O(4)	1.444(2)
C(3)-H(3A)	0.9900
C(3)-H(3B)	0.9900
C(4)-O(4)	1.434(2)
C(4)-C(5)	1.524(2)
C(4)-C(7)	1.547(2)
C(5)-C(6)	1.516(3)
C(5)-H(5A)	0.9900
C(5)-H(5B)	0.9900
C(6)-O(1)	1.4740(18)
C(6)-H(6A)	0.9900
C(6)-H(6B)	0.9900
C(7)-C(8)	1.512(2)
C(7)-H(7A)	0.9900
C(7)-H(7B)	0.9900
C(8)-C(13)	1.386(3)
C(8)-C(9)	1.398(3)
C(9)-C(10)	1.387(3)
C(9)-H(9)	0.9500
C(10)-C(11)	1.382(3)
C(10)-H(10)	0.9500
C(11)-C(12)	1.376(3)

C(11)-H(11)	0.9500
C(12)-C(13)	1.396(3)
C(12)-H(12)	0.9500
C(13)-H(13)	0.9500
N(1)-S(1)	1.6081(13)
N(1)-H(1N)	0.770(19)
O(1)-S(1)	1.5692(11)
O(2)-S(1)	1.4328(12)
O(3)-S(1)	1.4228(13)
N(1)-C(1)-C(2)	115.20(13)
N(1)-C(1)-C(4)	114.98(13)
C(2)-C(1)-C(4)	102.49(13)
N(1)-C(1)-H(1)	107.9
C(2)-C(1)-H(1)	107.9
C(4)-C(1)-H(1)	107.9
C(1)-C(2)-C(3)	101.42(13)
C(1)-C(2)-H(2A)	111.5
C(3)-C(2)-H(2A)	111.5
C(1)-C(2)-H(2B)	111.5
C(3)-C(2)-H(2B)	111.5
H(2A)-C(2)-H(2B)	109.3
O(4)-C(3)-C(2)	107.93(13)
O(4)-C(3)-H(3A)	110.1
C(2)-C(3)-H(3A)	110.1
O(4)-C(3)-H(3B)	110.1
C(2)-C(3)-H(3B)	110.1
H(3A)-C(3)-H(3B)	108.4
O(4)-C(4)-C(5)	108.02(13)
O(4)-C(4)-C(7)	110.21(12)
C(5)-C(4)-C(7)	112.73(14)

O(4)-C(4)-C(1)	100.22(12)
C(5)-C(4)-C(1)	112.44(13)
C(7)-C(4)-C(1)	112.41(13)
C(6)-C(5)-C(4)	115.42(14)
C(6)-C(5)-H(5A)	108.4
C(4)-C(5)-H(5A)	108.4
C(6)-C(5)-H(5B)	108.4
C(4)-C(5)-H(5B)	108.4
H(5A)-C(5)-H(5B)	107.5
O(1)-C(6)-C(5)	110.22(14)
O(1)-C(6)-H(6A)	109.6
C(5)-C(6)-H(6A)	109.6
O(1)-C(6)-H(6B)	109.6
C(5)-C(6)-H(6B)	109.6
H(6A)-C(6)-H(6B)	108.1
C(8)-C(7)-C(4)	113.99(13)
C(8)-C(7)-H(7A)	108.8
C(4)-C(7)-H(7A)	108.8
C(8)-C(7)-H(7B)	108.8
C(4)-C(7)-H(7B)	108.8
H(7A)-C(7)-H(7B)	107.6
C(13)-C(8)-C(9)	118.70(16)
C(13)-C(8)-C(7)	120.59(15)
C(9)-C(8)-C(7)	120.70(16)
C(10)-C(9)-C(8)	120.50(19)
C(10)-C(9)-H(9)	119.7
C(8)-C(9)-H(9)	119.7
C(11)-C(10)-C(9)	120.03(19)
C(11)-C(10)-H(10)	120.0
C(9)-C(10)-H(10)	120.0
C(12)-C(11)-C(10)	120.20(18)

C(12)-C(11)-H(11)	119.9
C(10)-C(11)-H(11)	119.9
C(11)-C(12)-C(13)	119.9(2)
C(11)-C(12)-H(12)	120.0
C(13)-C(12)-H(12)	120.0
C(8)-C(13)-C(12)	120.60(19)
C(8)-C(13)-H(13)	119.7
C(12)-C(13)-H(13)	119.7
C(1)-N(1)-S(1)	119.98(11)
C(1)-N(1)-H(1N)	121.3(13)
S(1)-N(1)-H(1N)	113.0(13)
C(6)-O(1)-S(1)	119.74(10)
C(4)-O(4)-C(3)	107.40(12)
O(3)-S(1)-O(2)	118.26(8)
O(3)-S(1)-O(1)	111.93(7)
O(2)-S(1)-O(1)	102.06(7)
O(3)-S(1)-N(1)	107.53(8)
O(2)-S(1)-N(1)	111.53(7)
O(1)-S(1)-N(1)	104.71(6)

Symmetry transformations used to generate equivalent atoms:

Table 4. Anisotropic displacement parameters ($\text{\AA}^2 \times 10^3$) for art_2_157s. The anisotropic displacement factor exponent takes the form: $-2\pi^2 [h^2 a^2 U_{11} + \dots + 2 h k a^* b^* U_{12}]$

	U11	U22	U33	U23	U13	U12
C(1)	23(1)	21(1)	25(1)	1(1)	4(1)	1(1)
C(2)	24(1)	27(1)	31(1)	-1(1)	1(1)	-1(1)
C(3)	26(1)	30(1)	40(1)	2(1)	3(1)	-2(1)
C(4)	25(1)	20(1)	24(1)	0(1)	6(1)	1(1)
C(5)	41(1)	21(1)	23(1)	-2(1)	3(1)	1(1)
C(6)	45(1)	23(1)	24(1)	0(1)	-6(1)	-3(1)
C(7)	28(1)	21(1)	24(1)	-1(1)	4(1)	1(1)
C(8)	38(1)	17(1)	27(1)	-2(1)	4(1)	3(1)
C(9)	42(1)	23(1)	34(1)	4(1)	7(1)	1(1)
C(10)	65(1)	30(1)	33(1)	7(1)	16(1)	1(1)
C(11)	93(2)	30(1)	26(1)	2(1)	2(1)	-7(1)
C(12)	76(2)	32(1)	35(1)	1(1)	-20(1)	-11(1)
C(13)	48(1)	23(1)	33(1)	1(1)	-3(1)	-8(1)
N(1)	25(1)	18(1)	26(1)	0(1)	4(1)	2(1)
O(1)	43(1)	19(1)	28(1)	3(1)	-2(1)	-5(1)
O(2)	39(1)	28(1)	30(1)	10(1)	-2(1)	-3(1)
O(3)	28(1)	36(1)	47(1)	9(1)	5(1)	-3(1)
O(4)	27(1)	29(1)	31(1)	1(1)	11(1)	2(1)
S(1)	26(1)	22(1)	26(1)	5(1)	1(1)	-3(1)

Table 5. Hydrogen coordinates ($\times 10^4$) and isotropic displacement parameters ($\text{\AA}^2 \times 10^3$) for art_2_157s.

	x	y	z	U(eq)
H(1)	3810	7832	6812	28
H(2A)	5405	9573	7346	33
H(2B)	3874	10718	7068	33
H(3A)	5925	10973	6196	38
H(3B)	7217	9659	6411	38
H(5A)	1865	7991	5160	34
H(5B)	3123	7024	5645	34
H(6A)	-863	7872	5954	37
H(6B)	-386	6457	5582	37
H(7A)	239	10165	6036	29
H(7B)	2215	11079	6097	29
H(9)	4321	11359	5018	39
H(10)	4101	11858	3884	51
H(11)	1129	11452	3310	59
H(12)	-1655	10605	3869	57
H(13)	-1457	10115	5009	42
H(1N)	580(30)	9323(19)	7172(8)	19(5)

Table 6. Torsion angles [°] for art_2_157s.

N(1)-C(1)-C(2)-C(3)	-158.15(14)
C(4)-C(1)-C(2)-C(3)	-32.54(15)
C(1)-C(2)-C(3)-O(4)	9.31(17)
N(1)-C(1)-C(4)-O(4)	170.72(12)
C(2)-C(1)-C(4)-O(4)	44.98(14)
N(1)-C(1)-C(4)-C(5)	-74.78(18)
C(2)-C(1)-C(4)-C(5)	159.47(14)
N(1)-C(1)-C(4)-C(7)	53.72(18)
C(2)-C(1)-C(4)-C(7)	-72.03(16)
O(4)-C(4)-C(5)-C(6)	164.56(13)
C(7)-C(4)-C(5)-C(6)	-73.43(18)
C(1)-C(4)-C(5)-C(6)	54.90(19)
C(4)-C(5)-C(6)-O(1)	-70.71(18)
O(4)-C(4)-C(7)-C(8)	64.35(17)
C(5)-C(4)-C(7)-C(8)	-56.42(19)
C(1)-C(4)-C(7)-C(8)	175.23(14)
C(4)-C(7)-C(8)-C(13)	107.15(18)
C(4)-C(7)-C(8)-C(9)	-73.1(2)
C(13)-C(8)-C(9)-C(10)	-1.6(3)
C(7)-C(8)-C(9)-C(10)	178.62(16)
C(8)-C(9)-C(10)-C(11)	0.2(3)
C(9)-C(10)-C(11)-C(12)	1.0(3)
C(10)-C(11)-C(12)-C(13)	-0.8(3)
C(9)-C(8)-C(13)-C(12)	1.8(3)
C(7)-C(8)-C(13)-C(12)	-178.38(16)
C(11)-C(12)-C(13)-C(8)	-0.6(3)
C(2)-C(1)-N(1)-S(1)	-153.96(12)
C(4)-C(1)-N(1)-S(1)	87.17(15)
C(5)-C(6)-O(1)-S(1)	97.26(15)

C(5)-C(4)-O(4)-C(3)	-157.65(13)
C(7)-C(4)-O(4)-C(3)	78.80(15)
C(1)-C(4)-O(4)-C(3)	-39.84(14)
C(2)-C(3)-O(4)-C(4)	19.97(17)
C(6)-O(1)-S(1)-O(3)	62.73(13)
C(6)-O(1)-S(1)-O(2)	-169.83(12)
C(6)-O(1)-S(1)-N(1)	-53.46(13)
C(1)-N(1)-S(1)-O(3)	-149.62(12)
C(1)-N(1)-S(1)-O(2)	79.20(13)
C(1)-N(1)-S(1)-O(1)	-30.42(13)

Symmetry transformations used to generate equivalent atoms:

Table 7. Hydrogen bonds for art_2_157s [\AA and $^\circ$].

D-H...A	d(D-H)	d(H...A)	d(D...A)	$\angle(\text{DHA})$
N(1)-H(1N)...O(2)#1	0.770(19)	2.28(2)	3.0407(19)	170.3(17)

Symmetry transformations used to generate equivalent atoms:

#1 $-x, y+1/2, -z+3/2$

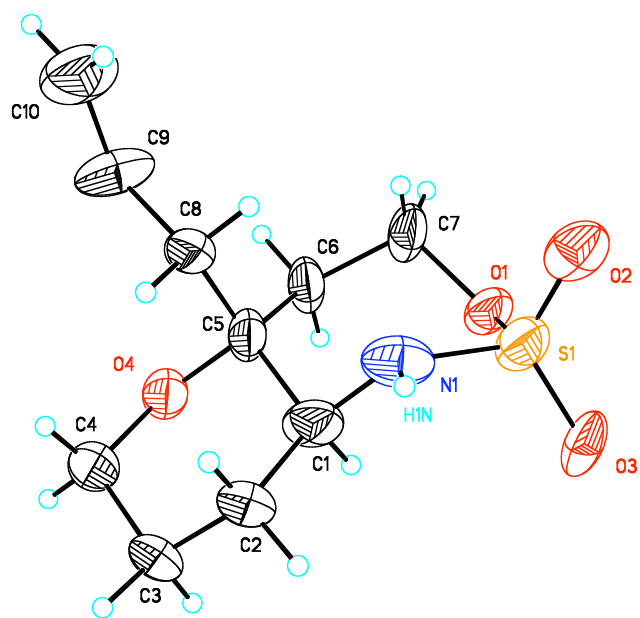
5a-allyloctahydropyrano[3,2-d][1,2,3]oxathiazepine 2,2-dioxide (25).

Table 1. Crystal data and structure refinement for oxathiazepane **25**.

Identification code	art_2_158s	
Empirical formula	C ₁₀ H ₁₇ N O ₄ S	
Formula weight	247.31	
Temperature	173(2) K	
Wavelength	1.54178 Å	
Crystal system	Monoclinic	
Space group	C2/c	
Unit cell dimensions	a = 27.957(7) Å	α = 90°.
	b = 7.6891(17) Å	β = 98.949(13)°.
	c = 11.327(2) Å	γ = 90°.
Volume	2405.3(9) Å ³	
Z	8	
Density (calculated)	1.366 Mg/m ³	
Absorption coefficient	2.418 mm ⁻¹	
F(000)	1056	
Crystal size	0.25 x 0.09 x 0.02 mm ³	
Theta range for data collection	5.97 to 55.96°.	
Index ranges	-30 ≤ h ≤ 28, -8 ≤ k ≤ 8, -12 ≤ l ≤ 11	
Reflections collected	3309	
Independent reflections	1405 [R(int) = 0.1054]	
Completeness to theta = 55.96°	89.2 %	
Absorption correction	Semi-empirical from equivalents	
Max. and min. transmission	0.9646 and 0.5832	
Refinement method	Full-matrix least-squares on F ²	
Data / restraints / parameters	1405 / 0 / 146	
Goodness-of-fit on F ²	1.140	
Final R indices [I > 2σ(I)]	R1 = 0.1341, wR2 = 0.2789	
R indices (all data)	R1 = 0.2518, wR2 = 0.3531	
Extinction coefficient	0.0009(3)	
Largest diff. peak and hole	0.734 and -1.000 e.Å ⁻³	

Table 2. Atomic coordinates ($\times 10^4$) and equivalent isotropic displacement parameters ($\text{\AA}^2 \times 10^3$) for ART2_158s. $U(\text{eq})$ is defined as one third of the trace of the orthogonalized U^{ij} tensor.

	x	y	z	$U(\text{eq})$
C(1)	1738(6)	3880(20)	6092(19)	76(6)
C(2)	2061(6)	5220(20)	5645(19)	82(6)
C(3)	2322(5)	6280(20)	6724(17)	73(6)
C(4)	1943(6)	7010(20)	7433(18)	78(6)
C(5)	1352(6)	4623(19)	6730(20)	77(7)
C(6)	1120(6)	3249(19)	7411(17)	72(6)
C(7)	880(6)	1787(18)	6658(17)	69(6)
C(8)	984(5)	5810(20)	6010(20)	87(7)
C(9)	628(6)	6770(30)	6604(19)	92(7)
C(10)	227(7)	7520(30)	5880(20)	114(9)
N(1)	1460(5)	2980(20)	5024(14)	77(5)
O(1)	1244(3)	625(13)	6309(12)	73(4)
O(2)	993(4)	505(15)	4103(12)	77(4)
O(3)	1822(4)	-84(13)	5076(11)	70(4)
O(4)	1627(4)	5662(13)	7732(11)	66(3)
S(1)	1387(2)	901(6)	5014(6)	76(2)

Table 3. Bond lengths [\AA] and angles [$^\circ$] for ART2_158s.

C(1)-N(1)	1.50(2)
C(1)-C(5)	1.50(2)
C(1)-C(2)	1.51(2)
C(1)-H(1)	1.0000
C(2)-C(3)	1.55(2)
C(2)-H(2A)	0.9900
C(2)-H(2B)	0.9900
C(3)-C(4)	1.53(2)
C(3)-H(3A)	0.9900
C(3)-H(3B)	0.9900
C(4)-O(4)	1.434(17)
C(4)-H(4A)	0.9900
C(4)-H(4B)	0.9900
C(5)-O(4)	1.50(2)
C(5)-C(6)	1.51(2)
C(5)-C(8)	1.51(2)
C(6)-C(7)	1.50(2)
C(6)-H(6A)	0.9900
C(6)-H(6B)	0.9900
C(7)-O(1)	1.454(16)
C(7)-H(7A)	0.9900
C(7)-H(7B)	0.9900
C(8)-C(9)	1.48(2)
C(8)-H(8A)	0.9900
C(8)-H(8B)	0.9900
C(9)-C(10)	1.40(2)
C(9)-H(9)	0.9500
C(10)-H(10A)	0.9500
C(10)-H(10B)	0.9500

N(1)-S(1)	1.613(16)
N(1)-H(1N)	0.7472
O(1)-S(1)	1.594(12)
O(2)-S(1)	1.420(14)
O(3)-S(1)	1.426(11)
N(1)-C(1)-C(5)	104.0(14)
N(1)-C(1)-C(2)	107.9(16)
C(5)-C(1)-C(2)	114.4(15)
N(1)-C(1)-H(1)	110.1
C(5)-C(1)-H(1)	110.1
C(2)-C(1)-H(1)	110.1
C(1)-C(2)-C(3)	109.1(17)
C(1)-C(2)-H(2A)	109.9
C(3)-C(2)-H(2A)	109.9
C(1)-C(2)-H(2B)	109.9
C(3)-C(2)-H(2B)	109.9
H(2A)-C(2)-H(2B)	108.3
C(4)-C(3)-C(2)	108.9(13)
C(4)-C(3)-H(3A)	109.9
C(2)-C(3)-H(3A)	109.9
C(4)-C(3)-H(3B)	109.9
C(2)-C(3)-H(3B)	109.9
H(3A)-C(3)-H(3B)	108.3
O(4)-C(4)-C(3)	111.4(13)
O(4)-C(4)-H(4A)	109.4
C(3)-C(4)-H(4A)	109.4
O(4)-C(4)-H(4B)	109.4
C(3)-C(4)-H(4B)	109.4
H(4A)-C(4)-H(4B)	108.0
O(4)-C(5)-C(1)	104.2(14)

O(4)-C(5)-C(6)	101.4(15)
C(1)-C(5)-C(6)	112.2(13)
O(4)-C(5)-C(8)	108.2(12)
C(1)-C(5)-C(8)	116.6(18)
C(6)-C(5)-C(8)	112.6(14)
C(7)-C(6)-C(5)	115.0(16)
C(7)-C(6)-H(6A)	108.5
C(5)-C(6)-H(6A)	108.5
C(7)-C(6)-H(6B)	108.5
C(5)-C(6)-H(6B)	108.5
H(6A)-C(6)-H(6B)	107.5
O(1)-C(7)-C(6)	110.2(13)
O(1)-C(7)-H(7A)	109.6
C(6)-C(7)-H(7A)	109.6
O(1)-C(7)-H(7B)	109.6
C(6)-C(7)-H(7B)	109.6
H(7A)-C(7)-H(7B)	108.1
C(9)-C(8)-C(5)	120.2(19)
C(9)-C(8)-H(8A)	107.3
C(5)-C(8)-H(8A)	107.3
C(9)-C(8)-H(8B)	107.3
C(5)-C(8)-H(8B)	107.3
H(8A)-C(8)-H(8B)	106.9
C(10)-C(9)-C(8)	118.3(19)
C(10)-C(9)-H(9)	120.9
C(8)-C(9)-H(9)	120.9
C(9)-C(10)-H(10A)	120.0
C(9)-C(10)-H(10B)	120.0
H(10A)-C(10)-H(10B)	120.0
C(1)-N(1)-S(1)	120.7(12)
C(1)-N(1)-H(1N)	111.6

S(1)-N(1)-H(1N)	106.6
C(7)-O(1)-S(1)	117.1(11)
C(4)-O(4)-C(5)	117.9(14)
O(2)-S(1)-O(3)	118.8(8)
O(2)-S(1)-O(1)	111.3(6)
O(3)-S(1)-O(1)	102.6(7)
O(2)-S(1)-N(1)	107.5(8)
O(3)-S(1)-N(1)	114.9(7)
O(1)-S(1)-N(1)	100.1(7)

Symmetry transformations used to generate equivalent atoms:

Table 4. Anisotropic displacement parameters ($\text{\AA}^2 \times 10^3$) for ART2_158s. The anisotropic displacement factor exponent takes the form: $-2\pi^2 [h^2 a^2 U_{11} + \dots + 2 h k a^* b^* U_{12}]$

	U11	U22	U33	U23	U13	U12
C(1)	52(10)	69(12)	112(19)	17(11)	35(11)	-4(9)
C(2)	46(9)	72(12)	130(20)	-10(12)	23(11)	-14(9)
C(3)	52(9)	61(11)	109(18)	-2(10)	22(10)	-21(8)
C(4)	62(10)	58(11)	122(18)	1(11)	36(11)	-9(9)
C(5)	66(10)	38(9)	140(20)	-22(11)	46(12)	-9(8)
C(6)	80(11)	41(9)	108(17)	-24(10)	51(12)	-17(8)
C(7)	82(11)	33(8)	102(16)	-5(9)	48(11)	-3(8)
C(8)	44(9)	49(10)	160(20)	0(12)	6(11)	-5(9)
C(9)	53(10)	150(20)	77(16)	7(14)	17(11)	32(12)
C(10)	73(13)	140(20)	130(20)	-21(17)	29(14)	24(14)
N(1)	55(8)	113(13)	64(12)	8(10)	16(8)	-6(8)
O(1)	54(6)	47(7)	127(12)	-1(7)	43(7)	0(5)
O(2)	72(7)	71(8)	98(11)	17(7)	46(8)	6(6)
O(3)	97(8)	52(6)	73(9)	-8(6)	49(7)	16(6)
O(4)	65(7)	51(7)	86(10)	-4(6)	28(7)	-2(6)
S(1)	64(3)	54(3)	119(5)	2(3)	40(3)	3(2)

Table 5. Hydrogen coordinates ($\times 10^4$) and isotropic displacement parameters ($\text{\AA}^2 \times 10^3$) for ART2_158s.

	x	y	z	U(eq)
H(1)	1938	3017	6615	91
H(2A)	1865	6012	5072	99
H(2B)	2303	4642	5228	99
H(3A)	2552	5522	7243	88
H(3B)	2508	7247	6436	88
H(4A)	2109	7557	8176	94
H(4B)	1750	7910	6954	94
H(6A)	1371	2751	8031	87
H(6B)	875	3816	7825	87
H(7A)	666	1131	7117	83
H(7B)	679	2267	5936	83
H(8A)	1166	6678	5615	104
H(8B)	799	5093	5369	104
H(9)	670	6874	7449	111
H(10A)	189	7402	5039	137
H(10B)	-7	8141	6240	137
H(1N)	1556	3207	4464	92

Table 6. Torsion angles [°] for ART2_158s.

N(1)-C(1)-C(2)-C(3)	175.3(13)
C(5)-C(1)-C(2)-C(3)	60(2)
C(1)-C(2)-C(3)-C(4)	-53.5(19)
C(2)-C(3)-C(4)-O(4)	52(2)
N(1)-C(1)-C(5)-O(4)	-174.8(13)
C(2)-C(1)-C(5)-O(4)	-57(2)
N(1)-C(1)-C(5)-C(6)	76(2)
C(2)-C(1)-C(5)-C(6)	-166.3(17)
N(1)-C(1)-C(5)-C(8)	-55.6(18)
C(2)-C(1)-C(5)-C(8)	62(2)
O(4)-C(5)-C(6)-C(7)	-170.1(13)
C(1)-C(5)-C(6)-C(7)	-59(2)
C(8)-C(5)-C(6)-C(7)	74.5(19)
C(5)-C(6)-C(7)-O(1)	74.4(19)
O(4)-C(5)-C(8)-C(9)	-55.5(19)
C(1)-C(5)-C(8)-C(9)	-172.5(16)
C(6)-C(5)-C(8)-C(9)	56(2)
C(5)-C(8)-C(9)-C(10)	-165.3(18)
C(5)-C(1)-N(1)-S(1)	-100.9(14)
C(2)-C(1)-N(1)-S(1)	137.3(12)
C(6)-C(7)-O(1)-S(1)	-97.7(16)
C(3)-C(4)-O(4)-C(5)	-57.1(19)
C(1)-C(5)-O(4)-C(4)	56.7(17)
C(6)-C(5)-O(4)-C(4)	173.3(12)
C(8)-C(5)-O(4)-C(4)	-68.0(16)
C(7)-O(1)-S(1)-O(2)	-66.4(12)
C(7)-O(1)-S(1)-O(3)	165.5(10)
C(7)-O(1)-S(1)-N(1)	47.0(12)
C(1)-N(1)-S(1)-O(2)	161.4(10)

C(1)-N(1)-S(1)-O(3)	-64.0(14)
C(1)-N(1)-S(1)-O(1)	45.1(12)

Symmetry transformations used to generate equivalent atoms:

Table 7. Hydrogen bonds for ART2_158s [\AA and $^\circ$].

D-H...A	d(D-H)	d(H...A)	d(D...A)	$\angle(\text{DHA})$
N(1)-H(1N)...O(4)#1	0.75	2.18	2.902(18)	162.0

Symmetry transformations used to generate equivalent atoms:

#1 $x, -y+1, z-1/2$

11b-benzyl-4a-methyl-2,3,4,4a,5,11b-hexahydrobenzo[f]pyrano[3,2-d][1,2,3]oxathiazepine 6,6-dioxide (40).

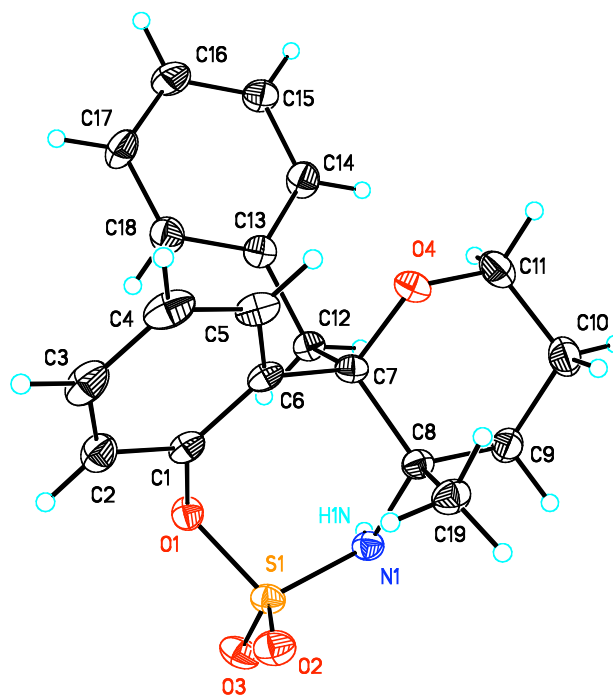


Table 1. Crystal data and structure refinement for oxathiazepane **40**.

Identification code	art3_066s	
Empirical formula	C ₁₉ H ₂₁ N O ₄ S	
Formula weight	359.43	
Temperature	173(2) K	
Wavelength	1.54178 Å	
Crystal system	Triclinic	
Space group	P-1	
Unit cell dimensions	a = 7.3392(2) Å	α = 100.1810(10)°.
	b = 9.7040(2) Å	β = 98.9240(10)°.
	c = 12.7562(3) Å	γ = 99.4360(10)°.
Volume	866.09(4) Å ³	
Z	2	
Density (calculated)	1.378 Mg/m ³	
Absorption coefficient	1.866 mm ⁻¹	
F(000)	380	
Crystal size	0.44 x 0.41 x 0.18 mm ³	
Theta range for data collection	8.38 to 66.18°.	
Index ranges	-7<=h<=8, -11<=k<=10, -14<=l<=12	
Reflections collected	4246	
Independent reflections	2161 [R(int) = 0.0125]	
Completeness to theta = 66.18°	71.0 %	
Absorption correction	Semi-empirical from equivalents	
Max. and min. transmission	0.7300 and 0.4974	
Refinement method	Full-matrix least-squares on F ²	
Data / restraints / parameters	2161 / 0 / 227	
Goodness-of-fit on F ²	1.051	
Final R indices [I>2sigma(I)]	R1 = 0.0328, wR2 = 0.0913	
R indices (all data)	R1 = 0.0334, wR2 = 0.0918	

Largest diff. peak and hole

0.197 and -0.440 e.Å⁻³

Table 2. Atomic coordinates ($\times 10^4$) and equivalent isotropic displacement parameters ($\text{\AA}^2 \times 10^3$) for ART3_066s. $U(\text{eq})$ is defined as one third of the trace of the orthogonalized U^{ij} tensor.

	x	y	z	$U(\text{eq})$
C(1)	-435(3)	3514(2)	6688(2)	25(1)
C(2)	-1210(3)	3824(2)	5718(2)	31(1)
C(3)	-921(3)	3054(2)	4754(2)	37(1)
C(4)	152(3)	2015(2)	4775(2)	36(1)
C(5)	904(3)	1718(2)	5755(2)	30(1)
C(6)	608(2)	2436(2)	6742(2)	24(1)
C(7)	1357(2)	2026(2)	7809(2)	23(1)
C(8)	2895(3)	3284(2)	8563(2)	23(1)
C(9)	3884(3)	2763(2)	9529(2)	30(1)
C(10)	4699(3)	1460(2)	9143(2)	36(1)
C(11)	3186(3)	318(2)	8386(2)	34(1)
C(12)	-317(3)	1538(2)	8362(2)	24(1)
C(13)	-1674(3)	191(2)	7718(2)	26(1)
C(14)	-1677(3)	-1108(2)	8040(2)	33(1)
C(15)	-2910(3)	-2352(2)	7476(2)	33(1)
C(16)	-4203(3)	-2309(2)	6570(2)	39(1)
C(17)	-4259(3)	-1006(2)	6241(2)	36(1)
C(18)	-3007(3)	211(2)	6816(2)	33(1)
C(19)	4348(3)	3852(2)	7919(2)	30(1)
N(1)	2047(2)	4464(2)	9083(1)	23(1)
O(1)	-843(2)	4329(1)	7632(1)	26(1)

O(2)	1989(2)	6150(1)	7818(1)	32(1)
O(3)	-2(2)	6197(1)	9204(1)	32(1)
O(4)	2271(2)	856(1)	7508(1)	28(1)
S(1)	879(1)	5418(1)	8441(1)	24(1)

Table 3. Bond lengths [\AA] and angles [$^\circ$] for ART3_066s.

C(1)-C(2)	1.383(3)
C(1)-C(6)	1.398(3)
C(1)-O(1)	1.421(2)
C(2)-C(3)	1.387(3)
C(2)-H(2)	0.9500
C(3)-C(4)	1.379(3)
C(3)-H(3)	0.9500
C(4)-C(5)	1.384(3)
C(4)-H(4)	0.9500
C(5)-C(6)	1.394(3)
C(5)-H(5)	0.9500
C(6)-C(7)	1.531(3)
C(7)-O(4)	1.435(2)
C(7)-C(12)	1.559(2)
C(7)-C(8)	1.578(2)
C(8)-N(1)	1.493(2)
C(8)-C(19)	1.534(3)
C(8)-C(9)	1.538(3)
C(9)-C(10)	1.522(3)
C(9)-H(9A)	0.9900
C(9)-H(9B)	0.9900
C(10)-C(11)	1.509(3)
C(10)-H(10A)	0.9900
C(10)-H(10B)	0.9900
C(11)-O(4)	1.438(2)
C(11)-H(11A)	0.9900
C(11)-H(11B)	0.9900
C(12)-C(13)	1.521(3)
C(12)-H(12A)	0.9900

C(12)-H(12B)	0.9900
C(13)-C(14)	1.393(3)
C(13)-C(18)	1.396(3)
C(14)-C(15)	1.388(3)
C(14)-H(14)	0.9500
C(15)-C(16)	1.388(3)
C(15)-H(15)	0.9500
C(16)-C(17)	1.406(3)
C(16)-H(16)	0.9500
C(17)-C(18)	1.381(3)
C(17)-H(17)	0.9500
C(18)-H(18)	0.9500
C(19)-H(19A)	0.9800
C(19)-H(19B)	0.9800
C(19)-H(19C)	0.9800
N(1)-S(1)	1.6043(16)
N(1)-H(1N)	1.0015
O(1)-S(1)	1.5971(13)
O(2)-S(1)	1.4174(13)
O(3)-S(1)	1.4261(14)
C(2)-C(1)-C(6)	122.91(19)
C(2)-C(1)-O(1)	115.10(17)
C(6)-C(1)-O(1)	121.93(17)
C(1)-C(2)-C(3)	118.9(2)
C(1)-C(2)-H(2)	120.5
C(3)-C(2)-H(2)	120.5
C(4)-C(3)-C(2)	119.92(19)
C(4)-C(3)-H(3)	120.0
C(2)-C(3)-H(3)	120.0
C(3)-C(4)-C(5)	120.0(2)

C(3)-C(4)-H(4)	120.0
C(5)-C(4)-H(4)	120.0
C(4)-C(5)-C(6)	122.1(2)
C(4)-C(5)-H(5)	119.0
C(6)-C(5)-H(5)	119.0
C(5)-C(6)-C(1)	116.04(18)
C(5)-C(6)-C(7)	121.00(18)
C(1)-C(6)-C(7)	122.95(18)
O(4)-C(7)-C(6)	105.34(15)
O(4)-C(7)-C(12)	110.19(14)
C(6)-C(7)-C(12)	109.57(14)
O(4)-C(7)-C(8)	107.47(14)
C(6)-C(7)-C(8)	110.88(14)
C(12)-C(7)-C(8)	113.08(15)
N(1)-C(8)-C(19)	110.67(14)
N(1)-C(8)-C(9)	103.82(15)
C(19)-C(8)-C(9)	109.81(15)
N(1)-C(8)-C(7)	112.07(14)
C(19)-C(8)-C(7)	110.25(15)
C(9)-C(8)-C(7)	110.03(14)
C(10)-C(9)-C(8)	111.03(17)
C(10)-C(9)-H(9A)	109.4
C(8)-C(9)-H(9A)	109.4
C(10)-C(9)-H(9B)	109.4
C(8)-C(9)-H(9B)	109.4
H(9A)-C(9)-H(9B)	108.0
C(11)-C(10)-C(9)	109.93(16)
C(11)-C(10)-H(10A)	109.7
C(9)-C(10)-H(10A)	109.7
C(11)-C(10)-H(10B)	109.7
C(9)-C(10)-H(10B)	109.7

H(10A)-C(10)-H(10B)	108.2
O(4)-C(11)-C(10)	111.57(15)
O(4)-C(11)-H(11A)	109.3
C(10)-C(11)-H(11A)	109.3
O(4)-C(11)-H(11B)	109.3
C(10)-C(11)-H(11B)	109.3
H(11A)-C(11)-H(11B)	108.0
C(13)-C(12)-C(7)	114.09(15)
C(13)-C(12)-H(12A)	108.7
C(7)-C(12)-H(12A)	108.7
C(13)-C(12)-H(12B)	108.7
C(7)-C(12)-H(12B)	108.7
H(12A)-C(12)-H(12B)	107.6
C(14)-C(13)-C(18)	117.33(18)
C(14)-C(13)-C(12)	120.71(17)
C(18)-C(13)-C(12)	121.91(17)
C(15)-C(14)-C(13)	122.05(19)
C(15)-C(14)-H(14)	119.0
C(13)-C(14)-H(14)	119.0
C(14)-C(15)-C(16)	119.52(18)
C(14)-C(15)-H(15)	120.2
C(16)-C(15)-H(15)	120.2
C(15)-C(16)-C(17)	119.66(19)
C(15)-C(16)-H(16)	120.2
C(17)-C(16)-H(16)	120.2
C(18)-C(17)-C(16)	119.43(19)
C(18)-C(17)-H(17)	120.3
C(16)-C(17)-H(17)	120.3
C(17)-C(18)-C(13)	121.98(19)
C(17)-C(18)-H(18)	119.0
C(13)-C(18)-H(18)	119.0

C(8)-C(19)-H(19A)	109.5
C(8)-C(19)-H(19B)	109.5
H(19A)-C(19)-H(19B)	109.5
C(8)-C(19)-H(19C)	109.5
H(19A)-C(19)-H(19C)	109.5
H(19B)-C(19)-H(19C)	109.5
C(8)-N(1)-S(1)	124.97(13)
C(8)-N(1)-H(1N)	110.9
S(1)-N(1)-H(1N)	108.9
C(1)-O(1)-S(1)	117.03(11)
C(7)-O(4)-C(11)	116.08(15)
O(2)-S(1)-O(3)	119.90(8)
O(2)-S(1)-O(1)	108.42(8)
O(3)-S(1)-O(1)	103.59(8)
O(2)-S(1)-N(1)	111.06(8)
O(3)-S(1)-N(1)	106.74(8)
O(1)-S(1)-N(1)	106.12(7)

Symmetry transformations used to generate equivalent atoms:

Table 4. Anisotropic displacement parameters ($\text{\AA}^2 \times 10^3$) for ART3_066s. The anisotropic displacement factor exponent takes the form: $-2\pi^2 [h^2 a^{*2} U^{11} + \dots + 2 h k a^* b^* U^{12}]$

	U ¹¹	U ²²	U ³³	U ²³	U ¹³	U ¹²
C(1)	25(1)	25(1)	22(1)	3(1)	5(1)	-2(1)
C(2)	32(1)	32(1)	27(1)	10(1)	0(1)	0(1)
C(3)	41(1)	40(1)	22(1)	10(1)	0(1)	-8(1)
C(4)	45(1)	35(1)	22(1)	2(1)	11(1)	-6(1)

C(5)	35(1)	25(1)	27(1)	1(1)	10(1)	-2(1)
C(6)	24(1)	22(1)	23(1)	2(1)	6(1)	-3(1)
C(7)	25(1)	20(1)	23(1)	2(1)	7(1)	4(1)
C(8)	24(1)	21(1)	24(1)	3(1)	5(1)	3(1)
C(9)	26(1)	30(1)	31(1)	8(1)	0(1)	2(1)
C(10)	30(1)	37(1)	45(1)	15(1)	3(1)	11(1)
C(11)	34(1)	29(1)	44(1)	13(1)	10(1)	12(1)
C(12)	26(1)	24(1)	22(1)	6(1)	6(1)	3(1)
C(13)	26(1)	26(1)	27(1)	7(1)	10(1)	3(1)
C(14)	32(1)	33(1)	33(1)	12(1)	3(1)	2(1)
C(15)	35(1)	24(1)	40(1)	13(1)	5(1)	0(1)
C(16)	33(1)	29(1)	47(2)	2(1)	4(1)	-5(1)
C(17)	28(1)	40(1)	34(1)	7(1)	-2(1)	-3(1)
C(18)	31(1)	32(1)	36(1)	12(1)	3(1)	3(1)
C(19)	26(1)	29(1)	35(1)	5(1)	9(1)	0(1)
N(1)	26(1)	21(1)	19(1)	4(1)	4(1)	3(1)
O(1)	26(1)	29(1)	24(1)	4(1)	5(1)	8(1)
O(2)	38(1)	28(1)	29(1)	10(1)	9(1)	2(1)
O(3)	49(1)	26(1)	27(1)	6(1)	13(1)	15(1)
O(4)	33(1)	23(1)	31(1)	4(1)	10(1)	9(1)
S(1)	31(1)	21(1)	21(1)	5(1)	6(1)	5(1)

Table 5. Hydrogen coordinates ($\times 10^4$) and isotropic displacement parameters ($\text{\AA}^2 \times 10^3$) for ART3_066s.

	x	y	z	U(eq)
H(2)	-1930	4553	5713	37
H(3)	-1461	3243	4081	44
H(4)	376	1503	4116	43
H(5)	1646	1002	5755	36
H(9A)	4907	3539	9969	35
H(9B)	2971	2517	9995	35
H(10A)	5735	1734	8762	44
H(10B)	5217	1085	9775	44
H(11A)	3753	-488	8088	41
H(11B)	2241	-46	8798	41
H(12A)	192	1370	9084	28
H(12B)	-1023	2321	8477	28
H(14)	-808	-1144	8664	39
H(15)	-2870	-3226	7708	40
H(16)	-5047	-3156	6175	47
H(17)	-5150	-964	5628	43
H(18)	-3055	1089	6590	39
H(19A)	3749	4323	7379	45
H(19B)	4836	3056	7552	45
H(19C)	5385	4540	8415	45
H(1N)	1356	4161	9648	29

Table 6. Torsion angles [°] for ART3_066s.

C(6)-C(1)-C(2)-C(3)	-1.1(3)
O(1)-C(1)-C(2)-C(3)	-178.47(16)
C(1)-C(2)-C(3)-C(4)	-1.1(3)
C(2)-C(3)-C(4)-C(5)	1.5(3)
C(3)-C(4)-C(5)-C(6)	0.3(3)
C(4)-C(5)-C(6)-C(1)	-2.3(3)
C(4)-C(5)-C(6)-C(7)	176.30(17)
C(2)-C(1)-C(6)-C(5)	2.8(3)
O(1)-C(1)-C(6)-C(5)	179.93(16)
C(2)-C(1)-C(6)-C(7)	-175.85(16)
O(1)-C(1)-C(6)-C(7)	1.3(3)
C(5)-C(6)-C(7)-O(4)	-0.7(2)
C(1)-C(6)-C(7)-O(4)	177.81(15)
C(5)-C(6)-C(7)-C(12)	-119.25(18)
C(1)-C(6)-C(7)-C(12)	59.3(2)
C(5)-C(6)-C(7)-C(8)	115.23(18)
C(1)-C(6)-C(7)-C(8)	-66.2(2)
O(4)-C(7)-C(8)-N(1)	-170.01(14)
C(6)-C(7)-C(8)-N(1)	75.36(18)
C(12)-C(7)-C(8)-N(1)	-48.2(2)
O(4)-C(7)-C(8)-C(19)	66.24(18)
C(6)-C(7)-C(8)-C(19)	-48.40(19)
C(12)-C(7)-C(8)-C(19)	-171.92(15)
O(4)-C(7)-C(8)-C(9)	-55.03(18)
C(6)-C(7)-C(8)-C(9)	-169.67(15)
C(12)-C(7)-C(8)-C(9)	66.81(19)
N(1)-C(8)-C(9)-C(10)	175.18(15)
C(19)-C(8)-C(9)-C(10)	-66.5(2)
C(7)-C(8)-C(9)-C(10)	55.1(2)

C(8)-C(9)-C(10)-C(11)	-53.8(2)
C(9)-C(10)-C(11)-O(4)	53.9(2)
O(4)-C(7)-C(12)-C(13)	-51.3(2)
C(6)-C(7)-C(12)-C(13)	64.16(19)
C(8)-C(7)-C(12)-C(13)	-171.60(14)
C(7)-C(12)-C(13)-C(14)	105.4(2)
C(7)-C(12)-C(13)-C(18)	-77.3(2)
C(18)-C(13)-C(14)-C(15)	1.8(3)
C(12)-C(13)-C(14)-C(15)	179.29(18)
C(13)-C(14)-C(15)-C(16)	-0.8(3)
C(14)-C(15)-C(16)-C(17)	-0.6(3)
C(15)-C(16)-C(17)-C(18)	0.9(3)
C(16)-C(17)-C(18)-C(13)	0.2(3)
C(14)-C(13)-C(18)-C(17)	-1.5(3)
C(12)-C(13)-C(18)-C(17)	-178.94(18)
C(19)-C(8)-N(1)-S(1)	60.73(19)
C(9)-C(8)-N(1)-S(1)	178.50(12)
C(7)-C(8)-N(1)-S(1)	-62.79(18)
C(2)-C(1)-O(1)-S(1)	-113.31(15)
C(6)-C(1)-O(1)-S(1)	69.31(19)
C(6)-C(7)-O(4)-C(11)	176.93(14)
C(12)-C(7)-O(4)-C(11)	-64.98(19)
C(8)-C(7)-O(4)-C(11)	58.64(18)
C(10)-C(11)-O(4)-C(7)	-59.6(2)
C(1)-O(1)-S(1)-O(2)	43.85(14)
C(1)-O(1)-S(1)-O(3)	172.25(12)
C(1)-O(1)-S(1)-N(1)	-75.53(13)
C(8)-N(1)-S(1)-O(2)	-59.60(16)
C(8)-N(1)-S(1)-O(3)	168.05(13)
C(8)-N(1)-S(1)-O(1)	58.03(15)

Symmetry transformations used to generate equivalent atoms:

Table 7. Hydrogen bonds for ART3_066s [\AA and $^\circ$].

D-H...A	d(D-H)	d(H...A)	d(D...A)	$\angle(\text{DHA})$
N(1)-H(1N)...O(3)#1	1.00	1.94	2.939(2)	173.4

Symmetry transformations used to generate equivalent atoms:

#1 $-x, -y+1, -z+2$

References

- (1) (a) Diver, S. T.; Giessert, A. J. *Chem. Rev.* **2004**, *104*, 1317. (b) Mori, M. *Top. Organomet. Chem.* **1998**, *1*, 133. (c) Hansen, E. C.; Lee, D. *Acc. Chem. Res.* **2006**, *39*, (8), 509.
- (2) Rogers, M.M.; Stahl, S. S. *Top. Organomet. Chem.* **2007**, *21*, 21.
- (3) Milczek, E.; Boudet, N.; Blakey, S. *Angew. Chem. Int. Ed.* **2008**, *47*, 6825.
- (4) Nishiyama, H.; Itoh, Y.; Matsumoto, H.; Park, S.-B.; Itoh, K. *J. Am. Chem. Soc.* **1994**, *116*, 2223.
- (5) For reviews see: (a) Muller, P.; Fruit, C. *Chem. Rev.* **2003**, *103*, 2905. (b) Dick, A. R.; Sanford, M. S. *Tetrahedron* **2006**, *62*, 2439. (c) Davies, H. M. L.; Long, M. S. *Angew. Chem. Int. Ed.* **2005**, *44*, 3518.
- (6) (a) Nowlan, D. T., III; Gregg, T. M.; Davies, H. M. L.; Singleton, D. A. *J. Am. Chem. Soc.* **2003**, *125*, 15902-15911. (b) Wong, F. M.; Wang, J.; Hengge, A. C.; Wu, W. *Org. Lett.*, **2007**, *9* (9), 1663.
- (7) (a) Hoye, T.; Dinsmore, C. J.; *J. Am. Chem. Soc.* **1991**, *113*, 4343. (b) Padwa, A. *J. Organomet. Chem.* **2001**, 617. (c) Padwa, A.; Austin, D. J.; Chiacchio, U.; Kassir, J. M.; Rescifina, A.; Xu, S. L. *Tetrahedron Lett.* **1991**, *32*, 5923. (c) Padwa, A. *J. Organomet. Chem.* **2001**, *617*, 3. (d) Panne, P.; Fox, J. M. *J. Am. Chem. Soc.* **2007**, *129*, 22.
- (8) In general, homopropargylic alcohols were prepared in an analogous manner to: Delorme, D.; Girard, Y.; Rokach, J. *J. Org. Chem.* **1989**, *54*, 3635.
- (9) Espino, C. G.; Wehn, P. M.; Chow, J.; Du Bois, J. *J. Am. Chem. Soc.* **2001**, *123*, 6935.

-
- (10) (a) Trnka, T. M.; Grubbs, R. H. *Acc. Chem. Res.* **2001**, *34*, 18. (b) Sanford, M. S.; Love, J. A.; Grubbs, R. H. *J. Am. Chem. Soc.* **2001**, *123*, 6543. (c) Sanford, M. S.; Ulman, M.; Grubbs, R. H. *J. Am. Chem. Soc.* **2001**, *123*, 749. (d) Trnka, T. M.; Morgan, J. P.; Sanford, M. S.; Wilhelm, T. E.; Scholl, M.; Choi, T.-L.; Ding, S.; Day, M. W.; Grubbs, R. H. *J. Am. Chem. Soc.* **2003**, *125*, 2546.
- (11) Blakey, S. B.; Musaev, D. G.; Bon, J. *Unpublished results* **2010**.
- (12) Doyle, M. P.; Phillips, I. M.; Hu, W. *J. Am. Chem. Soc.*, **2001**, *123* (22), 5366.
- (13) Stephen, A.; Hashmi, K. *Chem. Rev.*, **2007**, *107* (7), pp 3180.
- (14) Catino, A. J.; Nichols, J. M.; Forslund, R. E.; Doyle, M. P. *Org. Lett.* **2005**, *7*, 2787.
- (15) Espino, C. G.; Fiori, K. W.; Kim, M.; Du Bois, J. *J. Am. Chem. Soc.* **2004**, *126*, 15378.
- (16) Muller, P.; Fruit, C. *Chem. Rev.* **2003**, *103*, 2905.
- (17) Method adapted from Fruit, C.; Müller, P. *Tetrahedron Asymm.* **2004**, *15*, 1019.
- (18) Chinchilla, R.; Nájera, C. *Chem. Rev.* **2007**, *107*, (3), 874
- (19) Thornton, A. R.; Blakey, S. B. *J. Am. Chem. Soc.* **2008**, *130*, 5020.
- (20) Thornton, A. R.; Martin, V. I.; Blakey, S. B. *J. Am. Chem. Soc.* **2009**, *131*, 2434.
- (21) Qian, M.; Negishi, E. *Tet. Lett.* **2005**, *46*, 2927.
- (22) Ferreira, E. M.; Stoltz, B. M. *J. Am. Chem. Soc.* **2003**, *125*, (32), 9578.
- (23) Micuch, P.; Seebach, D. *Helv. Chim. Acta* **2002**, *85*, (6), 1567.
- (24) Duran, F.; Leman, L.; Ghini, A.; Burton, G.; Dauban, P.; Dodd, R. H. *Org. Lett.* **2002**, *4*, (15), 2481.

-
- (25) Razon, P.; N'Zoutani, M.-A.; Dhulut, S.; Bezzenine-Lafollée, S.; Pancrazi, A.; Ardisson, J. *Synthesis* **2005**, *1*, 109.
- (26) Madelaine, C.; Ouhamou, N.; Chiaroni, A.; Vedrenne, E.; Grimaud, L.; Six, Y. *Tetrahedron* **2008**, *64*, 37, 8878.
- (27) Francka, X.; Vaz Araujo, M. E.; Julliana, J.-C.; Hocquemillera, R.; Figadère, B. *Tetrahedron Letters* **2001**, *9*, 2801.
- (28) Schomaker, J. M.; Pulgam, V. R.; Borhan, B. *J. Am. Chem. Soc.* **2004**, *126*, 13600.
- (29) Francka, X.; Vaz Araujo, M. E.; Julliana, J.-C.; Hocquemillera, R.; Figadère, B. *Tetrahedron Letters* **2001**, *9*, 2801.
- (30) Pinchuk, A. N.; Rampy, M. A.; Longino, M. A.; Skinner, R. W.; Gross, M. D.; Weichert, J. P.; Counsell, R. E. *J. Med. Chem.* **2006**, *49*, 7, 2155.
- (31) Shimizu, T.; Murakoshi, K.; Yasui, K.; Sodeoka, M. *Synthesis* **2008**, *20* 3209.
- (32) Charette, A. B.; Molinaro, C.; Brochu, C. *J. Am. Chem. Soc.* **2001**, 12160.
- (33) Dijkink, J.; Speckamp, W. N. *Tetrahedron* **1978**, *34*, 173.
- (34) Stambuli, J. P.; Stauffer, S. R.; Shaughnessy, K.H.; Hartwig, J. F. *J. Am. Chem. Soc.* **2001**, 2677.
- (35) Beck, A. L.; Mascal, M.; Moody, C. J.; Coates, W. J. *J. Chem. Soc., Perkin Trans. 1*, **1992**, *7*, 813.
- (36) Schmidt, R. R.; Abele, W. *Angew. Chem.* **1982**, *94*, 299.

Chapter 3:

Application of Metallonitrene/Alkyne Cascade Reactions:

Towards the Synthesis of the Securinega Alkaloids and the

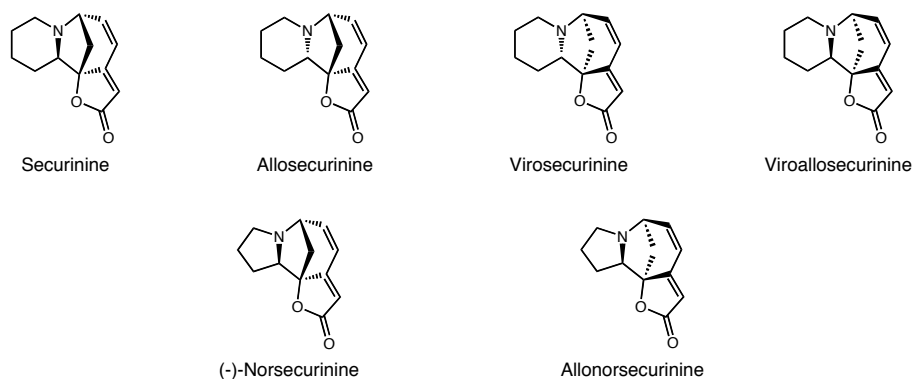
Development of Intermolecular Cascade Termination

3.1. The Securinega Alkaloids

3.1.1. Introduction

Inspired by our new reaction's ability to construct molecular complexity in a rapid fashion, we were immediately attracted to the possibility of using this technology to streamline the synthesis of biologically interesting and medicinally relevant natural products. A review of the literature revealed that a small set of natural products, known as the Securinega alkaloids (Figure 3.1), had been the efforts of significant research.^{1,2} While a number of interesting synthetic approaches to these medicinally useful natural products have been developed (*vide infra*),² we felt that the use of our newly developed methodology could significantly streamline the production of these molecules, and has therefore motivated our research efforts.

Figure 3.1. Representative members of the Securinega alkaloids.



3.1.2. History and Biological Importance

The Securinega alkaloids are a relatively small family of natural products, consisting of approximately 20 members that are generally isolated from a variety of plants from the Euphorbiaceae family, including those from the *Securinega*, *Phyllanthus*, *Flueggea*, *Margaritaria*, and *Brenia* genera.^{1,3} (-)-Securinine, the most abundant member of this family, was first isolated in 1956 from the leaves of *Securinega suffruticosa*, and structural elucidation by Horii and co-workers through chemical degradation and spectroscopic studies was completed in 1965.^{1c,4} Subsequent confirmation of this structure was provided in 1966 through X-ray crystallography.^{4b} Following this, (-)-allosecurinine, the C-2 epimer of (-)-securinine, was isolated from the same plant, and later from the *Phyllanthus* species, in minor amounts.^{1a} Additionally, the enantiomers of both alkaloids, virosecurinine and viroallosecurinine, have also been discovered and characterized.⁵ Subsequent work has led to the discovery of a number of other Securinega alkaloids, including the five-membered A-ring congener, (-)- and (+)-norsecurinine. The two major classes of Securinega alkaloids (securinine-type and norsecurinine-type) consist of numerous structural similarities including the presence of and interesting $\alpha,\beta,\delta,\gamma$ -unsaturated lactone moiety, as well as a core consisting of an azabicyclo [3.2.1] ring system.

In addition to these interesting structural features, the Securinega alkaloids also display a range of powerful biological activities. In fact, plants containing the Securinega alkaloids have been used in traditional Chinese medicine for many years as remedies for a range of illnesses.^{1c} One member of the family, securinine, has been studied *in vivo* for

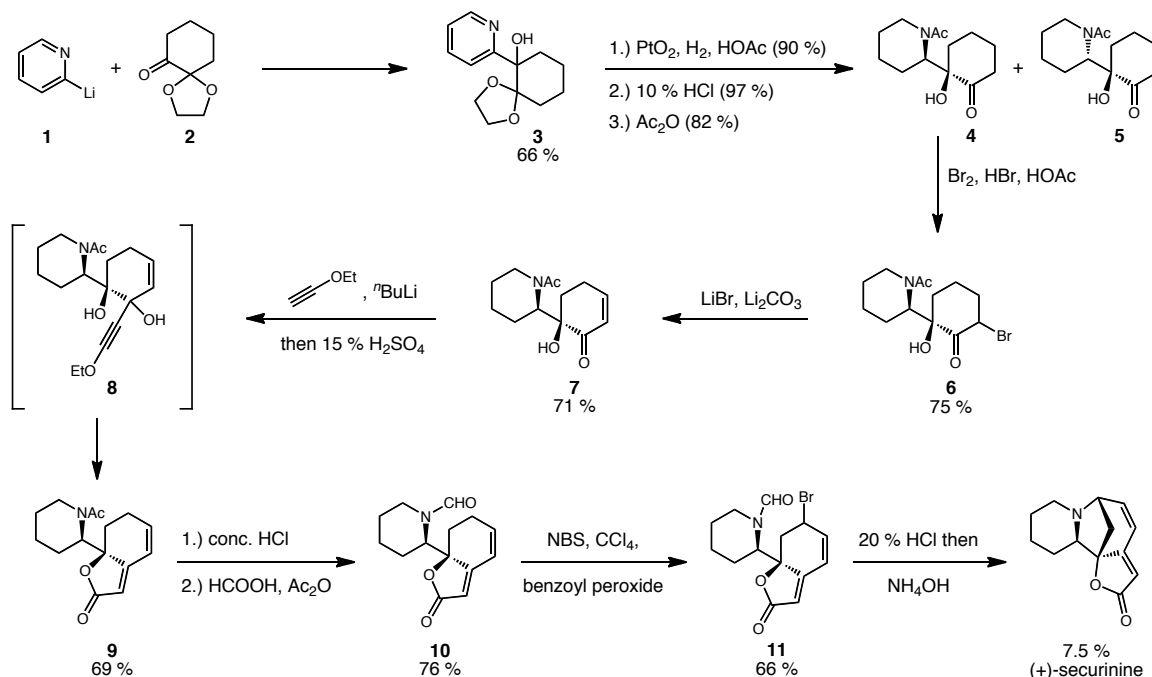
the treatment of symptoms resulting from ALS, Bell's palsy, and poliomyelitis.^{1b} More recently, this same alkaloid has been shown to possess antimalarial, antibacterial, and cytotoxic activity.⁶ Because of these interesting structural features and powerful biological activities, multiple research groups have developed synthetic approaches to these natural products.²

3.1.3. Recent Syntheses of The Securinega Alkaloids

The first total synthesis of racemic securinine (a 1:1 mixture of securinine and virosecurinine) was completed in 1966 by Horii and co-workers and is outlined in Scheme 3.1.^{2f} Their work commenced with the addition of lithiate **1** to ketal ketone **2**, producing alcohol **3** in 66 % yield. The pyridine moiety of this addition product was then reduced through catalytic hydrogenation with PtO₂ and H₂ in 90 % yield. The resulting mixture of diastereomers then underwent ketal hydrolysis and *N*-acetylation with Ac₂O to give **4** and **5**, now separable. The desired diastereomer **4** was then brominated and eliminated under basic condition to afford enone **7** in 71 % yield. This enone then underwent 1,2-addition by the lithiate formed via deprotonation of ethoxyacetylene. This was immediately followed by acidic hydrolysis to give $\alpha,\beta,\gamma,\delta$ -unsaturated lactone **9** in 69 % yield. Removal of the acetyl protecting group through acidic hydrolysis and subsequent reaction with formic acid and Ac₂O yielded the desired formamide **10** in 76 % yield. The total synthesis of (\pm)-securinine was then completed following radical bromination with NBS/CCl₄/benzoyl peroxide and subsequent S_N2 ring closure. Importantly, this allylic activation/S_N2 ring closure strategy has been employed by a

number of other groups in later syntheses of this molecule, and other Securinega alkaloids.

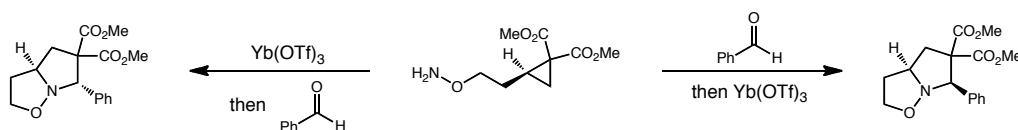
Scheme 3.1. Horii's synthesis of (\pm)-securinine.



Interestingly, it was not until over 20 years later that the next member of the Securinega alkaloids was constructed in Heathcock's 1987 synthesis of (\pm)-norsecurinine.^{2p} Since this work, syntheses of securinine, norsecurinine, and other members of this family have all been completed.² However, it was not until 2008 that the first synthesis of (-)-allosecurinine was completed by Kerr and co-workers.⁷ Their synthesis focused on the use of methodology that was previously developed by within their group for the synthesis of densely functionalized pyrrolidines (Scheme 3.2).⁸ For example, they have shown that intramolecular additions to cyclopropane diesters by tethered oxime ethers, formed via condensation with aldehydes, in the presence of a

Lewis acid catalyst leads to the stereoselective formation of pyrroloisoxazolidines in good yield. Additionally, they have shown that by simply switching the order of addition of the aldehyde and Lewis acid catalyst, the same enantiopure cyclopropane diester can be smoothly transformed into each heterocyclic diastereomer.

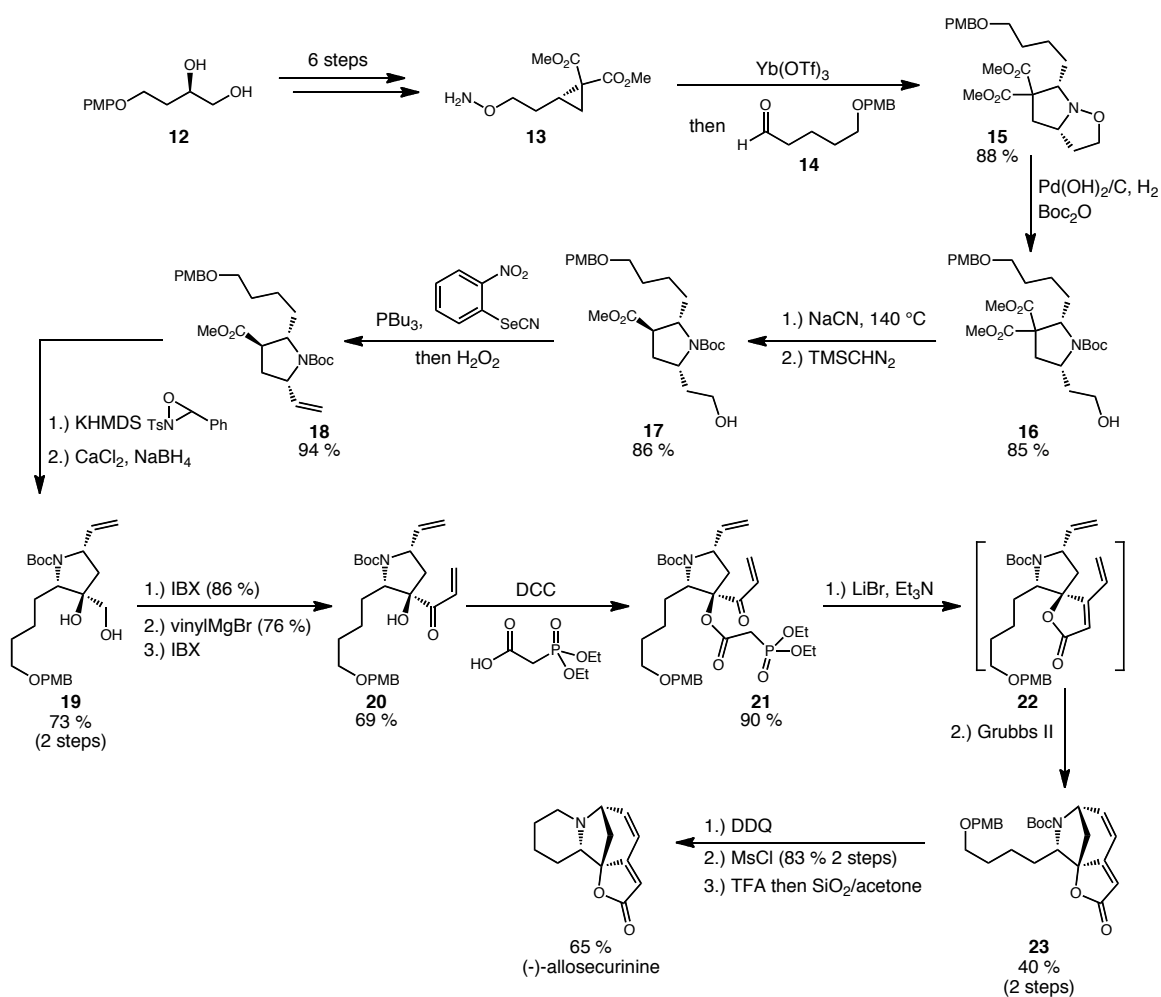
Scheme 3.2. Kerr's method for the synthesis of densely functionalized pyrrolidines.



With this in mind, the construction of (-)-allosecurinine commenced with the synthesis of enantiopure cyclopropane diester **13** from enantiopure PMP-protected triol **12**. This enantiopure substrate was produced through the use of Sharpless asymmetric dihydroxylation, and following its synthesis, a straight-forward six-step sequence provided enantiopure cyclopropane diester **13**. This intermediate was then treated with $\text{Yb}(\text{OTf})_3$ followed by aldehyde **14**, in an analogous manner to the previously discussed methodology, to provide heterocycle **15** in 88 % yield. Hydrogenolysis of this substrate's N-O bond and concurrent Boc protection was carried out using Pearlman's catalyst in the presence of Boc_2O , leading to **16** in 85 % yield. Krapcho decarboxylation led to a mixture of monoester **17** and its corresponding carboxylic acid which was then easily re-esterified using TMS-diozomethane.⁹ Under conditions developed by Grieco, primary alcohol **17** was eliminated to afford olefin **18** in 94 % yield.¹⁰ α -Oxygenation was then carried out through enolization of **18** followed by stereoselective addition to Davis oxaziridine.¹¹ Subsequent reduction of the ester then gave diol **19** in 73 % yield over two

steps. Oxidation of this primary alcohol with IBX was followed by addition of vinylmagnesium bromide and re-oxidation with IBX to give α -hydroxy enone **20**. This tertiary alcohol was then converted to phosphonate ester **21** through DCC mediated coupling in 90 % yield. This substrate was poised for an intramolecular Horner-Wadsworth-Emmons reaction to give butenolide **22**. This compound proved to be unstable so subsequent ring-closing metathesis was then carried out in a one-pot procedure to give **23** in 40 % yield over those two steps. The total synthesis of (-)-allosecurinine was then completed following removal of the PMB protecting group, activation of this alcohol with MsCl, and finally removal of the Boc protecting group and S_N2 ring-closure.

Scheme 3.3. Kerr's synthesis of (-)-allosecurinine.

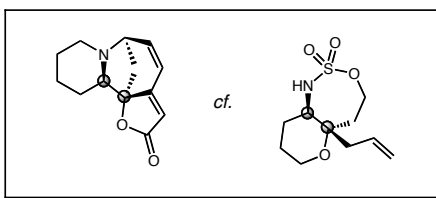


While the completion of the first total synthesis of (-)-allosecurinine was significant, it is worth noting that it was completed in over 20 steps, many of which were simple oxidation state or functional group alterations. This lack of efficiency highlights the need for alternative methods to construct this class of molecules, and has motivated us to examine the potential use of our metallonitrene/alkyne cascade reaction to streamline the synthesis of the Securinega alkaloids.

3.1.4. Metallonitrene/Alkyne Cascade Reactions to Streamline Synthesis

While a number of interesting and powerful syntheses of various members of the Securinega alkaloids have been developed, we felt that our methodology could lend an aspect of utility that had not been seen prior. When designing this project we realized that the methods discussed earlier are only applicable to a single specific member of the Securinega alkaloids. This, combined with the need for multiple functional group interconversions and oxidation state alterations, motivated us to develop a synthesis that would address both of these shortcomings. With this in mind, we felt that our methodology could be used to construct the 1,2-amino oxygenated stereocenters at the core of the Securinega alkaloids in a single transformation (Figure 3.2).

Figure 3.2. Metallonitrene/alkyne cascade reaction constructs the 1,2-amino oxygenated core of the Securinega alkaloids in a single reaction.



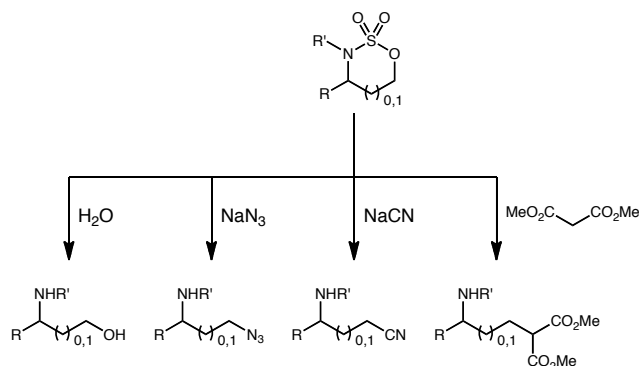
While our method provides the ability to construct the 1,2-amino oxygenated core of the Securinega alkaloids, because of the use of a sulfamate ester nitrene precursor, it also leads to the construction of a seven-membered cyclic sulfamidate. This functionality is clearly not present within this class of natural products and thus must be removed in subsequent reactions.

3.2. Synthetic Utility of Cyclic Sulfamidates

3.2.1. Previous Methods for the Use of 1,2- and 1,3-Cyclic Sulfamidates

Cyclic sulfamidates have been used extensively in the field of organic synthesis.¹² These versatile electrophilic intermediates are known to undergo a wide range of regioselective nucleophilic ring-opening reactions at the *O*-bearing carbon center. This characteristic makes 1,2- and 1,3-cyclic sulfamidates reactive equivalents to aziridines and azetidines respectively. Previous work has established that a range of simple nucleophiles, including CN^- , F^- , N_3^- and others, may be introduced to construct range of 1,2- and 1,3-amino functionalized products (Scheme 3.4). Additionally, it has been reported that more functionalized *C*-based nucleophiles, including stabilized enolates and cuprates, may also be used. In these reactions nucleophilic attack proceeds through an $\text{S}_{\text{N}}2$ pathway at the *O*-bearing carbon center. This regioselective ring-opening results in the formation of the corresponding *N*-sulfate, which can then be readily hydrolyzed under mildly acidic conditions to yield the final 1,2- or 1,3-amino functionalized products.^{12a}

Scheme 3.4. 1,2- and 1,3-cyclic sulfamidates as versatile electrophilic reagents.

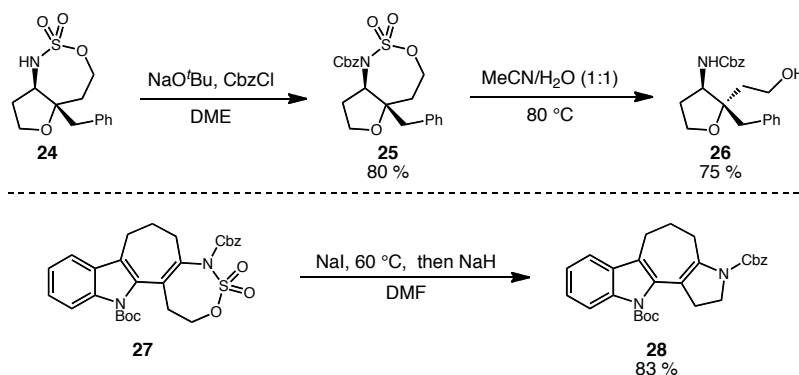


While the ring-opening of 1,2-cyclic sulfamidates proceeds at ambient temperature with a range of nucleophiles and various nitrogen substituents, due to the lessened ring strain associated with 1,3-cyclic sulfamidates, often more forcing reaction conditions are employed. Many times higher reaction temperatures as well as electron withdrawing substituents on the nitrogen, such as amide or carbamate protecting groups, are necessary.

3.2.2. Seven-Membered Oxathiazepane Ring-Opening

With our newly developed metallonitrene/alkyne cascade reaction we are now able to access densely functionalized 1,4-cyclic sulfamidates.¹³ Similar to 1,3-cyclic sulfamidates, we observe that *N*-acylation is necessary for efficient ring-opening reactions. Thus, following protection of oxathiazepane **24** with CbzCl and NaO^tBu in DME, reaction of this intermediate with H₂O in MeCN at 80 °C furnishes Cbz-protected 1,4-amino alcohol **26** in 75 % yield (Scheme 3.5). Additionally, due to the ability of our metallonitrene/alkyne cascade reaction to construct 1,4-cyclic sulfamidates, we have been able to develop a one-pot tandem ring-opening/ring-closing reaction for the synthesis of functionalized pyrrolidines. Thus, when *N*-acylated oxathiazepane **27** is heated with NaI in DMF at 60 °C followed by addition of NaH, we observe the formation of *N*-Cbz 1,2-dihydropyrrolidine **28** in 83 % yield.^{13b} Overall, this results in the extrusion of SO₃ and allows for the construction of densely functionalized pyrrolodines in a highly efficient manner.

Scheme 3.5. Ring-opening reactions of *N*-acyl oxathiazepanes and the development of NaI mediated pyrrolidine synthesis.



With our new reaction's ability to construct the 1,2-amino oxygenated stereocenters at the core of the Securinega alkaloids, as well as the versatility of our cyclization adducts, we were now set to pursue the total synthesis of the Securinega alkaloids.

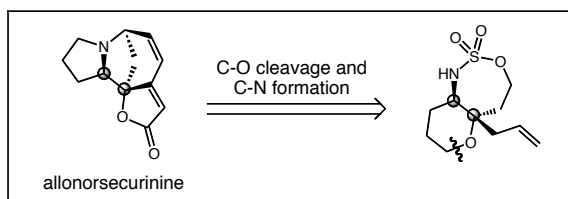
3.3. First Generation Approach Towards (±)-Allonorsecurinine

3.3.1. Retrosynthetic Analysis of (±)-Allonorsecurinine

With this previous work established, we hoped to utilize our newly developed metallonitrene/alkyne cascade reaction to streamline the synthesis of allonorsecurinine. While we were confident in this reaction's ability to construct the 1,2-amino oxygenated stereocenters at the core of allonorsecurinine, we knew that this method still needed further development if our efforts were to be successful. Namely, due to the constraint of intramolecular cascade termination, this process results in the formation of bicyclic ring

structures. When compared to the Securinega alkaloids it becomes clear that the carbon tether that was used for intramolecular trapping of the reactive intermediate would now need to be used to construct the second pyrrolidine moiety of allonorsecurinine (Scheme 3.6). Thus, if we were to utilize this methodology in the context of the Securinega alkaloids, we would be required to use an intramolecular trap that would allow us to then cleave the newly formed C-O bond.

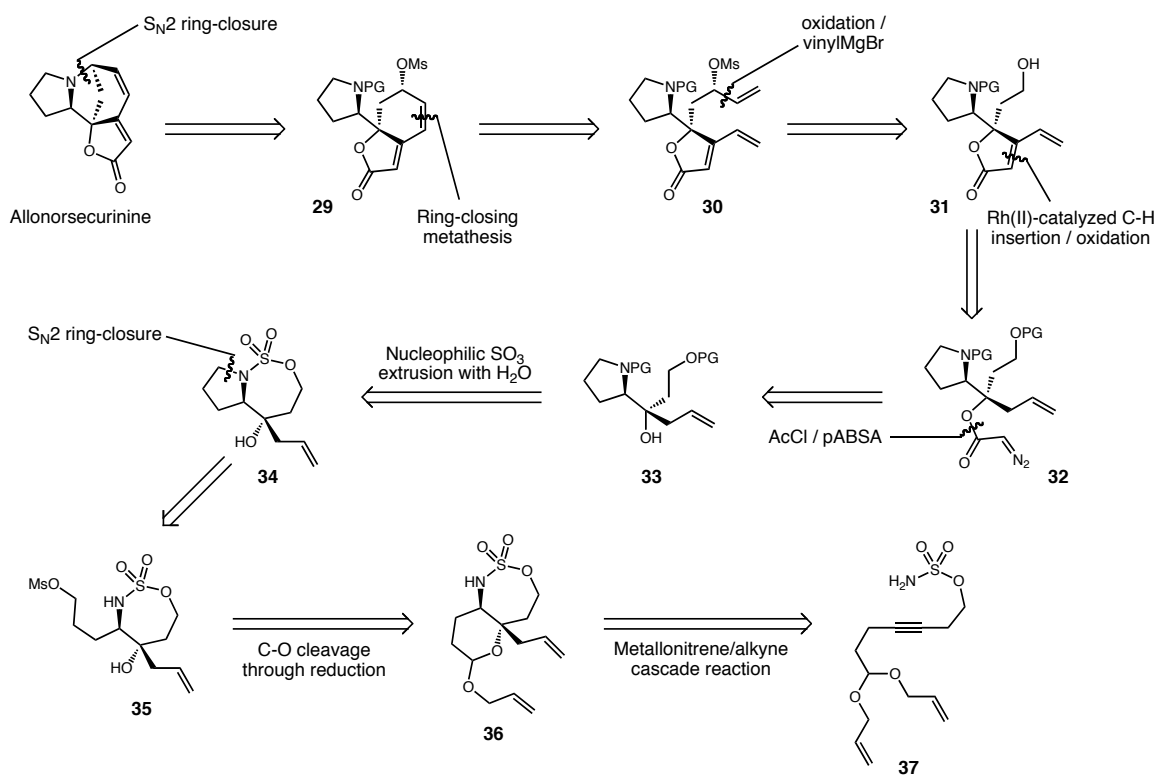
Scheme 3.6. Securinega alkaloids inspire the development of novel metallonitrene/alkyne cascade reaction termination.



Taking this into consideration, we have developed the following retrosynthetic analysis (Scheme 3.7). We felt that allonorsecurinine could be constructed through a final S_N2 ring-closure from pyrrolidine **29**, similar to the completion of Horii's original synthesis of norsecurinine. This pyrrolidine would be constructed from the ring-closing metathesis of **30**, accessed by addition of vinylmagnesium bromide to the aldehyde derived from oxidation of alcohol **31**. The butenolide ring-system of **31** could be accessed through the Rh(II)-catalyzed insertion of the carbene derived from α -diazo ester **32** into its γ -allylic C-H bonds. α -Diazo ester **32** could be accessed from tertiary alcohol **33** after acetylation and diazotization. This alcohol would arise from the nucleophilic extrusion of SO_3 from oxathiazepane **34** with H_2O . The pyrrolidine ring-system of **34** would arise from ring-opening through C-O bond cleavage of the metallonitrene/alkyne

cascade reaction product **36**, followed by nucleophilic displacement of the tethered activated alcohol. Thus, in pursuing the total synthesis of allonorsecurinine we felt that the construction of tertiary alcohol **35** would be crucial. With this in mind, we envisioned the use of acetal tethered alkynyl sulfamate ester **37** for use in our metallonitrene/alkyne cascade reaction. We postulated that this substrate would lead to the formation of hemiacetal **36** through an analogous oxonium ylide formation and [2,3] allyl group migration. This cyclization adduct could then be reduced to yield the desired tertiary alcohol with a tethered allyl-protected primary alcohol functionality. Thus, our synthetic efforts began with the construction of acetal tethered alkynyl sulfamate ester **37**.

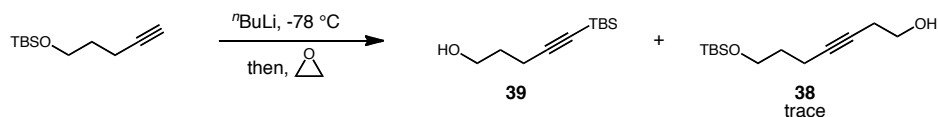
Scheme 3.7. Retrosynthetic analysis for the construction of allonorsecurinine through a metallonitrene/alkyne cascade reaction strategy.



3.3.2. Towards the Synthesis of (±)-Allonorsecurinine Through Allyl Acetal Tethered Alkynyl Sulfamate Ester **37**

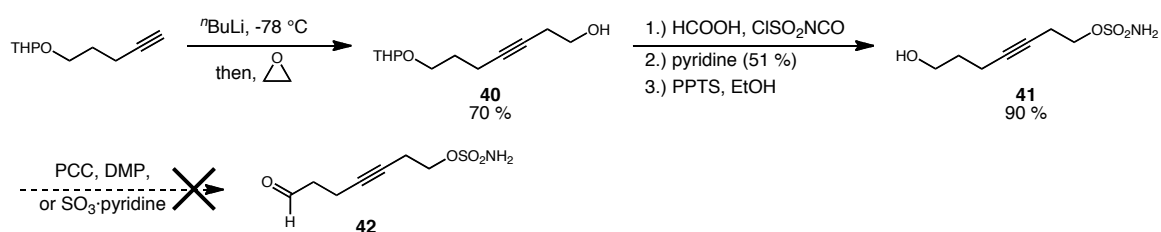
Following the plan laid out in Scheme 3.7, we began our synthesis of allonorsecurinine by first attempting to construct the metallonitrene/alkyne cascade reaction precursor, acetal tethered alkynyl sulfamate ester **37**. Our first attempts at constructing this substrate were met with significant difficulties. Our initial route began with the deprotonation of TBS-protected 4-pentyn-1-ol at $-78\text{ }^{\circ}\text{C}$ followed by addition to oxirane (Scheme 3.8).¹⁴ While similar substrates have been successfully constructed in an analogous manner, in this case, use of a silicon-based protecting group was not amenable to our reaction conditions. In this reaction we observed only minor amounts of the desired alcohol **38**, and the major side product isolated from the resulting complex mixture was tentatively assigned as the TBS-acetylene **39**, containing a free hydroxyl group. It is hypothesized that this product simply arises from addition of the alkynyl lithiate formed via deprotonation to the silicon protecting group itself, resulting in the formation of the less basic alkoxide anion which is then protonated upon mildly acidic work-up.

Scheme 3.8. Initial route to cyclization precursor **37** and unsuccessful attempts at oxirane opening.



Identifying that silicon-based protecting groups were not amenable to the opening of oxirane under the conditions examined motivated us to pursue the use of an alternate protecting group. Thus, THP-protected 4-pentyn-1-ol underwent addition to oxirane leading to homopropargylic alcohol **40** in 70 % yield (Scheme 3.9).¹⁵ This alcohol was then converted to its corresponding sulfamate ester in 51 % yield and THP-removal with PPTS in EtOH provided alcohol tethered alkynyl sulfamate ester **41**. In order to convert **41** to the desired cyclization precursor, we first needed to oxidize this substrate to its corresponding aldehyde, **42**. While there is no literature precedent for carrying out such a transformation in the presence of a sulfamate ester moiety, we felt that the concise nature of this route, and the ease with which alcohol **41** could be constructed, warranted the examination of this oxidation. Unfortunately, while a number of typical oxidations were attempted, including PCC, SO₃·pyridine, DMP, and Swern oxidations, only minimal amounts of the desired aldehyde **42** were ever isolated, and this route was subsequently abandoned.

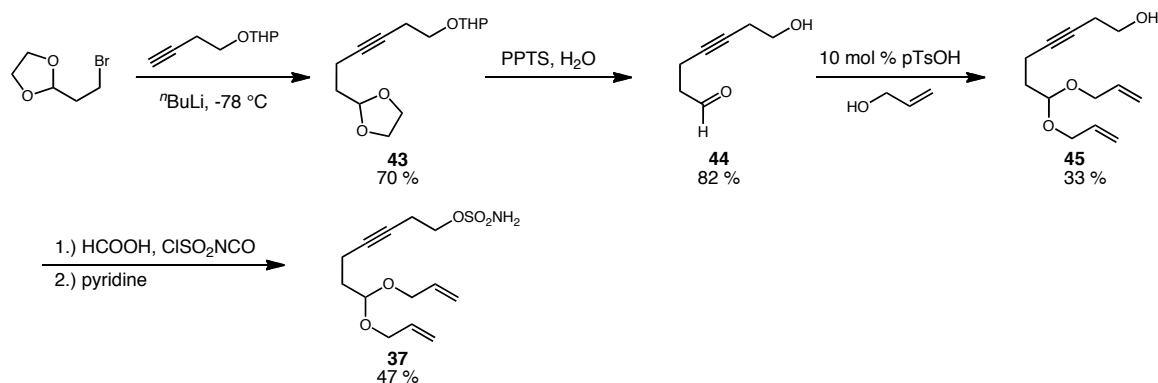
Scheme 3.9. Attempted synthesis of cyclization precursor **37** and unsuccessful oxidation protocols.



With these unsuccessful attempts behind us, we then examined a different synthetic strategy to obtain acetal tethered alkynyl sulfamate ester **37**. We chose to

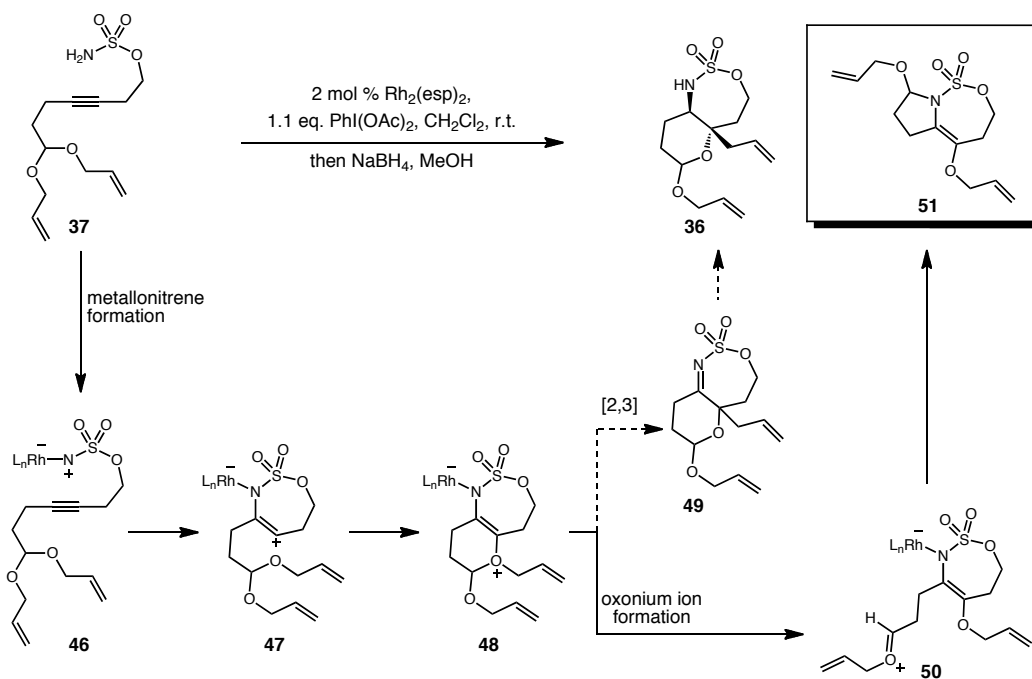
pursue this same substrate through the coupling of THP-protected 3-butyn-1-ol with commercially available 2-(2-bromoethyl)-1,3-dioxolane (Scheme 3.10). Thus, S_N2 displacement of this bromide with deprotonated THP-protected 3-butyn-1-ol was carried out in 70 % yield. This was followed by the removal of both the THP and dioxolane protecting groups under mildly acidic conditions to afford aldehyde **44** in 82 % yield. This aldehyde was then converted to allyl acetal **45** in 33 % yield. While typical dehydrative conditions, such as Dean-Stark and the use of 3 Å mol sieves, were attempted, only the use of neat allyl alcohol with 10 mol % pTsOH afforded the desired product, albeit in low yield. Finally, the homopropargylic alcohol of this substrate was converted to its corresponding sulfamate ester under standard conditions, providing **37** in 47 % yield. It is postulated that the low yield associated with this reaction is potentially due to the acidic lability of the allyl acetal moiety in conjunction with the use of excess formic acid needed to prepare sulfamoyl chloride prior to addition of the alcohol **45**. Even with these sequential low-yielding steps we were now in a position to examine the possibility of terminating our metallonitrene/alkyne cascade reaction with a tethered allyl acetal moiety.

Scheme 3.10. Synthesis of allyl acetal tethered alkynyl sulfamate ester **37**.



With substrate **37** in hand we next turned our attention to the key cyclization reaction (Scheme 3.11). When exposing this substrate to our general reaction conditions for the intramolecular termination of this metallonitrene/alkyne cascade reaction (2 mol % $\text{Rh}_2(\text{esp})_2$ and 1.1 equivalents $\text{PhI}(\text{OAc})_2$ in CH_2Cl_2 at ambient temperature followed by the addition of NaBH_4 and MeOH) we observed the formation of a complex mixture of products. Multiple attempts at purification provided one constituent of this complex mixture in trace amounts that we have tentatively assigned as compound **51**, as determined by ^1H NMR analysis and MS. This cyclization adduct could potentially arise from initial attack of a tethered allyl acetal oxygen atom leading to zwitterion **48**, while this intermediate was expected to undergo the typical [2,3] allyl migration, it appears that formation of oxonium ion **50** is faster. This oxonium ion can then undergo nucleophilic attack by the oxathiazepane nitrogen to yield bicyclic compound **51**.

Scheme 3.11. Cyclization of sulfamate ester **37** yields an unexpected product.



While the formation of bicyclic compound **51** was interesting, we felt that it was not viable to carry on our synthetic strategy through the use of an allyl acetal to terminate this cascade process, and accordingly, we re-examined our synthetic strategy. In our initial retrosynthetic analysis (Scheme 3.7) we identified that tertiary alcohol **35** was key to our proposed synthesis of the Securinega alkaloids. To access this alcohol we focused on an intramolecular cascade termination strategy that would allow us to subsequently cleave the resulting C-O bond of the bicyclic cyclization adduct. In re-examining this strategy, we realized that a more efficient route would circumvent the need for C-O bond cleavage, and in turn has inspired us to develop conditions for the intermolecular termination of our metallonitrene/alkyne cascade reaction.

3.4. Intermolecular Metallonitrene/Alkyne Cascade Reaction Termination

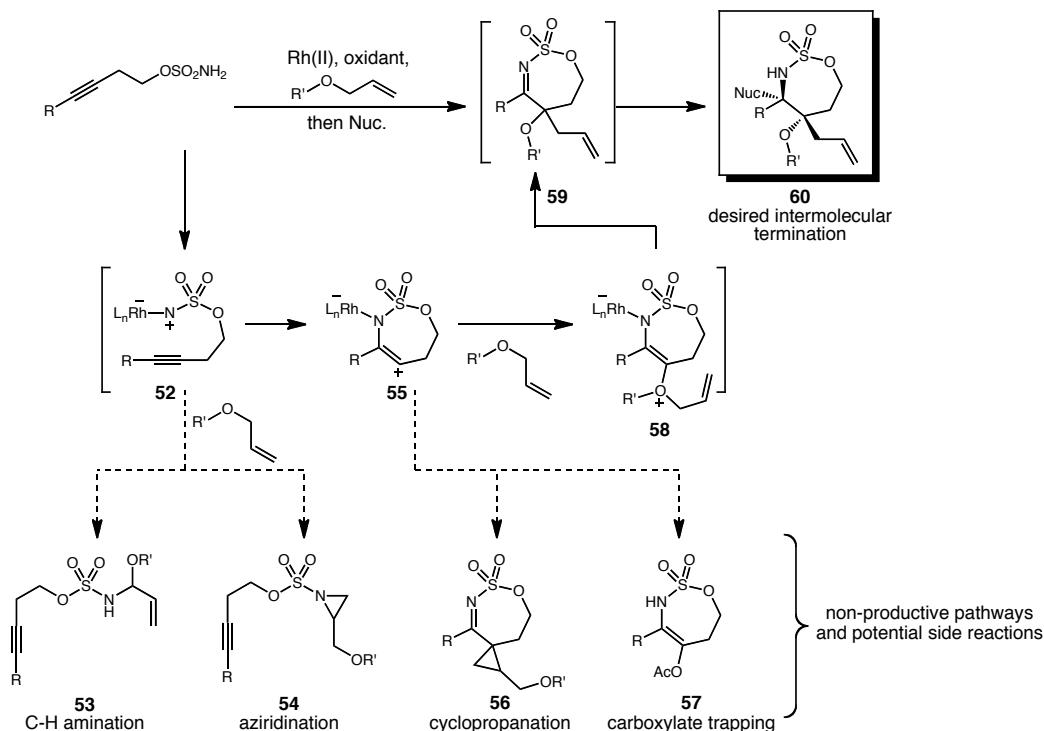
3.4.1. Concept and Preliminary Results

The intermolecular termination of this metallonitrene/alkyne cascade reaction represents a powerful concept for the rapid construction of densely functionalized *N*-containing molecules. This reaction allows for the combination of readily accessible sulfamate esters and commercially available allyl ethers to build significant complexity in a single transformation. However, even with this potential utility, there still remained a

number of obstacles that must be overcome before devising a synthetic strategy towards the Securinega alkaloids.

When examining a potential mechanism for this transformation a number of potential competing processes immediately present themselves (Scheme 3.12). First, there are a number of potential side reactions that the reactive metallonitrene (**52**) could take part in. For example, as discussed in Chapter 1, reactive metallonitrenes are known to undergo both C-H amination and azirindination reactions. If we hope to terminate this cascade process through the addition of an allyl ether nucleophile, we will in turn be exposing the reactive metallonitrene to both activated (ethereal and allylic) C-H bonds, as well as olefins, potentially leading to products **53** and **54** respectively. Second, if the metallonitrene does react preferentially with the tethered alkyne, there are still competing processes that will need to be suppressed for this reaction to be successful. For example, our previous results indicate that this reactive intermediate (**55**) may undergo cascade termination through cyclopropanation as well as intermolecular carboxylate trapping, both of which are potential side reactions in the cascade process (**56** and **57**). Thus, if this reaction is to lead to our desired intermolecular termination product **60**, a considerable amount of selectivity will need to be attained in order to suppress multiple non-productive pathways.

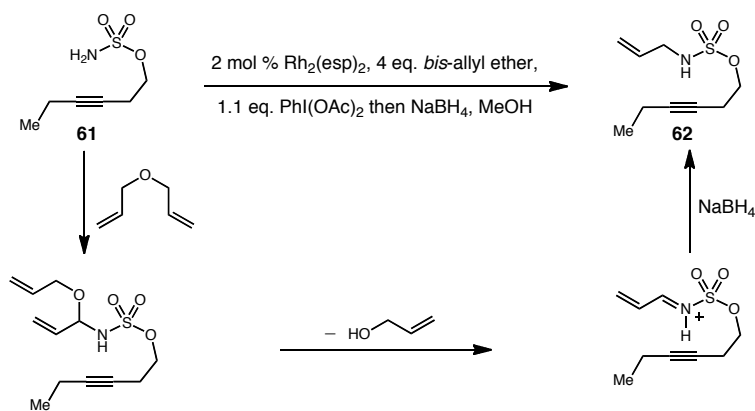
Scheme 3.12. Mechanism for the intermolecular termination of metallonitrene/alkyne cascade reactions and potential non-productive pathways.



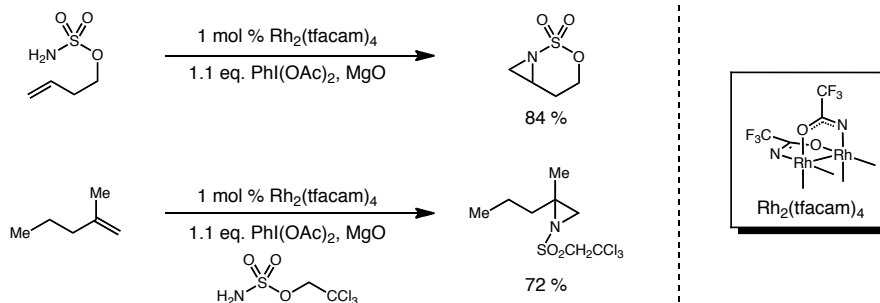
With this concept established, we commenced our studies into the intermolecular termination of this cascade process using sulfamate ester **61**. This substrate was produced in a single step from its corresponding commercially available homopropargylic alcohol, and possesses a simple alkyl group tethered to the alkyne as to remove any complications that could arise from intramolecular termination of the cascade process. To begin our studies we first simply introduced an excess of our desired nucleophile, *bis*-allyl ether, into the reaction mixture under standard reaction conditions (Scheme 3.13). However, when sulfamate ester **61** was combined with 2 mol % $\text{Rh}_2(\text{esp})_2$, 1.1 equivalents $\text{PhI}(\text{OAc})_2$, and 4 equivalents *bis*-allyl ether in CH_2Cl_2 at ambient temperature, followed by *in situ* reduction with NaBH_4 and MeOH , we did not observe formation of the desired cyclization adduct. Instead, the only isolable product

from the resulting complex mixture arose from intermolecular C-H amination of this substrate with *bis*-allyl ether, followed by reduction of the resulting hemi-aminol.

Scheme 3.13. Preliminary examination of intermolecular cascade termination with *bis*-allyl ether leads to intermolecular C-H amination products.

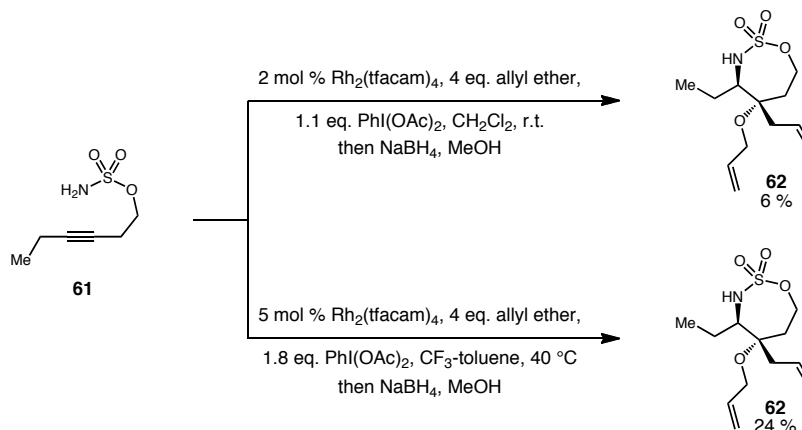


While discouraged by these preliminary results, we also knew that a major advantage to the use of Rh(II) catalysts is the fact that it has been illustrated that simple alterations in catalyst structure can have profound effects on reactivity and reaction efficiency.¹⁶ With this in mind, we were immediately drawn to a recent publication from the Du Bois group in which they utilized $\text{Rh}_2(\text{tfacam})_4$ for selective intra- and intermolecular aziridination reactions (Scheme 3.14).¹⁷ In this paper they state that this catalyst “*displays a strong bias for π -bond functionalization over σ -C-H insertion.*” While olefins and alkynes obviously display a number of differences, we felt that this statement justified the examination of this catalyst for our metallonitrene/alkyne cascade reaction.

Scheme 3.14. Du Bois' $\text{Rh}_2(\text{tfacam})_4$ for intra- and intermolecular aziridination reactions.

Du Bois' $\text{Rh}_2(\text{tfacam})_4$ is easily prepared through ligand exchange with commercially available $\text{Rh}_2(\text{OAc})_4$ and tri-fluoro acetamide in refluxing ClC_6H_5 over six days. After producing this catalyst in 74 % yield we then turned to examining its use in our metallonitrene/alkyne cascade reaction. Thus, exposing sulfamate ester **61** to 2 mol % $\text{Rh}_2(\text{tfacam})_4$, 1.1 equivalents PhI(OAc)_2 , and 4 equivalents *bis*-allyl ether in CH_2Cl_2 at ambient temperature followed by *in situ* reduction with NaBH_4 and MeOH furnished the desired cyclization adduct in 6 % yield (Scheme 3.15). While 6 % yield for our desired cyclization adduct is not synthetically useful, the observation that C-H amination was effectively suppressed gave us confidence in pursuing the further development of this transformation. A brief optimization revealed that conducting these reactions in CF_3 -toluene at 40 °C with 5 mol % catalyst and an excess of oxidant significantly increased our isolated yields of **62**, now to 24 %. Again, while 24 % yield is still not synthetically viable, these findings provided proof-of-principle for this new transformation, and we felt that the further development of this reaction was thus justified. In working towards the larger goal of constructing the Securinega alkaloids, we felt that it was pertinent to continue this optimization study with the use of a substrate that could potentially be useful to construct this class of natural products.

Scheme 3.15. Catalyst tuning provides proof-of-principle for intermolecular cascade termination.

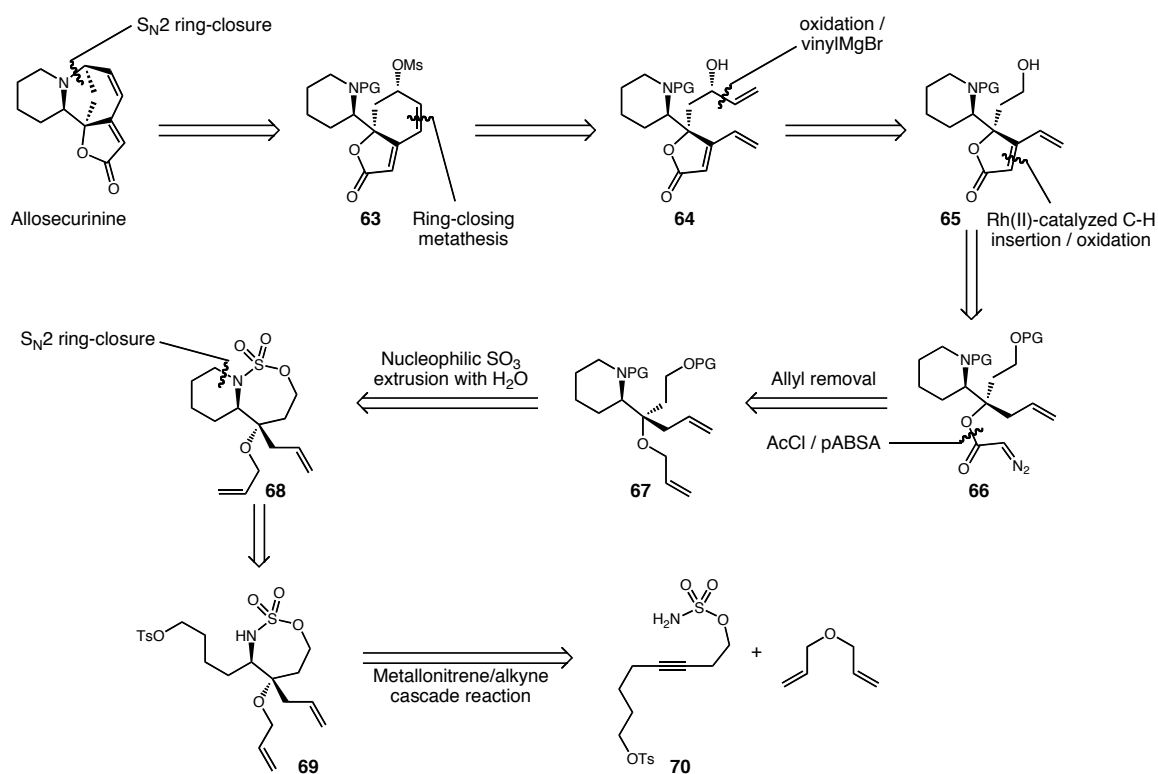


3.4.2. Retrosynthetic Analysis for (±)-Allosecurinine Through Intermolecular Cascade Termination

With these preliminary results established we next turned to devising a retrosynthesis for the construction of allosecurinine through the use of this intermolecular cascade termination methodology. Similar to our previously discussed retrosynthetic analysis (Scheme 3.7), we envisioned the total synthesis of allosecurinine being completed through an $\text{S}_{\text{N}}2$ ring-closure of allylic mesylate **63** (Scheme 3.16). This intermediate was planned to arise from ring-closing metathesis of substrate **64**, which in turn could be produced from the addition of vinylmagnesium bromide to the aldehyde resulting from oxidation of alcohol **65**. The butenolide ring-system was envisioned to arise from a similar C-H insertion strategy from α -diazo ester **66**, as discussed in our prior retrosynthetic analysis. The tertiary alcohol needed to install this α -diazo ester functionality would arise from removal of the allyl protecting group from piperidine **67**. This intermediate was envisioned to come from nucleophilic extrusion of SO_3 from

oxathiazepane **68** with H₂O. This bicyclic oxathiazepane could be accessed through S_N2 ring-closure of the primary tosylate **69** which would result from the intermolecular termination of our metallonitrene/alkyne cascade reaction with *bis*-allyl ether using alkynyl sulfamate ester **70**. Thus, our efforts towards the synthesis of allosecurinine began with the construction of cyclization precursor, alkynyl sulfamate ester **70**.

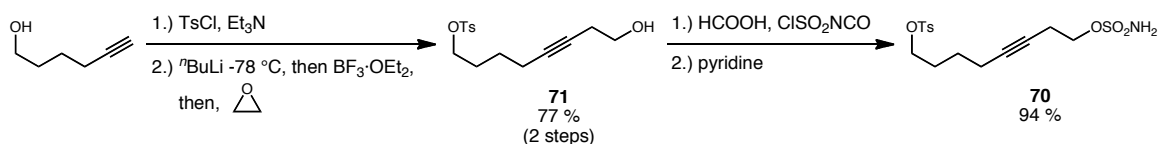
Scheme 3.16. Retrosynthetic analysis for the construction of allosecurinine through intermolecular cascade termination.



3.4.3. Towards the Synthesis of Allosecurinine Through Intermolecular Cascade Termination

To begin our studies towards the synthesis of allosecurinine we first constructed alkynyl sulfamate ester **70**. Thus, after tosylation of 5-hexyn-1-ol with TsCl and Et₃N, the resulting terminal alkyne was deprotonated at -78 °C with ⁿBuLi and underwent BF₃·OEt₂ assisted addition to oxirane (Scheme 3.17).¹⁸ This modified procedure for oxirane opening was adopted as to avoid dimerization of the alkyne. In this procedure, the lithiate formed via deprotonation with ⁿBuLi is first exposed to 1.2 equivalents of BF₃·OEt₂, presumably leading to the corresponding alkynyl borane. While maintaining the reaction temperature at -78 °C oxirane was then added. The oxophilic alkynyl borane then readily undergoes addition to this electrophile, resulting in complete consumption of starting material with 25 minutes and an isolated yield of homopropargylic alcohol **71** in 77 % over two steps. Sulfamate ester **70** was then produced in 94 % yield through the use of standard reaction conditions.

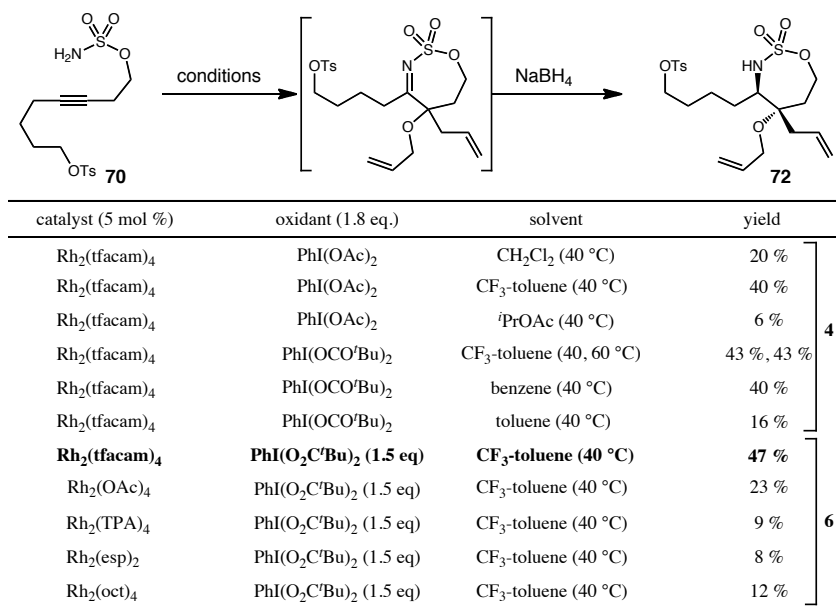
Scheme 3.17. Synthesis of alkynyl sulfamate ester **70**.



With an efficient and high-yielding synthesis of sulfamate ester **70** established, we next turned to optimizing this new reaction. As outlined in Scheme 3.18, our studies began with an examination of various solvents. Thus, under the conditions outlined

earlier, it was once again found that CF₃-toluene and benzene provided the best isolated yields. Additionally, it was found that higher yields were obtained when PhI(O₂C^tBu)₂ was employed as an oxidant. This finding may be attributed to the fact that this oxidant is substantially more soluble in our solvent of choice, CF₃-toluene. Because of this increased solubility, we were then able to reduce the amount of oxidant that was needed. While we were not able to isolate any products arising from trapping of the reactive intermediate with the carboxylic acid byproduct of our oxidant, we hoped that reducing the amount of oxidant present, while increasing the amount of nucleophile in solution, could increase our isolated yields. Thus, lowering the equivalents of oxidant from 1.8 to 1.5, and increasing the equivalents of *bis*-allyl ether from four to six, led to our highest isolated yield of **72** in 47 % with a diastereomeric ratio of 10:1 (*vide infra*). Lastly, to determine if Rh₂(tfacam)₄ was to credit for this reaction's efficiency, we underwent an examination of other potential Rh(II) catalysts. To date, all other Rh(II)-tetracarboxylates have led to significantly lower yields of our desired cyclization adduct, in turn confirming that the use of the electron-rich Rh₂(tfacam)₄ catalyst is superior for this metallonitrene/alkyne cascade reaction.

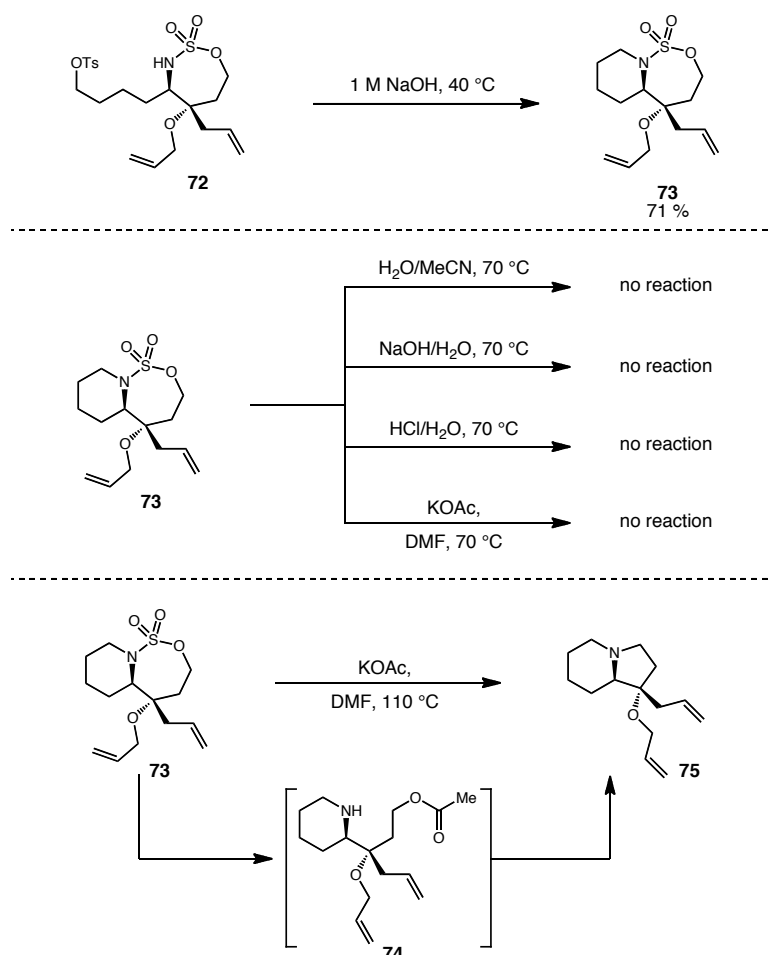
Scheme 3.18. Optimization of intermolecular cascade termination with *bis*-allyl ether towards the synthesis of allosecurinine.



While the formation of cyclization adduct **72** in 47 % yield is significant, we were cognizant of the challenges associated with carrying out a synthesis with such a low-yielding step. Nonetheless, due to this reaction's ability to form such molecular complexity in a single transformation, we were still motivated to continue our synthetic efforts. Thus, after this key cyclization reaction, treatment of the resulting oxathiazepane with 1 M aqueous NaOH in THF led to an intramolecular S_N2 displacement of the primary tosylate, leading to bicyclic amine **73** in 71 % yield (Scheme 3.19). At this stage we next turned to examining conditions for the ring-opening of this *N*-alkyl oxathiazepane with *O*-based nucleophiles. First, we examined the use of H₂O as a potential nucleophile for this transformation. Unfortunately, under a variety of conditions we observed no reactivity and starting material was cleanly recovered. Additionally, when KOAc was examined at 70 °C in DMF we saw no reactivity.

However, when a mixture of KOAc and oxathiazepane **73** was heated to 110 °C in DMF for 24 hours, we observed our first positive results. While the desired product **74** was not observed, we believe that the isolated bicyclic amine **75** comes from the initial nucleophilic addition of acetate anion to form **74**, but under the elevated reaction temperatures, this intermediate can then undergo displacement of acetate to give **75**.

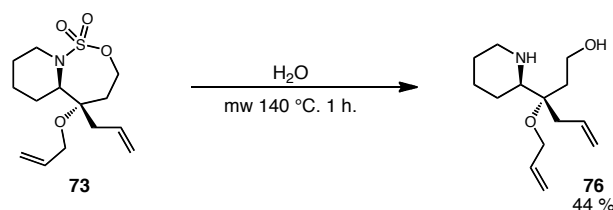
Scheme 3.19. Unsuccessful attempts at *N*-alkyl oxathiazepane ring-opening and initial positive results.



While this reaction was not productive for our synthesis of allosecurinine, it illustrated the significantly decreased reactivity of these *N*-alkyl oxathiazepanes, and

suggested that increased reaction temperatures were necessary for the introduction of *O*-based nucleophiles. Taking this into consideration, we examined a variety of conditions for the introduction of H₂O under elevated temperatures. After considerable effort it was found that H₂O could be successfully introduced when *N*-alkyl oxathiazepane **73** was heated to 140 °C in a 1:1 mixture of H₂O/dioxane under microwave irradiation for 1 hour in 44 % yield (Scheme 3.20). However, due to this reaction's low yield, as well as issues of reproducibility, it was determined that this strategy would not be amenable to the synthesis of allosecurinine.

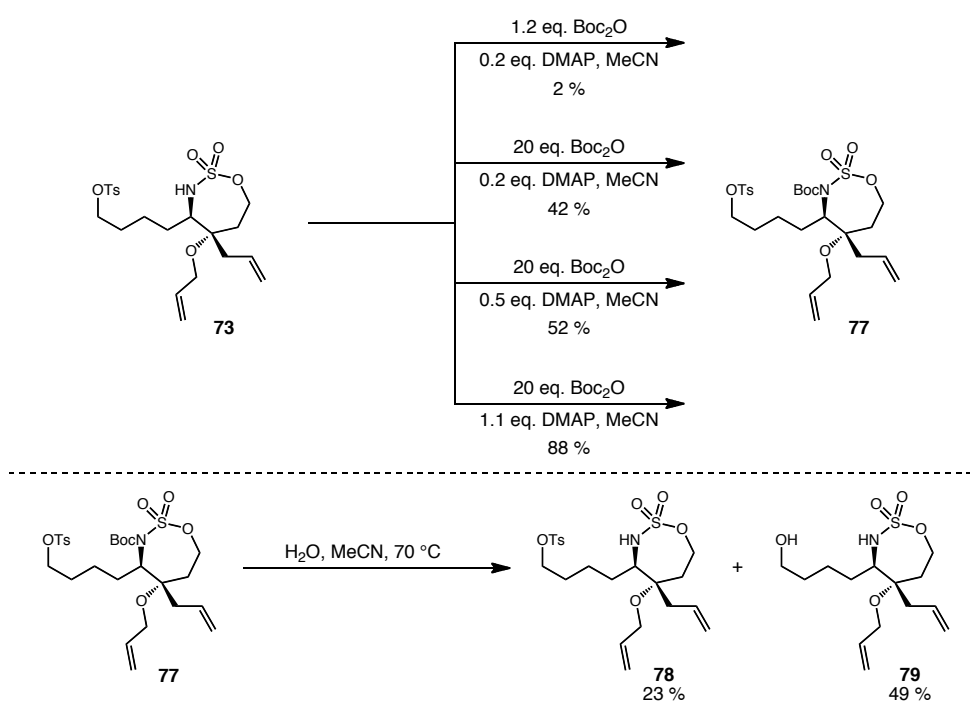
Scheme 3.20. Limited success at *N*-alkyl oxathiazepane ring-opening with H₂O.



Because of the difficulties associated with the ring-opening of *N*-alkyl oxithiazepane **73** with *O*-based nucleophiles, we next examined the possibility of acylating cyclization adduct **72** prior to ring-opening (Scheme 3.21). Multiple attempts at acylating this *N*-atom with Boc₂O and DMAP resulted in the undesired S_N2 ring-closure product **73**. However, it was determined that conducting the reaction with a large excess of Boc₂O (20 equivalents) as well as a full equivalent of DMAP provided the desired *N*-acylated oxathiazepane **77** in 88 % yield while suppressing the formation of the intramolecular S_N2 ring-closure product **73**. We then attempted the opening of this *N*-Boc oxathiazepane under conditions that had been successful for the opening of similar

N-acylated oxathiazepanes. Thus, when heating a mixture of **77** with H₂O and MeCN at 70 °C we observe the formation of multiple products. It was determined that products **78**, resulting from hydrolysis of the Boc protecting group, as well as **79**, resulting from displacement of the primary tosylate, were produced as the major products in 23 % and 49 % yield respectively, without our desired ring-opened product being produced.

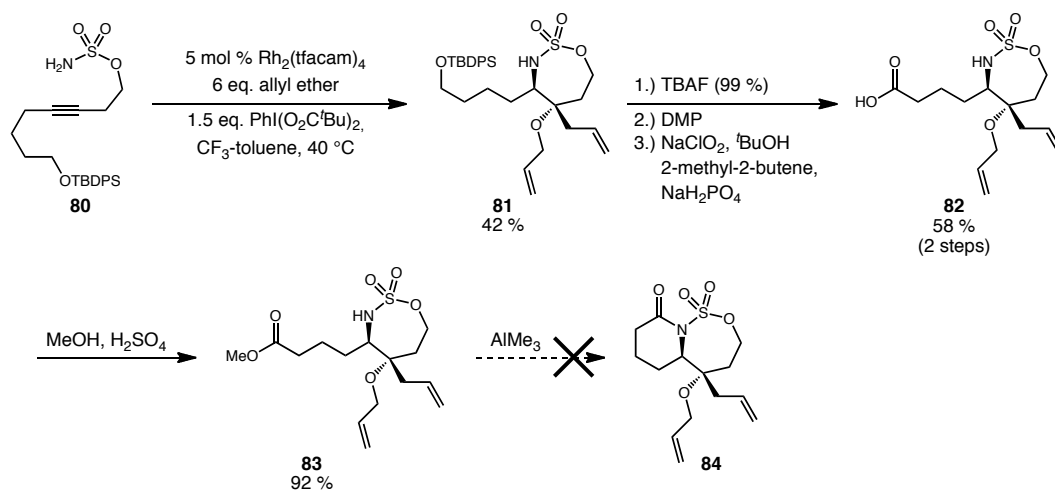
Scheme 3.21. Attempts at *N*-acylation and unsuccessful ring-opening with H₂O.



Because of these issues associated with the ring-opening of the resulting cyclization adduct, we were forced us to re-evaluate our synthetic approach once again. Thus, it was determined that instead of utilizing tosylated alkynyl sulfamate ester **70** in our metallonitrene/alkyne cascade reaction, the use of TBDPS-protected substrate **80** could be beneficial. This substrate was constructed in an analogous manner as previously discussed tosylated substrate, and underwent cyclization under our optimized reaction

conditions in 42 % yield (Scheme 3.22). This substrate was designed so that once the tethered alcohol functionality was released, we could potentially oxidize and subsequently cyclize in an intramolecular fashion to give amide **84**, an *N*-acylated oxathiazepane that could undergo facile ring-opening with H₂O. Thus, following Rh(II)-catalyzed cyclization, removal the silicon-based protecting group was accomplished in 99 % yield using TBAF. Next, this alcohol was oxidized to its corresponding carboxylic acid using a standard two-step protocol. Thus, use of Dess-Martin periodinane was followed by immediate exposure of the resulting aldehyde to Pinnick oxidation conditions to yield carboxylic acid tethered oxathiazepane **82** in 58 % yield over two steps. Subsequent attempts at coupling this acid with DCC were unsuccessful and it was determined based on literature precedent that conversion of acid **82** to methyl ester **83** could be beneficial for this coupling.¹⁹ Following esterification of this acid in 92 % yield, we attempted to close this second ring-system through the use of AlMe₃. Unfortunately, these attempts were once again unsuccessful and the resulting complex mixture of products was abandoned.

Scheme 3.22. Unsuccessful attempts to produce bicyclic *N*-acylated oxathiazepane **84**.



While initially we felt that our methodology could help to streamline the synthesis of allosecurinine, it soon became clear that sequential low-yielding steps were hampering our synthetic strategy. After multiple attempts at constructing this class of natural products it was determined that the investment of our resources would be better directed away for the realm of total synthesis, and instead in the further development of this intermolecular cascade termination methodology. Thus, we next looked to re-evaluate this reaction and its ability to construct *N*-containing molecules.

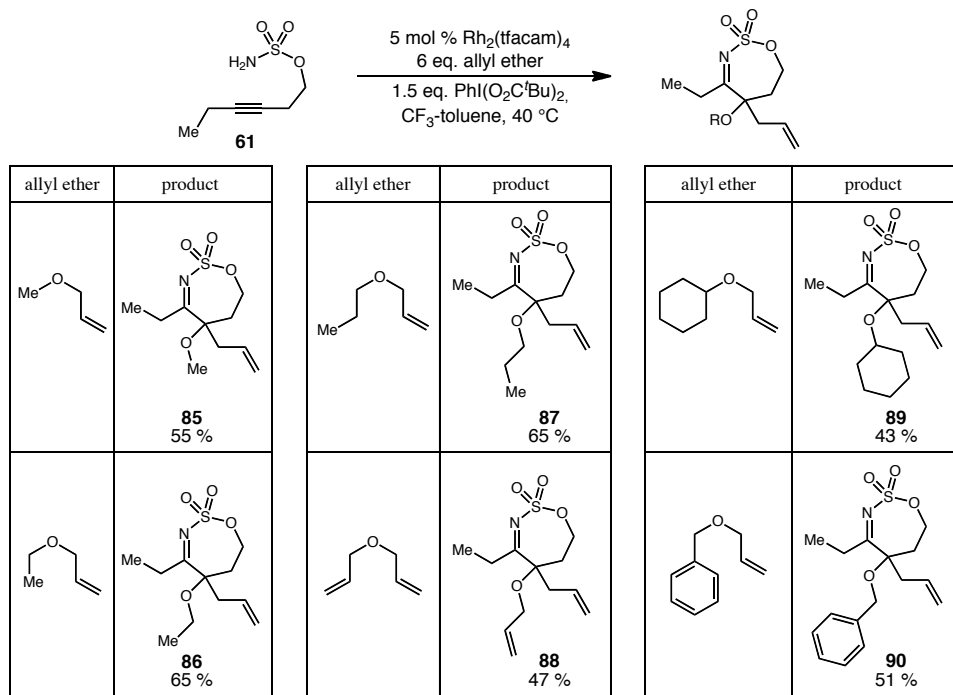
3.5. Re-evaluation of Cascade Termination Through Intermolecular Ylide Fomation/Allyl Migration

3.5.1 Examination of Etheral Traps

In the development of this intermolecular cascade termination reaction strategy towards the synthesis of the Securinega alkaloids, all of our previous efforts focused on the use of *bis*-allyl ether for cascade termination. In working towards the further development of this transformation we felt that a more thorough examination of etheral traps was necessary (Scheme 3.23). With this in mind, we have shown that a variety of commercially available etheral traps may be used to terminate this cascade process. Simple alkyl-allyl ethers result in the highest yields for this process to date, with methyl-, ethyl-, and propyl-allyl ethers terminating the cascade process in 55 %, 65 %, and 65 % yield respectively (**85**, **86**, and **87**). It is postulated that these increased yields may be attributed to the increased nucleophilicity of these etheral *O*-atoms relative to the others examined. We have also determined that increasing the steric bulk adjacent to this nucleophilic *O*-atom leads to a drop in isolated leads, with cyclohexyl-allyl ether terminating this cascade process in 43 % yield (**89**). Interestingly, the transfer of allyl groups is selective. For example, when benzyl-allyl ether is used to trap the reactive intermediate in this cascade process, we observe almost complete selectivity for allyl group migration (**90**), with the benzyl migration product being isolated in <5 % yield. This selectivity now allows for the incorporation of *O*-functionality with a commonly used benzyl protecting group, suggesting that this revised process could be useful in the

realm of organic synthesis. Importantly, in all cases this cascade process leads to densely functionalized *N*-containing molecules in a single transformation from incredibly simple starting materials and commercially available reagents.

Scheme 3.23. Examination of various ethereal traps for intermolecular cascade termination.

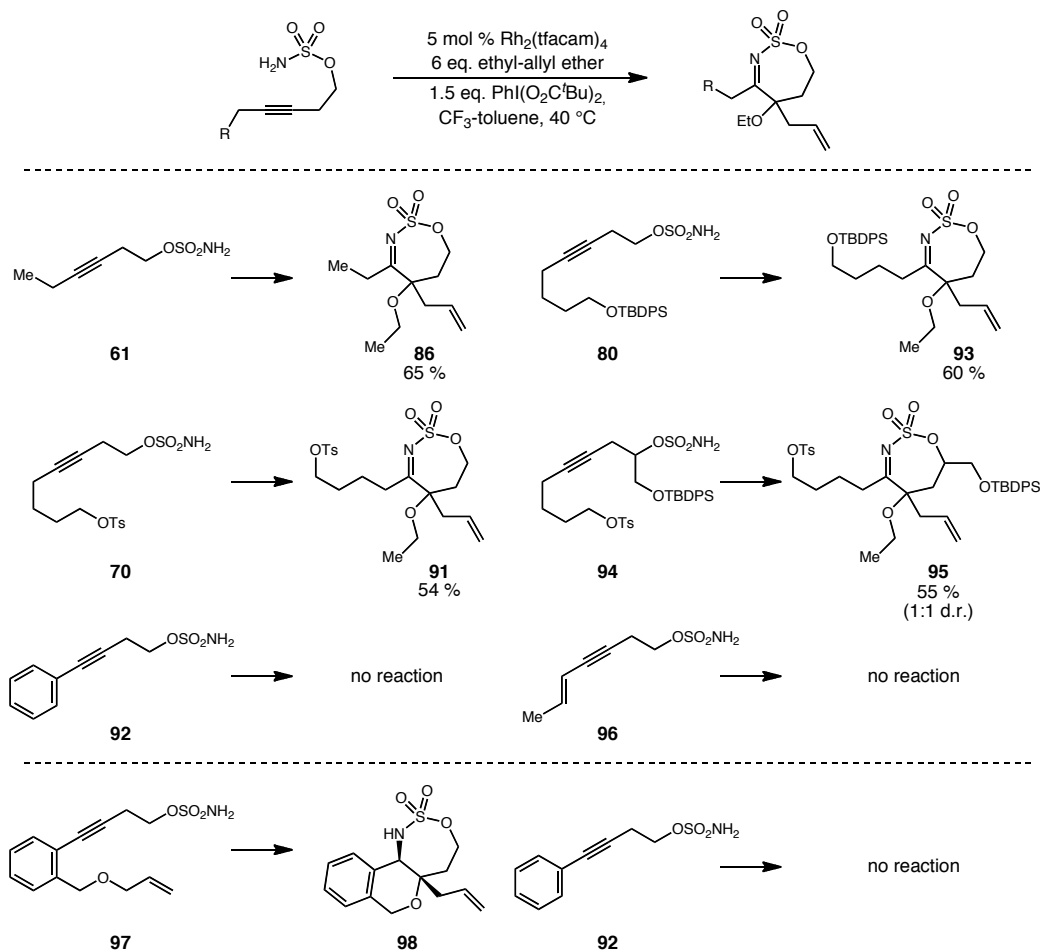


3.5.2. Examination of Alkyne Substitution

In addition to this diversity in terms of ethereal traps, we have also shown that a range of substitution patterns on the alkyne may be tolerated (Scheme 3.24). For example, both simple alkyl (**61**), as well as more functionalized alkyl substitution patterns (**70** and **80**) may be used, and as discussed earlier, heteroatom deactivation through the use of sulfonyl or silicon-based protecting groups is necessary for efficient intermolecular

cascade termination. Additionally, we examined the use of a sulfamate ester derived from a secondary homopropargylic alcohol, **94**. This substrate was cyclized under our standard reaction conditions to give *N*-sulfonyl imine **93** in 60 % yield. However, the existing chiral center in this substrate did not impart any diastereoselectivity on the cascade process, and a 1:1 mixture of diastereomers was isolated as determined by ¹H NMR. Interestingly, conjugated alkynes such as enyne **96** and phenyl substituted alkyne **92** are not reactive under these conditions. The reason for this lack of reactivity is unclear at this point, especially when aromatic alkynes **97** and **92** are compared. In the case of **97** we see intramolecular cascade termination to give product **98** in 98 % yield. However, when we move to cascade termination in an intermolecular fashion, we see no reaction with alkynyl sulfamate ester **92**, suggesting that the incoming nucleophile assists in the initial cyclization of the alkyne and metallonitrene, and that it is not simply due to the conjugation itself.

Scheme 3.24. Examination of alkyne substitution patterns and interesting reactivity differences.

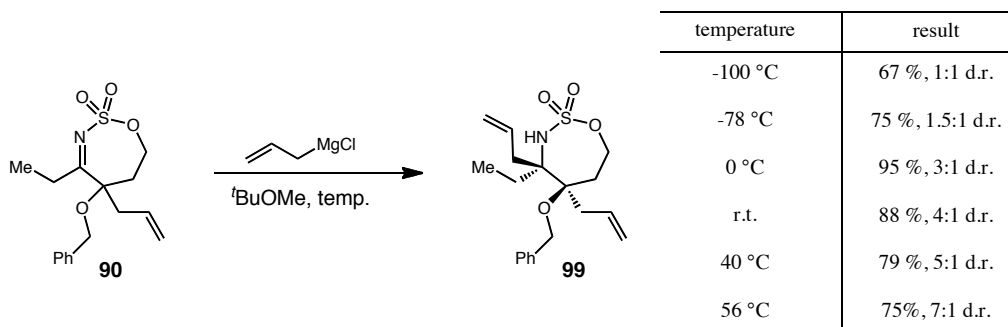


3.5.3. Utility of Intermolecular Cascade Termination Cyclization Adducts

With the a better understanding of this intermolecular cascade termination reaction we have also attempted to understand the unique reactivity patterns that these cyclization adducts possess. The ability to isolate the resulting imine of these cyclization reactions allows us to undergo a systematic study of the addition of Grignard reagents, as opposed to an *in situ* addition protocol which was necessary in our earlier work.

To illustrate this reaction's synthetic utility, we have shown that certain Grignard reagents undergo addition to these cyclization adducts efficiently. As illustrated in Scheme 3.25, we began our studies by examining the addition of allylmagnesium chloride to *N*-sulfonyl imine **90**. We have found that this nucleophile undergoes addition to this imine quite efficiently. Interestingly, we have observed that the facial selectivity for the addition of this nucleophile is highly dependent on reaction temperature, and we observe better diastereoselectivity at higher reaction temperatures. For example, the addition of allylmagnesium chloride to imine **90** at -100 °C takes place in 67 % yield, but results in a 1:1 mixture of diastereomers. As the reaction temperature is raised we observe a consistent improvement in the diastereoselectivity of addition, progressing all the way to a 7:1 diastereomeric ratio when the reaction is conducted at 56 °C (reflux).

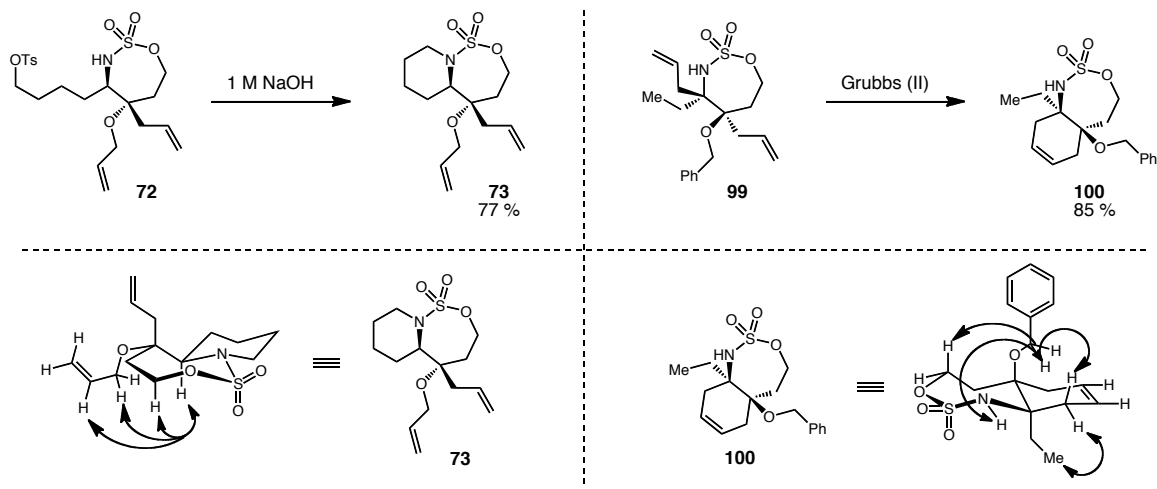
Scheme 3.25. Temperature dependent facial selectivity for the addition of allylmagnesium chloride to *N*-sulfonyl imine **90**.



This type of observation is not an isolated phenomenon, and there are multiple examples for this temperature dependent facial selectivity in the addition of organometallic reagents to α -oxygenated imines and aldehydes.²⁰ However, because of this characteristic it is difficult to invoke typical predictive stereochemical models such as

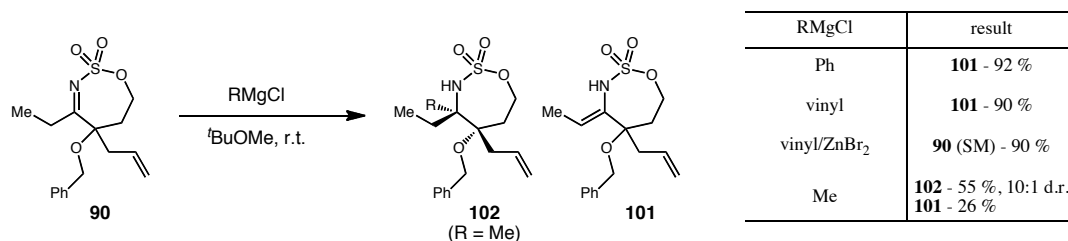
chelate and Felkin-Ahn control. This is due to the fact that these classical models do not take entropic factors, such as reaction temperature, solvent effects, or aggregation states of the Grignard reagent, into consideration.²⁰ Even with these difficulties, we have observed that the addition of various nucleophiles (NaBH₄, LAH, DIBAL-H, and allylmagnesium chloride) all take place from the same face as the α -oxygenated center, as determined by nOe experiments on the either addition products themselves or derivatives there of (Figure 3.3). For example, nOe experiments on addition product **99** proved to be inconclusive, however, when this substrate undergoes ring-closing metathesis, the resulting bicyclic system is now significantly rigidified and we are able to successfully determine the relative stereochemistry of this compound, and therefore the addition product as well. Likewise, nOe studies on compound **72** were inconclusive while the rigidified *N*-alkyl oxathiazepane **73** allowed for the successful determination of relative stereochemistry. Observing that the addition of different nucleophiles all occur for the same face as each other allows us to predictably install further functionalization to these cyclization adducts, and further highlights the utility of this transformation.

Figure 3.3. Key nOe correlations for oxathiazepane **73** and ring-closed product **100**.

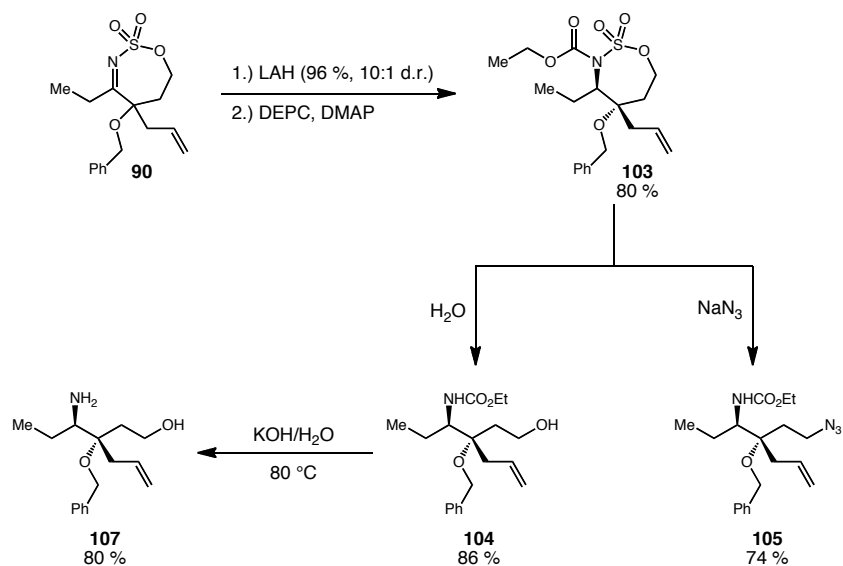


In addition to allylmagnesium chloride, we have also examined the addition of other sp^3 and sp^2 hybridized organometallic reagents (Scheme 3.26). While allylmagnesium chloride underwent selective 1,2-additions to *N*-sulfonyl imine **90**, sp^2 hybridized Grignard reagents phenylmagnesium chloride and vinylmagnesium chloride led to the formation of enamine **101**, resulting from α -deprotonation, in 92 % and 90 % yield respectively. In an attempt to attenuate the basicity of vinylmagnesium chloride, the addition of $ZnBr_2$ only resulted in the return of starting material in 90 % yield. Also, sp^3 hybridized methylmagnesium chloride led to a mixture of the desired 1,2-addition product **102** and the same α -deprotonation product **101** in 55 % and 26 % yield respectively.

Scheme 3.26. Examination of Grignard reagents.

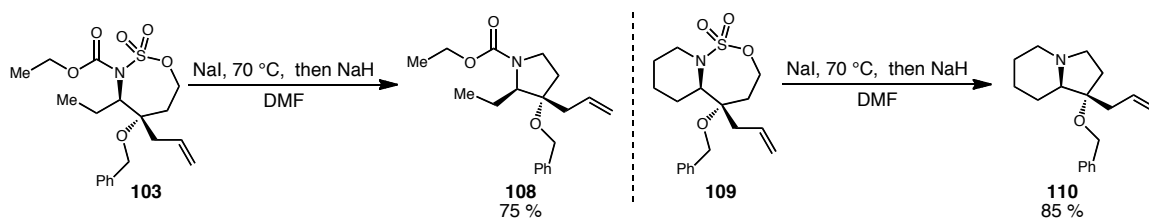


In addition to the introduction of Grignard reagents, we have also examined the use of these cyclization adducts to form a diverse range of *N*-containing compounds. For example, we have shown that a single cyclization adduct, *N*-sulfonyl imine **90**, may be converted to three different classes of *N*-containing molecules. As shown in Scheme 3.27, this imine may be reduced with LAH at 40 °C in 96 % yield and a 10:1 diastereomeric ratio. The resulting amine may then be acylated with di-ethyl pyrocarbonate and DMAP to furnish acylated oxathiazepane **103** in 80 % yield. While a more typical protecting group, such as Cbz, has been utilized in the past, we have found that acylation under typical conditions (NaO^tBu and CbzCl in DME) is not amenable to this substrate. While some uncertainty remains, we hypothesize that this is due to the increased steric bulk adjacent to this oxathiazepane *N*-atom. However, the use (EtOCO)₂O with DMAP proceeds in high yields and provides the electronic bias that is needed for the ring-opening of these 1,4-cyclic sulfamidates. Thus, **103** may undergo subsequent reaction with a range of nucleophiles, including H₂O and NaN₃ in 86 % and 74 % yield respectively, leading to the synthesis of various functionalized aliphatic amines (**104** and **105**). Lastly, the ethyl carbamate protecting group may be cleaved under strongly basic conditions, freeing the amino group and leading to the production of **107** in 80 % yield.

Scheme 3.27. Synthesis of aliphatic amines via intermolecular cascade termination.

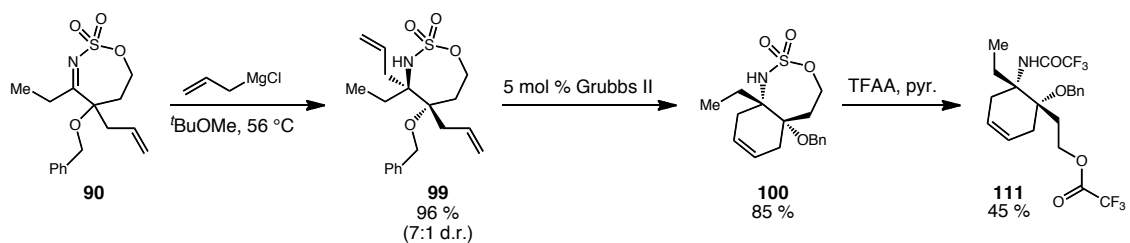
In addition to aliphatic amines, using the same methodology that was discussed earlier (Scheme 3.5), we are also able to access densely functionalized pyrrolidines (Scheme 3.28). For example, the same *N*-acyl oxathiazepane **103** may undergo tandem ring-opening/ring-closing reaction with NaI in DMF to give functionalized pyrrolidine **108** in 75 %. Also, we have found that bicyclic *N*-alkyl oxathiazepane **109** can undergo this same reaction in 85 % yield. This stands in contrast to the continued troubles that we faced when attempting to open a similar *N*-alkyl oxathiazepane with *O*-based nucleophiles (Scheme 3.19). The ease with which **109** undergoes tandem ring-opening/ring-closing with NaI suggests that the nature of the nucleophile plays a larger role in this process than we initially anticipated, and that more polarizable nucleophiles (I *cf.* H_2O) may be more efficient for addition to these systems.

Scheme 3.28. Synthesis of *N*-heterocycles via intermolecular cascade termination.



Lastly, we have illustrated that carbocycles may be accessed through the use of this methodology. For example, as discussed earlier, *N*-sulfonyl imine **90** undergoes addition by allylmagnesium chloride to yield oxathiazepane **99** in 96 % yield (Scheme 3.29). Subsequent ring-closing metathesis using Grubbs II catalyst led to the formation of bicyclic compound **100** in 85 % yield. While a variety of techniques for the acylation of this intermediate, including the use CbzCl, Boc₂O, Ac₂O, AcCl, (EtOCO)₂O, and (Cbz)₂O, proved to be unsuccessful, we found that the use of neat TFAA and pyridine led to the formation of functionalized carbocyclic amine **111** in 45 % yield. It is postulated that this product arises from the initial addition of **100** to pyridine-activated TFAA complex to give the corresponding trifluoroacetamide. Due to the intense electron-withdrawing nature of this protecting group, the trifluoroacetate anion byproduct of TFAA is then capable of undergoing addition at the *O*-bearing carbon of this intermediate to in turn yield the observed carbocyclic product in 45 % yield.

Scheme 3.29. Synthesis of functionalized carbocycles via intermolecular cascade termination.



3.6. Conclusions and Future Directions

Motivated by the disparate reactivity between similar intermediates, our research efforts have focused on the development of new metallonitrene mediated transformations. Based on a novel metallonitrene/alkyne metathesis reaction concept, we have successfully developed powerful Rh(II)-catalyzed metallonitrene/alkyne cascade reaction. To date we have shown that a wide range of heterocyclic structures can be formed selectively and predictably with this new technology. Importantly, these transformations utilize readily available starting materials and reagents, to in turn generate significant molecular complexity in a rapid fashion.

While we believe this cascade process to be powerful, we also realize that shortcomings exist. For example, we have found that only sulfamate esters derived from homopropargylic alcohols are useful for these transformations. In turn, I believe that the ability to use alternate nitrene precursors, in conjunction with varying tether lengths, would significantly advance this chemistry. Additionally, while we are able to construct these complex structures in a diastereoselective fashion, the extension of this work to an enantioselective manifold would also constitute a major achievement. Preliminary work

by Véronique Martin has illustrated that the use of certain chiral Rh(II)-catalysts can effect this transformation enantioselectively, however, if real progress is to be made, new catalysts will need to be developed and there is considerable work to be done.

The development of this new reaction goes beyond its specific ability to generate multiple bonds and stereocenters in a single transformation. The successful development of this process plainly illustrates that our motivations are justified, and that the field of metallonitrene chemistry is still significantly underdeveloped. Providing further evidence for this, since the development of this transformation, our lab has also developed a second novel metallonitrene mediated transformation. The work of Dr. Armin Stoll has shown that metallonitrenes can also undergo reaction with tethered allenes. In turn generating a new reactive intermediate that may undergo cycloadditions with aldehydes, imines, and nitrones.²¹ Similar to our metallonitrene/alkyne cascade reaction, this new reaction is able to transform readily available starting materials into valuable functionalized materials.

With these things in mind, future work within the Blakey group will go beyond the further development of these specific reactions. In moving forward, the efforts of this group will remain focused on new reaction discovery, and development, within the field of metallonitrene chemistry.

Experimental Procedures and Compound Characterization

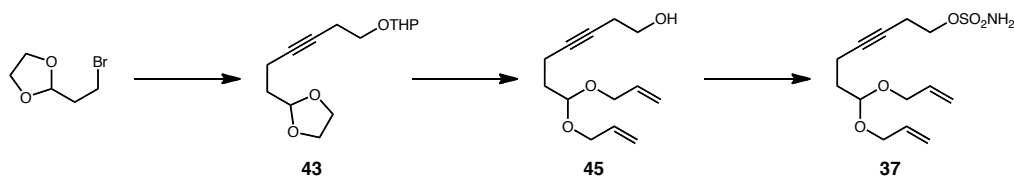
General Information.

^1H and ^{13}C NMR spectra were recorded on a Varian Inova 600 spectrometer (600 MHz ^1H , 150 MHz ^{13}C) at room temperature in CDCl_3 with internal CHCl_3 as the reference (7.27 ppm for ^1H and 77.23 ppm for ^{13}C). Chemical shifts (δ values) were reported in parts per million (ppm) and coupling constants (J values) in Hz. Multiplicity is indicated using the following abbreviations: s = singlet, d = doublet, t = triplet, q = quartet, qn = quintet, m = multiplet, b = broad signal.). Infrared (IR) spectra were recorded using Thermo Electron Corporation Nicolet 380 FT-IR spectrometer. High resolution mass spectra were obtained using a Thermo Electron Corporation Finigan LTQFTMS (at the Mass Spectrometry Facility, Emory University). We acknowledge the use of shared instrumentation provided by grants from the NIH and the NSF. Melting points (mp) were taken using a Fisher-Johns melting point apparatus and are not corrected. Analytical thin layer chromatography (TLC) was performed on precoated glass backed EMD 0.25 mm silica gel 60 plates. Visualization was accomplished with UV light or ethanolic anisaldehyde, followed by heating. Flash column chromatography was carried out using EMD Geduran® silica gel 60 (40-63 μm).

All reactions were conducted with anhydrous solvents in oven dried or flame-dried and argon-charged glassware. Anhydrous solvents were purified by passage through activated alumina using a *Glass Contours* solvent purification system unless otherwise noted. Benzene and trifluorotoluene was dried over activated 4 Å molecular sieves. Solvents used in workup, extraction and column chromatography were used as

received from commercial suppliers without prior purification. All reagents were purchased from Sigma-Aldrich and used as received unless otherwise noted. $\text{PhI}(\text{OAc})_2$ and $\text{PhI}(\text{O}_2\text{C}^t\text{Bu})_2$ was dried under vacuum (0.02 mmHg) for 12 hours prior to use. Pyridine was purified by distillation from calcium hydride. Rhodium catalysts were purchased from Strem chemical company and used as received.

Towards the Synthesis of (\pm)-Allonorsecurinine.

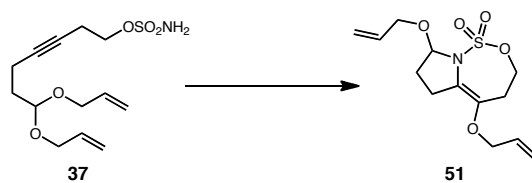


2-((6-(1,3-dioxolan-2-yl)hex-3-yn-1-yl)oxy)tetrahydro-2H-pyran (43). $n\text{BuLi}$ (0.83 mL, 1.18 mmol) was added dropwise to a solution of THP-protected 3-butyn-1-ol (0.20 g, 1.3 mmol) in THF (5.5 mL) at $-78\text{ }^\circ\text{C}$. After stirring at $-78\text{ }^\circ\text{C}$ for 2 h, a solution of 2-(2-bromoethyl)-1,3-dioxolane (0.14 mL, 1.2 mmol) in DMPU (1.5 mL) was added slowly. The resulting solution was warmed to ambient temperature and stirred 14 h. After this time the reaction was quenched by the addition of 1 N HCl at $0\text{ }^\circ\text{C}$. The organic layer was separated and the aqueous layer was extracted with Et_2O (2 x 20 mL). The combined organic extracts were dried over MgSO_4 , filtered, and concentrated *in vacuo*. Purification by flash column chromatography (8:1 \rightarrow 2:1 hexanes/EtOAc) afforded 2-((6-(1,3-dioxolan-2-yl)hex-3-yn-1-yl)oxy)tetrahydro-2H-pyran (**43**) (0.15 g, 52 %) as a clear viscous oil; R_f 0.45 (3:1 hexanes/EtOAc); **IR** (thin film, cm^{-1}) 2939, 2874, 1135, 1121, 1033; **$^1\text{H NMR}$** (CDCl_3 , 600 MHz) δ 4.97 (t, 1H, $J = 4.7$ Hz), 4.64 (t, 1H, $J = 3.3$

Hz), 3.97-3.95 (m, 2H), 3.90-3.84 (m, 2H), 3.78 (q, 1H, $J = 7.1$ Hz), 2.45 (t, 2H, $J = 7.1$ Hz), 2.29 (t, 2H, $J = 7.6$ Hz), 1.85-1.81 (m, 3H), 1.74-1.69 (m, 1H), 1.61-1.52 (m, 4H); ^{13}C NMR (CDCl_3 , 150 MHz) δ 119.4, 103.6, 103.4, 98.9, 80.3, 66.3, 65.1, 62.4, 33.4, 30.8, 25.6, 20.4, 19.6, 13.9; HRMS (+ ESI) calculated for $\text{C}_{14}\text{H}_{23}\text{O}_4$ 255.1596, found 255.1518 $[\text{M}+\text{H}]^+$.

7,7-Bis(allyloxy)hept-3-yn-1-ol (45). PPTS (0.63 g, 2.3 mmol) was added as a solid in a single portion to 2-(((6-(1,3-dioxolan-2-yl)hex-3-yn-1-yl)oxy)tetrahydro-2H-pyran (43) in a mixture of acetone/ H_2O (2:1, 12 mL total) at ambient temperature. The resulting solution was warmed to 50 °C and stirred for 14 h. After this time the mixture was diluted with H_2O (15 mL) and extracted with CH_2Cl_2 (2 x 30 mL). The combined organic extracts were dried over MgSO_4 , filtered, and concentrated *in vacuo*. The resulting crude oil was immediately dissolved in allyl alcohol (5 mL) and pTsOH (44 mg, 0.23 mmol) was added as a solid in a single portion. The resulting solution was stirred at ambient temperature for 2 h. After this time the reaction mixture was concentrated *in vacuo*. The resulting crude oil was purified by flash column chromatography (4:1→2:1 hexanes/EtOAc) to afford 7,7-bis(allyloxy)hept-3-yn-1-ol (45) (90 mg, 33 %) as a clear oil; R_f 0.25 (3:1 hexanes/EtOAc); ^1H NMR (CDCl_3 , 600 MHz) δ 5.90 (d, 2H, 4.7 Hz), 5.28 (d, 1H, $J = 7.1$ Hz), 5.16 (d, 1H, $J = 3.2$ Hz), 4.71 (t, 1H, $J = 6.7$ Hz), 4.10 (d, 2H, $J = 7.1$ Hz), 4.20 (d, 2H), 3.66-3.40 (m, 2H), 2.41 (bs, 2H), 2.25 (bs, 2H), 2.09 (bs, 1H), 1.83, (q, 2H, $J = 6.2$ Hz); ^{13}C NMR (CDCl_3 , 150 MHz) δ 134.8, 116.9, 101.6, 101.3, 80.6, 66.7, 64.4, 61.5, 32.9, 32.8, 23.4, 20.5, 14.6; HRMS (+ ESI) calculated for $\text{C}_{13}\text{H}_{21}\text{O}_3$ 225.1491, found 225.1464 $[\text{M}+\text{H}]^+$.

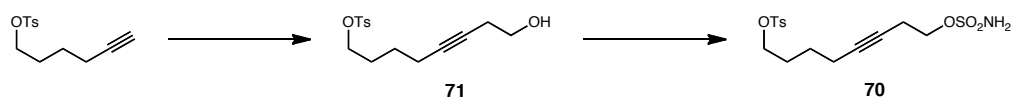
7,7-Bis(allyloxy)hept-3-yn-1-sulfamate (37). Formic acid (0.05 mL, 1.3 mmol) was added to neat chlorosulfonyl isocyanate (0.05 mL, 1.3 mmol) at 0 °C with stirring. The resulting white solid was dissolved in MeCN (4.3 mL), warmed to room temperature and stirred for 14 h. After this time the reaction mixture was cooled to 0 °C and a solution of 7,7-bis(allyloxy)hept-3-yn-1-ol (**45**) (0.20 g, 0.89 mmol) and 2,6-lutidine (0.16 mL, 1.3 mmol) in DMA (0.25) was added dropwise. The resulting mixture was warmed to ambient temperature and stirred until thin layer chromatography indicated complete consumption of starting material. H₂O and EtOAc were added. The organic phase was collected and the aqueous phase was extracted with EtOAc (2 x 15 mL). The combined organic extracts were washed with brine, dried over MgSO₄ and concentrated *in vacuo*. Purification by flash chromatography (4:1 → 2:1 hexanes/EtOAc) afforded 7,7-bis(allyloxy)hept-3-yn-1-sulfamate (**37**) (0.13 g, 47 %) as a clear oil; **R_f** 0.15 (3:1 hexanes/EtOAc); **¹H NMR** (CDCl₃, 600 MHz) δ 5.92-5.88 (m, 2H), 5.30-5.01 (m, 4H), 5.02 (bs, 2H), 4.82-4.10 (m, 2H), 4.28-4.21 (m, 2H), 4.18-4.00 (m, 4H), 3.60 (sext, 1H, *J* = 4.5 Hz), 2.64-2.56 (m, 2H), 2.43 (t, 2H, *J* = 7.2 Hz), 1.90-1.78 (m, 3 H); **HRMS** (+ESI) calculated for C₁₃H₂₂NO₅S 304.1219, found 304.1122 [M+H]⁺.



5,8-Bis(allyloxy)-4,6,7,8-tetrahydro-3H-pyrrolo[1,2-c][1,2,3]oxathiazepine 1,1-dioxide (51). 7,7-bis(allyloxy)hept-3-yn-1-sulfamate (**37**) (27 mg, 0.088 mmol),

$\text{PhI}(\text{OAc})_2$ (31 mg, 0.096 mmol), and $\text{Rh}_2(\text{esp})_2$ (1.3 mg, 0.0028 mmol) were combined in a 2 dram reaction vial and sealed with a Teflon lined cap. CH_2Cl_2 (0.50 mL) was added and the reaction was stirred at ambient temperature for 45 mins. After this time MeOH (0.75 mL) and NaBH_4 (9.9 mg, 0.26 mmol) were added and stirring was continued at ambient temperature for 3 h. After this time the reaction mixture was concentrated *in vacuo* and purified by flash column chromatography to afford 5,8-bis(allyloxy)-4,6,7,8-tetrahydro-3*H*-pyrrolo[1,2-*c*][1,2,3]oxathiazepine 1,1-dioxide (**51**) (5.6 mg, 21 %) as a colorless oil; R_f 0.13 (3:1 hexanes/EtOAc); **IR** (thin film, cm^{-1}) 2924, 1371, 1173, 999; **$^1\text{H NMR}$** (CDCl_3 , 600 MHz) δ 6.10-5.85 (m, 2H), 5.85-5.67 (m, 1H), 5.38-5.18 (m, 4H), 4.58-4.54 (m, 2H), 4.44-4.17 (m, 4H), 4.07 (ddt, 1H), 2.88-2.60 (m, 3H), 2.14-2.02 (m, 1H), 2.01-1.94 (m, 1H); **$^{13}\text{C NMR}$** (CDCl_3 , 150 MHz) δ 139.9, 133.9, 133.9, 119.6, 118.3, 117.7, 93.0, 71.0, 70.7, 69.2, 31.0, 30.8, 25.9; **HRMS** (+ ESI) calculated for $\text{C}_{13}\text{H}_{20}\text{NO}_5\text{S}$ 302.1062, found 302.0921 $[\text{M}+\text{H}]^+$.

Towards the Synthesis of (\pm)-Allosecurinine.

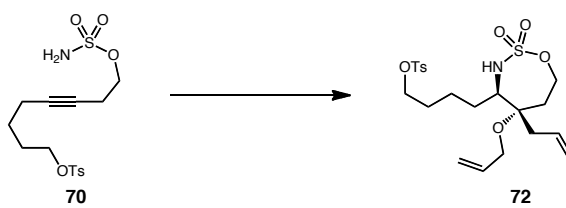


8-hydroxyoct-5-yn-1-yl 4-methylbenzenesulfonate (71). $n\text{BuLi}$ (6.2 mL, 15.5 mmol) was added dropwise to a solution of hex-5-yn-1-yl 4-methylbenzenesulfonate²² (3.0 g, 12 mmol) in THF (60 mL) at $-78\text{ }^\circ\text{C}$. After stirring at $-78\text{ }^\circ\text{C}$ for 40 mins. $\text{BF}_3\cdot\text{OEt}_2$ (1.7 mL, 14 mmol) was added slowly followed by freshly distilled oxirane (1.0 mL, 16 mmol). The resulting solution was stirred 30 min at $-78\text{ }^\circ\text{C}$. After this time the reaction was

quenched by the addition of 1 N HCl at 0 °C. The organic layer was separated and the aqueous layer was extracted with Et₂O (2 x 20 mL). The combined organic extracts were dried over MgSO₄, filtered, and concentrated *in vacuo*. Purification by flash column chromatography (2:1→1:1 hexanes/EtOAc) afforded 8-hydroxyoct-5-yn-1-yl 4-methylbenzenesulfonate (**71**) (2.4 g, 68 %) as a colorless viscous oil; **R_f** 0.10 (3:1 hexanes/EtOAc); **IR** (thin film, cm⁻¹) 3396, 2941, 1353, 1173; **¹H NMR** (CDCl₃, 600 MHz) δ 7.78 (d, 2H, *J* = 8.5), 7.35 (d, 2H, *J* = 8.5 Hz), 4.05 (t, 2H, *J* = 6.1 Hz), 3.66 (t, 2H, *J* = 6.4 Hz), 2.45 (s, 3H), 2.40 (tt, 2H, *J* = 6.1, 2.4 Hz), 2.15 (tt, 2H, *J* = 7.0, 2.4 Hz), 1.83 (bs, 1H), 1.79-1.72 (m, 2H), 1.52 (qn, 2H, *J* = 7.0 Hz); **¹³C NMR** (CDCl₃, 150 MHz) δ 144.9, 133.2, 130.0, 128.0, 81.5, 77.5, 70.3, 61.5, 28.1, 24.9, 23.3, 21.8, 18.3; **HRMS** (+ESI) calculated for C₁₅H₂₁NO₄S 297.1161, found 297.1157 [M+H]⁺.

8-(tosyloxy)oct-3-yn-1-sulfamate (70). Formic acid (0.77 mL, 20 mmol) was added to neat chlorosulfonyl isocyanate (1.7 mL, 20 mmol) at 0 °C with stirring. The resulting white solid was dissolved in MeCN (30 mL), warmed to ambient temperature and stirred for 14 h. After this time the reaction mixture was cooled to 0 °C and a solution of 8-hydroxyoct-5-yn-1-yl 4-methylbenzenesulfonate (**71**) (2.4 g, 8.1 mmol) and 2,6-lutidine (2.4 mL, 20 mmol) in DMA (15 mL) was added slowly. The resulting mixture was warmed to ambient temperature and stirred until thin layer chromatography indicated complete consumption of starting material. H₂O and EtOAc were added. The organic phase was collected and the aqueous phase was extracted with EtOAc (2 x 15 mL). The combined organic extracts were washed with brine, dried over MgSO₄ and concentrated *in vacuo*. Purification by flash column chromatography (2:1→3:2 hexanes/EtOAc)

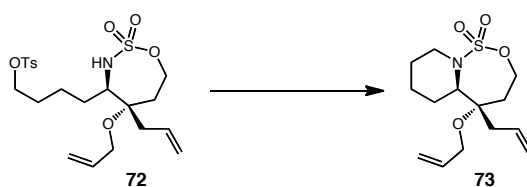
afforded 8-(tosyloxy)oct-3-yn-1-sulfamate (**70**) as an amorphous solid (2.7 g, 89 %); R_f 0.13 (3:1 hexanes/EtOAc); **IR** (thin film, cm^{-1}) 3374, 3282, 2955, 1354, 1174; $^1\text{H NMR}$ (CDCl_3 , 600 MHz) δ 7.78 (d, 2H, $J = 8.1$ Hz), 7.36 (d, 2H, $J = 8.1$ Hz), 4.96 (bs, 2H), 4.25 (t, 2H, $J = 6.7$ Hz), 4.08 (t, 2H, $J = 6.7$ Hz), 2.62-2.60 (m, 2H), 2.46 (s, 3H), 2.17-2.15 (m, 2H), 1.80 (tt, 2H, $J = 15.3, 6.2$ Hz), 1.53 (tt, 2H, $J = 15.3, 6.2$ Hz); $^{13}\text{C NMR}$ (CDCl_3 , 150 MHz) δ 145.1, 133.1, 130.1, 128.1, 81.9, 75.7, 70.4, 69.1, 28.1, 24.6, 21.9, 19.9, 18.2; **HRMS** (+ ESI) calculated for $\text{C}_{15}\text{H}_{22}\text{NO}_6\text{S}_2$ 376.0889, found 376.0886 $[\text{M}+\text{H}]^+$.



5-allyl-5-(allyloxy)-2,2-dioxido-1,2,3-oxathiazepan-4-yl)butyl

4-methylbenzenesulfonate (72). $\text{Rh}_2(\text{tfacam})_4$ (7.1 mg, 0.011 mmol) in trifluorotoluene (0.62 mL) was stirred in a round bottom flask at 40 °C. A solution of 8-(tosyloxy)oct-3-yn-1-sulfamate (**70**) (0.10 g, 0.22 mmol), $\text{PhI}(\text{O}_2\text{C}^t\text{Bu})_2$ (0.13 g, 0.33 mmol) and *bis*-allyl ether (0.16 mL, 1.31 mmol) in trifluorotoluene (0.62 mL) was added via syringe pump over 1.5 h. After complete addition the reaction was stirred for 15 min then MeOH (1 mL) and NaBH_4 (41 mg, 1.1 mmol) were added. Once the reaction was determined to be complete by thin layer chromatography the mixture was concentrated onto a pad of silica gel and immediately purified by flash column chromatography (4:1 \rightarrow 1:1 pentane/ether) to afford 5-allyl-5-(allyloxy)-2,2-dioxido-1,2,3-oxathiazepan-4-yl)butyl

4-methylbenzenesulfonate (**72**). (59 mg, 47 %) as a colorless oil; R_f 0.20 (3:1 hexanes/EtOAc); $^1\text{H NMR}$ (CDCl_3 , 600 MHz) δ 7.78 (d, 2H, $J = 8.6$ Hz), 7.35 (d, 2H, $J = 8.1$ Hz), 5.89-5.76 (m, 2H), 5.38-5.10 (m, 5H), 4.45 (t, 1H, $J = 6.2$ Hz), 4.13 (dt, 1H, $J = 11.0, 5.7$ Hz), 4.04-4.15 (m, 3H), 3.93-4.01 (m, 2H), 2.67 (dd, 1H, $J = 15.3, 6.2$ Hz), 2.45-2.40 (m, 4H), 2.06-2.00 (m, 1H), 1.99-1.84 (m, 2H), 1.77-1.60 (m, 3H), 1.45-1.30 (m, 2H); HRMS (+ESI) calculated for $\text{C}_{21}\text{H}_{32}\text{NO}_7\text{S}$ 474.1620, found 474.1588 $[\text{M}+\text{H}]^+$.

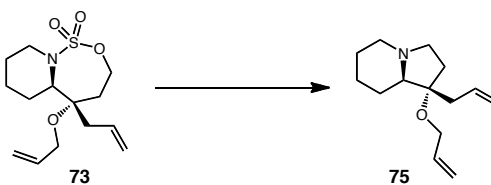
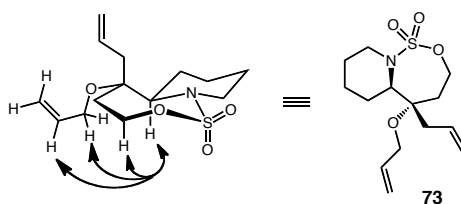


5-allyl-5-(allyloxy)octahydropyrido[1,2-c][1,2,3]oxathiazepine 1,1-dioxide (73).

Aqueous NaOH (1 M, 0.25 mL) was added dropwise to a solution of 4-5-allyl-5-(allyloxy)-2,2-dioxido-1,2,3-oxathiazepan-4-ylbutyl 4-methylbenzenesulfonate (**72**) (0.10 g, 0.21 mmol) in THF (0.25 mL) at ambient temperature. The resulting solution was stirred until thin layer chromatography indicated complete consumption of starting material. The reaction was neutralized with 1 N HCl and extracted with EtOAc (3 x 10 mL). The combined organic extracts were washed with brine, dried over MgSO_4 and concentrated *in vacuo*. Purification by flash column chromatography (10:1→8:1 hexanes/EtOAc) afforded 5-allyl-5-(allyloxy)octahydropyrido[1,2-c][1,2,3]oxathiazepine 1,1-dioxide (**73**) as an amorphous solid (48 mg, 77 %); R_f 0.75 (3:1 hexanes/EtOAc); IR (thin film, cm^{-1}) 2945, 2869, 1343, 1177; $^1\text{H NMR}$ (CDCl_3 , 600 MHz) δ 5.94-5.83 (m, 2H), 5.31-5.10 (m, 4H), 4.35-4.30 (m, 2H), 4.05-3.98 (m, 2H), 3.93-3.88 (m, 1H), 3.79-

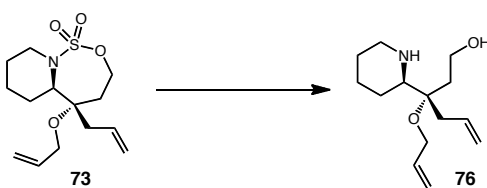
3.70 (m, 1H), 3.20-3.12 (m, 1H), 2.67 (dd, 1H, $J = 15.3, 6.2$ Hz), 2.44 (dd, 1H, $J = 15.3, 6.2$ Hz), 2.28 (tt, 1H, $J =$ Hz), 2.02-1.89 (m, 1H), 1.90-1.74 (m, 4H), 1.70-1.54 (m, 2H); ^{13}C NMR (CDCl_3 , 150 MHz) δ 134.5, 131.8, 119.5, 117.3, 78.3, 77.4, 63.4, 61.9, 55.9, 46.1, 39.2, 33.8, 23.6, 22.9; HRMS (+ ESI) calculated for $\text{C}_{14}\text{H}_{24}\text{NO}_4\text{S}$ 302.1426, found 302.1376 $[\text{M}+\text{H}]^+$.

Key nOe correlations for *N*-alkyl oxathiazepane **73.**



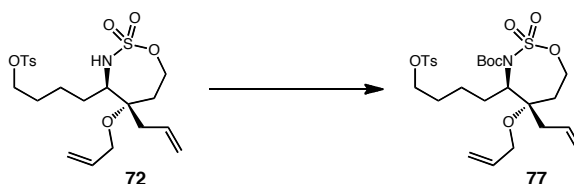
1-allyl-1-(allyloxy)octahydroindolizine (75). 5-allyl-5-(allyloxy)octahydroindolizine 1,1-dioxide (**73**) (30 mg, 0.10 mmol) and KOAc (100 mg, 1.0 mmol) in DMF (1.0 mL) was heated in a sealed tube to 110 °C for 24 h. After this time the reaction was cooled to ambient temperature, transferred to 50 mL round-bottom flask and concentrated *in vacuo*. The resulting crude oil was purified by flash column chromatography (10:1 $\text{CH}_2\text{Cl}_2/\text{MeOH}$ with 1 % conc. ammonium hydroxide added) to afford 1-allyl-1-(allyloxy)octahydroindolizine (**75**) as a colorless oil (13 mg, 61 %); **IR**

(thin film, cm^{-1}) 3074, 2933, 2855, 1157; $^1\text{H NMR}$ (CDCl_3 , 600 MHz) δ 5.96-5.85 (m, 2H), 5.32-4.80 (m, 4H), 4.00-3.88 (m, 2H), 3.10 (d, 1H), 2.96 (t, 1H), 2.65 (dd, 1H), 2.28 (q, 1H), 2.17-2.0 (m, 3H), 1.92-1.74 (m, 4H), 1.68-1.59 (m, 1H), 1.58-1.42 (m, 1H), 1.38-1.24 (m, 2H); $^{13}\text{C NMR}$ (CDCl_3 , 150 MHz) δ 135.6, 134.2, 117.9, 116.2, 85.1, 72.4, 64.0, 54.4, 53.8, 38.7, 35.0, 27.6, 25.3, 24.5; **HRMS** (+ ESI) calculated for $\text{C}_{14}\text{H}_{24}\text{NO}$ 222.1858, found 222.1853 $[\text{M}+\text{H}]^+$.

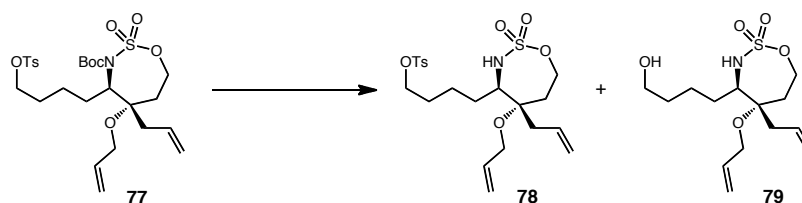


1-allyl-1-(allyloxy)octahydroindolizine (76). 5-allyl-5-(allyloxy)octahydropyrido[1,2-c][1,2,3]oxathiazepine 1,1-dioxide (**73**) (50 mg, 0.17 mmol) in $\text{H}_2\text{O}/1,4\text{-dioxane}$ (1:1, 4 mL total) was heated under microwave irradiation at $140\text{ }^\circ\text{C}$ for 1 h. After this time the reaction was cooled to ambient temperature, diluted with CH_2Cl_2 and transferred to 25 mL round-bottom flask. This solution was concentrated *in vacuo* and purified by flash column chromatography (10:1 \rightarrow 3:1 $\text{CH}_2\text{Cl}_2/\text{MeOH}$ with 1 % NH_4OH) to afford 1-allyl-1-(allyloxy)octahydroindolizine (**76**) (17 mg, 44 %) as a clear residue; **IR** (thin film, cm^{-1}) 3425, 2924, 2854, 1069; $^1\text{H NMR}$ (CDCl_3 , 600 MHz) δ 5.98 (dddd, 1H, $J = 11.4, 6.7, 3.2, 1.2$ Hz), 5.82-5.74 (m, 2H), 5.32-5.09 (m, 4H), 3.96 (dd, 1H, $J = 12.4, 4.8$ Hz), 3.88 (dd, 1H, $J = 11.1, 4.7$ Hz), 3.77-3.82 (m, 1H), 3.57 (dd, 1H, $J = 12.1, 6.7$ Hz), 2.99-2.86 (m, 1H), 2.73 (t, 1H, $J =$ Hz), 2.51 (dd, 1H, $J = 5.2, 3.8$ Hz), 2.26-2.17 (m, 1H), 1.96-1.84 (m, 5H), 1.80-1.60 (m, 6H); $^{13}\text{C NMR}$ (CDCl_3 , 150 MHz) δ 134.3, 132.1,

119.2, 117.3, 62.9, 61.6, 56.8, 55.8, 46.2, 39.3, 34.7, 29.9, 23.9, 23.7; **HRMS** (+ ESI) calculated for $C_{14}H_{25}NO_2$ 240.1964, found 240.1958 $[M+H]^+$.



^tButyl 5-allyl-5-(allyloxy)-4-(4-(tosyloxy)butyl)-1,2,3-oxathiazepane-3-carboxylate 2,2-dioxide (77). 4-5-allyl-5-(allyloxy)-2,2-dioxido-1,2,3-oxathiazepan-4-yl)butyl 4-methylbenzenesulfonate (**72**) (59 mg, 0.13 mmol) in MeCN (0.30 mL) was added dropwise to a solution of Boc_2O (0.55 g, 2.53 mmol) and DMAP (16 mg, 0.13 mmol) in MeCN (0.10 mL) at 0 °C. This solution was warmed to ambient temperature and after 1 h. the reaction was quenched by the addition of H_2O and diluted with EtOAc. The organic phase was separated and the aqueous phase was extracted with EtOAc (2 x 10 mL). The combined organic extracts were washed with brine, dried over $MgSO_4$ and concentrated *in vacuo*. Purification by flash column chromatography (3:1 hexanes/EtOAc) afforded ^tbutyl 5-allyl-5-(allyloxy)-4-(4-(tosyloxy)butyl)-1,2,3-oxathiazepane-3-carboxylate 2,2-dioxide (**77**) (52 mg, 88 %) as a colorless oil; R_f 0.30 (3:1 hexanes/EtOAc); 1H NMR ($CDCl_3$, 600 MHz) δ 7.78 (d, 2H, $J = 8.6$ Hz), 7.35 (d, 2H, $J = 8.1$ Hz), 5.89-5.76 (m, 2H), 5.38-5.10 (m, 4H), 4.89 (t, 1H, $J = 6.2$ Hz), 4.70 (dd, 1H, $J = 11.0, 5.7$ Hz), 4.28 (dd, 1H, $J = 12.4, 4.8$ Hz), 4.04-3.87 (m, 3H), 2.46 (s, 3H), 2.43-2.34 (m, 2H), 2.06-2.00 (m, 1H), 1.99-1.84 (m, 2H), 1.77-1.60 (m, 3H), 1.52 (s, 9H), 1.45-1.30 (m, 2H).



4-5-allyl-5-(allyloxy)-2,2-dioxido-1,2,3-oxathiazepan-4-yl)butyl

4-methylbenzenesulfonate (78) and 5-allyl-5-(allyloxy)-4-(4-hydroxybutyl)-1,2,3-

oxathiazepane 2,2-dioxide (79). 'Butyl 5-allyl-5-(allyloxy)-4-(4-(tosyloxy)butyl)-1,2,3-

oxathiazepane-3-carboxylate 2,2-dioxide (77) (30 mg, 0.052 mmol) was stirred in

H₂O/MeCN (1:1, 0.5 mL total) at 70 °C for 14 h. After this time the reaction was cooled

to ambient temperature and diluted with H₂O and EtOAc. The organic phase was

separated and the aqueous phase was extracted with EtOAc (2 x 10 mL). The combined

organic extracts were washed with brine, dried over MgSO₄ and concentrated *in vacuo*.

Purification by flash column chromatography (3:1→1:1 hexanes/EtOAc) afforded 4-5-

allyl-5-(allyloxy)-2,2-dioxido-1,2,3-oxathiazepan-4-yl)butyl 4-methylbenzenesulfonate

(78) as a colorless residue (5.7 mg, 23 %), and 5-allyl-5-(allyloxy)-4-(4-hydroxybutyl)-

1,2,3-oxathiazepane 2,2-dioxide (79) as a colorless oil (7.8 mg, 49 %); **R_f** 0.20 (3:1

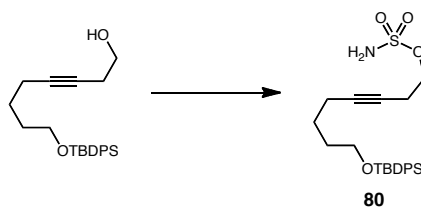
hexanes/EtOAc); **¹H NMR** (CDCl₃, 600 MHz) δ 5.95-5.85 (m, 1H), 5.77-5.70 (m, 1H),

5.33-5.15 (m, 4H), 4.45 (t, 1H, *J* = 6.2 Hz), 4.13 (dt, 1H, *J* = 11.0, 5.7 Hz), 3.97 (dd, 1H,

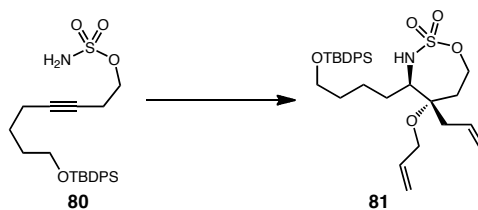
J = 12.4, 4.8 Hz), 3.87 (dd, 1H, *J* = 12.2, 5.7 Hz), 3.67-3.63 (m, 2H), 3.20 (d, 1H, *J* = 4.8

Hz), 2.43-2.34 (m, 1H), 2.21-2.28 (m, 1H), 2.04-1.88 (m, 4H), 1.74-1.40 (m, 6H);

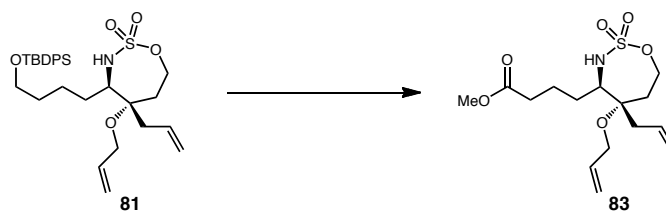
HRMS (+ESI) calculated for C₁₄H₂₆NO₅S 320.1532, found 320.1436 [M+H]⁺.



8-((tert-butyldiphenylsilyl)oxy)oct-3-yn-1-sulfamate (80). Formic acid (0.93 mL, 24 mmol) was added to neat chlorosulfonyl isocyanate (2.1 mL, 24 mmol) at 0 °C with stirring. The resulting white solid was dissolved in MeCN (36 mL), warmed to ambient temperature and stirred for 14 h. After this time the reaction mixture was cooled to 0 °C and a solution of 8-((tert-butyldiphenylsilyl)oxy)oct-3-yn-1-ol (3.7 g, 9.7 mmol) and 2,6-lutidine (2.8 mL, 24 mmol) in DMA (22 mL) was added slowly. The resulting mixture was warmed to ambient temperature and stirred until thin layer chromatography indicated complete consumption of starting material. H₂O and EtOAc were added. The organic phase was collected and the aqueous phase was extracted with EtOAc (2 x 25 mL). The combined organic extracts were washed with brine, dried over MgSO₄ and concentrated *in vacuo*. Purification by flash column chromatography (6:1 → 1:1 hexanes/EtOAc) afforded 8-((tert-butyldiphenylsilyl)oxy)oct-3-yn-1-sulfamate (**80**) as an amorphous solid (3.1 g, 70 %); **IR** (thin film, cm⁻¹) 3322, 3284, 2931, 2858, 1361, 1181, 1109, 701; **¹H NMR** (CDCl₃, 600 MHz) δ 7.68-7.38 (m, 10H), 4.88 (bs, 2H), 4.24 (t, 2H, *J* = 7.1 Hz), 3.69 (t, 2H, *J* = 6.2 Hz), 2.61 (tt, 2H, *J* = 7.2, 2.4 Hz), 2.16 (tt, 2H, *J* = 6.7, 2.4 Hz), 1.67 (qn, 2H, *J* = 6.7 Hz), 1.57 (qn, 2H, *J* = 7.1 Hz), 1.06 (s, 9H); **¹³C NMR** (CDCl₃, 150 MHz) δ 135.7, 134.1, 129.8, 127.8, 83.0, 74.8, 69.3, 63.7, 31.8, 27.1, 25.3, 19.9, 19.4, 18.6; **HRMS** (+ESI) calculated for C₂₄H₃₄NO₄SSi 460.1978, found 460.1922 [M+H]⁺.



5-allyl-5-(allyloxy)-4-(4-((tert-butyldiphenylsilyloxy)butyl)-1,2,3-oxathiazepane 2,2-dioxide (81). $\text{Rh}_2(\text{tfacam})_4$ (7.1 mg, 0.011 mmol) in trifluorotoluene (0.62 mL) was stirred in a round bottom flask at 40 °C. A solution of 8-((tert-butyldiphenylsilyloxy)oct-3-yn-1-sulfamate (**80**) (0.10 g, 0.22 mmol), $\text{PhI}(\text{O}_2\text{C}^t\text{Bu})_2$ (0.13 g, 0.33 mmol) and *bis*-allyl ether (0.16 mL, 1.31 mmol) in trifluorotoluene (0.62 mL) was added via syringe pump over 1.5 h. After complete addition the reaction was stirred for 15 min then MeOH (1 mL) and NaBH_4 (41 mg, 1.1 mmol) were added. Once the reaction was determined to be complete by thin layer chromatography the mixture was concentrated onto a pad of silica gel and immediately purified by flash column chromatography (4:1 \rightarrow 1:1 pentane/ether) to afford 5-allyl-5-(allyloxy)-4-(4-((tert-butyldiphenylsilyloxy)butyl)-1,2,3-oxathiazepane 2,2-dioxide (**81**) (53 mg, 44 %) as a colorless oil; R_f 0.30 (3:1 hexanes/EtOAc); $^1\text{H NMR}$ (CDCl_3 , 600 MHz) δ 7.70-7.36 (m, 10H), 5.94-5.88 (m, 1H), 5.76-5.68 (m, 1H), 5.33-5.07 (m, 5H), 4.42 (t, 1H, $J = 6.7$ Hz), 4.12 (tt, 1H, $J = 8.6, 7.2$ Hz), 3.96 (dd, 1H, $J = 5.2, 3.8$ Hz), 3.72-3.64 (m, 2H), 3.19 (d, 1H, $J = 14.8$ Hz), 2.42 (dd, 1H, $J = 5.2, 3.8$ Hz), 2.20-2.41 (m, 1H), 2.02-1.80 (m, 4H), 1.62-1.40 (m, 5H), 1.06 (s, 9H); **HRMS** (+ESI) calculated for $\text{C}_{30}\text{H}_{44}\text{NO}_5\text{SSi}$ 558.2709, found 558.1689 $[\text{M}+\text{H}]^+$.



Methyl 4-5-allyl-5-(allyloxy)-2,2-dioxido-1,2,3-oxathiazepan-4-yl)butanoate 83.

TBAF (1 M in THF, 0.08 mL 0.080 mmol) was added dropwise to a solution of 5-allyl-5-(allyloxy)-4-(4-((tert-butyl diphenylsilyl)oxy)butyl)-1,2,3-oxathiazepane 2,2-dioxide **81** (22 mg, 0.039 mmol) in THF (0.20 mL) at 0 °C. The resulting solution was warmed to ambient temperature and stirred for 2 h. After this time the reaction was quenched by the addition of H₂O. The organic phase was separated and the aqueous phase was extracted with EtOAc (2 x 10 mL). The combined organic extracts were washed with brine, dried over MgSO₄, concentrated *in vacuo* and the resulting colorless oil was immediately dissolved in CH₂Cl₂ (0.25 mL) and stirred at ambient temperature. To this solution was added DMP (27 mg, 0.063 mmol). The resulting solution was stirred for 1h. After this time the reaction was quenched by the addition of saturated aqueous NaHCO₃/20 % aqueous Na₂SO₃ (1:1, 5 mL total). The organic layer was separated and the aqueous layer was extracted with Et₂O (2 x 20 mL). The combined organic extracts were washed with brine, dried over MgSO₄ and concentrated *in vacuo*. The resulting colorless oil was immediately dissolved in CH₂Cl₂ (0.10 mL). ^tBuOH (0.32 mL) and 2-Me-2-butene (0.22 M aqueous solution, 0.17 mL) were added. To this solution was added NaClO₂ (34 mg, 0.37 mmol) and NaH₂PO₄ (36 mg, 0.29 mmol) in H₂O (0.34 mL) and the reaction was stirred until determined to be complete by thin layer chromatography. After this time the reaction was quenched with brine and extracted with Et₂O (2 x 15 mL). The combined

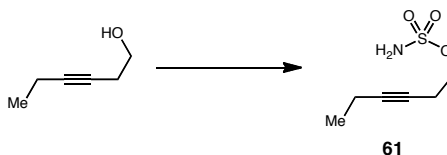
organic extracts were washed with brine, dried over MgSO_4 and concentrated *in vacuo*. The resulting crude oil was immediately dissolved in MeOH (1 mL) and concentrated. H_2SO_4 (0.10 mL) was added dropwise at ambient temperature. After 1 h. the reaction was diluted with H_2O and neutralized with 6 M NaOH. The resulting mixture was then extracted with Et_2O (3 x 15 mL). The combined organic extracts were washed with brine, dried over MgSO_4 and concentrated *in vacuo*. Purification by flash column chromatography (3:1 \rightarrow 1:1 hexanes/EtOAc) afforded methyl 4-5-allyl-5-(allyloxy)-2,2-dioxido-1,2,3-oxathiazepan-4-yl)butanoate (**83**) as a colorless oil (17 mg, 53 %); R_f 0.20 (3:1 hexanes/EtOAc); $^1\text{H NMR}$ (CDCl_3 , 600 MHz) δ 5.90 (dddd, 1H, $J = 11.4, 6.7, 3.2, 1.2$ Hz), 5.76-5.69 (m, 1H), 5.33-5.13 (m, 5H), 4.43 (t, 1H, $J = 6.7$ Hz), 4.12 (m, 1H), 3.97 (dd, 1H, $J = 11.4, 6.7$ Hz), 3.87 (dd, 1H, $J = 11.4, 6.7$ Hz), 3.68 (s, 3H), 3.20 (d, 1H, $J = 8.6$ Hz), 2.50-2.22 (m, 4H), 2.34-1.86 (m, 4H), 1.72-1.60 (m, 2H); **HRMS** (+ESI) calculated for $\text{C}_{15}\text{H}_{25}\text{NO}_6\text{S}$ 347.1403, found 347.1422 $[\text{M}]^+$.

Re-Evaluation of Intermolecular Cascade Termination.

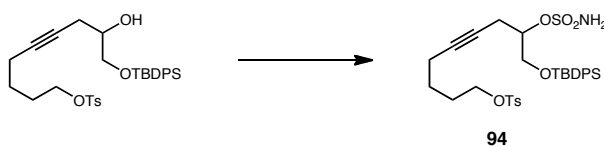
General Procedure (A) for the preparation of sulfamate esters.

Formic acid (2.5 eq.) was added to neat chlorosulfonyl isocyanate (2.5 eq.) at 0 °C with stirring. The resulting white solid was dissolved in MeCN (2.0 M), warmed to room temperature and stirred for 14 h. After this time the reaction mixture was cooled to 0 °C and a solution of the starting alcohol (1.0 eq.) and 2,6 lutidine (2.5 eq.) in DMA (1.4 M) was added dropwise. The resulting mixture was warmed to room temperature and stirred until thin layer chromatography indicated complete consumption of starting material.

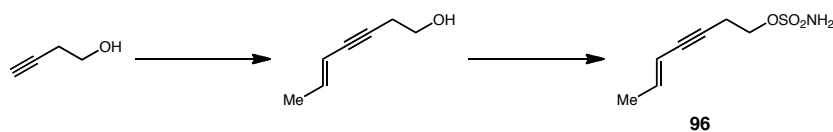
H₂O and EtOAc were added. The organic phase was collected and the aqueous phase was extracted with EtOAc. The combined organic extracts were washed with brine, dried over MgSO₄ and concentrated *in vacuo*. Purification by flash chromatography as indicated afforded the desired sulfamate ester.



Hex-3-yn-1-sulfamate (61). Prepared according to general procedure A using hex-3-yn-1-ol (3.0 g, 30.6 mmol), chlorosulfonyl isocyanate (6.6 mL, 77 mmol) and formic acid (2.9 mL, 77 mmol). After 3.5 h the reaction was quenched by the addition of EtOAc (50 mL) and H₂O (45 mL). Flash chromatography (3:1 → 1:1 hexanes/EtOAc) afforded hex-3-yn-1-sulfamate (**61**) as an amorphous solid (5.2 g, 96 %); **R_f** 0.30 (3:1 hexanes/EtOAc); **IR** (thin film, cm⁻¹) 3372, 3273, 2983, 1529, 1338, 1170, 981; **¹H NMR** (CDCl₃, 600 MHz) δ 5.05 (bs, 2H), 4.25 (t, 2H, *J* = 7.1 Hz), 2.63 (tt, 2H, *J* = 6.7, 2.4 Hz), 2.16 (qt, 2H, *J* = 7.2, 1.9 Hz), 1.12 (t, 2H, *J* = 7.1 Hz); **¹³C NMR** (CDCl₃, 150 MHz) δ 84.6, 73.8, 69.4, 19.9, 14.2, 12.5; **HRMS** (+ESI) calculated for C₆H₁₂NO₃S 178.0538, found 178.0555 [M+H]⁺.



1-((tert-butyldiphenylsilyloxy)-9-(tosyloxy)non-4-yn-2-sulfamate (94). Prepared according to general procedure **A** using 9-((tert-butyldiphenylsilyloxy)-8-hydroxynon-5-yn-1-yl 4-methylbenzenesulfonate (0.64 g, 1.1 mmol), chlorosulfonyl isocyanate (0.25 mL, 2.8 mmol) and formic acid (0.11 mL, 2.8 mmol). After 4 h the reaction was quenched by addition of EtOAc (10 mL) and H₂O (5 mL). Flash chromatography (3:1→1:1 hexanes/EtOAc) afforded 1-((tert-butyldiphenylsilyloxy)-9-(tosyloxy)non-4-yn-2-sulfamate (**94**) as a pale yellow oil (0.51 g, 70 %); **R_f** 0.25 (3:1 hexanes/EtOAc); **IR** (thin film, cm⁻¹) 3350, 3285, 2931, 2858, 1357, 1187, 1175, 933; **¹H NMR** (CDCl₃, 600 MHz) δ 7.78 (d, 2H *J* = 8.6 Hz), 7.69-7.34 (m, 10H), 4.82 (bs, 2H), 4.68 (qn, 1H, *J* = 4.8 Hz), 4.02 (t, 2H, *J* = 6.2 Hz), 3.92 (d, 2H, *J* = 4.3 Hz), 2.69-2.61 (m, 2H), 2.45 (s, 3H), 2.09 (t, 2H, *J* = 6.7 Hz), 1.72 (qn, 2H, *J* = 6.2), 1.47 (qn, 2H, *J* = 6.7 Hz), 1.08 (s, 9H); **¹³C NMR** (CDCl₃, 150 MHz) δ 145.0, 135.9, 135.7, 133.0, 130.3, 130.2, 130.1, 128.1, 82.4, 81.7, 75.3, 70.3, 64.5, 60.6, 28.1, 27.0, 24.6, 21.9, 19.4, 18.2, 14.4; **HRMS** (+ESI) calculated for C₃₂H₄₂NO₇S₂Si 644.2172, found 644.2110 [M+H]⁺.



(E)-hept-5-en-3-yn-1-ol. To a solution of Pd(PPh₃)₄ (0.49 g, 0.43 mmol) and CuI (0.14 g, 0.71 mmol) in Et₃N (2.7 mL) was added a 3-butyn-1-ol (0.93 mL, 14 mmol) in Et₃N (2.7 mL) at ambient temperature. (E)-1-bromoprop-1-ene (2.1 g, 17 mmol) in Et₃N (2.7 mL) was then added and the reaction was stirred for 8 h. After this time H₂O was added and the mixture was extracted with Et₂O (3 x 20 mL). The combined organic extracts

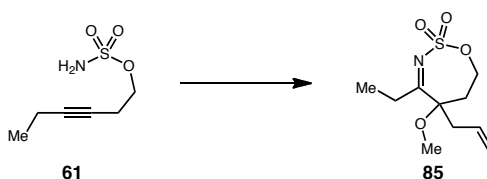
were washed with brine, dried over MgSO_4 and concentrated *in vacuo*. The resulting crude oil was purified by flash column chromatography (5:1→2:1 hexanes/EtOAc) to afford (*E*)-hept-5-en-3-yn-1-ol (0.72 g, 46 %) as a pale yellow oil; R_f 0.40 (3:1 hexanes/EtOAc); **IR** (thin film, cm^{-1}) 3347, 2938, 2914, 1043; **^1H NMR** (CDCl_3 , 600 MHz) δ 6.11 (dq, 1H $J = 13.3, 6.4$ Hz), 5.48 (dq, 1H, $J = 15.6, 1.8$ Hz), 3.73 (dd, 2H, $J = 6.4, 5.9$ Hz), 2.57 (t, 2H, $J = 4.6$ Hz), 1.81-1.77 (m, 5H); **^{13}C NMR** (CDCl_3 , 150 MHz) δ 139.4, 110.8, 84.6, 81.4, 61.4, 23.9, 18.7; **HRMS** (+ESI) calculated for $\text{C}_7\text{H}_{11}\text{O}$ 111.0810, found 111.0802 $[\text{M}+\text{H}]^+$.

(*E*)-hept-5-en-3-yn-1-sulfamate (96). Prepared according to general procedure **A** using (*E*)-hept-5-en-3-yn-1-ol (0.72 g, 6.5 mmol), chlorosulfonyl isocyanate (1.4 mL, 16 mmol) and formic acid (0.63 mL, 16 mmol). After 4 h the reaction was quenched by addition of EtOAc and H_2O . Flash chromatography (3:1 to 1:1 hexanes/EtOAc) afforded (*E*)-hept-5-en-3-yn-1-sulfamate (**96**) as a pale yellow oil (0.70 g, 57 %); R_f 0.25 (3:1 hexanes/EtOAc); **IR** (thin film, cm^{-1}) 3374, 3276, 1342, 1174, 989; **^1H NMR** (CDCl_3 , 600 MHz) δ 6.12 (dq, 1H $J = 13.5, 6.7$ Hz), 5.45 (dd, 1H, $J = 15.8, 2.1$ Hz), 4.82 (bs, 2H), 4.30 (t, 2H, $J = 7.0$ Hz), 2.76 (t, $J = 7.0$ Hz), 1.77 (d, 3H, $J = 6.7$ Hz); **^{13}C NMR** (CDCl_3 , 150 MHz) δ 140.1, 110.4, 101.9, 82.3, 81.6, 69.0, 20.4, 18.8; **HRMS** (-ESI) calculated for $\text{C}_7\text{H}_{10}\text{NO}_3\text{S}$ 188.0381, found 188.0389 $[\text{M}-\text{H}]^-$.

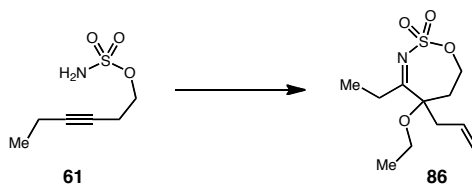
General procedure (B) for intermolecular cascade termination.

$\text{Rh}_2(\text{tfacam})_4$ (5 mol %) in trifluorotoluene (0.025 M) was stirred in a round bottom flask at 40 °C. A solution of sulfamate ester (1 eq.), $\text{PhI}(\text{O}_2\text{C}^t\text{Bu})_2$ (1.6 eq.) and allyl ether (6

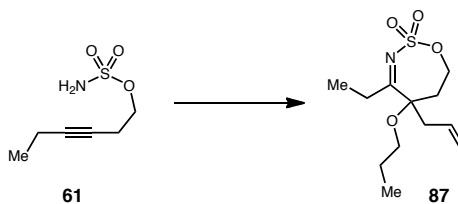
eq.) in trifluorotoluene (0.025 M) was added via syringe pump over 1.5 h. After complete addition the reaction was stirred until thin layer chromatography indicated complete consumption of starting sulfamate ester (5-20 min). Once judged to be complete the reaction mixture was concentrated onto a pad of silica gel and immediately purified by flash column chromatography on silica gel as indicated.



5-allyl-4-ethyl-5-methoxy-1,2,3-oxathiazepane 2,2-dioxide (85). Prepared by general procedure **B** using hex-3-yn-1-sulfamate (**61**) (50 mg, 0.28 mmol), $\text{PhI}(\text{O}_2\text{C}^t\text{Bu})_2$ (0.18 g, 0.45 mmol), methyl-allyl ether (0.12 mg, 1.7 mmol) and $\text{Rh}_2(\text{tfacam})_4$ (9.2 mg, 0.014 mmol). Flash chromatography (5:1 hexanes/EtOAc) afforded 5-allyl-4-ethyl-5-methoxy-6,7-dihydro-5H-1,2,3-oxathiazepine 2,2-dioxide (**85**) as a colorless oil (38 mg, 55 %); R_f 0.47 (3:1 hexanes/EtOAc); **IR** (thin film, cm^{-1}) 2977, 2938, 1626, 1363, 1178; **$^1\text{H NMR}$** (CDCl_3 , 600 MHz) δ 5.96-5.89 (m, 1H), 5.24-5.21 (m, 2H), 4.43 (dd, 1H, $J = 11.4, 6.7$ Hz), 4.30 (dt, 1H, $J = 11.4, 4.8$ Hz), 3.27 (s, 3H), 2.92 (dt, 1H, $J = 12.4, 6.7$ Hz), 2.80 (dq, 1H, $J = 20.9, 7.1$ Hz), 2.64-2.58 (m, 2H), 2.52 (dd, 1H, $J = 14.8, 8.6$ Hz), 1.99 (dd, 1H, $J = 14.8, 4.3$ Hz), 1.13 (t, 3H, $J = 7.2$ Hz); **$^{13}\text{C NMR}$** (CDCl_3 , 150 MHz) δ 193.2, 131.3, 120.2, 84.7, 64.7, 52.9, 39.7, 31.4, 30.1, 10.2; **HRMS** (+APCI) calculated for $\text{C}_{10}\text{H}_{18}\text{NO}_4\text{S}$ 248.0957, found 248.0949 $[\text{M}+\text{H}]^+$.

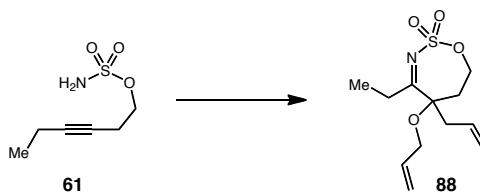


5-allyl-5-ethoxy-4-ethyl-6,7-dihydro-5H-1,2,3-oxathiazepine 2,2-dioxide 86. Prepared by general procedure **B** using hex-3-yn-1-sulfamate (**61**) (50 mg, 0.28 mmol), $\text{PhI}(\text{O}_2\text{C}^t\text{Bu})_2$ (0.18 g, 0.45 mmol), ethyl-allyl ether (0.19 mL, 1.7 mmol) and $\text{Rh}_2(\text{tfacam})_4$ (9.2 mg, 0.014 mmol). Flash chromatography (6:1 hexanes/EtOAc) afforded 5-allyl-5-ethoxy-4-ethyl-6,7-dihydro-5H-1,2,3-oxathiazepine 2,2-dioxide (**86**) as a colorless oil (48 mg, 65 %); R_f 0.50 (3:1 hexanes/EtOAc); **IR** (thin film, cm^{-1}) 2978, 2934, 1626, 1363, 1178; **$^1\text{H NMR}$** (CDCl_3 , 600 MHz) δ 5.96 (dddd, 1H, $J = 14.0, 9.8, 8.8, 5.5$ Hz), 5.24-5.20 (m, 2H), 4.40 (ddd, 1H, $J = 11.6, 7.0, 1.5$ Hz), 4.28 (dt, 1H, $J = 12.5, 4.3$ Hz), 3.59 (tq, 1H, $J = 6.7, 1.8$ Hz), 3.19 (tq, 1H, $J = 7.0, 1.8$ Hz), 2.98-2.89 (m, 1H), 2.82 (dq, 1H, $J = 21.4, 7.0$ Hz), 2.62-2.47 (m, 3H), 2.01 (ddd, 1H, $J = 15.0, 4.6, 1.2$ Hz), 1.25 (t, 3H, $J = 7.0$ Hz), 1.13 (t, 3H, $J = 7.3$ Hz); **$^{13}\text{C NMR}$** (CDCl_3 , 150 MHz) δ 193.7, 131.5, 119.9, 84.5, 64.8, 60.7, 39.8, 32.0, 29.9, 15.5, 10.2; **HRMS** (+APCI) calculated for $\text{C}_{11}\text{H}_{20}\text{NO}_4\text{S}$ 262.1113, found 262.1106 $[\text{M}+\text{H}]^+$.



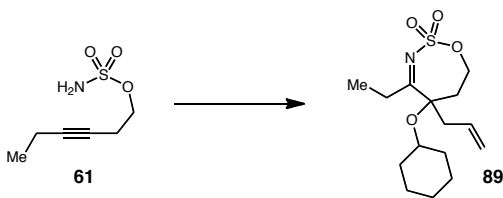
5-allyl-4-ethyl-5-propoxy-6,7-dihydro-5H-1,2,3-oxathiazepine 2,2-dioxide (87).

Prepared by general procedure **B** using hex-3-yn-1-sulfamate (**61**) (50 mg, 0.28 mmol), $\text{PhI}(\text{O}_2\text{C}^t\text{Bu})_2$ (0.18 g, 0.45 mmol), propyl-allyl ether (0.22 mL, 1.7 mmol) and $\text{Rh}_2(\text{tfacam})_4$ (9.2 mg, 0.014 mmol). Flash chromatography (5:1 \rightarrow 4:1 hexanes/EtOAc) afforded 5-allyl-4-ethyl-5-propoxy-6,7-dihydro-5H-1,2,3-oxathiazepine 2,2-dioxide (**87**) as a colorless oil (50 mg, 65 %); R_f 0.53 (3:1 hexanes/EtOAc); **IR** (thin film, cm^{-1}) 2969, 2937, 2878, 1626, 1364, 1178; **$^1\text{H NMR}$** (CDCl_3 , 600 MHz) δ 5.98-5.91 (m, 1H), 5.23-5.18 (m, 2H), 4.41 (ddd, 1H, $J = 11.4, 6.7, 1.4$ Hz), 4.28 (dt, 1H, $J = 12.4, 4.8$ Hz), 3.44 (dt, 1H, $J = 8.6, 6.7$ Hz), 3.13 (dt, 1H, $J = 8.6, 6.2$ Hz), 2.97-2.89 (m, 1H), 2.83-2.76 (m, 1H), 2.62-2.49 (m, 3H), 2.01 (dd, 1H, $J = 15.2, 4.8$ Hz), 1.65-1.59 (m, 2H), 1.12 (t, 3H, $J = 6.7$ Hz), 0.96 (t, 3H, $J = 7.2$ Hz); **$^{13}\text{C NMR}$** (CDCl_3 , 150 MHz) δ 193.7, 131.5, 119.9, 84.2, 66.4, 64.8, 39.8, 32.0, 30.0, 27.2, 23.4, 10.7, 10.3; **HRMS** (+APCI) calculated for $\text{C}_{12}\text{H}_{22}\text{NO}_4\text{S}$ 276.1270, found 276.1260 $[\text{M}+\text{H}]^+$.

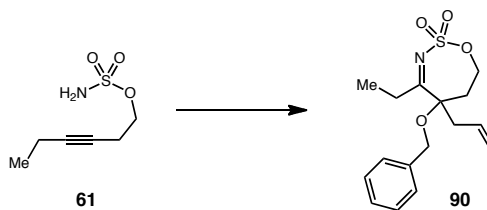


5-allyl-5-(allyloxy)-4-ethyl-6,7-dihydro-5H-1,2,3-oxathiazepine 2,2-dioxide (88).

Prepared by general procedure **B** using hex-3-yn-1-sulfamate (**61**) (50 mg, 0.28 mmol), $\text{PhI}(\text{O}_2\text{C}^t\text{Bu})_2$ (0.18 g, 0.45 mmol), *bis*-allyl ether (0.21 mL, 1.7 mmol) and $\text{Rh}_2(\text{tfacam})_4$ (9.2 mg, 0.014 mmol). Flash chromatography (5:1 \rightarrow 4:1 hexanes/EtOAc) afforded 5-allyl-5-(allyloxy)-4-ethyl-6,7-dihydro-5H-1,2,3-oxathiazepine 2,2-dioxide (**88**) as a colorless oil (35 mg, 45 %); R_f 0.40 (3:1 hexanes/EtOAc); **IR** (thin film, cm^{-1}) 2877, 2837, 1627, 1362, 1178; **$^1\text{H NMR}$** (CDCl_3 , 600 MHz) δ 6.02-5.86 (m, 2H), 5.36 (dq, 2H, $J = 17.2, 1.4$ Hz), 5.23 (d, 2H, $J = 10.5$ Hz), 4.41 (ddd, 1H, $J = 11.4, 6.7, 0.9$ Hz), 4.30 (dt, 1H, $J = 11.4, 4.8$ Hz), 4.06 (ddt, 1H, $J = 12.9, 5.2, 1.4$ Hz), 3.74 (ddt, 1H, $J = 12.9, 4.8, 1.9$ Hz), 2.94 (dt, 1H, $J = 13.8, 6.7$ Hz), 2.79 (dq, 1H, $J = 18.6, 7.2$ Hz), 2.67-2.53 (m, 3H), 2.05 (ddd, 1H, $J = 14.8, 4.3, 0.9$ Hz), 1.12 (t, 3H, $J = 6.7$ Hz); **$^{13}\text{C NMR}$** (CDCl_3 , 150 MHz) δ 193.2, 133.5, 131.4, 120.2, 117.1, 84.8, 66.1, 64.7, 39.9, 32.2, 30.1, 10.2; **HRMS** (+APCI) calculated for $\text{C}_{12}\text{H}_{20}\text{NO}_4\text{S}$ 274.1113, found 274.1122 $[\text{M}+\text{H}]^+$.

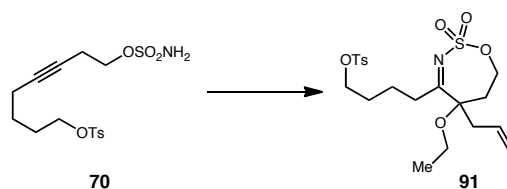


5-allyl-5-(cyclohexyloxy)-4-ethyl-6,7-dihydro-5H-1,2,3-oxathiazepine 2,2-dioxide (89). Prepared by general procedure **B** using hex-3-yn-1-sulfamate (**61**) (50 mg, 0.28 mmol), $\text{PhI}(\text{O}_2\text{C}^t\text{Bu})_2$ (0.18 g, 0.45 mmol), cyclohexyl-allyl ether (0.24 g, 1.7 mmol) and $\text{Rh}_2(\text{tfacam})_4$ (9.2 mg, 0.014 mmol). Flash chromatography (5:1 \rightarrow 4:1 hexanes/EtOAc) afforded 5-allyl-5-(cyclohexyloxy)-4-ethyl-6,7-dihydro-5H-1,2,3-oxathiazepine 2,2-dioxide (**89**) as a colorless oil (37 mg, 43 %); R_f 0.50 (3:1 hexanes/EtOAc); **IR** (thin film, cm^{-1}) 2934, 2857, 1625, 1366, 1178; **$^1\text{H NMR}$** (CDCl_3 , 600 MHz) δ 5.97-5.90 (m, 1H), 5.22-5.19 (m, 2H), 4.41 (ddd, 1H, $J = 11.9, 6.7, 1.4$ Hz), 4.26 (dt, 1H, $J = 11.9, 4.3$ Hz), 3.47 (tt, 1H, $J = 9.1, 3.3$ Hz), 2.87 (dt, 1H, $J = 13.3, 6.7$ Hz), 2.79-2.71 (m, 2H), 2.63 (dd, 1H, $J = 14.3, 5.7$ Hz), 2.45 (dd, 1H, $J = 14.3, 8.1$ Hz), 2.13 (ddd, 1H, $J = 14.8, 4.3, 1.4$ Hz), 1.84-1.74 (m, 4H), 1.55-1.53 (m, 1H), 1.47-1.19 (m, 5H), 1.11 (t, 3H, $J = 7.2$ Hz); **$^{13}\text{C NMR}$** (CDCl_3 , 150 MHz) δ 194.3, 131.7, 119.9, 84.7, 73.4, 65.0, 39.7, 35.0, 33.2, 30.8, 27.2, 25.6, 24.5; **HRMS** (+APCI) calculated for $\text{C}_{15}\text{H}_{26}\text{NO}_4\text{S}$ 316.1583, found 316.1573 $[\text{M}+\text{H}]^+$.

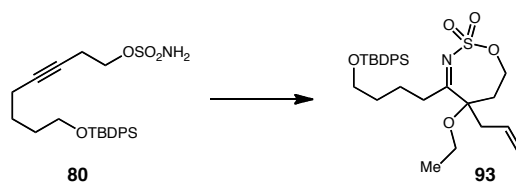


5-allyl-5-(benzyloxy)-4-ethyl-6,7-dihydro-5H-1,2,3-oxathiazepine 2,2-dioxide (90).

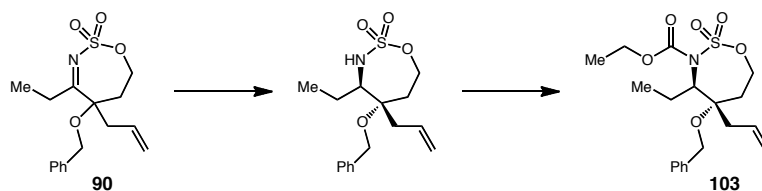
Prepared by general procedure **B** using hex-3-yn-1-sulfamate (**61**) (50 mg, 0.28 mmol), $\text{PhI}(\text{O}_2\text{C}^t\text{Bu})_2$ (0.18 g, 0.45 mmol), benzyl-allyl ether (0.26 mL, 1.7 mmol) and $\text{Rh}_2(\text{tfacam})_4$ (9.2 mg, 0.014 mmol). Flash chromatography (5:1→3:1 hexanes/EtOAc) afforded 5-allyl-5-(benzyloxy)-4-ethyl-6,7-dihydro-5H-1,2,3-oxathiazepine 2,2-dioxide (**90**) as a white amorphous solid (45 mg, 51 %); R_f 0.40 (3:1 hexanes/EtOAc); **IR** (thin film, cm^{-1}) 2977, 2937, 1627, 1365, 1181; **¹H NMR** (CDCl_3 , 600 MHz) δ 7.40-7.33 (m, 5H), 6.07-6.00 (m, 1H), 5.29-5.26 (m, 2H), 4.62 (d, 1H, $J = 11.4$ Hz), 4.46 (ddd, 1H, $J = 11.4, 6.7, 1.0$ Hz), 4.36-4.31 (m, 2H), 3.05 (dt, 1H, $J = 14.8, 6.7$ Hz), 2.86 (dq, 1H, $J = 19.1, 7.1$ Hz), 2.72 (ddd, 1H, $J = 14.3, 5.2, 1.0$ Hz), 2.68-2.60 (m, 2H), 2.13 (dd, 1H, $J = 14.3, 3.8$ Hz), 1.13 (t, 3H, $J = 7.2$ Hz); **¹³C NMR** (CDCl_3 , 150 MHz) δ 192.9, 137.3, 131.3, 128.8, 128.1, 126.8, 120.4, 84.9, 66.9, 64.7, 39.9, 32.3, 30.3, 10.3; **HRMS** (+APCI) calculated for $\text{C}_{16}\text{H}_{22}\text{NO}_4\text{S}$ 324.1270, found 324.1259 $[\text{M}+\text{H}]^+$.



4-(5-allyl-5-ethoxy-2,2-dioxido-6,7-dihydro-5H-1,2,3-oxathiazepin-4-yl)butyl 4-methylbenzenesulfonate (91). Prepared by general procedure **B** using 8-(tosyloxy)oct-3-yn-1-sulfamate (**70**) (106 mg, 0.28 mmol), $\text{PhI}(\text{O}_2\text{C}^t\text{Bu})_2$ (0.18 g, 0.45 mmol), ethyl-allyl ether (0.19 mL, 1.7 mmol) and $\text{Rh}_2(\text{tfacam})_4$ (9.2 mg, 0.014 mmol). Flash chromatography (4:1 \rightarrow 1:1 hexanes/EtOAc) afforded 4-(5-allyl-5-ethoxy-2,2-dioxido-6,7-dihydro-5H-1,2,3-oxathiazepin-4-yl)butyl 4-methylbenzenesulfonate (**91**) as a colorless oil (64 mg, 53 %); R_f 0.40 (3:1 hexanes/EtOAc); **IR** (thin film, cm^{-1}) 2876, 1627, 1356, 1173; **$^1\text{H NMR}$** (CDCl_3 , 600 MHz) δ 7.78 (d, 2H, $J = 8.6$ Hz), 7.35 (d, 2H, $J = 8.1$ Hz), 5.97-5.90 (m, 1H), 5.22-5.19 (m, 2H), 4.39 (dd, 1H, $J = 11.0, 5.7$ Hz), 4.27 (dt, 1H, $J = 12.4, 4.8$ Hz), 4.02 (t, 2H, $J = 6.2$ Hz), 3.57 (tt, 1H, $J = 13.8, 6.7$ Hz), 3.16 (tt, 1H, $J = 13.8, 6.7$ Hz), 2.87 (dt, 1H, $J = 14.8, 6.7$ Hz), 2.76 (dt, 1H, $J = 18.6, 8.1$ Hz), 2.56-2.45 (m, 5H), 2.01 (dd, 1H, $J = 13.8, 3.3$ Hz), 1.71-1.60 (m, 5H), 1.23 (t, 3H, $J = 7.2$ Hz); **$^{13}\text{C NMR}$** (CDCl_3 , 150 MHz) δ 145.0, 132.9, 131.3, 130.1, 128.0, 120.1, 84.3, 70.3, 64.8, 60.6, 39.6, 35.6, 31.9, 28.2, 21.8, 21.7, 15.5; **HRMS** (+APCI) calculated for $\text{C}_{20}\text{H}_{30}\text{NO}_7\text{S}_2$ 460.1464, found 460.1455 $[\text{M}+\text{H}]^+$.

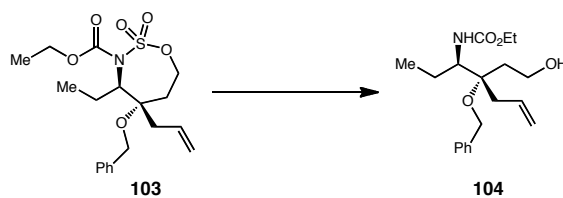


5-allyl-4-(4-((tert-butyldiphenylsilyloxy)butyl)-5-ethoxy-6,7-dihydro-5H-1,2,3-oxathiazepine 2,2-dioxide (93). Prepared by general procedure **B** using 8-((tert-butyldiphenylsilyloxy)oct-3-yn-1-sulfamate (**80**) (0.13 g, 0.28 mmol), $\text{PhI}(\text{O}_2\text{C}^t\text{Bu})_2$ (0.18 g, 0.45 mmol), ethyl-allyl ether (0.19 mL, 1.7 mmol) and $\text{Rh}_2(\text{tfacam})_4$ (9.2 mg, 0.014 mmol). Flash chromatography (5:1 \rightarrow 2:1 hexanes/EtOAc) afforded 5-allyl-4-(4-((tert-butyldiphenylsilyloxy)butyl)-5-ethoxy-6,7-dihydro-5H-1,2,3-oxathiazepine 2,2-dioxide (**93**) as a colorless oil (89 mg, 59 %); R_f 0.30 (3:1 hexanes/EtOAc); **IR** (thin film, cm^{-1}) 2931, 2858, 1628, 1363, 1181, 1106, 701; **^1H NMR** (CDCl_3 , 600 MHz) δ 7.68-7.38 (m, 10H), 5.99-5.92 (m, 1H), 5.23-5.21 (m, 2H), 4.40 (dd, 1H, $J = 11.4, 6.7$ Hz), 4.27 (dt, 1H, $J = 12.4, 4.8$ Hz), 3.69 (t, 3H, $J = 6.7$ Hz), 3.60-3.55 (m, 1H), 3.16 (dq, 1H, $J = 8.6, 7.2$ Hz), 2.93 (dq, 1H, $J = 14.8, 7.2$ Hz), 2.82-2.75 (m, 1H), 2.59-2.46 (m, 3H), 2.00 (dd, 1H, $J = 5.2, 3.8$ Hz), 1.80-1.57 (m, 4H), 1.22 (t, 3H, $J = 7.1$ Hz), 1.07 (s, 9H); **^{13}C NMR** (CDCl_3 , 150 MHz) δ 192.6, 135.7, 134.1, 131.5, 129.7, 127.8, 119.9, 84.4, 64.7, 63.7, 60.7, 39.6, 36.1, 32.0, 31.9, 27.2, 27.1, 22.5, 19.4, 15.6; **HRMS** (+APCI) calculated for $\text{C}_{29}\text{H}_{41}\text{NNaO}_5\text{SSi}$ 566.2372, found 566.2359 $[\text{M}+\text{Na}]^+$.

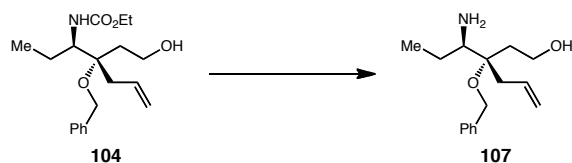


5-allyl-5-(benzyloxy)-4-ethyl-1,2,3-oxathiazepane 2,2-dioxide. To a solution of 5-allyl-5-(benzyloxy)-4-ethyl-6,7-dihydro-5H-1,2,3-oxathiazepine 2,2-dioxide (**90**) (0.18 g, 0.56 mmol) in THF (2.9 mL) at ambient temperature was added LAH (0.56 mL, 1.1 mmol, 2 M solution in THF). Once thin layer chromatography indicated complete consumption of starting material the reaction mixture was poured into a vigorously stirring solution of Et₂O (50 mL) and a saturated aqueous Rochelle's salt solution (25 mL). Et₂O (100 mL) was added and the resulting biphasic mixture was stirred vigorously for approximately 3 h. The organic layer was separated, washed with brine, dried over MgSO₄ and concentrated *in vacuo*. Flash chromatography (5:1→2:1 hexanes/EtOAc) afforded 5-allyl-5-(benzyloxy)-4-ethyl-1,2,3-oxathiazepane 2,2-dioxide as a colorless oil (0.17 g, 96 %); **R_f** 0.33 (3:1 hexanes/EtOAc); **IR** (thin film, cm⁻¹) 3355, 2967, 2877, 1361, 1177, 736; **¹H NMR** (CDCl₃, 600 MHz) δ 7.41-7.33 (m, 5H), 5.86-5.76 (m, 1H), 5.25-5.16 (m, 3H), 4.53-4.45 (m, 2H), 4.39 (d, 1H, *J* = 10.7 Hz), 4.19-4.10 (m, 1H), 3.15 (bd, 1H, *J* = 12.2 Hz), 2.60 (dd, 1H, *J* = 15.6, 6.1 Hz), 2.34 (dd, 1H, *J* = 15.6, 8.2 Hz), 2.15 (dd, 1H, *J* = 16.2, 4.9 Hz), 2.08-2.00 (m, 2H), 1.96-1.86 (m, 1H), 1.65 (sext, 1H, *J* = 7.3 Hz), 1.27 (t, 3H, *J* = 7.0 Hz), 1.41 (t, 3H, *J* = 7.3 Hz); **¹³C NMR** (CDCl₃, 150 MHz) δ 137.6, 131.5, 128.9, 128.2, 127.5, 119.5, 79.9, 64.8, 63.7, 62.4, 38.2, 33.7, 19.6, 11.9; **HRMS** (+ESI) calculated for C₁₆H₂₄NO₄S 326.1426, found 326.1418 [M+H]⁺.

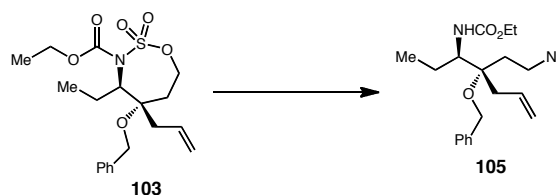
Ethyl 5-allyl-5-(benzyloxy)-4-ethyl-1,2,3-oxathiazepane-3-carboxylate 2,2-dioxide (103). To a solution of 5-allyl-5-(benzyloxy)-4-ethyl-1,2,3-oxathiazepane 2,2-dioxide (0.18 g, 0.55 mmol) and DMAP (20 mg, 0.17 mmol) in THF (2.0 mL) at 0 °C was added diethylpyrocarbonate (0.16 mL, 1.1 mmol) neat. This solution was warmed to ambient temperature and once thin layer chromatography indicated complete consumption of starting material (1-3 h) the reaction was quenched by the addition of H₂O (10 mL). This biphasic mixture was transferred to a separatory funnel and the aqueous layer was extracted with Et₂O (2 X 20 mL). The combined organic extracts were washed with brine, dried over MgSO₄ and concentrated *in vacuo*. Flash chromatography (5:1→4:1 hexanes/EtOAc) afforded ethyl 5-allyl-5-(benzyloxy)-4-ethyl-1,2,3-oxathiazepane-3-carboxylate 2,2-dioxide (**103**) as a colorless oil (0.15 g, 70 %); **R_f** 0.40 (3:1 hexanes/EtOAc); **IR** (thin film, cm⁻¹) 2978, 1724, 1388, 1367, 1275, 955; **¹H NMR** (CDCl₃, 600 MHz) δ 7.38-7.25 (m, 5H), 5.89-5.82 (m, 1H), 5.24-5.19 (m, 2H), 5.00 (t, 1H, *J* = 13.3 Hz), 4.87 (d, 1H, *J* = 11.9), 4.63 (d, 1H, *J* = 11.0 Hz), 4.45 (d, 1H, *J* = 11.5 Hz), 4.34 (dt, 1H, *J* = 11.5, 1.8 Hz), 4.31-4.22 (m, 2H), 4.13 (q, 1H, *J* = 5.5 Hz), 2.54 (ddd, 1H, *J* = 36.2, 15.6, 6.9 Hz), 2.19-2.05 (m, 3H), 1.97 (t, 1H, *J* = 15.6 Hz), 1.65-1.59 (m, 1H), 1.26 (m, 3H), 1.06 (t, 3H, *J* = 7.3 Hz); **¹³C NMR** (CDCl₃, 150 MHz) δ 154.3, 138.2, 131.8, 128.5, 127.5, 126.9, 119.8, 77.5, 69.4, 65.5, 64.5, 63.7, 60.6, 40.2, 33.2, 22.5, 14.3, 11.3; **HRMS** (+ESI) calculated for C₁₉H₂₈NO₆S 398.1637, found 398.1644 [M+H]⁺.



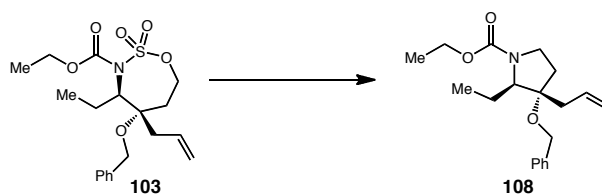
Ethyl 4-(benzyloxy)-4-(2-hydroxyethyl)hept-6-en-3-ylcarbamate (104). A solution of ethyl 5-allyl-5-(benzyloxy)-4-ethyl-1,2,3-oxathiazepane-3-carboxylate 2,2-dioxide (**103**) (25 mg, 0.06 mmol) in MeCN/H₂O (1:1, 0.4 mL total) was heated to 80 °C for 20 h. After this time the reaction was cooled to ambient temperature and Et₂O (1 mL) and 1 M aqueous HCl (2 mL) was added. The resulting biphasic mixture was stirred 2 h. after which point it was transferred to a separatory funnel and extracted with EtOAc (2 x 10 mL). The combined organic extracts were dried over MgSO₄ and concentrated *in vacuo*. Flash chromatography (3:1 → 1:1 hexanes/EtOAc) afforded ethyl 4-(benzyloxy)-4-(2-hydroxyethyl)hept-6-en-3-ylcarbamate (**104**) as a colorless oil (18 mg, 86 %); **R_f** 0.15 (3:1 hexanes/EtOAc); **IR** (thin film, cm⁻¹) 3400, 3312, 2971, 2932, 2875, 1693, 1537, 1071; **¹H NMR** (CDCl₃, 600 MHz) δ 7.35-7.27 (m, 5H), 5.93 (sext, 1H, *J* = 7.6 Hz), 5.23 (bd, 1H, *J* = 9.1 Hz), 5.18-5.14 (m, 2H), 4.58 (d, 1H, *J* = 11.0 Hz), 4.46 (d, 1H, *J* = 11.0 Hz), 4.12-4.08 (m, 2H), 3.93 (dt, 1H, *J* = 11.0, 6.2 Hz), 3.85 (bs, 1H), 3.76 (dt, 1H, *J* = 11.0, 5.7 Hz), 2.58 (dd, 1H, *J* = 15.2, 6.7 Hz), 2.47 (dd, 1H, *J* = 14.8, 8.1 Hz) 1.97 (t, 2H, *J* = 6.2 Hz), 1.78 (sext, 1H, *J* = 6.7 Hz), 1.40-1.35 (m, 1H), 1.22 (t, 3H, *J* = 6.7 Hz), 0.97 (t, 3H, *J* = 7.6 Hz); **¹³C NMR** (CDCl₃, 150 MHz) δ 157.4, 138.9, 134.2, 128.5, 127.6, 127.4, 118.5, 80.3, 64.0, 61.0, 58.6, 57.6, 40.3, 35.9, 24.1, 14.8, 11.4; **HRMS** (+ESI) calculated for C₁₉H₃₀NO₄ 336.2175, found 336.2168 [M+H]⁺.



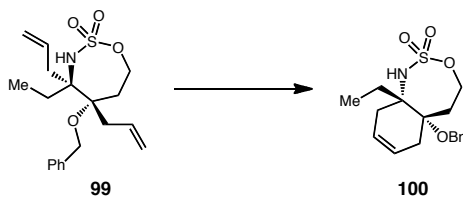
3-(1-aminopropyl)-3-(benzyloxy)hex-5-en-1-ol (107). Saturated aqueous KOH (pH 14, 1 mL) was added slowly to ethyl 4-(benzyloxy)-4-(2-hydroxyethyl)hept-6-en-3-ylcarbamate (**104**) (5 mg, 0.015 mmol) in MeOH (1 mL) at ambient temperature. The resulting solution was heated to 80 °C for 14 h. After this time the reaction was cooled to ambient temperature and neutralized with 6 N HCl. This solution was transferred to 25 mL round-bottom flask and concentrated *in vacuo*. Once dry the flask was washed with CH₂Cl₂ and filtered. The filtrate was then concentrated *in vacuo* to yield 3-(1-aminopropyl)-3-(benzyloxy)hex-5-en-1-ol (**107**) as a white amorphous solid (3 mg, 80 %); *R_f* 0.10 (5:1 CH₂Cl₂/MeOH); ¹H NMR (CDCl₃, 600 MHz) δ 7.37-7.28 (m, 5H), 5.85-5.78 (m, 1H), 5.23-5.1 (m, 2H), 4.49 (d, 1H, *J* = 10.5 Hz), 4.35 (d, 1H, *J* = 10.5 Hz), 3.78-3.65 (m, 3H), 3.15 (d, 1H, *J* = 10.5 Hz), 2.60 (dt, 2H, *J* = 15.7, 4.8 Hz), 2.32 (d, 2H, *J* = 15.7 Hz), 1.95-1.85 (m, 4H), 1.69-1.56 (m, 6H), 1.06 (t, 1H, *J* = 7.2 Hz); ¹³C NMR (CDCl₃, 150 MHz) δ 137.7, 132.3, 128.8, 128.1, 127.9, 119.2, 63.7, 57.5, 55.9, 39.5, 35.2, 29.9, 27.9, 22.6, 11.8, **HRMS** (+ESI) calculated for C₁₆H₂₆NO₂ 264.1964, found 264.1954 [M+H]⁺.



Ethyl-4-(2-azidoethyl)-4-(benzyloxy)hept-6-en-3-ylcarbamate (105). NaN₃ (8.0 mg, 0.13 mmol) was added to a solution of ethyl 5-allyl-5-(benzyloxy)-4-ethyl-1,2,3-oxathiazepane-3-carboxylate 2,2-dioxide (**103**) (25 mg, 0.063 mmol) in DMSO (0.15 mL) and heated to 70 °C for 14 h. After this time the reaction was cooled to ambient temperature and diluted with saturated aqueous NH₄Cl (3 mL) and stirred 2 h. After this time the mixture was transferred to a separatory funnel and extracted with EtOAc (3 x 10 mL). The combined organic extracts were washed with brine, dried over MgSO₄ and concentrated *in vacuo*. Flash chromatography (3:1 → 1:2 hexanes/ EtOAc) afforded ethyl-4-(2-azidoethyl)-4-(benzyloxy)hept-6-en-3-ylcarbamate (**105**) as a colorless oil (17 mg, 74 %); **R_f** 0.10 (3:1 hexanes/EtOAc); **IR** (thin film, cm⁻¹) 2975, 2933, 11694, 1414, 1103; **¹H NMR** (CDCl₃, 600 MHz) δ 7.33-7.04 (m, 5H), 5.80 (sept, 1H, *J* = 7.6 Hz), 5.01 (t, 1H, *J* = 11.0 Hz), 4.16-4.00 (m, 4H), 2.25 (dd, 1H, *J* = 15.2, 6.7 Hz), 1.96 (dd, 2H, *J* = 14.8, 8.1 Hz), 1.80 (dd, 1H, *J* = 14.3, 7.4 Hz), 1.46-1.22 (m, 3H), 1.05 (m, 3H); **HRMS** (+ESI) calculated for C₁₉H₂₉N₄O₃ 361.2240, found 361.2233 [M+H]⁺.

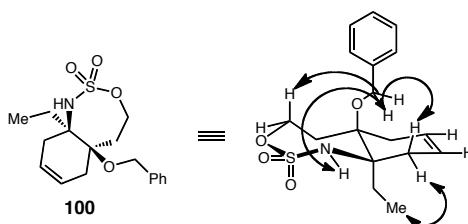


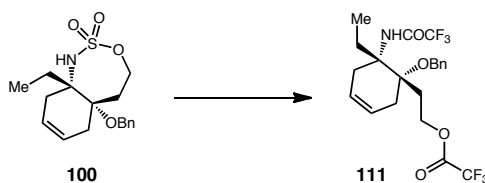
Ethyl 3-allyl-3-(benzyloxy)-2-ethylpyrrolidine-1-carboxylate (108). A mixture of ethyl 5-allyl-5-(benzyloxy)-4-ethyl-1,2,3-oxathiazepane-3-carboxylate 2,2-dioxide (**103**) (3 mg, 0.008 mmol) and NaI (2.2 mg, 0.02 mmol) in DMF (0.1 mL) was heated to 70 °C for 6 h. The reaction was cooled to ambient temperature and NaH (1.0 mg, 0.023 mmol, 60% dispersion in mineral oil) was added in a single portion. The resulting mixture was warmed to 40 °C and stirred 14 h. This solution was cooled to ambient temperature and quenched by the addition of saturated aqueous NH₄Cl (0.25 mL). This mixture was extracted with EtOAc (3 x 5 mL), the organic extracts were combined, dried over MgSO₄ and concentrated *in vacuo*. Flash chromatography (4:1→2:1 hexanes/ EtOAc) afforded ethyl 3-allyl-3-(benzyloxy)-2-ethylpyrrolidine-1-carboxylate (**108**) as a colorless residue (2.3 mg, 98 %); *R_f* 0.25 (3:1 hexanes/EtOAc); **IR** (thin film, cm⁻¹) 2917, 2849, 1692, 732; **¹H NMR** (CDCl₃, 600 MHz) δ 7.37-7.25 (m, 5H), 5.90-5.81 (m, 1H), 5.13-5.06 (m, 2H), 4.54-4.49 (m, 2H), 3.91 (tt, 1H, *J* = 36.6, 6.7 Hz), 3.50-3.39 (m, 2H), 2.53-2.32 (m, 2H), 2.14-2.03 (m, 2H), 1.87-1.79 (m, 1H), 1.45 (qn, 1H, *J* = 7.1 Hz), 1.06 (t, 3H, *J* = 7.3 Hz); **¹³C NMR** (CDCl₃, 150 MHz) δ 154.3, 138.2, 131.8, 128.5, 127.5, 126.9, 119.8, 70.5, 65.4, 62.5, 61.5, 61.3, 60.6, 40.2, 33.2, 22.5, 14.3, 11.3; **HRMS** (+ESI) calculated for C₁₉H₂₈NO₃ 318.2069, found 318.1983 [M+H]⁺.



5a-(benzyloxy)-9a-ethyl-4,5,5a,6,9,9a-hexahydro-1H-benzo[d][1,2,3]oxathiazepine 2,2-dioxide (100). 4,5-diallyl-5-(benzyloxy)-4-ethyl-1,2,3-oxathiazepane 2,2-dioxide (**99**) (10 mg, 0.03 mmol) in benzene (1.2 mL) was added to a solution of Grubbs second generation catalyst (1.1 mg, 0.001 mmol) in benzene (7.0 mL). This solution was stirred at ambient temperature for 20 h. The reaction mixture was then concentrated onto a pad of SiO₂ and purified via flash chromatography (5:1→3:1 hexanes/ EtOAc) to afford 5a-(benzyloxy)-9a-ethyl-4,5,5a,6,9,9a-hexahydro-1H-benzo[d][1,2,3]oxathiazepine 2,2-dioxide (**100**) as a white amorphous solid (7 mg, 77 %); **R_f** 0.33 (3:1 hexanes/EtOAc); **IR** (thin film, cm⁻¹) 3357, 3031, 2922, 1356, 1180; **¹H NMR** (CDCl₃, 600 MHz) δ 7.36-7.26 (m, 5H), 5.69 (bs, 1H), 5.52 (bs, 1H), 5.05 (s, 1H), 5.55 (t, 1H, *J* = 12.4 Hz), 4.43 (d, 1H, *J* = 10.5 Hz), 4.31 (d, 1H, *J* = 10.5 Hz), 4.13 (bd, 1H, *J* = 12.8 Hz), 2.54 (dd, 1H, *J* = 19.7, 4.1 Hz), 2.32 (dd, 1H, *J* = 17.9, 5.5 Hz), 2.22-2.05 (m, 5H), 1.55 (sext, 2H, *J* = 7.3 Hz), 1.07 (t, 3H, *J* = 6.9 Hz); **¹³C NMR** (CDCl₃, 150 MHz) δ 138.0, 128.8, 128.1, 127.6, 125.8, 122.2, 79.3, 64.5, 64.2, 63.8, 33.7, 32.7, 21.7, 21.3, 8.6; **HRMS** (-APCI) calculated for C₁₇H₂₂NO₄S 335.1275, found 336.1274 [M-H]⁻.

Key nOe correlations for compound 100





1-(benzyloxy)-6-ethyl-6-(2,2,2-trifluoroacetamido)cyclohex-3-en-1-yl)ethyl 2,2,2-trifluoroacetate (111). To a solution of 5a-(benzyloxy)-9a-ethyl-4,5,5a,6,9,9a-hexahydro-1H-benzo[d][1,2,3]oxathiazepine 2,2-dioxide (**100**) (21 mg, 0.06 mmol) in pyridine (.10 mL) was added trifluoroacetic anhydride (0.17 mL, 1.2 mmol) at 0 °C. The resulting solution was warmed to ambient temperature and stirred 50 h. After this time the reaction was diluted with Et₂O (7 mL) and quenched with H₂O (5 mL). The resulting biphasic mixture was transferred to a separatory funnel and extracted with Et₂O (2 x 10 mL). The combined organic extracts were dried over MgSO₄ and concentrated *in vacuo*. Flash chromatography (3:1→1:1 hexanes/ EtOAc) afforded 1-(benzyloxy)-6-ethyl-6-(2,2,2-trifluoroacetamido)cyclohex-3-en-1-yl)ethyl 2,2,2-trifluoroacetate (**111**) as a colorless oil (12 mg, 41 %); **R_f** 0.20 (3:1 hexanes/EtOAc); **IR** (thin film, cm⁻¹) 3395, 2925, 1786, 1731, 1221, 1154; ; **¹H NMR** (CDCl₃, 600 MHz) δ 7.41-7.27 (m, 5H), 6.50 (bs, 1H), 5.69 (dd, 2H, *J* = 12.0, 9.8), 4.60-4.49 (m, 4H), 3.44 (bd, 1H, *J* = 12.1 Hz), 2.55 (d, 1H, *J* = 14.0 Hz), 2.45 (d, 1H, *J* = 14.1 Hz), 2.29-2.14 (m, 4H), 1.65 (sext, 1H, *J* = 6.2 Hz), 0.97 (t, 3H, *J* = 6.2 Hz); **¹³C NMR** (CDCl₃, 150 MHz) δ 138.0, 128.8, 128.1, 127.6, 125.8, 122.2, 79.3, 64.5, 64.2, 63.8, 33.7, 32.7, 21.7, 21.3, 8.6; **¹³C NMR** (CDCl₃, 150 MHz) δ 150.6, 137.9, 128.9, 128.2, 127.4, 125.5, 123.1, 79.6, 65.7, 64.9, 64.1, 32.5, 32.3, 31.3, 29.9, 26.6, 8.7; **HRMS** (+ESI) calculated for C₂₁H₂₄F₆NO₄ 468.1610, found 468.1683 [M+H]⁺.

References

- (1) For reviews, see: (a) Snieckus, V. "The Securinega Alkaloids" in *The Alkaloids*, ed. R. H. F. Manske, 1975, vol. 14, pp. 425. (b) Beutler, J. A.; Brubaker, A. N. *Drugs Fut.* **1987**, *12*, 957. (c) Weinreb, S. M. *Nat. Prod Rep.* **2009**, *26*, 758.
- (2) Syntheses of the Securinega alkaloids: (a) Liu, P.; Hong, S.; Weinreb, S. M. *J. Am. Chem. Soc.* **2008**, *130*, 7562. (b) Alibes, R.; Bayón, P.; de March, P.; Figueredo, M.; Font, J.; Garcia-Garcia, E.; Gonzalez-Galvez, D. *Org. Lett.* **2005**, *7*, 5107. (c) Honda, T.; Namiki, H.; Watanabe, M.; Mizutani, M. *Tetrahedron Lett.* **2004**, *45*, 5211. (d) Honda, T.; Namiki, H.; Kaneda, K.; Mizutani, H. *Org. Lett.* **2004**, *6*, 87. (e) Alibes, R.; Ballbe, E.; Busque, F.; de March, P.; Elias, L.; Figueredo, M.; Font, J. *Org. Lett.* **2004**, *6*, 1813. (f) Kammler, R.; Polborn, K.; Wanner, K. T. *Tetrahedron* **2003**, *59*, 3359. (g) Honda, T.; Namiki, H.; Kudoh, M.; Nagase, H.; Mizutani, H. *Heterocycles* **2003**, *59*, 169. (h) Liras, S.; Davoren, J. E.; Bordner, J. *Org. Lett.* **2001**, *3*, 70. (i) Han, G.; LaPorte, M. G.; Folmer, J. J.; Werner, K. M.; Weinreb, S. M. *Angew. Chem. Int. Ed.* **2000**, *39*, 237. (j) Han, J.; LaPorte, M. G.; Folmer, J. J.; Werner, K. M.; Weinreb, S. M. *J. Org. Chem.* **2000**, *65*, 6293. (k) Honda, T.; Namiki, H.; Kudoh, M.; Watanabe, N.; Nagase, H.; Mizutani, H. *Tetrahedron Lett.* **2000**, *41*, 5927. (l) Magnus, P.; Rodríguez-López, J.; Mulholland, K.; Matthews, I. *Tetrahedron* **1993**, *49*, 8059. (m) Magnus, P.; Rodríguez-López, J.; Mulholland, K.; Matthews, I. *J. Am. Chem. Soc.* **1992**, *114*, 382. (n) Jacobi, P. A.; Blum, C. A.; DeSimone, R. W.; Udodong, U. E. S. *J. Am. Chem. Soc.* **1991**, *113*, 5384. (o) Jacobi, P. A.; Blum, C. A.; DeSimone, R. W.; Udodong, U. E. S. *Tetrahedron Lett.* **1989**, *30*, 7173. (p) Heathcock, C. H.; von Geldern, T. W. *Heterocycles* **1987**, *25*, 75. (q) Horii, Z.; Hanaoka, M.; Yamawaki, Y.; Tamura, Y.; Saito, S.; Shigematsu, N.;

-
- Kotera, K.; Yoshikawa, H.; Sato, Y.; Nakai, H.; Sugimoto, N. *Tetrahedron* **1967**, *23*, 1165. (r) Saito, S.; Yoshikawa, H., Sato, Y.; Nakai, H.; Sugimoto, N.; Horii, Z.; Hanaoka, N.; Tamura, Y. *Chem. Pharm. Bull.* **1966**, *14*, 313
- (3) Imado, S.; Shiro, M.; Horii, Z. *Chem. Pharm. Bull.* **1965**, *13*, 643 and references cited.
- (4) (a) A. Ohsaki, Y. Kobayashi, K. Yoneda, A. Kishida and H. Ishiyama, *J. Nat. Prod.* **2007**, *70*, 2003. (b) For a more recent X-ray structure of securinine, see: Luger, P.; Weber, M.; Dung, N. X.; Ky, P. T.; Long, P. K. *Acta Crystallogr. Sect. C: Cryst. Struct. Commun.* **1995**, *C51*, 127.
- (5) For the isolation of virosecurinine, see: (a) Nakano, T.; Yang, T. H.; Terao, S. *Tetrahedron* **1963**, *19*, 609; For the isolation of viroallosecurinine, see: (b) Saito, S.; Iwamoto, T.; Tanaka, T.; Matsumura, C.; Sugimoto, N.; Horii, Z.; Tamura, Y. *Chem. Ind.* **1964**, *28*, 1263.
- (6) (a) Weenen, H.; Nkunya, M. H. H.; Bray, D. H.; Mwasumbi, L. B.; Kinabo, L. S.; Kilimali, V. A.; Wijnberg, J. B. *Planta Med.* **1990**, *56*, 371. (b) Mensah, J. L.; Lagarde, I.; Ceschin, C.; Michel, G.; Gleye, J.; Fouraste, I. *J. Ethnopharmacol.* **1990**, *28*, 129. (c) Tatematsu, H.; Mori, M.; Yang, T.-H.; Chang, J.-J.; Lee, T. T.-Y. ; Lee, K.-H. *J. Pharm. Sci.*, **1991**, *80*, 325. (d) Dong, N. Z.; Gu, Z. L.; Chou, W. H.; Kwok, C. Y. *Acta Pharmacol. Sinica* **1999**, *20*, 267.
- (7) Leduc, A. B.; Kerr, M. A. *Angew. Chem. Int. Ed.* **2008**, *47*, 7945.
- (8) Jackson, S. K.; Karadeolian, A.; Driega, A. B.; Kerr, M. A. *J. Am. Chem. Soc.* **2008**, *130*, 4196.
- (9) (a) Krapcho, A. P.; Glynn, G. A.; Grenon, B. J. *Tetrahedron Lett.* **1967**, *8*, 215.

-
- (b) Krapcho, A. P.; Mundy, B. P. *Tetrahedron* **1970**, *26*, 5437.
- (10) Grieco, P. A.; Gilman, S.; Nishizawa, M. *J. Org. Chem.* **1976**, *41*, 1485.
- (11) Davis, F. A.; Lamendola, J.; Nadir, U.; Lluger, E. W.; Sedergran, T. C.; Panunto, T. W.; Billmers, R.; Jenkins, R.; Turchi, I. J.; Watson, W. H.; Chen, J. S.; Kimura, M. *J. Am. Chem. Soc.* **1980**, *102*, 2000.
- (12) For a review see: (a) Meléndez R. E. Lubell, W. D. *Tetrahedron* **2003**, *59*, 2581.
- (b) Atfani, M.; Wei, L.; Lubell, W. D. *Org. Lett.* **2001**, *3*, 2965.
- (13) (a) Thornton, A. R.; Blakey, S. B. *J. Am. Chem. Soc.* **2008**, *130*, 5020. (b) Thornton, A. R.; Martin, V. I.; Blakey, S. B. *J. Am. Chem. Soc.* **2009**, *131*, 2434.
- (14) Sato, Y.; Aso, Y.; Shindo, M. *Tetrahedron Lett.* **2009**, *50*, 28, 4164.
- (15) Paquette, L. A.; Begland, R. W. *J. Am. Chem. Soc.* **1968**, *90*, 19, 5159.
- (16) Panne, P.; Fox, J. M. *J. Am. Chem. Soc.* **2007**, *129*, 22.
- (17) Guthikonda, K.; Du Bois, J. *J. Am. Chem. Soc.* **2002**, *124*, 13672.
- (18) Yamaguchi, M.; Hirao, I. *Tetrahedron Lett.* **1983**, *24*, 391.
- (19) Hurley, P. B.; Dake, G. R. *J. Org. Chem.* **2008**, *73*, (11), 4131.
- (20) Cainelli, G.; Giacomini, D.; Galletti, P. *Chem. Commun.* **1999**, 567.
- (21) Stoll, A. H.; Blakey, S. B. *J. Am. Chem. Soc.* **2010**, *132* (7), 2108.
- (22) Hoye, T. R.; Vyvyan, J. R. *J. Org. Chem.* **1995**, *60*, (13), 4184.

Appendix:

Copper-Catalyzed Olefin Aminoacetoxylation

A.1. Background and Previous Studies on Olefin Aminoacetoxylation

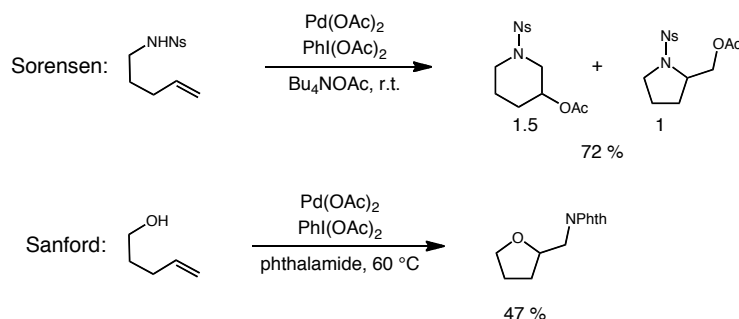
A.1.1. Introduction and Background

Olefin difunctionalization represents a powerful class of reactions with significant synthetic potential. These reactions have received a considerable amount of attention due to their ability to install useful functional handles into easily accessible olefin-containing substrates.^{1,2} This is exemplified by the osmium-catalyzed asymmetric olefin dihydroxylation reaction developed by Sharpless and co-workers.^{1a} This reaction has become commonplace among the synthetic community due to its ability to construct important dioxygenated stereocenters from simple alkene starting materials. In addition to this reaction, Sharpless has extended this methodology to the formation of 1,2-aminoxygenated stereocenters through the use of a similar osmium-catalyzed asymmetric olefin aminohydroxylation reaction.³ Again, because of this reaction's ability to generate an immensely important structural motif from simple olefin-containing starting materials, it has remained useful to the synthetic community.

However, while the Os-catalyzed dihydroxylation reaction remains prominent, the analogous aminohydroxylation reaction has not experienced this same distinction. While powerful, this reaction still suffers from issues of regioselectivity as well catalyst toxicity due to the use of osmium. Because of this, numerous reports for the amino-oxygenation of olefins have been reported in recent years.⁴ In an attempt to avoid the use of toxic Os-based reagents, recent reports have focused on the use of more environmentally benign metals, such as palladium and copper.

Recent advances in the area of 1,2-amino-alcohol synthesis include reports by Sorensen, Stahl, and Sanford for the hypervalent iodine induced palladium-catalyzed intramolecular variants of this transformation (Scheme A.1).^{4e,f,g} These reactions allow for the construction of functionalized furans and pyrrolidines from simple alcohol- or amino-tethered alkene starting materials. While these advances are significant, there remain limitations in each methodology. For example, in the case of Sorensen's work there remain issues of regioselectivity, and often times a mixture of the corresponding piperidine and pyrrolidine regioisomers are formed. Sanford's work suffers from a practicality standpoint, with the use of the nucleophile, phthalimide, as the limiting reagent. In addition, often times cyclization must be induced by the use of substrates which take advantage of the Thorpe-Ingold effect, resulting in this reaction's limited applicability to synthesis.

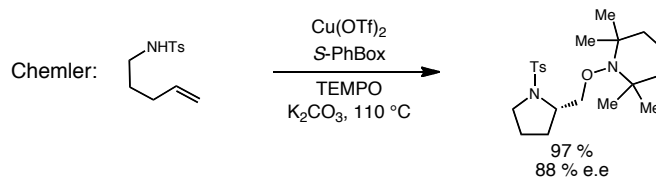
Scheme A.1. Previously developed Pd-catalyzed olefin aminooxygenation methodologies.



In addition to these Pd-catalyzed methods, copper-based systems for this transformation have also been reported.⁵ The work of Chemler and co-workers has made considerable headway in the development and application of these reactions, establishing

both diastereo- and enantioselective protocols (Scheme A.2). However, while powerful, these reactions still suffer from the need for elevated temperatures to effect cyclization.

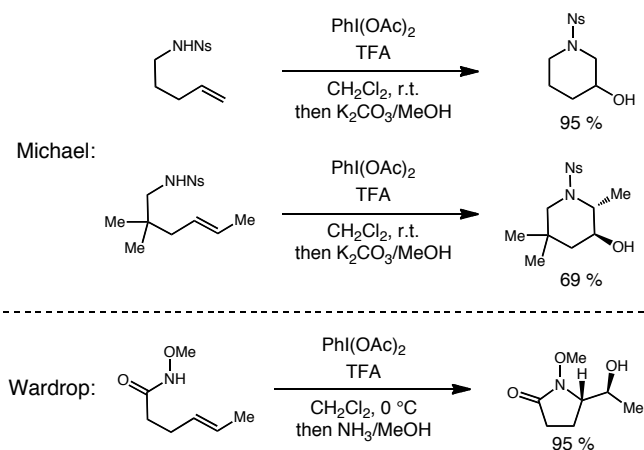
Scheme A.2. Chemler's Cu-catalyzed olefin aminooxygenation methodology.



In addition to the previously mentioned limitations, all of these methods lack the ability to cyclize 1,2-disubstituted olefins. In fact, in a recent publication from the Stahl group,^{4f} it was stated that “*in general, internal olefins appear to be ineffective substrates*”, indicating that such olefins are beyond the scope of these methodologies. Additionally, all of the previously mentioned work only allows for the synthesis of pyrrolidine structures, with no such methods for the selective construction of the regioisomeric piperidine products. These shortcomings have motivated our efforts to develop an intramolecular aminooxygenation reaction that allows for the selective production of functionalized piperidines.

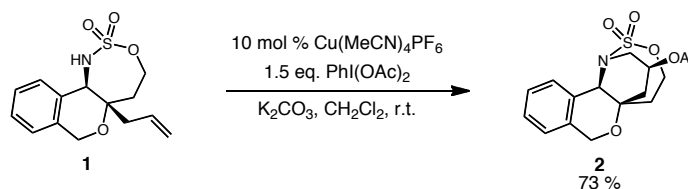
While pursuing this goal, reports from both the Michael and Wardrop groups showed that this transformation could be accomplished in a metal-free reaction manifold (Scheme A.3).^{6,7} However, in both cases strongly acidic conditions must be employed to attain useful yields of the desired cyclization adducts. Thus, both groups utilize stoichiometric amounts of TFA to promote cyclization.

Scheme A.3. Metal-free aminooxygenation reactions for the synthesis of functionalized piperidines.

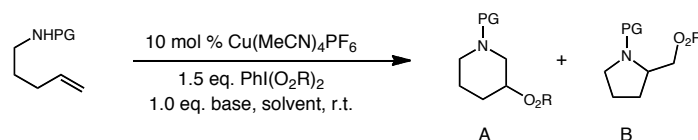


A.1.2. Previous Studies Within the Blakey Group

While pursuing the development of new catalysts for our metallonitrene/alkyne cascade reaction methodology, Dr. Armin Stoll discovered that oxathiazepane **1** could be converted to oxygenated piperidine **2** in 73 % when exposed to 10 mol % $\text{Cu}(\text{MeCN})_4\text{PF}_6$, 1.5 equivalents $\text{PhI}(\text{OAc})_2$, 1.1 equivalents of K_2CO_3 in CH_2Cl_2 at ambient temperature (Scheme A.4). This aminooxygenation reaction resulted in the exclusive formation of piperidine cyclization adduct **2**, and thus stood in contrast to previously developed methods which almost exclusively result in pyrrolidine formation. This realization prompted the further investigation of this new reaction to determine if this was simply due the rigid nature of bicyclic compound **1**, or if this was in fact a general feature of this reaction.

Scheme A.4. Cu(I)-catalyzed olefin aminoacetoxylation reaction discovery.

Subsequent efforts by Danny Mancheno established that this selectivity for piperidine formation is in fact a general feature of this transformation (Table A.1). In addition, his work has established a general reaction protocol that we have been able to apply to a wide range of olefin-containing substrates (*vide infra*). His studies determined that while other electron-withdrawing *N*-substituents are possible, highest yields were observed when the 4-Ns protecting group was utilized (Entries 1-4). Additionally, it was found that a range of carboxylate nucleophiles may be incorporated into the piperidine product, with acetate, pivaloate, and dimethylphenyl acetate all effectively integrated (Entries 1, 5, and 6). The use of CH₂Cl₂ as solvent and the K₂CO₃ as a base provided the highest yields.

Table A.1. Optimization studies for Cu(I)-catalyzed olefin aminoacetoxylation.

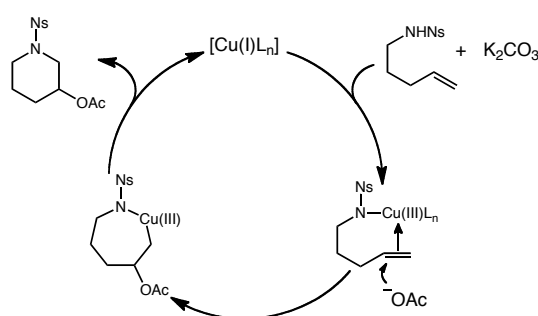
entry	PG	R	Solvent	Base	% yield	A:B
1	Ns	OAc	CH ₂ Cl ₂	K ₂ CO ₃	88	9:1
2	Ts	OAc	CH ₂ Cl ₂	K ₂ CO ₃	47	8:2
3	Ac	OAc	CH ₂ Cl ₂	K ₂ CO ₃	--	--
4	Boc	OAc	CH ₂ Cl ₂	K ₂ CO ₃	--	--
5	Ns	OPiv	CH ₂ Cl ₂	K ₂ CO ₃	73	9:1
6	Ns	OCMe ₂ Ph	CH ₂ Cl ₂	K ₂ CO ₃	70	9:1
7	Ns	OAc	THF	K ₂ CO ₃	--	--
8	Ns	OAc	C ₆ H ₆	K ₂ CO ₃	29	95:5
9	Ns	OAc	CF ₃ C ₆ H ₅	K ₂ CO ₃	72	92:8
10	Ns	OAc	CH ₃ C ₆ H ₅	K ₂ CO ₃	18	70:30
11	Ns	OAc	MeCN	K ₂ CO ₃	6	--
12	Ns	OAc	CH ₂ Cl ₂	Bu ₄ NOAc	34	9:1
13	Ns	OAc	CH ₂ Cl ₂	Cs ₂ CO ₃	72	9:1
14	Ns	OAc	CH ₂ Cl ₂	KO ^t Bu	43	9:1

These studies led to the development of general reaction conditions that could then be applied to a range of simple γ -aminoolefins. Importantly, these reactions lead to formation of piperidine cyclization adducts with good selectivity under mild reaction conditions. These features distinguish this method from previously discussed Pd- and Cu-catalyzed amino-oxygenation protocols, and provide complementary reaction conditions to the work of Michael and Wardrop.

We believe that this difference in regioselectivity may be explained by an alternate mechanism, consistent with our results from the ensuing study (*vide infra*). Thus, we propose a mechanism in which the Cu-catalyst and the *N*-Ns amine combine under the oxidative reaction conditions to form an electrophilic Cu(III) amido species.

Coordination of the tethered olefin to the Cu-center activates it for intermolecular addition by acetate anion at the olefinic position best able to stabilize the build-up of a positive charge. The resulting cyclic Cu(III) species may then undergo reductive elimination to yield the observed aminoacetoxylation product, in turn regenerating a Cu(I) species.

Figure A.1. Proposed mechanism for Cu(I)-catalyzed intramolecular aminoacetoxylation.



In conjunction with the efforts of Danny Mancheno and Dr. Armin Stoll, I began the synthesis and examination of more complex γ -aminoolefins to determine the scope of, and to help establish the mechanism for, this new olefin aminoacetoxylation reaction.⁸

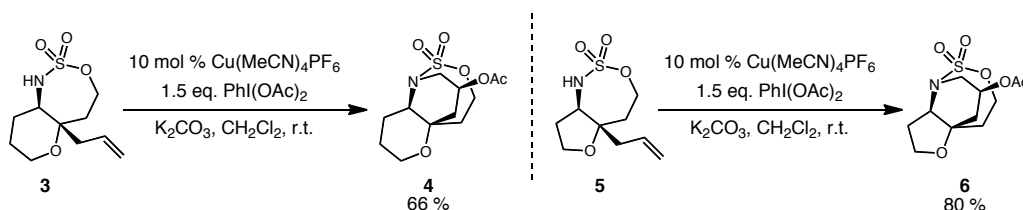
A.2. Results and Discussion

A.2.1. Intramolecular Olefin Aminoacetoxylation

Motivated by this reaction's ability to cyclize oxathiazepane products resulting from our metallonitrene/alkyne cascade reaction chemistry (Scheme A.4), my studies began by examining the use of other such bicyclic oxathiazepane systems (Scheme A.5).

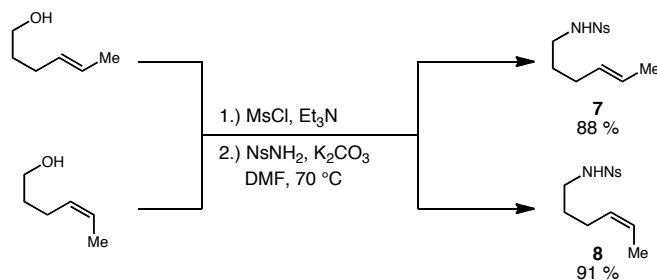
Thus, when both 6,7- and 5,7-bicyclic oxathiazepanes **3** and **5** were exposed to the previously developed general reaction conditions, we observed the formation of the corresponding aminoacetoxylation products **4** and **6** in 66 % and 80 % yield as single diastereomers determined by ^1H NMR. The relative stereochemistry of these products were assigned by analogy to Dr. Stoll's cyclization adduct **2**, determined by X-ray crystallography.

Scheme A.5. Intramolecular aminoacetoxylation of metallonitrene/alkyne cyclization adducts **3** and **5**.



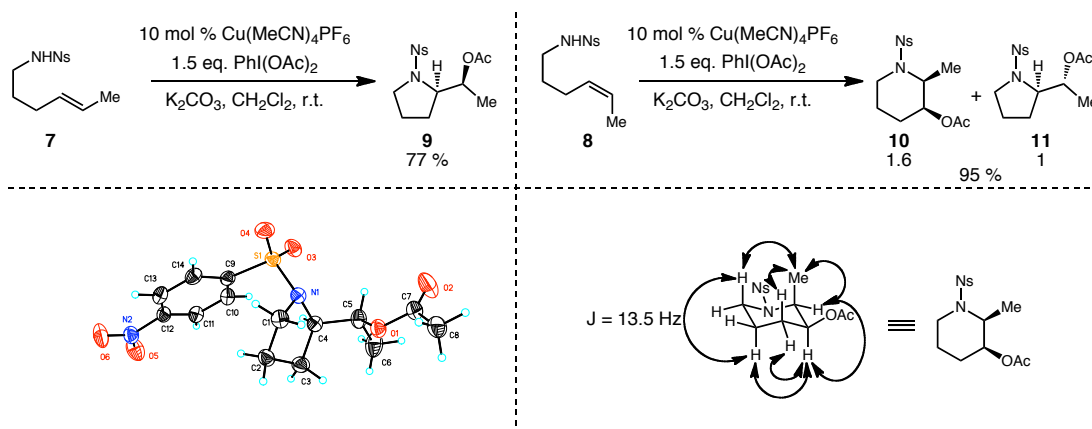
Following these studies, we next examined the possibility of utilizing 1,2-disubstituted olefins for this aminoacetoxylation reaction. We felt that this feature could potentially distinguish this reaction from previously developed aminoxygenation methods, and in turn provide a distinct advantage. Thus, the synthesis of a series of 1,2-disubstituted olefins was undertaken. First, *cis*- and *trans*-Me *N*-Ns substituted γ -aminoolefins **7** and **8** were constructed from their corresponding commercially available alcohols through a one-pot, two-step procedure involving mesylation followed by displacement with 4-NsNH₂, providing **7** and **8** in 88 % and 91 % yield respectively (Scheme A.6).

Scheme A.6. Synthesis of 1,2-disubstituted γ -aminoolefins **7** and **8**.



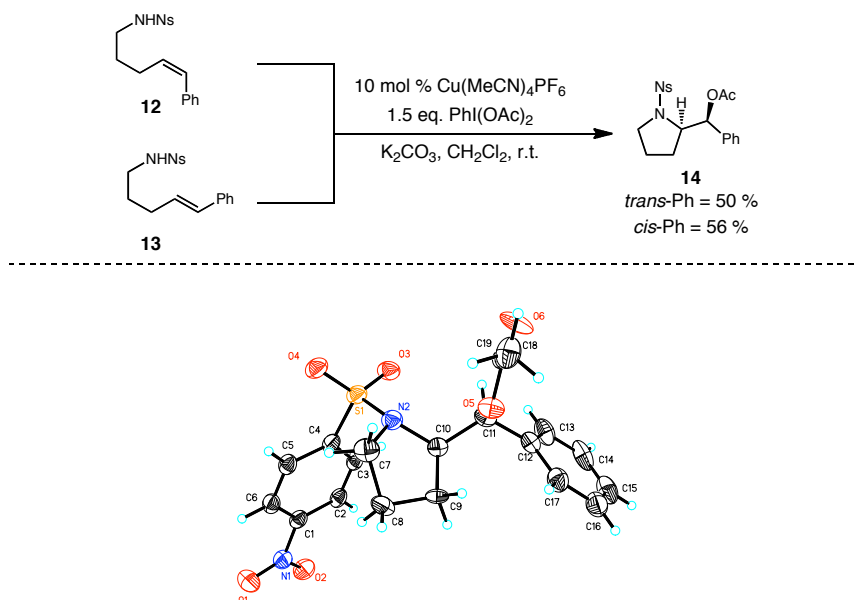
When *trans*-Me γ -aminoolefin **7** was exposed to our general aminoacetoxylation reaction conditions we observe complete consumption of starting material with 30 minutes, leading to the formation of pyrrolidine **9** in 77 % yield as a single diastereomer, determined by X-ray crystallography (Scheme A.7). However, when *cis*-Me γ -aminoolefin **8** was exposed to the same reaction conditions we isolate a mixture of piperidine **10** and pyrrolidine **11** in 95 % overall yield in a 1.6:1 ratio determined by ^1H NMR. The relative stereochemistry of piperidine **10** was determined by nOe NMR experiments, while the relative stereochemistry of pyrrolidine **11** was determined by comparison of spectral data obtained from its diastereomer, pyrrolidine **9**.

Scheme A.7. Cyclization of 1,2-disubstituted γ -aminoolefins **7** and **8**.



This reaction's ability to cyclize traditionally less reactive 1,2-disubstituted olefins provides a distinct advantage, and stands in contrast to, previously developed methods. Additionally, these reactions provide evidence for our proposed mechanism. For example, the cyclizations of both **7** and **8** are diastereoselective and result from the overall *anti* addition of the amine and acetate nucleophiles. This is consistent with the proposed bimolecular addition of acetate anion to the Cu(III)-olefin complex (Figure A.1). The explanation for the complete reversal in regioselectivity for the cyclization of *trans*-olefin **7**, versus the formation of a mixture of regioisomers with *cis*-olefin **8**, is not apparent at this point. However, because there is no obvious electronic bias (positive charge stabilization) within these dialkyl substituted systems, the most likely explanation is due to subtle geometric factors that cannot be predicted at this time. To determine if these features are general for the cyclization of 1,2-disubstituted olefins, we next investigated the cyclization of electronically biased systems.

The cyclization of *cis*- and *trans*-phenyl γ -aminoolefins **12** and **13** was thus pursued (Scheme A.8). We observe that both olefins **12** and **13** converge upon a single pyrrolidine product **14** when exposed to our general reaction conditions. The relative stereochemistry of **14** was confirmed by X-ray crystallography.

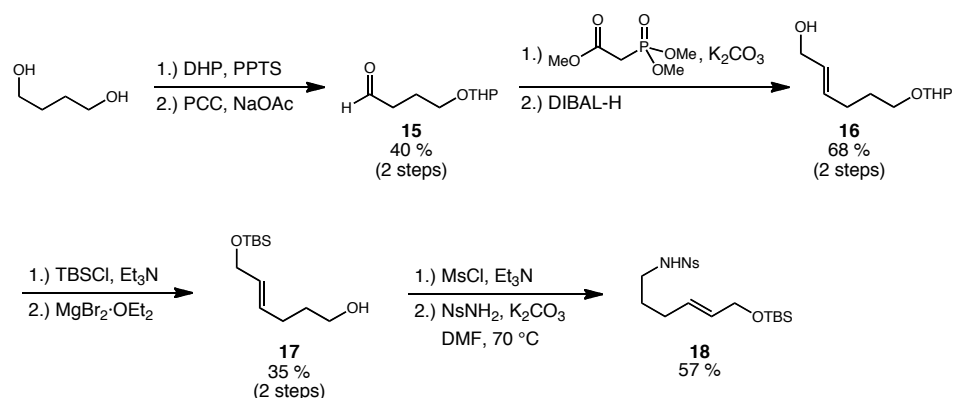
Scheme A.8. Cyclization of *cis*- and *trans*-phenyl γ -aminoolefins **12** and **13**.

With these electronically biased systems we now see that the addition of the acetate nucleophile occurs at the position which is most able to stabilize the ensuing positive charge (benzylic). The fact that both geometric isomers converge to a single product may be explained by the formation of discrete carbocation intermediate, thereby leading to a loss in stereochemical bias from the starting olefin.

Lastly, to display the versatility of this new reaction we looked to examine 1,2-disubstituted olefins with more complex functionalities. Thus, we chose to pursue TBS-protected allylic alcohol γ -aminoolefin **18**. This substrate was constructed in a straight-forward manner according to Scheme A.9. Thus, mono THP protection of 1,4-butane diol was followed immediately by PCC oxidation to give aldehyde **15** in 40 % yield over two steps. Subsequent Horner-Wadsworth-Emmons olefination was then followed by reduction of the resulting methyl ester to give allylic alcohol **16** in 68 % yield over two steps. To complete the synthesis of **18** TBS protection was followed by

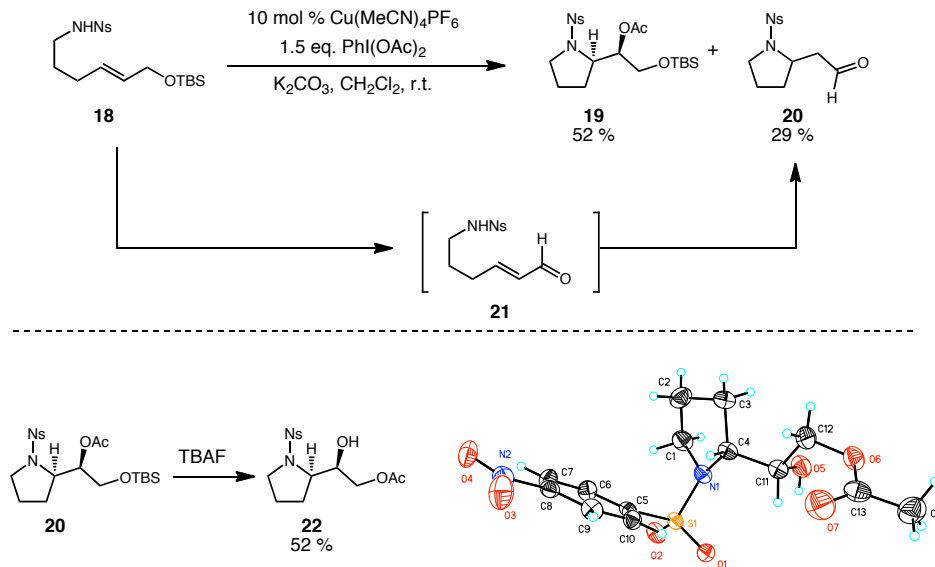
THP removal to give **17** in 35 % yield over two steps. Lastly, one-pot mesylation and S_N2 displacement furnished γ -aminoolefin **18** in 57 % yield.

Scheme A.9. Synthesis of TBS-protected γ -aminoolefin **18**.



Interestingly, the cyclization of TBS-protected γ -aminoolefin **18** resulted in the formation of pyrrolidine **19** and aldehyde **20** in 52 % and 29 % respectively. The relative stereochemistry of **19** was determined by X-ray crystallography following TBS removal and subsequent acetate migration. The formation of aldehyde **20** could potentially arise from oxidative removal of the silyl-protecting group to give α,β -unsaturated aldehyde **21**, and under the mildly basic reaction conditions this intermediate may then undergo intramolecular conjugate addition to give the observed aldehyde **20**.

Scheme A.10. Cyclization of TBS-protected γ -aminoolefin **18**.



A.3. Conclusions

In conclusion we have developed a new Cu-catalyzed olefin aminoacetoxylation reaction. This transformation provides complimentary reaction conditions to those recently disclosed by Michael and Wardrop for the cyclization of various γ -aminoolefins. Importantly, this reaction is able to induce cyclization in traditionally less reactive 1,2-disubstituted olefins under very mild reaction conditions. Based on our mechanistic hypothesis, future work in our group will focus on the use of alternate nucleophiles towards the development of multiple amino-functionalization reactions.

Experimental Procedures and Compound Characterization

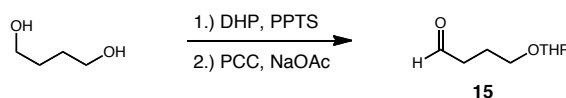
General Information.

^1H and ^{13}C NMR spectra were recorded on a Varian Inova 600 spectrometer (600 MHz ^1H , 150 MHz ^{13}C), a Varian Unity plus 600 (600 MHz ^1H , 150 MHz ^{13}C) or a Varian Inova 400 spectrometer (400 MHz ^1H , 100 MHz ^{13}C) at room temperature in CDCl_3 with internal CHCl_3 as the reference (7.27 ppm for ^1H and 77.23 ppm for ^{13}C) or C_6D_6 (7.16 ppm for ^1H and 128.39 ppm for ^{13}C). Chemical shifts (δ values) were reported in parts per million (ppm) and coupling constants (J values) in Hz. Multiplicity is indicated using the following abbreviations: s = singlet, d = doublet, t = triplet, q = quartet, qn = quintet, hep = heptet, m = multiplet, b = broad signal). Infrared (IR) spectra were recorded using Thermo Electron Corporation Nicolet 380 FT-IR spectrometer. High resolution mass spectra were obtained using a Thermo Electron Corporation Finigan LTQFTMS (at the Mass Spectrometry Facility, Emory University). We acknowledge the use of shared instrumentation provided by grants from the NIH and the NSF. Melting points (mp) were taken using a Fisher-Johns melting point apparatus and are not corrected. Analytical thin layer chromatography (TLC) was performed on precoated glass backed EMD 0.25 mm silica gel 60 plates. Visualization was accomplished with UV light, ethanolic anisaldehyde, phosphomolybdic acid or CAM stain (Verghn's), followed by heating. Flash column chromatography was carried out using EMD Geduran® silica gel 60 (40-63 μm) or Fluka® aluminum oxide (0.05-0.15 mm); pH 7.0.

All reactions were conducted with anhydrous solvents in oven dried or flame-dried and argon-charged glassware. Anhydrous solvents were purified by passage

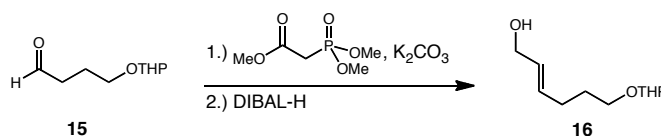
through activated alumina using a *Glass Contours* solvent purification system unless otherwise noted. Solvents used in workup, extraction and column chromatography were used as received from commercial suppliers without prior purification. All reagents were purchased from Sigma-Aldrich and used as received unless otherwise noted. (Diacetoxyiodo)benzene was dried at 98 °C under vacuum (0.02 mmHg) for 12 hours prior to use.

Preparation of Olefinic Alcohols



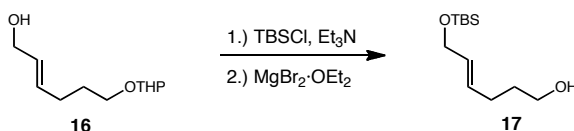
4-((tetrahydro-2H-pyran-2-yl)oxy)butanal (15). To a solution of 3,4-dihydro-2H-pyran (7.74 mL, 85.4 mmol) and PPTS (5.86 g, 23.3 mmol) in CH_2Cl_2 (150 mL) was added 1,4-butanediol (7.0 g, 77.7 mmol) in CH_2Cl_2 (150 mL) at ambient temperature. The resulting mixture was stirred 2 h. at which point H_2O (400 mL) was added. The biphasic mixture was extracted with CH_2Cl_2 (2 x 200 mL) and the combined organic extracts were washed with brine (600 mL) and dried over MgSO_4 . Concentration *in vacuo* provided a viscous oil that was then dissolved in CH_2Cl_2 (200 mL), equipped with a magnetic stir bar, and cooled to 0 °C. To this solution was added NaOAc (9.55 g, 116.5 mmol) and pyridinium chlorochromate (25.11 g, 116.5 mmol) in single portions as solids. The resulting orange slurry was warmed to ambient temperature and stirred 4 h. The mixture was then diluted with Et_2O (500 mL) and stirred 30 min. The resulting mixture was then decanted and filtered through a pad of Celite. The filtrate was concentrated *in*

vacuo and purified by flash column chromatography (5:1→3:1 Hexanes/EtOAc) affording 4-((tetrahydro-2H-pyran-2-yl)oxy)butanal (**15**) (5.39 g, 40 %) as a clear oil. **IR** (thin film, cm^{-1}) 2955, 2927, 2855, 1742, 1473, 1234, 1163, 838; **$^1\text{H NMR}$** (CDCl_3 , 400 MHz) δ 9.80 (t, 1H, $J = 1.8$ Hz), 4.58 (t, 1H, $J = 3.1$ Hz), 3.90-3.76 (m, 2H), 3.54-3.48 (m, 1H), 3.41 (dt, 1H, $J = 9.8, 6.1$ Hz), 2.55 (tt, 1H, $J = 7.0, 1.8$ Hz), 1.96 (qn, 2H, 6.4 Hz), 1.83-1.66 (m, 3H), 1.63-1.50 (m, 4H); **$^{13}\text{C NMR}$** (CDCl_3 , 100 MHz) δ 202.7, 99.1, 66.6, 62.5, 41.3, 30.8, 25.6, 22.9, 19.7; **HRMS** (+APCI) calculated for $\text{C}_9\text{H}_{17}\text{O}_3$ 173.1178, found 173.1172 $[\text{M}+\text{H}]^+$.



(E)-6-((tetrahydro-2H-pyran-2-yl)oxy)hex-2-en-1-ol (16). 4-((Tetrahydro-2H-pyran-2-yl)oxy)butanal (**15**) (5.39 g, 31.3 mmol) was added to a solution of K_2CO_3 (8.65 g, 62.6 mmol) and trimethylphosphorylacetate (5.42 mL, 37.6 mmol) in H_2O (6.24 mL). The mixture was stirred 24 h. at ambient temperature. After this time it was diluted with H_2O (60 mL) and extracted with CH_2Cl_2 (2 x 45 mL). The combined organic extracts were washed with brine (70 mL), dried with MgSO_4 and concentrated *in vacuo* affording a viscous oil. This oil was immediately dissolved in CH_2Cl_2 (157 mL), equipped with a magnetic stir bar, and cooled to -78 °C, diisobutylaluminum hydride (68.8 mL, 1 M solution in CH_2Cl_2) was then added slowly. This solution was stirred at -78 °C for 3 h. at which point it was poured into an Erlenmeyer flask containing Et_2O (600 mL). To this dilute solution was added potassium sodium tartrate 4-hydrate (25 mL, sat. aq. solution)

and stirred vigorously for 3 h. The organic layer was then decanted and the aqueous layer was extracted with Et₂O (2 x 40 mL). The combined organic extracts were washed with brine (200 mL), dried over MgSO₄, and concentrated *in vacuo*. The resulting oil was purified by flash column chromatography (3:1 Hexanes/EtOAc → 100 % EtOAc) to afford (*E*)-6-((tetrahydro-2H-pyran-2-yl)oxy)hex-2-en-1-ol (**16**) (4.29 g, 68 %) as a clear oil. **IR** (thin film, cm⁻¹) 3392, 2939, 2868, 1119, 1022; **¹H NMR** (CDCl₃, 400 MHz) δ 5.74-5.65 (m, 2H), 4.58 (t, 1H, *J* = 3.7 Hz), 4.10 (t, 1H, *J* = 5.0), 3.89-3.85 (m, 1H), 3.75 (dt, 1H, *J* = 9.6, 6.4 Hz), 3.52-3.49 (m, 1H), 3.40 (dt, 1H, *J* = 9.6, 6.4 Hz), 2.17-2.14 (m, 2H), 1.86-1.81 (m, 1H), 1.74-1.65 (m, 3H), 1.61-1.52 (m, 5H), 1.33-1.31 (m, 1H); **¹³C NMR** (CDCl₃, 100 MHz) δ 132.8, 129.6, 99.1, 67.1, 63.9, 62.6, 30.9, 29.3, 29.1, 25.7, 19.9; **HRMS** (+APCI) calculated for C₁₁H₂₁O₃ 201.1491, found 201.1485 [M+H]⁺.



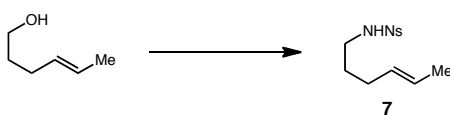
(*E*)-6-(tert-butyldimethylsilyloxy)hex-4-en-1-ol (17). (*E*)-6-((tetrahydro-2H-pyran-2-yl)oxy)hex-2-en-1-ol (**16**) (2.14 g, 10.7 mmol) in THF (3.45 mL) was added to a solution of TBSCl (2.39 mL, 12.8 mmol) and imidazole (1.46 g, 21.4 mmol) in THF (50.0 mL). The mixture was stirred 1.5 h. at ambient temperature. After this time it was quenched with H₂O (60 mL) and extracted with Et₂O (2 x 45 mL). The combined organic extracts were washed with brine (75 mL), dried with MgSO₄ and concentrated *in vacuo* to afford a viscous oil. This oil was immediately dissolved in Et₂O (71.3 mL), equipped with a magnetic stir bar, and cooled to 0 °C, MgBr₂·OEt₂ (11.04 g, 42.7 mmol) in Et₂O (10 mL)

was then added slowly. This solution was warmed to ambient temperature and stirred overnight at which point it was quenched with H₂O (50 mL) and extracted with CH₂Cl₂ (2 x 40 mL). The combined organic extracts were washed with a saturated aqueous solution of NH₄Cl (100 mL), dried over MgSO₄, and concentrated *in vacuo* affording a clear oil that was purified by flash column chromatography (4:1 Hexanes/EtOAc→2:1 Hexanes/EtOAc) to afford (*E*)-6-(tert-butyldimethylsilyloxy)hex-4-en-1-ol (**17**) (0.88 g, 35 %) as a clear oil. **IR** (thin film, cm⁻¹) 3358, 2929, 2857, 1471, 1255; **¹H NMR** (CDCl₃, 400 MHz) δ 5.69-5.64 (m, 1H), 5.61-5.63 (m, 1H), 4.13 (dd, 2H, *J* = 3.8, 1.4), 3.67 (t, 2H, *J* = 6.7 Hz), 2.13 (dt, 2H, *J* = 7.2, 6.7 Hz), 1.67 (qn, 2H, *J* = 6.7 Hz), 1.30 (bs, 1H), 0.91 (s, 9H), 0.08 (s, 6H); **¹³C NMR** (CDCl₃, 100 MHz) δ 130.6, 130.1, 64.1, 62.7, 32.3, 28.7, 26.2, 18.7, -4.9; **HRMS** (+APCI) calculated for C₁₂H₂₇O₂Si 231.1780, found 231.1775 [M+H]⁺

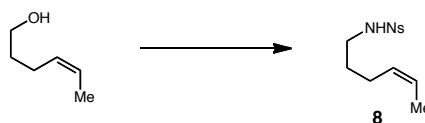
General Procedure (A) for the preparation of *N*-Nosyl Protected γ -Aminoolefins.

To a solution of olefinic alcohol (1 eq.) in CH₂Cl₂ (0.2 M) was added methanesulfonyl chloride, (1.5 eq.) at room temperature. The mixture was then cooled with an ice bath to 0 °C. Triethylamine (3.5 eq.) was slowly added over the course of 5 min. The solution obtained was removed from the ice bath and warmed to ambient temperature. Once the reaction was judged to be complete by TLC (slurry may develop), it was quenched with H₂O (10 mL). The biphasic mixture was then extracted with CH₂Cl₂ (2 x 30 mL). The combined organic extracts were washed with brine (10 mL), dried over solid Na₂SO₄ and concentrated *in vacuo*. The resulting crude oil was immediately dissolved in DMF (0.3 M). To this solution was added K₂CO₃ (4 eq.) and 4-nitrobenzene-sulfonamide (4 eq.) as

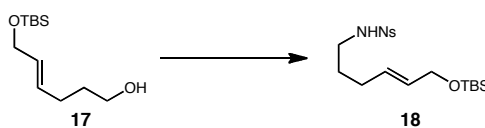
solids at room temperature. The yellow slurry obtained was heated to 70 °C until the reaction was judged to be complete by TLC. The reaction was then cooled to room temperature and quenched with H₂O (20 mL). The mixture was extracted with EtOAc (2 x 30 mL). The combined organic extracts were washed with 2N HCl (10 mL), water (2 x 10 mL), brine (10 mL) and dried over Na₂SO₄. Concentration *in vacuo* yielded the crude product that was purified by flash column chromatography on silica gel.



(E)-N-(hex-4-enyl)-4-nitrobenzenesulfonamide (7). Prepared according to general procedure and **A** using (*E*)-hex-4-en-1-ol (500 mg, 4.9 mmol), methanesulfonyl chloride, (0.72 mL, 7.5 mmol), triethylamine (2.4 mL, 18 mmol), K₂CO₃ (3.5 g, 25 mmol), and 4-nitrobenzene-sulfonamide (5.0 g, 25 mmol). Purification by flash column chromatography (5:2 Hexanes/EtOAc, R_f = 0.40) afforded (*E*)-N-(hex-4-enyl)-4-nitrobenzenesulfonamide (**7**) (1.2 g, 88 %) as a yellow amorphous solid. **IR** (thin film, cm⁻¹) 3291, 3105, 2936, 1530, 1349, 1163; **¹H NMR** (CDCl₃, 600 MHz) δ 8.38 (d, 2H, *J* = 9.0 Hz), 8.06 (d, 2H, *J* = 8.6 Hz), 5.43-5.38 (m, 1H), 5.33-5.28 (m, 1H), 4.57 (t, 1H, *J* = 5.7 Hz), 3.03 (dt, 2H, *J* = 7.1, 6.2 Hz), 2.00 (q, 2H, *J* = 7.2 Hz), 1.62 (dd, 3H, *J* = 5.2, 0.9 Hz), 1.58-1.53 (m, 3H); **¹³C NMR** (CDCl₃, 150 MHz) δ 150.3, 146.2, 129.5, 128.5, 126.8, 124.6, 43.1, 29.6, 29.5, 18.1; **HRMS** (+APCI) calculated for C₁₂H₁₇N₂O₄S 285.0915, found 285.0903 [M+H]⁺.



(Z)-N-(hex-4-enyl)-4-nitrobenzenesulfonamide (8). Prepared according to general procedure **A** using (Z)-hex-4-en-1-ol (0.25 g, 2.5 mmol), methanesulfonyl chloride, (0.36 mL, 3.7 mmol), triethylamine (1.2 mL, 8.8 mmol), K_2CO_3 (1.7 g, 13 mmol), and 4-nitrobenzene-sulfonamide (2.5 g, 13 mmol). Purification by flash column chromatography (5:2 Hexanes/EtOAc, $R_f = 0.40$) afforded (Z)-N-(hex-4-enyl)-4-nitrobenzenesulfonamide (**8**) (0.64 g, 91 %) as a yellow amorphous solid. **IR** (thin film, cm^{-1}) 3290, 3106, 2937, 1529, 1349, 1163; **1H NMR** ($CDCl_3$, 600 MHz) δ 8.36 (d, 2H, $J = 8.6$ Hz), 8.06 (d, 2H, $J = 8.6$ Hz), 5.49-5.43 (m, 1H), 5.28-5.24 (m, 1H), 5.08 (t, 1H, $J = 6.2$ Hz), 3.01 (q, 2H, $J = 6.7$ Hz), 2.03 (q, 2H, $J = 7.2$ Hz), 1.57-1.53 (m, 5H); **^{13}C NMR** ($CDCl_3$, 150 MHz) δ 150.2, 146.1, 128.7, 128.5, 125.6, 124.6, 43.2, 29.5, 23.9, 12.9; **HRMS** (+APCI) calculated for $C_{12}H_{17}N_2O_4S$ 285.0915, found 285.0924 $[M+H]^+$.

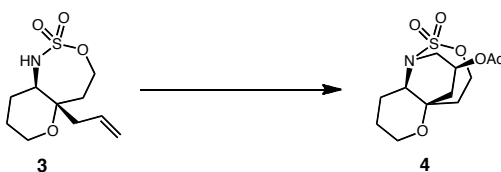


(E)-N-(6-(tert-butyldimethylsilyloxy)hex-4-enyl)-4-nitrobenzenesulfonamide (18). Prepared according to general procedure and **A** using (E)-6-((tert-butyldimethylsilyloxy)hex-4-en-1-ol (**17**) (880 mg, 3.8 mmol), methanesulfonyl chloride, (0.55 mL, 5.7 mmol), triethylamine (1.86 mL, 13.4 mmol), K_2CO_3 (2.64 g, 19.1 mmol), and 4-nitrobenzene-sulfonamide (3.86 g, 19.1 mmol). Purification by flash

column chromatography (2:1 Hexanes/EtOAc, $R_f = 0.25$) afforded (*E*)-*N*-(6-(tert-butyltrimethylsilyloxy)hex-4-enyl)-4-nitrobenzenesulfonamide (**18**) (910 mg, 57 %) as a yellow oil. **IR** (thin film, cm^{-1}) 3294, 2930, 2856, 1531, 1349, 1164; **$^1\text{H NMR}$** (CDCl_3 , 600 MHz) δ 8.37 (d, 2H, $J = 8.6$ Hz), 8.06 (d, 2H, $J = 9.1$ Hz), 5.57-5.50 (m, 2H), 4.63 (bs, 1H), 4.09 (d, 2H, $J = 3.3$ Hz), 3.03 (q, 2H, $J = 6.7$ Hz), 2.05 (q, 2H, $J = 6.7$ Hz), 1.60 (qn, 3H, $J = 7.1$ Hz), 0.90 (s, 11H), 0.06 (s, 6H); **$^{13}\text{C NMR}$** (CDCl_3 , 150 MHz) δ 150.3, 146.3, 131.0, 128.9, 128.5, 124.6, 63.8, 43.1, 29.3, 29.3, 26.2, 18.63, -4.9; **HRMS** (+APCI) calculated for $\text{C}_{18}\text{H}_{31}\text{N}_2\text{O}_5\text{SSi}$ 415.1728, found 415.1717 $[\text{M}+\text{H}]^+$.

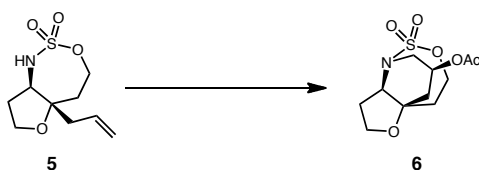
General Procedure B for copper catalyzed olefin aminoacetoxylation.

N-Nosyl protected olefinic amine (1.0 eq.) with $\text{PhI}(\text{OAc})_2$ (1.50 eq.), K_2CO_3 (1.0 eq.), and $\text{Cu}(\text{CH}_3\text{CN})_4\text{PF}_6$ (10 mol%) in a round bottom flask was equipped with a magnetic stir bar and sealed with a septum. After flushing with argon, CH_2Cl_2 (0.2 M) was added and the reaction was stirred at room temperature. After the reaction was judged to be complete by TLC, it was quenched with saturated NH_4Cl solution. The biphasic mixture was then extracted with EtOAc (2 x 10 mL). The combined organic extracts were washed with saturated NH_4Cl solution and dried over Na_2SO_4 . Concentration *in vacuo* yielded the crude product that was purified by flash column chromatography on silica gel.



2,2-dioxidohexahydro-1,5a-propanopyrano[3,2-*d*][1,2,3]oxathiazepin-11-yl acetate

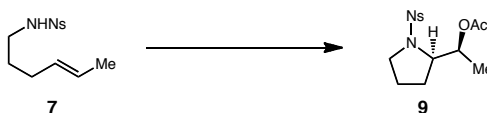
(4). Prepared according to general procedure **B** using 5-allyloctahydropyrano[3,2-*d*][1,2,3]oxathiazepine 2,2-dioxide (**3**)^{Error! Bookmark not defined.a} (50 mg, 0.2 mmol), $\text{PhI}(\text{OAc})_2$ (98 mg, 0.3 mmol), K_2CO_3 (28 mg, 0.2 mmol) and $\text{Cu}(\text{CH}_3\text{CN})_4\text{PF}_6$ (7.5 mg, 0.02 mmol). Purification by flash column chromatography (3:1→1:1 Hexanes/EtOAc) afforded piperidine (**4**) (48 mg, 80 %) as an amorphous solid. **IR** (thin film, cm^{-1}) 2947, 1741, 1389, 1362, 1188; **¹H NMR** (CDCl_3 , 600 MHz) δ 5.21 (sp, 1H, $J = 5.5$ Hz), 4.51 (ddd, 1H, $J = 13.7, 7.8, 3.2$), 4.38 (ddd, 1H, $J = 13.7, 8.7, 2.8$ Hz), 3.98 (dd, 1H, $J = 14.7, 5.5$ Hz), 3.84 (dd, 1H, $J = 12.4, 4.6$ Hz), 3.67 (dd, 1H, $J = 11.9, 4.6$ Hz), 3.55 (dt, 1H, $J = 11.9, 3.2$ Hz), 3.00 (dd, 1H, $J = 14.7, 11.5$), 2.34-2.27 (m, 2H), 2.18-2.13 (m, 1H), 2.07 (s, 3H), 2.01 (dq, 1H, $J = 12.8, 5.0$ Hz), 1.91-1.88 (m, 2H), 1.78-1.70 (m, 2H); **¹³C NMR** (CDCl_3 , 150 MHz) δ 169.9, 73.9, 67.5, 65.9, 60.7, 54.2, 43.7, 43.1, 33.7, 25.6, 23.1, 21.1; **HRMS** (+APCI) calculated for $\text{C}_{12}\text{H}_{20}\text{NO}_6\text{S}$ 306.1011, found 306.1005 $[\text{M}+\text{H}]^+$.



2,2-dioxidotetrahydro-4*H*-1,5a-propanofuro[3,2-*d*][1,2,3]oxathiazepin-10-yl acetate

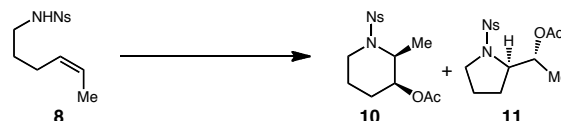
(6). Prepared according to general procedure **B** using 5-allylhexahydro-1*H*-furo[3,2-

d][1,2,3]oxathiazepine 2,2-dioxide (**5**)^{Error! Bookmark not defined.a} (30 mg, 0.13 mmol), PhI(OAc)₂ (62 mg, 0.19 mmol), K₂CO₃ (18 mg, 0.13 mmol) and Cu(CH₃CN)₄PF₆ (5 mg, 0.01 mmol). Purification by flash column chromatography (3:1 Hexanes/EtOAc) afforded piperidine (**6**) (24 mg, 66 %) as an amorphous solid. **IR** (thin film, cm⁻¹) 2955, 1742, 1364, 1237, 1181, 1026; **¹H NMR** (CDCl₃, 600 MHz) δ 5.16 (tt, 1H, *J* = 11.4, 5.2 Hz), 4.69 (ddd, 1H, *J* = 13.8, 10.0, 3.8), 4.41 (ddd, 1H, *J* = 13.3, 5.7, 3.8 Hz), 4.36 (t, 1H, *J* = 10 Hz), 4.09-4.02 (m, 2H), 3.96 (ddd, 1H, *J* = 14.8, 5.2, 1.4 Hz), 3.06 (dd, 1H, *J* = 14.8, 11.4 Hz), 2.41 (ddd, 1H, *J* = 15.7, 9.5, 3.8 Hz), 2.35-2.28 (m, 1H), 2.26-2.18 (m, 2H), 2.13 (dd, 1H, *J* = 12.9, 4.8 Hz), 1.80 (t, 1H, *J* = 12.9 Hz); **¹³C NMR** (CDCl₃, 150 MHz) δ 169.9, 78.9, 69.1, 65.1, 64.3, 57.2, 43.6, 39.7, 38.1, 24.9, 21.2; **HRMS** (+APCI) calculated for C₁₁H₁₈NO₆S 292.0855, found 292.0910 [M+H]⁺.



1-(1-((4-nitrophenyl)sulfonyl)pyrrolidin-2-yl)ethyl acetate (9). Prepared according to general procedure **B** using (*E*)-*N*-(hex-4-enyl)-4-nitrobenzenesulfonamide (**7**) (110 mg, 0.4 mmol), PhI(OAc)₂ (193 mg, 0.6 mmol), K₂CO₃ (83 mg, 0.6 mmol) and Cu(CH₃CN)₄PF₆ (15 mg, 0.04 mmol). Purification by flash column chromatography (4:1→3:2 Hexanes/EtOAc) afforded 1-(1-((4-nitrophenyl)sulfonyl)pyrrolidin-2-yl)ethyl acetate (**9**) (100 mg, 77 %) as a white crystalline solid. **IR** (thin film, cm⁻¹) 3106, 2982, 1734, 1528, 1348, 1239, 1162; **¹H NMR** (CDCl₃, 600 MHz) δ 8.37 (d, 2H, *J* = 8.6 Hz), 8.02 (d, 2H, *J* = 9.0 Hz), 5.15 (dq, 1H, *J* = 6.7, 4.3), 3.88 (dt, 1H, *J* = 8.6, 3.8 Hz), 3.39-

3.30 (m, 2H), 2.00 (s, 3H), 1.95-1.88 (m, 2H), 1.71-1.65 (m, 1H), 1.65-1.56 (m, 1H), 1.25 (d, 3H, $J = 6.7$ Hz); $^{13}\text{C NMR}$ (CDCl_3 , 150 MHz) δ 170.2, 150.3, 144.4, 128.8, 124.5, 71.9, 63.3, 49.6, 26.6, 24.9, 21.4, 17.1; **HRMS** (+APCI) calculated for $\text{C}_{14}\text{H}_{18}\text{N}_2\text{O}_6\text{S}$ 342.0886, found 343.0955 $[\text{M}+\text{H}]^+$.

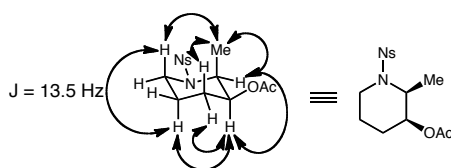


2-Methyl-1-(4-nitrophenylsulfonyl)piperidin-3-yl acetate (**10**) and

1-(4-Nitrophenylsulfonyl)pyrrolidin-2-yl ethyl acetate (**11**). Prepared according to general procedure **B** using (*Z*)-*N*-(hex-4-enyl)-4-nitrobenzenesulfonamide (**8**) (110 mg, 0.4 mmol), $\text{PhI}(\text{OAc})_2$ (193 mg, 0.6 mmol), K_2CO_3 (83 mg, 0.6 mmol) and $\text{Cu}(\text{CH}_3\text{CN})_4\text{PF}_6$ (15 mg, 0.04 mmol). Purification by flash column chromatography (4:1 \rightarrow 3:1 Hexanes/EtOAc) afforded 2-methyl-1-(4-nitrophenylsulfonyl)piperidin-3-yl acetate (**10**) (77 mg, 59 %) as an amorphous solid. **IR** (thin film, cm^{-1}) 2954, 1736, 1530, 1350, 1241, 740; $^1\text{H NMR}$ (CDCl_3 , 600 MHz) δ 8.36 (d, 2H, $J = 8.7$ Hz), 8.04 (d, 2H, $J = 8.7$ Hz), 4.60 (dt, 1H, $J = 11.9, 5.0$ Hz), 4.45 (qn, 1H, $J = 6.4$ Hz), 3.76 (dd, 1H, $J = 13.7, 4.9$ Hz), 3.00 (dt, 1H, $J = 13.7, 3.2$ Hz), 2.04 (s, 3H), 1.77-1.69 (m, 2H), 1.64-1.57 (m, 2H), 1.42 (qt, 1H, $J = 13.3, 4.6$ Hz), 1.10 (d, 3H, $J = 6.8$ Hz); $^{13}\text{C NMR}$ (CDCl_3 , 150 MHz) δ 170.1, 150.0, 147.8, 124.9, 70.2, 50.4, 39.8, 24.1, 23.9, 21.1, 10.3; **HRMS** (+APCI) calculated for $\text{C}_{14}\text{H}_{19}\text{N}_2\text{O}_6\text{S}$ 343.0964, found 343.1033 $[\text{M}+\text{H}]^+$, and 1-(4-nitrophenylsulfonyl)pyrrolidin-2-yl ethyl acetate (**11**) (47 mg, 36 %) as a white crystalline solid. **IR** (thin film, cm^{-1}) 3106, 2981, 1734, 1528, 1350, 1239, 1162;

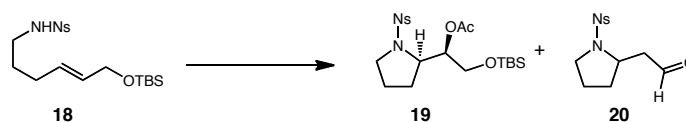
^1H NMR (CDCl_3 , 600 MHz) δ 8.39 (d, 2H, $J = 8.6$ Hz), 8.07 (d, 2H, $J = 9.0$ Hz), 5.21 (qn, 1H, $J = 6.4$ Hz), 3.80 (dq, 1H, $J = 4.1, 0.9$ Hz), 3.49 (dt, 1H, $J = 11.0, 5.9$ Hz), 3.29 (dt, 1H, $J = 11, 6.4$ Hz), 2.07 (s, 3H), 1.88-1.79 (m, 2H), 1.63-1.50 (m, 4H), 1.28 (d, 3H, $J = 6.7$ Hz); **^{13}C NMR** (CDCl_3 , 150 MHz) δ 170.6, 150.4, 143.4, 129.1, 124.6, 71.4, 61.9, 49.9, 27.1, 24.6, 21.5, 15.3; **HRMS** (+APCI) calculated for $\text{C}_{14}\text{H}_{19}\text{N}_2\text{O}_6\text{S}$ 3423.0964, found 343.1056 $[\text{M}+\text{H}]^+$.

Key nOe correlations for piperidine product 10.



1-(4-Nitrophenylsulfonyl)pyrrolidin-2-yl(phenyl)methyl acetate (14). Prepared according to general procedure **B** using (*Z*)-5-phenylpent-4-enyl 4-methylbenzenesulfonate (**13**) (50 mg, 0.14 mmol), $\text{PhI}(\text{OAc})_2$ (70 mg, 0.22 mmol), K_2CO_3 (19 mg, 0.14 mmol) and $\text{Cu}(\text{CH}_3\text{CN})_4\text{PF}_6$ (5.2 mg, 0.014 mmol). Purification by flash column chromatography (4:1 \rightarrow 3:1 Hexanes/EtOAc) afforded 1-(4-nitrophenylsulfonyl)pyrrolidin-2-yl(phenyl)methyl acetate (**14**) as a white crystalline solid (17 mg, 29 %, 10:1 d.r.). **IR** (thin film, cm^{-1}) 3105, 2980, 1741, 1529, 1350, 1232, 1163; **^1H NMR** (CDCl_3 , 600 MHz) δ 8.35 (d, 2H, $J = 8.6$ Hz), 8.0 (d, 2H, $J = 8.6$), 7.38-

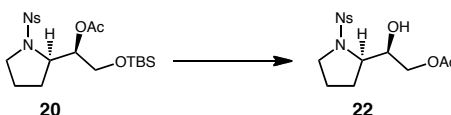
7.23 (m, 5H), 6.10 (d, 1H, $J = 2.9$ Hz), 4.21 (dt, 1H, $J = 8.6, 3.3$ Hz), 3.34-3.25 (m, 2H), 2.15 (s, 3H), 2.01-1.97 (m, 1H), 1.75-1.68 (m, 1H), 1.56-1.51 (m, 2H); $^{13}\text{C NMR}$ (CDCl_3 , 150 MHz) δ 170.0, 150.3, 144.2, 137.3, 128.9, 128.8, 128.7, 128.5, 126.6, 124.6, 63.9, 49.8, 26.6, 24.8, 21.4; **HRMS** (+APCI) calculated for $\text{C}_{19}\text{H}_{20}\text{N}_2\text{O}_6\text{S} - [\text{C}_2\text{H}_3\text{O}_2]$ 345.0909, found 345.0898 $[\text{M}-\text{OAc}]^+$.



2-(tert-butyldimethylsilyloxy)-1-(1-(4-nitrophenylsulfonyl)pyrrolidin-2-yl)ethyl acetate (19) and 2-(1-((4-nitrophenyl)sulfonyl)pyrrolidin-2-yl)acetaldehyde (20).

Prepared according to general procedure **B** using (*E*)-*N*-(6-(tert-butyldimethylsilyloxy)hex-4-enyl)-4-nitrobenzenesulfonamide (**18**) (50 mg, 0.12 mmol), $\text{PhI}(\text{OAc})_2$ (58 mg, 0.18 mmol), K_2CO_3 (17 mg, 0.12 mmol) and $\text{Cu}(\text{CH}_3\text{CN})_4\text{PF}_6$ (4.5 mg, 0.012 mmol). Purification by flash column chromatography (4:1 \rightarrow 2:1 Hexanes/EtOAc) afforded 2-(tert-butyldimethylsilyloxy)-1-(1-(4-nitrophenylsulfonyl)pyrrolidin-2-yl)ethyl acetate (**19**) as a colorless oil (29 mg, 52 %). **IR** (thin film, cm^{-1}) 2954, 2856, 1742, 1530, 1349, 1232, 1164; $^1\text{H NMR}$ (CDCl_3 , 600 MHz) δ 8.37 (d, 2H, $J = 9.2$ Hz), 8.03 (d, 2H, $J = 8.9$), 5.24 (ddd, 1H, $J = 6.1, 5.8, 3.7$ Hz), 4.05 (dt, 1H, $J = 8.5, 3.7$ Hz), 3.78 (dd, 1H, $J = 10.7, 5.5$ Hz), 3.65 (dd, 1H, $J = 10.7, 6.4$ Hz), 3.39-3.27 (m, 2H), 2.05 (s, 3H), 2.02-1.98 (m, 1H), 1.96-1.85 (m, 1H), 1.66-1.54 (m, 2H), 0.91 (s, 9H), 0.08 (d, 6H, $J = 10.7$ Hz); $^{13}\text{C NMR}$ (CDCl_3 , 150 MHz) δ 170.1, 150.3, 143.8, 128.9, 124.5, 75.1, 62.2, 60.1, 49.6, 26.7, 25.9, 24.9, 21.3, 18.4, -5.2, -5.4; **HRMS**

(+APCI) calculated for $C_{20}H_{33}N_2O_7SSi$ 473.1779, found 473.1776 $[M+H]^+$, and 2-(1-((4-nitrophenyl)sulfonyl)pyrrolidin-2-yl)acetaldehyde (**20**) as a colorless oil (29 %). **IR** (thin film, cm^{-1}) 3106, 2875, 1720, 1529, 1350, 1162, 737; **1H NMR** ($CDCl_3$, 600 MHz) δ 9.81 (s, 1H), 8.40 (d, 2H, $J = 8.9$), 8.03 (d, 2H, 8.9 Hz), 4.07 (m, 1H), 3.53 (dt, 1H, $J = 10.4$, 6.2 Hz), 3.22 (dd, 1H, $J = 18.1$, 3.8 Hz), 3.17-3.13 (m, 1H), 2.78 (dd, 1H, $J = 18.1$, 9.1 Hz), 1.92-1.82 (m, 2H), 1.67-1.60 (m, 2H); **^{13}C NMR** ($CDCl_3$, 150 MHz) δ 200.2, 170.1, 150.4, 146.7, 142.9, 128.9, 124.7, 55.3, 50.9, 49.4, 32.4, 24.1; **HRMS** (+APCI) calculated for $C_{12}H_{15}N_2O_5S$ 299.0703, found 299.0692 $[M+H]^+$



Determination of the relative stereochemistry in 2-(tert-butyldimethylsilyloxy)-1-(1-(4-nitrophenyl)sulfonyl)pyrrolidin-2-yl)ethyl acetate (**20**) was determined through X-ray crystallography of the secondary alcohol obtained after removal of the silyl ether and subsequent acetate migration (**22**).

2-hydroxy-2-(1-(4-nitrophenyl)sulfonyl)pyrrolidin-2-yl)ethyl acetate (22). TBAF (0.89 mL, 0.89 mmol, 1M solution in THF) was added slowly to a solution of 2-(tert-butyldimethylsilyloxy)-1-(1-(4-nitrophenyl)sulfonyl)pyrrolidin-2-yl)ethyl acetate (**20**) in THF, 2.0 mL) at 0 °C. The resulting solution was warmed to ambient temperature and stirred 3.5 h. at which point H_2O (5.0 mL) was added. The biphasic mixture was extracted with Et_2O (2 x 10 mL) and the combined organic extracts were washed with

brine (15 mL) and dried over MgSO_4 . Concentration *in vacuo* provided a viscous oil that was purified by flash column chromatography (2:1 Hexanes/EtOAc) to yield 2-hydroxy-2-1-((4-nitrophenyl)sulfonyl)pyrrolidin-2-yl)ethyl acetate (**22**) white crystalline solid (62-mg, 41 %) as a crystalline solid. **IR** (thin film, cm^{-1}) 3809, 2957, 1736, 1529, 1351, 1163; **^1H NMR** (CDCl_3 , 600 MHz) δ 8.39 (d, 2H, $J = 8.6$ Hz), 8.04 (d, 2H, $J = 8.6$ Hz), 4.25-4.19 (m, 2H), 4.10 (dd, 1H, $J = 10.9, 7.1$ Hz), 3.67 (dt, 1H, $J = 8.6, 5.2$ Hz), 3.49 (dt, 1H, $J = 10.9, 6.7$ Hz), 3.33 (dt, 1H, $J = 10.5, 6.7$ Hz), 2.74 (bs, 1H), 2.13 (s, 3H), 2.01 (dq, 1H, $J = 12.4, 6.7$ Hz), 1.90 (sp, 1H, $J = 6.7$), 1.63 (dq, 1H, $J = 14.8, 7.1$ Hz), 1.45 (dq, 1H, $J = 12.4, 7.1$ Hz); **^{13}C NMR** (CDCl_3 , 150 MHz) δ 171.4, 150.5, 143.1, 128.9, 124.7, 71.5, 65.9, 62.8, 50.2, 26.6, 24.8, 21.1; **HRMS** (+APCI) calculated for $\text{C}_{14}\text{H}_{20}\text{N}_2\text{O}_7\text{S}$ 359.0915, found 359.0914 $[\text{M}+\text{H}]^+$.

X-Ray Crystallographic Data

1-(1-((4-nitrophenyl)sulfonyl)pyrrolidin-2-yl)ethyl acetate (9).

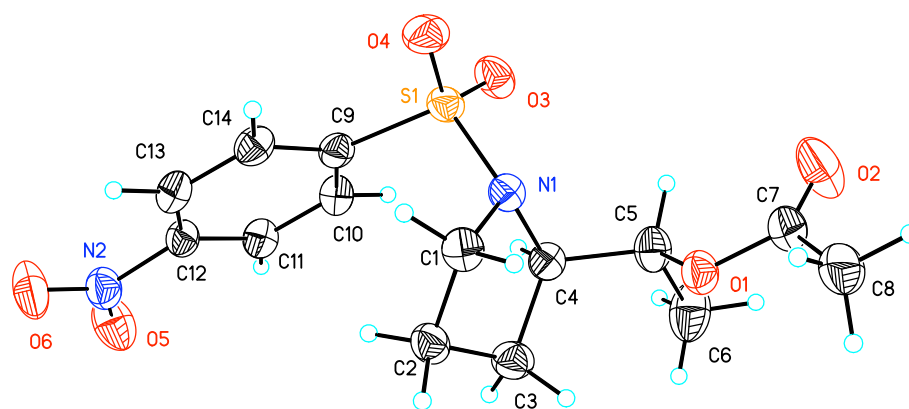


Table 1. Crystal data and structure refinement for **9**.

Identification code	ART_6_014	
Empirical formula	C ₁₄ H ₁₈ N ₂ O ₆ S	
Formula weight	342.36	
Temperature	173(2) K	
Wavelength	1.54178 Å	
Crystal system	Monoclinic	
Space group	P2(1)/n	
Unit cell dimensions	a = 8.0729(2) Å	α = 90°.
	b = 20.2011(5) Å	β = 103.3570(10)°.
	c = 10.0762(2) Å	γ = 90°.
Volume	1598.79(6) Å ³	
Z	4	
Density (calculated)	1.422 Mg/m ³	
Absorption coefficient	2.104 mm ⁻¹	
F(000)	720	
Crystal size	0.34 x 0.23 x 0.23 mm ³	
Theta range for data collection	4.38 to 66.41°.	
Index ranges	-8 ≤ h ≤ 8, -21 ≤ k ≤ 23, -11 ≤ l ≤ 10	
Reflections collected	11763	
Independent reflections	2438 [R(int) = 0.0171]	
Completeness to theta = 66.41°	86.7 %	
Absorption correction	Semi-empirical from equivalents	
Max. and min. transmission	0.6432 and 0.5348	
Refinement method	Full-matrix least-squares on F ²	
Data / restraints / parameters	2438 / 0 / 209	
Goodness-of-fit on F ²	1.028	
Final R indices [I > 2σ(I)]	R1 = 0.0312, wR2 = 0.0857	
R indices (all data)	R1 = 0.0322, wR2 = 0.0865	

Extinction coefficient	0.0036(3)
Largest diff. peak and hole	0.324 and -0.305 e.Å ⁻³

Table 2. Atomic coordinates ($\times 10^4$) and equivalent isotropic displacement parameters ($\text{\AA}^2 \times 10^3$) for ART_6_014s. U(eq) is defined as one third of the trace of the orthogonalized U_{ij} tensor.

	x	y	z	U(eq)
C(1)	2689(2)	1987(1)	792(2)	32(1)
C(2)	1720(2)	1888(1)	-669(2)	33(1)
C(3)	1107(2)	2587(1)	-1100(2)	35(1)
C(4)	765(2)	2917(1)	192(2)	28(1)
C(5)	1382(2)	3627(1)	452(2)	35(1)
C(6)	490(3)	4092(1)	-667(2)	54(1)
C(7)	4154(2)	4096(1)	1258(2)	38(1)
C(8)	5939(3)	4088(1)	1083(2)	48(1)
C(9)	-835(2)	1577(1)	1520(2)	28(1)
C(10)	-2332(2)	1762(1)	604(2)	30(1)
C(11)	-3300(2)	1285(1)	-202(2)	31(1)
C(12)	-2751(2)	636(1)	-63(2)	29(1)
C(13)	-1308(2)	438(1)	880(2)	32(1)
C(14)	-334(2)	917(1)	1681(2)	31(1)
N(1)	1645(2)	2477(1)	1339(1)	26(1)
N(2)	-3764(2)	136(1)	-975(2)	37(1)
O(1)	3203(2)	3629(1)	500(1)	34(1)
O(2)	3609(2)	4478(1)	1972(2)	62(1)
O(3)	-511(2)	2746(1)	2615(1)	38(1)
O(4)	1690(2)	1899(1)	3506(1)	40(1)

O(5)	-5037(2)	315(1)	-1790(2)	54(1)
O(6)	-3266(2)	-436(1)	-856(2)	57(1)
S(1)	534(1)	2205(1)	2384(1)	29(1)

Table 3. Bond lengths [\AA] and angles [$^\circ$] for ART_6_014s.

C(1)-N(1)	1.486(2)
C(1)-C(2)	1.513(2)
C(1)-H(1A)	0.9900
C(1)-H(1B)	0.9900
C(2)-C(3)	1.525(2)
C(2)-H(2A)	0.9900
C(2)-H(2B)	0.9900
C(3)-C(4)	1.542(2)
C(3)-H(3A)	0.9900
C(3)-H(3B)	0.9900
C(4)-N(1)	1.500(2)
C(4)-C(5)	1.522(2)
C(4)-H(4A)	1.0000
C(5)-O(1)	1.460(2)
C(5)-C(6)	1.515(3)
C(5)-H(5A)	1.0000
C(6)-H(6A)	0.9800
C(6)-H(6B)	0.9800
C(6)-H(6C)	0.9800
C(7)-O(2)	1.206(2)
C(7)-O(1)	1.340(2)
C(7)-C(8)	1.492(3)
C(8)-H(8A)	0.9800
C(8)-H(8B)	0.9800

C(8)-H(8C)	0.9800
C(9)-C(14)	1.392(2)
C(9)-C(10)	1.392(2)
C(9)-S(1)	1.7742(16)
C(10)-C(11)	1.380(2)
C(10)-H(10A)	0.9500
C(11)-C(12)	1.381(2)
C(11)-H(11A)	0.9500
C(12)-C(13)	1.382(2)
C(12)-N(2)	1.478(2)
C(13)-C(14)	1.382(2)
C(13)-H(13A)	0.9500
C(14)-H(14A)	0.9500
N(1)-S(1)	1.6267(13)
N(2)-O(5)	1.213(2)
N(2)-O(6)	1.221(2)
O(3)-S(1)	1.4313(13)
O(4)-S(1)	1.4304(13)
N(1)-C(1)-C(2)	103.82(13)
N(1)-C(1)-H(1A)	111.0
C(2)-C(1)-H(1A)	111.0
N(1)-C(1)-H(1B)	111.0
C(2)-C(1)-H(1B)	111.0
H(1A)-C(1)-H(1B)	109.0
C(1)-C(2)-C(3)	102.45(13)
C(1)-C(2)-H(2A)	111.3
C(3)-C(2)-H(2A)	111.3
C(1)-C(2)-H(2B)	111.3
C(3)-C(2)-H(2B)	111.3
H(2A)-C(2)-H(2B)	109.2

C(2)-C(3)-C(4)	105.60(13)
C(2)-C(3)-H(3A)	110.6
C(4)-C(3)-H(3A)	110.6
C(2)-C(3)-H(3B)	110.6
C(4)-C(3)-H(3B)	110.6
H(3A)-C(3)-H(3B)	108.8
N(1)-C(4)-C(5)	110.35(13)
N(1)-C(4)-C(3)	104.46(13)
C(5)-C(4)-C(3)	115.88(14)
N(1)-C(4)-H(4A)	108.6
C(5)-C(4)-H(4A)	108.6
C(3)-C(4)-H(4A)	108.6
O(1)-C(5)-C(6)	108.99(15)
O(1)-C(5)-C(4)	107.18(13)
C(6)-C(5)-C(4)	112.06(15)
O(1)-C(5)-H(5A)	109.5
C(6)-C(5)-H(5A)	109.5
C(4)-C(5)-H(5A)	109.5
C(5)-C(6)-H(6A)	109.5
C(5)-C(6)-H(6B)	109.5
H(6A)-C(6)-H(6B)	109.5
C(5)-C(6)-H(6C)	109.5
H(6A)-C(6)-H(6C)	109.5
H(6B)-C(6)-H(6C)	109.5
O(2)-C(7)-O(1)	123.49(18)
O(2)-C(7)-C(8)	125.02(17)
O(1)-C(7)-C(8)	111.48(16)
C(7)-C(8)-H(8A)	109.5
C(7)-C(8)-H(8B)	109.5
H(8A)-C(8)-H(8B)	109.5
C(7)-C(8)-H(8C)	109.5

H(8A)-C(8)-H(8C)	109.5
H(8B)-C(8)-H(8C)	109.5
C(14)-C(9)-C(10)	121.25(15)
C(14)-C(9)-S(1)	119.84(13)
C(10)-C(9)-S(1)	118.69(12)
C(11)-C(10)-C(9)	119.34(15)
C(11)-C(10)-H(10A)	120.3
C(9)-C(10)-H(10A)	120.3
C(12)-C(11)-C(10)	118.56(15)
C(12)-C(11)-H(11A)	120.7
C(10)-C(11)-H(11A)	120.7
C(11)-C(12)-C(13)	122.99(15)
C(11)-C(12)-N(2)	117.84(15)
C(13)-C(12)-N(2)	119.18(15)
C(14)-C(13)-C(12)	118.33(15)
C(14)-C(13)-H(13A)	120.8
C(12)-C(13)-H(13A)	120.8
C(13)-C(14)-C(9)	119.44(15)
C(13)-C(14)-H(14A)	120.3
C(9)-C(14)-H(14A)	120.3
C(1)-N(1)-C(4)	108.43(12)
C(1)-N(1)-S(1)	117.40(11)
C(4)-N(1)-S(1)	117.68(10)
O(5)-N(2)-O(6)	123.84(15)
O(5)-N(2)-C(12)	118.54(14)
O(6)-N(2)-C(12)	117.61(15)
C(7)-O(1)-C(5)	117.43(14)
O(3)-S(1)-O(4)	120.21(8)
O(3)-S(1)-N(1)	106.38(7)
O(4)-S(1)-N(1)	107.52(7)
O(3)-S(1)-C(9)	107.56(7)

O(4)-S(1)-C(9)	107.23(8)
N(1)-S(1)-C(9)	107.35(7)

Symmetry transformations used to generate equivalent atoms:

Table 4. Anisotropic displacement parameters ($\text{\AA}^2 \times 10^3$) for ART_6_014s. The anisotropic displacement factor exponent takes the form: $-2\pi^2 [h^2 a^{*2} U^{11} + \dots + 2 h k a^* b^* U^{12}]$

	U11	U22	U33	U23	U13	U12
C(1)	26(1)	32(1)	38(1)	-2(1)	10(1)	2(1)
C(2)	32(1)	35(1)	36(1)	-8(1)	13(1)	-7(1)
C(3)	35(1)	41(1)	28(1)	-2(1)	5(1)	-3(1)
C(4)	23(1)	31(1)	29(1)	1(1)	4(1)	-1(1)
C(5)	29(1)	30(1)	45(1)	-2(1)	8(1)	-1(1)
C(6)	47(1)	36(1)	73(2)	12(1)	1(1)	1(1)
C(7)	38(1)	36(1)	37(1)	-3(1)	5(1)	-9(1)
C(8)	41(1)	57(1)	46(1)	-9(1)	9(1)	-17(1)
C(9)	26(1)	31(1)	28(1)	1(1)	9(1)	-4(1)
C(10)	26(1)	26(1)	38(1)	1(1)	8(1)	0(1)
C(11)	24(1)	31(1)	36(1)	3(1)	4(1)	-1(1)
C(12)	29(1)	28(1)	33(1)	-1(1)	9(1)	-6(1)
C(13)	34(1)	26(1)	38(1)	6(1)	10(1)	0(1)
C(14)	28(1)	34(1)	32(1)	7(1)	5(1)	0(1)
N(1)	23(1)	28(1)	28(1)	-1(1)	5(1)	-1(1)
N(2)	37(1)	32(1)	42(1)	-4(1)	11(1)	-7(1)
O(1)	30(1)	33(1)	39(1)	-4(1)	8(1)	-7(1)
O(2)	52(1)	59(1)	77(1)	-36(1)	19(1)	-14(1)
O(3)	35(1)	41(1)	43(1)	-14(1)	17(1)	-7(1)

O(4)	37(1)	52(1)	28(1)	3(1)	0(1)	-11(1)
O(5)	41(1)	49(1)	61(1)	-14(1)	-9(1)	-3(1)
O(6)	68(1)	28(1)	68(1)	-9(1)	4(1)	-3(1)
S(1)	27(1)	35(1)	26(1)	-4(1)	6(1)	-6(1)

Table 5. Hydrogen coordinates ($\times 10^4$) and isotropic displacement parameters ($\text{\AA}^2 \times 10^3$) for ART_6_014s.

	x	y	z	U(eq)
H(1A)	2785	1567	1309	38
H(1B)	3846	2162	833	38
H(2A)	750	1582	-725	40
H(2B)	2471	1716	-1239	40
H(3A)	54	2573	-1834	42
H(3B)	1989	2834	-1434	42
H(4A)	-487	2904	138	34
H(5A)	1191	3780	1348	42
H(6A)	921	4542	-461	81
H(6B)	-738	4083	-724	81
H(6C)	709	3949	-1541	81
H(8A)	6599	4435	1648	72
H(8B)	5937	4167	123	72
H(8C)	6454	3656	1362	72
H(10A)	-2685	2211	535	36
H(11A)	-4322	1401	-839	37
H(13A)	-993	-16	976	39
H(14A)	669	796	2335	38

Table 6. Torsion angles [°] for ART_6_014s.

N(1)-C(1)-C(2)-C(3)	39.04(16)
C(1)-C(2)-C(3)-C(4)	-33.64(17)
C(2)-C(3)-C(4)-N(1)	15.46(17)
C(2)-C(3)-C(4)-C(5)	137.08(15)
N(1)-C(4)-C(5)-O(1)	61.98(17)
C(3)-C(4)-C(5)-O(1)	-56.44(19)
N(1)-C(4)-C(5)-C(6)	-178.49(15)
C(3)-C(4)-C(5)-C(6)	63.1(2)
C(14)-C(9)-C(10)-C(11)	-2.9(2)
S(1)-C(9)-C(10)-C(11)	171.76(13)
C(9)-C(10)-C(11)-C(12)	0.5(2)
C(10)-C(11)-C(12)-C(13)	2.3(3)
C(10)-C(11)-C(12)-N(2)	-177.50(15)
C(11)-C(12)-C(13)-C(14)	-2.7(3)
N(2)-C(12)-C(13)-C(14)	177.06(15)
C(12)-C(13)-C(14)-C(9)	0.3(2)
C(10)-C(9)-C(14)-C(13)	2.4(2)
S(1)-C(9)-C(14)-C(13)	-172.15(13)
C(2)-C(1)-N(1)-C(4)	-30.47(16)
C(2)-C(1)-N(1)-S(1)	105.93(13)
C(5)-C(4)-N(1)-C(1)	-116.01(15)
C(3)-C(4)-N(1)-C(1)	9.19(16)
C(5)-C(4)-N(1)-S(1)	107.72(14)
C(3)-C(4)-N(1)-S(1)	-127.08(12)
C(11)-C(12)-N(2)-O(5)	-0.8(2)
C(13)-C(12)-N(2)-O(5)	179.35(16)
C(11)-C(12)-N(2)-O(6)	179.36(16)

C(13)-C(12)-N(2)-O(6)	-0.4(2)
O(2)-C(7)-O(1)-C(5)	5.7(3)
C(8)-C(7)-O(1)-C(5)	-173.30(15)
C(6)-C(5)-O(1)-C(7)	86.52(19)
C(4)-C(5)-O(1)-C(7)	-152.00(14)
C(1)-N(1)-S(1)-O(3)	-172.59(11)
C(4)-N(1)-S(1)-O(3)	-40.22(12)
C(1)-N(1)-S(1)-O(4)	57.42(13)
C(4)-N(1)-S(1)-O(4)	-170.21(11)
C(1)-N(1)-S(1)-C(9)	-57.67(13)
C(4)-N(1)-S(1)-C(9)	74.70(12)
C(14)-C(9)-S(1)-O(3)	-151.65(13)
C(10)-C(9)-S(1)-O(3)	33.64(15)
C(14)-C(9)-S(1)-O(4)	-21.05(16)
C(10)-C(9)-S(1)-O(4)	164.23(13)
C(14)-C(9)-S(1)-N(1)	94.23(14)
C(10)-C(9)-S(1)-N(1)	-80.49(14)

Symmetry transformations used to generate equivalent atoms:

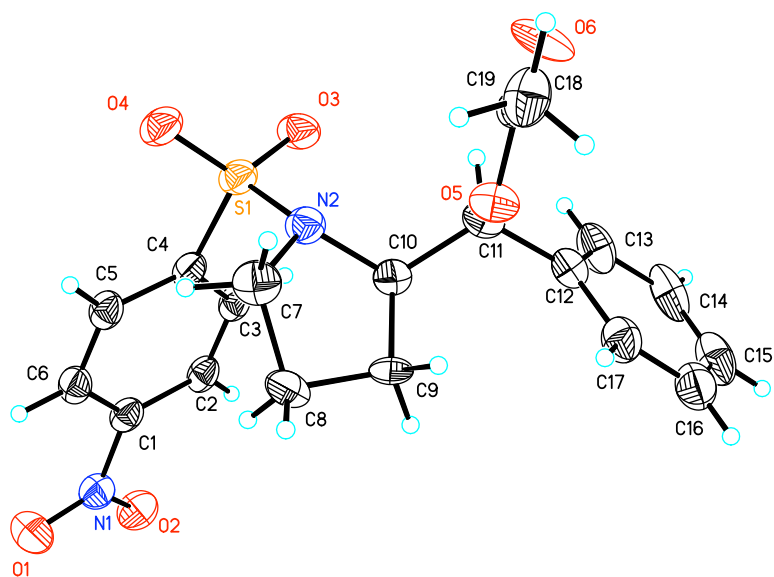
1-(4-Nitrophenylsulfonyl)pyrrolidin-2-yl)(phenyl)methyl acetate (14).

Table 1. Crystal data and structure refinement for **14**.

Identification code	art698s	
Empirical formula	C ₁₉ H ₂₀ N ₂ O ₆ S	
Formula weight	404.43	
Temperature	173(2) K	
Wavelength	0.71073 Å	
Crystal system	Monoclinic	
Space group	P2(1)/c	
Unit cell dimensions	a = 14.287(16) Å	α = 90°.
	b = 7.710(8) Å	β = 92.52(2)°.
	c = 17.145(19) Å	γ = 90°.
Volume	1887(4) Å ³	
Z	4	
Density (calculated)	1.424 Mg/m ³	
Absorption coefficient	0.211 mm ⁻¹	
F(000)	848	
Crystal size	0.15 x 0.13 x 0.13 mm ³	
Theta range for data collection	1.43 to 30.33°.	
Index ranges	-19 ≤ h ≤ 20, -10 ≤ k ≤ 10, -24 ≤ l ≤ 24	
Reflections collected	32759	
Independent reflections	5320 [R(int) = 0.1026]	
Completeness to theta = 30.33°	94.1 %	
Absorption correction	Semi-empirical from equivalents	
Max. and min. transmission	0.9730 and 0.9690	
Refinement method	Full-matrix least-squares on F ²	
Data / restraints / parameters	5320 / 5 / 292	
Goodness-of-fit on F ²	1.007	
Final R indices [I > 2σ(I)]	R1 = 0.0594, wR2 = 0.1495	
R indices (all data)	R1 = 0.1653, wR2 = 0.2002	
Largest diff. peak and hole	0.311 and -0.314 e.Å ⁻³	

Table 2. Atomic coordinates ($\times 10^4$) and equivalent isotropic displacement parameters ($\text{\AA}^2 \times 10^3$) for art698s. $U(\text{eq})$ is defined as one third of the trace of the orthogonalized U^{ij} tensor.

	x	y	z	$U(\text{eq})$
C(1)	92(2)	5936(4)	1282(2)	54(1)
C(2)	-42(2)	4215(4)	1459(2)	56(1)
C(3)	493(2)	2989(4)	1113(2)	55(1)
C(4)	1165(2)	3489(4)	597(2)	54(1)
C(5)	1266(2)	5223(4)	401(2)	57(1)
C(6)	732(2)	6458(4)	747(2)	58(1)
C(7)	3460(3)	3465(5)	892(2)	73(1)
C(8)	3385(8)	4191(11)	1688(5)	66(3)
C(9)	3300(10)	2529(16)	2133(8)	63(4)
C(8A)	3728(6)	3475(12)	1762(5)	67(2)
C(9A)	2980(9)	2643(14)	2220(7)	68(4)
C(10)	2729(3)	1187(4)	1629(2)	61(1)
C(11)	3178(2)	-597(4)	1713(2)	60(1)
C(12)	3067(2)	-1378(4)	2504(2)	56(1)
C(13)	2329(2)	-2473(4)	2636(2)	79(1)
C(14)	2205(3)	-3167(5)	3379(3)	92(1)
C(15)	2789(3)	-2719(5)	3975(3)	92(1)
C(16)	3536(3)	-1612(5)	3871(2)	85(1)
C(17)	3670(3)	-962(4)	3137(2)	72(1)
C(18)	4566(3)	-1501(4)	1079(2)	63(1)
C(19)	5573(2)	-1097(5)	981(2)	81(1)
N(1)	-459(2)	7262(4)	1680(2)	64(1)
N(2)	2853(2)	1903(3)	835(1)	59(1)
O(1)	-272(2)	8779(3)	1565(2)	88(1)
O(2)	-1059(2)	6785(3)	2119(1)	81(1)
O(3)	1508(2)	281(3)	271(1)	71(1)
O(4)	2244(2)	2579(3)	-501(1)	72(1)
O(5)	4171(2)	-380(3)	1557(1)	69(1)
S(1)	1943(1)	1939(1)	225(1)	60(1)
O(6)	4255(9)	-2814(14)	832(10)	91(4)

O(6A) 4020(10) -2407(19) 720(9) 99(5)
 Table 3. Bond lengths [Å] and angles [°] for art698s.

C(1)-C(2)	1.377(4)
C(1)-C(6)	1.383(4)
C(1)-N(1)	1.476(4)
C(2)-C(3)	1.368(4)
C(2)-H(2A)	0.9300
C(3)-C(4)	1.388(4)
C(3)-H(3A)	0.9300
C(4)-C(5)	1.387(4)
C(4)-S(1)	1.770(3)
C(5)-C(6)	1.371(4)
C(5)-H(5A)	0.9300
C(6)-H(6A)	0.9300
C(7)-C(8)	1.484(9)
C(7)-N(2)	1.486(4)
C(7)-C(8A)	1.524(8)
C(7)-H(7B)	0.96(3)
C(7)-H(7A)	0.96(3)
C(8)-C(9)	1.499(13)
C(8)-H(8A)	0.9700
C(8)-H(8B)	0.9700
C(9)-C(10)	1.556(12)
C(9)-H(9A)	0.9700
C(9)-H(9B)	0.9700
C(8A)-C(9A)	1.498(11)
C(8A)-H(8AA)	0.9700
C(8A)-H(8AB)	0.9700
C(9A)-C(10)	1.544(10)
C(9A)-H(9AA)	0.9700
C(9A)-H(9AB)	0.9700
C(10)-N(2)	1.487(4)
C(10)-C(11)	1.522(5)
C(10)-H(10)	0.93(3)

C(11)-O(5)	1.465(4)
C(11)-C(12)	1.499(4)
C(11)-H(11A)	0.9800
C(12)-C(13)	1.377(4)
C(12)-C(17)	1.394(5)
C(13)-C(14)	1.401(5)
C(13)-H(13A)	0.9300
C(14)-C(15)	1.337(6)
C(14)-H(14A)	0.9300
C(15)-C(16)	1.384(6)
C(15)-H(15A)	0.9300
C(16)-C(17)	1.376(5)
C(16)-H(16A)	0.9300
C(17)-H(17A)	0.9300
C(18)-O(6)	1.177(9)
C(18)-O(6A)	1.198(11)
C(18)-O(5)	1.333(4)
C(18)-C(19)	1.489(5)
C(19)-H(19A)	0.9600
C(19)-H(19B)	0.9600
C(19)-H(19C)	0.9600
N(1)-O(1)	1.218(4)
N(1)-O(2)	1.221(3)
N(2)-S(1)	1.631(3)
O(3)-S(1)	1.425(2)
O(4)-S(1)	1.423(2)
C(2)-C(1)-C(6)	122.0(3)
C(2)-C(1)-N(1)	118.9(3)
C(6)-C(1)-N(1)	119.1(3)
C(3)-C(2)-C(1)	119.0(3)
C(3)-C(2)-H(2A)	120.5
C(1)-C(2)-H(2A)	120.5
C(2)-C(3)-C(4)	120.0(3)
C(2)-C(3)-H(3A)	120.0
C(4)-C(3)-H(3A)	120.0

C(5)-C(4)-C(3)	120.3(3)
C(5)-C(4)-S(1)	119.4(2)
C(3)-C(4)-S(1)	120.3(2)
C(6)-C(5)-C(4)	119.9(3)
C(6)-C(5)-H(5A)	120.0
C(4)-C(5)-H(5A)	120.0
C(5)-C(6)-C(1)	118.8(3)
C(5)-C(6)-H(6A)	120.6
C(1)-C(6)-H(6A)	120.6
C(8)-C(7)-N(2)	107.5(5)
C(8)-C(7)-C(8A)	28.7(3)
N(2)-C(7)-C(8A)	100.9(4)
C(8)-C(7)-H(7B)	101(2)
N(2)-C(7)-H(7B)	112(2)
C(8A)-C(7)-H(7B)	128(2)
C(8)-C(7)-H(7A)	126(3)
N(2)-C(7)-H(7A)	102(3)
C(8A)-C(7)-H(7A)	103(3)
H(7B)-C(7)-H(7A)	108(4)
C(7)-C(8)-C(9)	99.0(7)
C(7)-C(8)-H(8A)	112.0
C(9)-C(8)-H(8A)	112.0
C(7)-C(8)-H(8B)	112.0
C(9)-C(8)-H(8B)	112.0
H(8A)-C(8)-H(8B)	109.6
C(8)-C(9)-C(10)	109.7(10)
C(8)-C(9)-H(9A)	109.7
C(10)-C(9)-H(9A)	109.7
C(8)-C(9)-H(9B)	109.7
C(10)-C(9)-H(9B)	109.7
H(9A)-C(9)-H(9B)	108.2
C(9A)-C(8A)-C(7)	110.9(8)
C(9A)-C(8A)-H(8AA)	109.5
C(7)-C(8A)-H(8AA)	109.5
C(9A)-C(8A)-H(8AB)	109.5
C(7)-C(8A)-H(8AB)	109.5

H(8AA)-C(8A)-H(8AB)	108.0
C(8A)-C(9A)-C(10)	96.8(7)
C(8A)-C(9A)-H(9AA)	112.4
C(10)-C(9A)-H(9AA)	112.4
C(8A)-C(9A)-H(9AB)	112.4
C(10)-C(9A)-H(9AB)	112.4
H(9AA)-C(9A)-H(9AB)	110.0
N(2)-C(10)-C(11)	110.8(2)
N(2)-C(10)-C(9A)	107.3(5)
C(11)-C(10)-C(9A)	120.7(6)
N(2)-C(10)-C(9)	100.5(6)
C(11)-C(10)-C(9)	109.9(6)
C(9A)-C(10)-C(9)	18.4(8)
N(2)-C(10)-H(10)	110.1(16)
C(11)-C(10)-H(10)	109.0(16)
C(9A)-C(10)-H(10)	97.9(16)
C(9)-C(10)-H(10)	116.2(17)
O(5)-C(11)-C(12)	110.6(2)
O(5)-C(11)-C(10)	106.7(3)
C(12)-C(11)-C(10)	112.8(2)
O(5)-C(11)-H(11A)	108.9
C(12)-C(11)-H(11A)	108.9
C(10)-C(11)-H(11A)	108.9
C(13)-C(12)-C(17)	117.7(3)
C(13)-C(12)-C(11)	120.5(3)
C(17)-C(12)-C(11)	121.8(3)
C(12)-C(13)-C(14)	120.8(4)
C(12)-C(13)-H(13A)	119.6
C(14)-C(13)-H(13A)	119.6
C(15)-C(14)-C(13)	119.8(4)
C(15)-C(14)-H(14A)	120.1
C(13)-C(14)-H(14A)	120.1
C(14)-C(15)-C(16)	121.3(4)
C(14)-C(15)-H(15A)	119.3
C(16)-C(15)-H(15A)	119.3
C(17)-C(16)-C(15)	118.9(4)

C(17)-C(16)-H(16A)	120.6
C(15)-C(16)-H(16A)	120.6
C(16)-C(17)-C(12)	121.5(4)
C(16)-C(17)-H(17A)	119.3
C(12)-C(17)-H(17A)	119.3
O(6)-C(18)-O(6A)	23.9(14)
O(6)-C(18)-O(5)	127.9(8)
O(6A)-C(18)-O(5)	114.2(8)
O(6)-C(18)-C(19)	119.4(8)
O(6A)-C(18)-C(19)	132.5(8)
O(5)-C(18)-C(19)	111.8(3)
C(18)-C(19)-H(19A)	109.5
C(18)-C(19)-H(19B)	109.5
H(19A)-C(19)-H(19B)	109.5
C(18)-C(19)-H(19C)	109.5
H(19A)-C(19)-H(19C)	109.5
H(19B)-C(19)-H(19C)	109.5
O(1)-N(1)-O(2)	123.7(3)
O(1)-N(1)-C(1)	117.7(3)
O(2)-N(1)-C(1)	118.6(3)
C(7)-N(2)-C(10)	109.5(3)
C(7)-N(2)-S(1)	118.4(2)
C(10)-N(2)-S(1)	118.0(2)
C(18)-O(5)-C(11)	118.5(2)
O(4)-S(1)-O(3)	120.54(13)
O(4)-S(1)-N(2)	107.71(15)
O(3)-S(1)-N(2)	106.64(14)
O(4)-S(1)-C(4)	107.40(15)
O(3)-S(1)-C(4)	107.67(16)
N(2)-S(1)-C(4)	106.03(14)

Symmetry transformations used to generate equivalent atoms:

Table 4. Anisotropic displacement parameters ($\text{\AA}^2 \times 10^3$) for art698s. The anisotropic displacement factor exponent takes the form: $-2\pi^2 [h^2 a^{*2} U_{11} + \dots + 2 h k a^* b^* U_{12}]$

	U11	U22	U33	U23	U13	U12
C(1)	55(2)	63(2)	45(2)	3(1)	-4(1)	-12(2)
C(2)	58(2)	66(2)	44(2)	12(1)	6(1)	-13(2)
C(3)	62(2)	57(2)	46(2)	11(1)	4(1)	-13(2)
C(4)	59(2)	60(2)	42(2)	5(1)	-3(1)	-14(2)
C(5)	61(2)	58(2)	52(2)	9(1)	2(1)	-15(2)
C(6)	63(2)	54(2)	57(2)	7(1)	-7(2)	-15(2)
C(7)	65(2)	76(2)	80(3)	-6(2)	3(2)	-13(2)
C(8)	69(7)	49(6)	80(6)	-16(4)	-3(5)	5(4)
C(9)	84(10)	64(7)	42(5)	-22(4)	22(6)	21(6)
C(8A)	60(5)	60(5)	82(5)	-15(4)	-1(4)	-1(4)
C(9A)	97(9)	47(5)	61(5)	-12(3)	22(5)	17(5)
C(10)	73(3)	58(2)	53(2)	-3(1)	7(2)	4(2)
C(11)	54(2)	55(2)	70(2)	-9(2)	4(2)	-4(1)
C(12)	50(2)	46(2)	74(2)	2(2)	4(2)	2(1)
C(13)	57(2)	57(2)	121(3)	17(2)	5(2)	-2(2)
C(14)	64(2)	56(2)	159(4)	35(3)	31(3)	10(2)
C(15)	90(3)	74(3)	114(3)	29(2)	43(3)	27(2)
C(16)	98(3)	73(2)	84(3)	12(2)	15(2)	15(2)
C(17)	76(2)	63(2)	77(2)	12(2)	12(2)	1(2)
C(18)	78(3)	62(2)	50(2)	3(2)	6(2)	-5(2)
C(19)	64(2)	99(3)	81(2)	27(2)	14(2)	-4(2)
N(1)	66(2)	68(2)	58(2)	0(1)	-4(1)	0(2)
N(2)	67(2)	56(2)	55(1)	-2(1)	9(1)	-6(1)
O(1)	96(2)	66(2)	103(2)	-4(1)	12(2)	1(1)
O(2)	82(2)	97(2)	66(1)	1(1)	20(1)	-1(1)
O(3)	90(2)	56(1)	67(1)	-10(1)	14(1)	-22(1)
O(4)	91(2)	77(1)	49(1)	0(1)	15(1)	-15(1)
O(5)	65(2)	66(1)	76(1)	-16(1)	10(1)	-7(1)
S(1)	73(1)	59(1)	47(1)	-2(1)	8(1)	-14(1)
O(6)	69(6)	56(4)	149(8)	-51(4)	17(4)	-8(4)

O(6A) 88(9) 122(11) 90(6) -46(7) 34(6) -10(7)

Table 5. Hydrogen coordinates ($\times 10^4$) and isotropic displacement parameters ($\text{\AA}^2 \times 10^3$) for art698s.

	x	y	z	U(eq)
H(2A)	-490	3891	1808	67
H(3A)	407	1820	1223	66
H(5A)	1695	5547	35	69
H(6A)	798	7625	624	70
H(8A)	2835	4917	1728	80
H(8B)	3940	4839	1855	80
H(9A)	2988	2744	2615	75
H(9B)	3919	2070	2265	75
H(8AA)	4313	2854	1853	81
H(8AB)	3822	4661	1937	81
H(9AA)	2458	3417	2299	82
H(9AB)	3220	2194	2718	82
H(11A)	2890	-1372	1317	71
H(13A)	1908	-2756	2226	94
H(14A)	1717	-3937	3458	111
H(15A)	2692	-3160	4470	110
H(16A)	3939	-1312	4290	102
H(17A)	4175	-229	3062	86
H(19A)	5834	-1927	634	121
H(19B)	5906	-1149	1479	121
H(19C)	5629	47	766	121
H(7B)	3210(30)	4410(40)	580(20)	105(14)
H(7A)	4020(30)	3070(60)	660(30)	144(19)
H(10)	2100(20)	1100(30)	1724(14)	46(8)

Table 6. Torsion angles [°] for art698s.

C(6)-C(1)-C(2)-C(3)	2.0(4)
N(1)-C(1)-C(2)-C(3)	-177.5(2)
C(1)-C(2)-C(3)-C(4)	0.5(4)
C(2)-C(3)-C(4)-C(5)	-3.1(4)
C(2)-C(3)-C(4)-S(1)	173.4(2)
C(3)-C(4)-C(5)-C(6)	3.2(4)
S(1)-C(4)-C(5)-C(6)	-173.3(2)
C(4)-C(5)-C(6)-C(1)	-0.7(4)
C(2)-C(1)-C(6)-C(5)	-1.9(4)
N(1)-C(1)-C(6)-C(5)	177.6(2)
N(2)-C(7)-C(8)-C(9)	35.5(9)
C(8A)-C(7)-C(8)-C(9)	-45.2(11)
C(7)-C(8)-C(9)-C(10)	-35.4(11)
C(8)-C(7)-C(8A)-C(9A)	78.4(15)
N(2)-C(7)-C(8A)-C(9A)	-28.2(8)
C(7)-C(8A)-C(9A)-C(10)	38.2(9)
C(8A)-C(9A)-C(10)-N(2)	-33.6(9)
C(8A)-C(9A)-C(10)-C(11)	94.6(8)
C(8A)-C(9A)-C(10)-C(9)	37(3)
C(8)-C(9)-C(10)-N(2)	21.7(10)
C(8)-C(9)-C(10)-C(11)	138.5(8)
C(8)-C(9)-C(10)-C(9A)	-92(4)
N(2)-C(10)-C(11)-O(5)	58.7(3)
C(9A)-C(10)-C(11)-O(5)	-68.0(6)
C(9)-C(10)-C(11)-O(5)	-51.5(6)
N(2)-C(10)-C(11)-C(12)	-179.7(3)
C(9A)-C(10)-C(11)-C(12)	53.7(6)
C(9)-C(10)-C(11)-C(12)	70.2(6)
O(5)-C(11)-C(12)-C(13)	-146.9(3)
C(10)-C(11)-C(12)-C(13)	93.7(4)
O(5)-C(11)-C(12)-C(17)	36.4(4)
C(10)-C(11)-C(12)-C(17)	-83.0(4)
C(17)-C(12)-C(13)-C(14)	-1.2(5)

C(11)-C(12)-C(13)-C(14)	-178.1(3)
C(12)-C(13)-C(14)-C(15)	2.2(5)
C(13)-C(14)-C(15)-C(16)	-1.7(6)
C(14)-C(15)-C(16)-C(17)	0.2(6)
C(15)-C(16)-C(17)-C(12)	0.8(5)
C(13)-C(12)-C(17)-C(16)	-0.3(5)
C(11)-C(12)-C(17)-C(16)	176.5(3)
C(2)-C(1)-N(1)-O(1)	173.9(3)
C(6)-C(1)-N(1)-O(1)	-5.7(4)
C(2)-C(1)-N(1)-O(2)	-4.4(4)
C(6)-C(1)-N(1)-O(2)	176.0(3)
C(8)-C(7)-N(2)-C(10)	-24.4(5)
C(8A)-C(7)-N(2)-C(10)	4.4(5)
C(8)-C(7)-N(2)-S(1)	114.8(5)
C(8A)-C(7)-N(2)-S(1)	143.6(4)
C(11)-C(10)-N(2)-C(7)	-114.5(3)
C(9A)-C(10)-N(2)-C(7)	19.2(6)
C(9)-C(10)-N(2)-C(7)	1.6(6)
C(11)-C(10)-N(2)-S(1)	106.1(3)
C(9A)-C(10)-N(2)-S(1)	-120.2(6)
C(9)-C(10)-N(2)-S(1)	-137.7(6)
O(6)-C(18)-O(5)-C(11)	-10.9(11)
O(6A)-C(18)-O(5)-C(11)	12.1(10)
C(19)-C(18)-O(5)-C(11)	179.8(3)
C(12)-C(11)-O(5)-C(18)	103.5(3)
C(10)-C(11)-O(5)-C(18)	-133.5(3)
C(7)-N(2)-S(1)-O(4)	47.5(3)
C(10)-N(2)-S(1)-O(4)	-176.7(2)
C(7)-N(2)-S(1)-O(3)	178.2(2)
C(10)-N(2)-S(1)-O(3)	-46.0(2)
C(7)-N(2)-S(1)-C(4)	-67.2(3)
C(10)-N(2)-S(1)-C(4)	68.5(2)
C(5)-C(4)-S(1)-O(4)	-28.5(3)
C(3)-C(4)-S(1)-O(4)	155.0(2)
C(5)-C(4)-S(1)-O(3)	-159.7(2)
C(3)-C(4)-S(1)-O(3)	23.8(3)

C(5)-C(4)-S(1)-N(2)	86.5(2)
C(3)-C(4)-S(1)-N(2)	-90.1(2)

Symmetry transformations used to generate equivalent atoms:

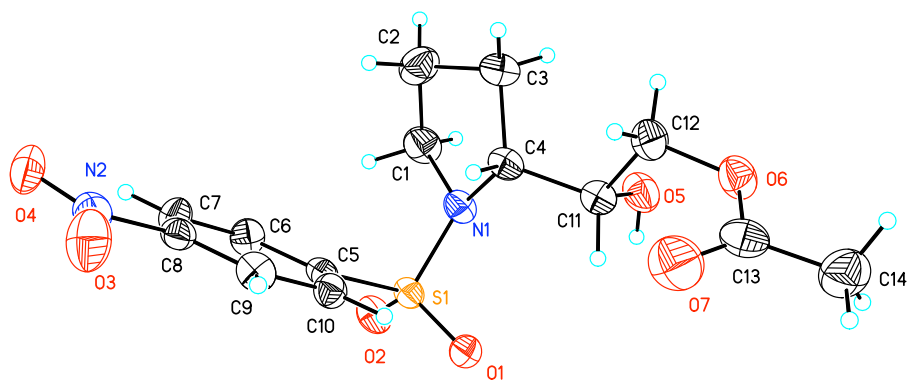
2-hydroxy-2-1-((4-nitrophenyl)sulfonyl)pyrrolidin-2-yl)ethyl acetate (22).

Table 1. Crystal data and structure refinement for **22**.

Identification code	art_6_182s	
Empirical formula	C ₁₄ H ₁₈ N ₂ O ₇ S	
Formula weight	358.36	
Temperature	293(2) K	
Wavelength	1.54178 Å	
Crystal system	Monoclinic	
Space group	P2(1)	
Unit cell dimensions	a = 7.5329(4) Å	α = 90°.
	b = 8.0154(4) Å	β = 93.700(3)°.
	c = 13.3032(7) Å	γ = 90°.
Volume	801.56(7) Å ³	
Z	2	
Density (calculated)	1.485 Mg/m ³	
Absorption coefficient	2.174 mm ⁻¹	
F(000)	376	
Crystal size	0.29 x 0.26 x 0.14 mm ³	
Theta range for data collection	3.33 to 66.29°.	
Index ranges	-8 ≤ h ≤ 8, -8 ≤ k ≤ 9, -13 ≤ l ≤ 15	
Reflections collected	5715	
Independent reflections	2277 [R(int) = 0.0170]	
Completeness to theta = 66.29°	90.8 %	
Absorption correction	Semi-empirical from equivalents	
Refinement method	Full-matrix least-squares on F ²	
Data / restraints / parameters	2277 / 1 / 217	
Goodness-of-fit on F ²	1.074	
Final R indices [I > 2σ(I)]	R1 = 0.0267, wR2 = 0.0741	
R indices (all data)	R1 = 0.0268, wR2 = 0.0742	
Absolute structure parameter	0.094(16)	
Largest diff. peak and hole	0.233 and -0.204 e.Å ⁻³	

Table 2. Atomic coordinates ($\times 10^4$) and equivalent isotropic displacement parameters ($\text{\AA}^2 \times 10^3$) for ART_6_182s. $U(\text{eq})$ is defined as one third of the trace of the orthogonalized U^{ij} tensor.

	x	y	z	$U(\text{eq})$
C(1)	7742(3)	5378(3)	388(2)	39(1)
C(2)	9189(4)	6098(4)	1104(2)	43(1)
C(3)	9813(3)	4581(3)	1706(2)	40(1)
C(4)	8099(3)	3628(3)	1900(2)	29(1)
C(5)	4406(3)	5808(3)	2027(2)	24(1)
C(6)	4322(3)	7450(3)	1705(2)	30(1)
C(7)	4089(3)	8714(3)	2388(2)	32(1)
C(8)	3913(3)	8274(3)	3389(2)	27(1)
C(9)	3980(3)	6647(3)	3719(2)	31(1)
C(10)	4236(3)	5392(3)	3035(2)	27(1)
C(11)	8333(3)	1744(3)	2022(2)	33(1)
C(12)	9755(3)	1419(3)	2861(2)	39(1)
C(13)	8755(3)	-809(4)	3846(2)	39(1)
C(14)	8989(4)	-2606(4)	4095(2)	54(1)
N(1)	6896(2)	4081(3)	1013(1)	29(1)
N(2)	3621(3)	9615(3)	4121(2)	36(1)
O(1)	4262(2)	2675(2)	1604(1)	30(1)
O(2)	3945(2)	4682(2)	198(1)	34(1)
O(3)	3250(3)	9185(3)	4974(1)	51(1)
O(4)	3749(2)	11080(2)	3853(1)	41(1)
O(5)	8909(2)	999(2)	1135(1)	40(1)
O(6)	9834(2)	-313(2)	3143(1)	39(1)
O(7)	7721(3)	121(3)	4227(2)	61(1)
S(1)	4777(1)	4195(1)	1153(1)	25(1)

Table 3. Bond lengths [\AA] and angles [$^\circ$] for ART_6_182s.

C(1)-N(1)	1.498(3)
C(1)-C(2)	1.515(4)
C(1)-H(1A)	0.9700
C(1)-H(1B)	0.9700
C(2)-C(3)	1.514(4)
C(2)-H(2A)	0.9700
C(2)-H(2B)	0.9700
C(3)-C(4)	1.537(3)
C(3)-H(3A)	0.9700
C(3)-H(3B)	0.9700
C(4)-N(1)	1.486(3)
C(4)-C(11)	1.527(3)
C(4)-H(4A)	0.9800
C(5)-C(6)	1.384(3)
C(5)-C(10)	1.395(3)
C(5)-S(1)	1.773(2)
C(6)-C(7)	1.379(3)
C(6)-H(6A)	0.9300
C(7)-C(8)	1.393(3)
C(7)-H(7A)	0.9300
C(8)-C(9)	1.376(3)
C(8)-N(2)	1.476(3)
C(9)-C(10)	1.378(3)
C(9)-H(9A)	0.9300
C(10)-H(10A)	0.9300
C(11)-O(5)	1.415(3)
C(11)-C(12)	1.519(3)
C(11)-H(11A)	0.9800
C(12)-O(6)	1.438(3)
C(12)-H(12A)	0.9700
C(12)-H(12B)	0.9700
C(13)-O(7)	1.212(3)
C(13)-O(6)	1.338(3)

C(13)-C(14)	1.486(5)
C(14)-H(14A)	0.9600
C(14)-H(14B)	0.9600
C(14)-H(14C)	0.9600
N(1)-S(1)	1.6222(16)
N(2)-O(4)	1.232(3)
N(2)-O(3)	1.236(3)
O(1)-S(1)	1.4231(17)
O(2)-S(1)	1.4338(16)
O(5)-H(5A)	0.8200
N(1)-C(1)-C(2)	103.31(18)
N(1)-C(1)-H(1A)	111.1
C(2)-C(1)-H(1A)	111.1
N(1)-C(1)-H(1B)	111.1
C(2)-C(1)-H(1B)	111.1
H(1A)-C(1)-H(1B)	109.1
C(3)-C(2)-C(1)	102.3(2)
C(3)-C(2)-H(2A)	111.3
C(1)-C(2)-H(2A)	111.3
C(3)-C(2)-H(2B)	111.3
C(1)-C(2)-H(2B)	111.3
H(2A)-C(2)-H(2B)	109.2
C(2)-C(3)-C(4)	104.6(2)
C(2)-C(3)-H(3A)	110.8
C(4)-C(3)-H(3A)	110.8
C(2)-C(3)-H(3B)	110.8
C(4)-C(3)-H(3B)	110.8
H(3A)-C(3)-H(3B)	108.9
N(1)-C(4)-C(11)	112.73(19)
N(1)-C(4)-C(3)	102.74(18)
C(11)-C(4)-C(3)	114.6(2)
N(1)-C(4)-H(4A)	108.8
C(11)-C(4)-H(4A)	108.8
C(3)-C(4)-H(4A)	108.8
C(6)-C(5)-C(10)	121.3(2)

C(6)-C(5)-S(1)	119.73(16)
C(10)-C(5)-S(1)	118.95(17)
C(7)-C(6)-C(5)	120.0(2)
C(7)-C(6)-H(6A)	120.0
C(5)-C(6)-H(6A)	120.0
C(6)-C(7)-C(8)	117.9(2)
C(6)-C(7)-H(7A)	121.1
C(8)-C(7)-H(7A)	121.1
C(9)-C(8)-C(7)	122.8(2)
C(9)-C(8)-N(2)	118.9(2)
C(7)-C(8)-N(2)	118.3(2)
C(8)-C(9)-C(10)	119.0(2)
C(8)-C(9)-H(9A)	120.5
C(10)-C(9)-H(9A)	120.5
C(9)-C(10)-C(5)	119.1(2)
C(9)-C(10)-H(10A)	120.5
C(5)-C(10)-H(10A)	120.5
O(5)-C(11)-C(12)	107.51(19)
O(5)-C(11)-C(4)	111.6(2)
C(12)-C(11)-C(4)	108.6(2)
O(5)-C(11)-H(11A)	109.7
C(12)-C(11)-H(11A)	109.7
C(4)-C(11)-H(11A)	109.7
O(6)-C(12)-C(11)	111.9(2)
O(6)-C(12)-H(12A)	109.2
C(11)-C(12)-H(12A)	109.2
O(6)-C(12)-H(12B)	109.2
C(11)-C(12)-H(12B)	109.2
H(12A)-C(12)-H(12B)	107.9
O(7)-C(13)-O(6)	123.0(3)
O(7)-C(13)-C(14)	125.0(2)
O(6)-C(13)-C(14)	112.0(2)
C(13)-C(14)-H(14A)	109.5
C(13)-C(14)-H(14B)	109.5
H(14A)-C(14)-H(14B)	109.5
C(13)-C(14)-H(14C)	109.5

H(14A)-C(14)-H(14C)	109.5
H(14B)-C(14)-H(14C)	109.5
C(4)-N(1)-C(1)	110.56(16)
C(4)-N(1)-S(1)	118.45(14)
C(1)-N(1)-S(1)	118.79(15)
O(4)-N(2)-O(3)	123.9(2)
O(4)-N(2)-C(8)	119.1(2)
O(3)-N(2)-C(8)	117.0(2)
C(11)-O(5)-H(5A)	109.5
C(13)-O(6)-C(12)	116.9(2)
O(1)-S(1)-O(2)	119.41(10)
O(1)-S(1)-N(1)	107.28(10)
O(2)-S(1)-N(1)	106.90(9)
O(1)-S(1)-C(5)	106.82(10)
O(2)-S(1)-C(5)	107.71(10)
N(1)-S(1)-C(5)	108.33(10)

Symmetry transformations used to generate equivalent atoms:

Table 4. Anisotropic displacement parameters ($\text{\AA}^2 \times 10^3$) for ART_6_182s. The anisotropic displacement factor exponent takes the form: $-2\pi^2 [h^2 a^{*2} U^{11} + \dots + 2 h k a^* b^* U^{12}]$

	U11	U22	U33	U23	U13	U12
C(1)	35(1)	43(1)	38(1)	11(1)	9(1)	1(1)
C(2)	47(1)	36(1)	47(2)	4(1)	9(1)	-7(1)
C(3)	28(1)	43(2)	49(2)	-2(1)	-1(1)	-4(1)
C(4)	24(1)	35(1)	29(1)	-1(1)	3(1)	1(1)
C(5)	18(1)	28(1)	26(1)	-2(1)	1(1)	1(1)
C(6)	35(1)	30(1)	26(1)	5(1)	6(1)	2(1)
C(7)	36(1)	24(1)	37(1)	4(1)	2(1)	1(1)
C(8)	21(1)	30(1)	29(1)	-5(1)	1(1)	-1(1)
C(9)	31(1)	37(1)	24(1)	-1(1)	1(1)	2(1)
C(10)	26(1)	26(1)	28(1)	5(1)	2(1)	2(1)
C(11)	28(1)	34(1)	38(1)	1(1)	2(1)	0(1)
C(12)	37(1)	36(1)	43(1)	6(1)	-5(1)	4(1)
C(13)	32(1)	53(2)	33(1)	-5(1)	-1(1)	-5(1)
C(14)	55(2)	55(2)	52(2)	13(2)	4(1)	-7(1)
N(1)	25(1)	33(1)	28(1)	3(1)	4(1)	4(1)
N(2)	30(1)	39(1)	38(1)	-10(1)	-2(1)	3(1)
O(1)	28(1)	27(1)	37(1)	-4(1)	0(1)	0(1)
O(2)	32(1)	43(1)	26(1)	-3(1)	-4(1)	7(1)
O(3)	70(1)	48(1)	33(1)	-12(1)	1(1)	12(1)
O(4)	52(1)	25(1)	47(1)	-4(1)	-1(1)	7(1)
O(5)	36(1)	42(1)	41(1)	-9(1)	-3(1)	7(1)
O(6)	36(1)	42(1)	38(1)	8(1)	4(1)	7(1)
O(7)	57(1)	66(2)	63(1)	-10(1)	20(1)	4(1)
S(1)	22(1)	28(1)	24(1)	-2(1)	0(1)	3(1)

Table 5. Hydrogen coordinates ($\times 10^4$) and isotropic displacement parameters ($\text{\AA}^2 \times 10^{-3}$) for ART_6_182s.

	x	y	z	U(eq)
H(1A)	6889	6228	165	46
H(1B)	8240	4881	-196	46
H(2A)	10145	6573	741	51
H(2B)	8720	6947	1534	51
H(3A)	10437	4910	2335	48
H(3B)	10599	3901	1327	48
H(4A)	7607	4077	2508	35
H(6A)	4423	7701	1029	36
H(7A)	4051	9825	2186	39
H(9A)	3855	6397	4394	37
H(10A)	4295	4284	3242	32
H(11A)	7207	1239	2194	40
H(12A)	10903	1761	2641	47
H(12B)	9506	2085	3444	47
H(14A)	8204	-2909	4605	81
H(14B)	10198	-2806	4338	81
H(14C)	8717	-3263	3502	81
H(5A)	8044	650	792	60

Table 6. Torsion angles [$^{\circ}$] for ART_6_182s.

N(1)-C(1)-C(2)-C(3)	35.8(2)
C(1)-C(2)-C(3)-C(4)	-40.7(2)
C(2)-C(3)-C(4)-N(1)	29.0(2)
C(2)-C(3)-C(4)-C(11)	151.7(2)
C(10)-C(5)-C(6)-C(7)	0.8(3)
S(1)-C(5)-C(6)-C(7)	-177.99(18)
C(5)-C(6)-C(7)-C(8)	-1.1(3)
C(6)-C(7)-C(8)-C(9)	0.7(3)
C(6)-C(7)-C(8)-N(2)	-178.6(2)
C(7)-C(8)-C(9)-C(10)	0.1(3)
N(2)-C(8)-C(9)-C(10)	179.40(19)
C(8)-C(9)-C(10)-C(5)	-0.5(3)
C(6)-C(5)-C(10)-C(9)	0.0(3)
S(1)-C(5)-C(10)-C(9)	178.83(16)
N(1)-C(4)-C(11)-O(5)	54.5(2)
C(3)-C(4)-C(11)-O(5)	-62.5(3)
N(1)-C(4)-C(11)-C(12)	172.88(18)
C(3)-C(4)-C(11)-C(12)	55.8(3)
O(5)-C(11)-C(12)-O(6)	-69.4(2)
C(4)-C(11)-C(12)-O(6)	169.7(2)
C(11)-C(4)-N(1)-C(1)	-130.3(2)
C(3)-C(4)-N(1)-C(1)	-6.4(2)
C(11)-C(4)-N(1)-S(1)	87.7(2)
C(3)-C(4)-N(1)-S(1)	-148.39(17)
C(2)-C(1)-N(1)-C(4)	-18.5(2)
C(2)-C(1)-N(1)-S(1)	123.37(19)
C(9)-C(8)-N(2)-O(4)	172.4(2)
C(7)-C(8)-N(2)-O(4)	-8.4(3)
C(9)-C(8)-N(2)-O(3)	-8.0(3)
C(7)-C(8)-N(2)-O(3)	171.3(2)
O(7)-C(13)-O(6)-C(12)	1.4(3)
C(14)-C(13)-O(6)-C(12)	-178.5(2)
C(11)-C(12)-O(6)-C(13)	-87.6(2)

C(4)-N(1)-S(1)-O(1)	-51.97(19)
C(1)-N(1)-S(1)-O(1)	169.14(16)
C(4)-N(1)-S(1)-O(2)	178.83(16)
C(1)-N(1)-S(1)-O(2)	39.94(19)
C(4)-N(1)-S(1)-C(5)	63.01(19)
C(1)-N(1)-S(1)-C(5)	-75.88(18)
C(6)-C(5)-S(1)-O(1)	-162.57(17)
C(10)-C(5)-S(1)-O(1)	18.59(19)
C(6)-C(5)-S(1)-O(2)	-33.1(2)
C(10)-C(5)-S(1)-O(2)	148.01(16)
C(6)-C(5)-S(1)-N(1)	82.14(19)
C(10)-C(5)-S(1)-N(1)	-96.70(17)

Symmetry transformations used to generate equivalent atoms:

Table 7. Hydrogen bonds for ART_6_182s [\AA and $^\circ$].

D-H...A	d(D-H)	d(H...A)	d(D...A)	$\angle(\text{DHA})$
O(5)-H(5A)...O(2)#1	0.82	2.08	2.896(2)	173.5

Symmetry transformations used to generate equivalent atoms:

#1 $-x+1, y-1/2, -z$

References

- (1) For reviews see: (a) Kolb, H. C.; VanNieuwenhze, M. S.; Sharpless, K. B. *Chem. Rev.* **1994**, *94*, 2483. (b) Jensen, K. H.; Sigman, M. S.; *Org. Biomol. Chem.* **2008**, *6*, 4083.
- (2) For examples of diamination see: (a) Bar, G. L. J.; Lloyd-Jones, G. C.; Booker-Milburn, K. I. *J. Am. Chem. Soc.* **2005**, *127*, 7308. (b) Streuff, J.; Hövelmann, C. H.; Nieger, M.; Muñoz, K. *J. Am. Chem. Soc.* **2005**, *127*, 14586. For examples of diacetoxylation see: Li, Y.; Song, D.; Dong, V. M. *J. Am. Chem. Soc.* **2008**, *130*, 2962.
- (c) Seayad, J.; Seayad, A. M.; Chai, C. L. L. *Org. Lett.*, **2010**, *12*, (7), 1412.
- (3) (a) Li, G.; Chang, H.-T.; Sharpless, K. B. *Angew. Chem., Int. Ed.* **1996**, *35*, 451. (b) Nilov, D.; Reiser, O. *Adv. Synth. Catal.* **2002**, *344*, 1169. (c) Muniz, K. *Chem. Soc. Rev.* **2004**, *33*, 166.
- (4) (a) Michaelis, D. J.; Shaffer, C. J.; Yoon, T. P. *J. Am. Chem. Soc.* **2007**, *129*, 1866. (b) Michaelis, D. J.; Ischay, M. A.; Yoon, T. P. *J. Am. Chem. Soc.* **2008**, *130*, 6610. (c) Michaelis, D. J.; Williamson, K. S.; Yoon, T. P. *Tetrahedron* **2009**, *65*, 5118. (d) Benkovics, T.; Du, J.; Guzei, I. A.; Yoon, T. P. *J. Org. Chem.* **2009**, *74*, 5545. (e) Alexanian, E. J.; Lee, C.; Sorensen, E. J. *J. Am. Chem. Soc.* **2005**, *127*, 7690. (f) Liu, G.; Stahl, S. S. *J. Am. Chem. Soc.* **2006**, *128*, 7179. (g) Desai, L. V.; Sanford, M. S. *Angew. Chem., Int. Ed.* **2007**, *46*, 5737.
- (5) (a) Fuller, P. H.; Kim, J.-W.; Chemler, S. R. *J. Am. Chem. Soc.* **2008**, *130*, 17638. (b) Paderes, M. C.; Chemler, S. R. *Org. Lett.* **2009**, *11*, 1915.
- (6) Lovick, H. M.; Michael, F. M. *J. Am. Chem. Soc.* **2010**, *132*, 1249.s
- (7) Wardrop, D. J.; Bowen, E. G.; Forslund, R. E.; Sussman, A. D.; Weerasekera, S.

L. J. Am. Chem. Soc. **2010**, *132*, 1188.

(8) Mancheno, D. E.; Thornton, A. R.; Stoll, A. H.; Kong, A.; Blakey, S. B. *Org. Lett.* **2010**, *12*, 18, 4110.